For My Family

Promotor: Prof. dr. Els J. M. Van Damme

Laboratory of Biochemistry and Glycobiology

Department of Molecular Biotechnology

Faculty of Bioscience Engineering, Ghent University

Dean: Prof. dr. ir. Guido Van Huylenbroeck

Rector: Prof. dr. Anne De Paepe

Chenjing Shang

Biological activity of ribosome-inactivating proteins from *Malus domestica* (apple) and *Sambucus nigra* (elderberry)

Thesis submitted in fulfillment of the requirements for the degree of Doctor (PhD) of Applied Biological Sciences: Cell and Gene Biotechnology

Nederlandse vertaling van de titel:

Biologische activiteiten van ribosoom-inactiverende proteïnen uit *Malus domestica* (appel) en *Sambucus nigra* (vlier).

Cover illustration:

EGFP fluorescence in protoplasts expressing type 2 RIP::EGFP fusion protein.

Refer to this thesis:

Shang C. (2015) Biological activity of ribosome-inactivating proteins from *Malus domestica* (apple) and *Sambucus nigra* (elderberry). PhD thesis, Faculty of Bioscience engineering, Ghent University, Ghent, Belgium.

ISBN: 978-90-5989-810-3

The promotor,   The author,
Prof. dr. Els J. M. Van Damme   Chenjing Shang

Members of the examination committee:

Prof. dr. ir. Nico Boon (chairman)

Lab. Microbial Ecology and Technology, Dept. Biochemical and Microbial Technology,
Faculty of Bioscience Engineering, Ghent University, Belgium

Prof. dr. Els J. M. Van Damme (promotor)

Lab. Biochemistry and Glycobiology, Dept. Molecular Biotechnology
Faculty of Bioscience Engineering, Ghent University, Belgium

Prof. dr. ir. Monica Höfte (secretary)

Lab. Phytopathology, Dept. Crop Protection
Faculty of Bioscience Engineering, Ghent University, Belgium

Prof. dr. Wim Van den Ende

Lab. Molecular Plant Biology, Institute of Botany and Microbiology
KU Leuven, Belgium

Prof. dr. ir. Winnok H. De Vos

Lab. Cell Biology and Histology, Dept. Veterinary Sciences
University of Antwerp, Belgium

Prof. dr. ir. Guy Smagghe

Lab. Agrozoology, Dept. Crop Protection
Faculty of Bioscience Engineering, Ghent University, Belgium

Prof. dr. Danny Geelen

Dept. Plant Production
Faculty of Bioscience Engineering, Ghent University, Belgium

Prof. dr. ir. Kris Audenaert

Dept. Applied Biosciences
Faculty of Bioscience Engineering, Ghent University, Belgium

Prof. dr. ir. John Van Camp

Dept. Food Safety and Food Quality
Faculty of Bioscience Engineering, Ghent University, Belgium

Table of Contents

List of abbreviations

AA	amino acid
ABA	abscisic acid
α2MG-R	α2-macroglobulin receptor
AOP	antioxidant protein
AOX 1	alcohol oxidase 1
BY-2	bright Yellow-2 (*Nicotiana tabacum* cell suspension culture)
cv	cultivated variety
CWDEs	cell wall-degrading enzymes
DAA	day after anthesis
D/PAMPs	damage/pathogen-associated molecular patterns
DPI	days post infection
EF	elongation factor
EGFP	enhanced green fluorescent protein
ER	endoplasmic reticulum
ERAD	reticulum-associated degradation
EST	expressed sequence tag
Fuc	fucose
FW	fresh weight
Gal	galactose
GAPDH	glyceraldehyde 3-phosphate dehydrogenase
GlcNAc	N-acetylglucosamine
GTPase	guanosine triphosphatase
HIV	human immunodeficiency virus
IC50	half maximal inhibitory concentration
IRAb	*Iris* agglutinin b
IRIP	*Iris* type 1 RIP
JA	jasmonic acid
JaCop	just another colocalization plugin
kDa	kiloDalton

LC50	50% lethal concentration
LRP	lipoprotein receptor-related proteins
Man	mannose
MeJA	methyl jasmonate
MS	Murashige-Skoog medium
MSMO	Murashige-Skoog medium with minimal organics
MVB	multivesicular bodies
MW	molecular weight
NEPs	necrosis and ethylene-inducing proteins
NLS	nuclear localization sequence
PAG	polynucleotide: adenosine glycosidase
PAMP	pathogen-associated molecular pattern
PAP	pokeweed antiviral protein
PBS	phosphate buffered saline
PR	pathogenesis-related
PSV	protein storage vacuoles
pv	pathovar
PVDF	polyvinylidene fluoride
qRT-PCR	quantitative reverse-transcriptase polymerase chain reaction
RFU	relative fluorescence units
RIP	ribosome-inactivating protein
ROS	reactive oxygen species
RTA	ricin toxin A chain
rRNA	ribosomal RNA
SA	salicylic acid
SE	standard error
SNA	*Sambucus nigra* agglutinin
SP	signal peptide
TBS	Tris-buffered saline
TGN	trans-Golgi network
TMV	tobacco mosaic virus
WT	wild type

Scope

In nature, agricultural plants are continuously suffering from a multitude of biotic stresses such as viral, bacterial and fungal infection, insect predation and herbivore attack… Every year, these factors cause great losses in global agricultural economy. Due to their immobility plants cannot escape from these pests and diseases. However each plant species has developed its own set of defense proteins to successfully cope with all hostile attacks. For instance plants accumulate carbohydrate binding proteins (lectins) and ribosome-inactivating proteins (RIPs) as part of their natural defense system. The first RIP was discovered more than a century ago and since then this class of proteins has been the subject of many research projects. Despite the detailed knowledge of the biological activities of the proteins the physiological role of RIPs is still poorly understood.

The family of RIPs is classically divided into type 1 RIPs composed of one domain with enzymatic activity, and type 2 RIPs in which the enzymatic domain is linked to carbohydrate binding domain. This PhD research focuses on the type 1 and type 2 RIPs from apple (*Malus* sp.), as well as the RIP family from *Sambucus nigra*. Apple is a major fruit crop, and more than one hundred countries are growing apples every year. Apple is a favorite fruit for many people. The presence of ricin-like proteins in common fruits like apple raises important questions. The statement, "An apple a day keeps the doctor away" indicates that apple is a healthy fruit for our daily consumption. There are many benefits of eating apples we heard from doctors, newspapers and internet, such as protecting against Parkinson's, reducing the risk of developing cancers, controlling your weight and so on. Definitely, all these evidences tell us that apple is a healthy fruit. In the first part of the PhD thesis we focus on the question why RIP sequences are present in the genome of *Malus domestica*? It is important and interesting to investigate the biological activities and the possible (cyto)toxic effects of RIPs expressed in edible fruits like apple. The thesis starts with a general introduction describing the occurrence, distribution and biological characterizes of RIPs from plants.

The first objective of this PhD project was the characterization of RIPs from apple. In **Chapter 2**, the focus of the research was on the cloning, the heterologous expression and the purification of recombinant type 1 and type 2 RIPs. Subsequently, the recombinant proteins have been characterized for what concerns their molecular structures and biological activity. The toxicity of the proteins for animal cells was

investigated in detail. In addition, the carbohydrate binding property of the type 2 RIP was analyzed using glycan arrays.

The second goal for this work was to study the localization of the type 1 and type 2 RIPs from apple in plant cells. In **Chapter 3**, the subcellular localization of the RIPs from apple was analyzed in different plant systems. Furthermore a quantitative analysis of the transcript levels of the apple RIPs was performed in different tissues from an apple tree and throughout fruit development.

The third aim of this PhD research was to study of the effects of the type 1 and type 2 RIPs from apple and their involvement in disease resistance. In **Chapter 4**, transgenic tobacco plants were constructed. These plants were used to study the effects of overexpression of the RIP genes on the overall growth as well as the development of the plants, and their disease resistance to tobacco mosaic virus and fungi. Furthermore, the insecticidal activity of the apple RIPs was analyzed by adding the recombinant proteins to an artificial diet.

In the second part of this PhD, the research focuses on the RIP family from *Sambucus nigra*. Besides the studies of RIPs in agriculture, RIPs are also important from a medical point of view because of their potential anti-tumor activity. However, selective targeting of cancer cells requires knowledge on their specific cytotoxic activity and working mechanism. This also requires enhanced insight in their binding affinity, internalization and intracellular destination in the cell. Although previous studies have addressed mechanisms of RIP induced cell death and the internalization of specific type 2 RIPs, mainly with galactose-recognition domains, for many RIPs, this information is still lacking or incomplete. In this context, two major questions are pending, namely, whether (i) translation-inhibition activity is the sole factor for RIP-induced apoptosis, and whether (ii) there is a direct contribution of the lectin chain to the cytotoxicity of the protein. An ideal model system for such studies is the family of elderberry lectins (SNA-II and SNA-IV)/RIPs (SNA-I, SNA-V and SNLRP). The availability of both RIPs and related non-RIP lectins with different carbohydrate-binding specificities offers an opportunity to study the contributions of the RIP domain and the lectin domain to the cytotoxicity of the protein, binding to the cell surface, internalization and trafficking in the cell.

The fourth objective of this research was to investigate the effects of RIPs from *Sambucus nigra* (elderberry) on mammalian cells. In **Chapter 5**, the carbohydrate specificities of RIPs and lectins from elderberry were analyzed and compared in

detail. In **Chapter 6**, the *in vitro* and *in vivo* activities of several *S. nigra* proteins have been characterized. We studied the cytotoxicity of several RIPs/lectins from elderberry towards human cells. In an attempt to explain the interaction of the proteins with the cells, the internalization and intracellular localization of the RIPs/lectins was determined and cell surface glycoproteins and glycolipids were analysed.

Chapter 7 aims to integrate all the data into a general discussion and some perspectives for future research are suggested.

Chapter 1
General introduction

Partly redrafted from:

Shang, C., Peumans, W. J. and Van Damme, E. J. M. (2014) Occurrence and taxonomical distribution of ribosome-inactivating proteins belonging to the ricin/shiga toxin superfamily. In: Ribosome-inactivating proteins: ricin and related proteins. Stirpe, F. and Lappi, D. A. (eds.) pp. 11-27. Wiley Blackwell Press, NJ, USA

Peumans, W. J., Shang, C. and Van Damme, E. J. M. (2014) Updated model of the molecular evolution of RIP genes. In: Ribosome-inactivating proteins: ricin and related proteins. Stirpe, F. and Lappi, D. A. (eds.) pp. 134-150. Wiley Blackwell Press, NJ, USA

Shang, C., Dang, L. and Van Damme, E. J. M. (2015) Plant AB toxins with lectin domains. In: Toxinology: Plant Toxins. Gopalakrishnakone, P., Carlini, C. R. and Ligabue-Braun, R. (eds.) Springer, Berlin, Germany. In press

1.1 General introduction of ribosome-inactivating proteins

1.1.1 Historical note

The scientific history of ribosome-inactivating proteins (RIPs) started in 1888 when Peter Hermann Stillmark discovered the lethal toxicity of a "ferment" in castor bean (*Ricinus communis*) seeds which he named "ricin" (Stillmark, 1888). Throughout more than a century, the properties of ricin and related proteins have been extensively investigated and described, including their molecular structures, enzymatic activities, biological roles and potential applications in agriculture as well as in medicine.

1.1.2 Definition

The observation that plant proteins can irreversibly inactivate ribosomes resulted in the term of "ribosome-inactivating proteins", which was first introduced by Stirpe (1982). Though the activity of ribosomes can be affected by different types of proteins/enzymes (e.g. proteases, RNases, ribosome-binding proteins), this contribution deals exclusively with proteins that by virtue of a well-defined RNA N-glycosidase activity are capable of depurinating a specific adenine in what is called the conserved α-sarcin/ricin loop of the large ribosomal RNA (Stirpe and Battelli, 2006). This depurination of the α-sarcin/ricin loop by RIPs can inhibit protein synthesis and cause cell death (Puri et al., 2012). At present, the family of RIPs groups all proteins with an RNA N-glycosidase domain (EC3.2.2.22). A more detailed description of the enzymatic activities of RIPs will be described in the part dealing with enzymatic activity (chapter 1.2.1.1).

1.1.3 Classification of RIPs

Plant RIPs are classically subdivided in three main groups namely the type 1 RIPs, type 2 RIPs and one type 3 RIP (Fig. 1.1).

Classification of RIPs
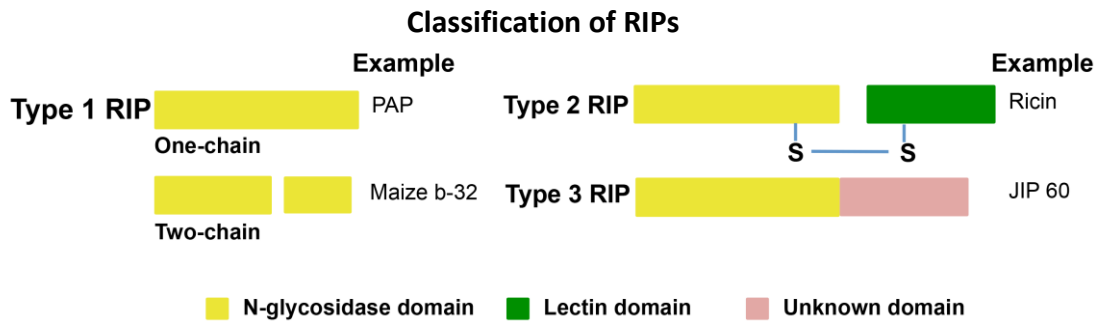
Figure 1.1 Schematic overview of the molecular structure of different types of RIPs. Examples of one-chain and two-chain type 1 RIPs refer to mature, catalytically active PAP and maize RIP b-32, respectively. The schematic structure of type 2 RIPs refers to mature ricin whereas that of type 3 RIPs refers to intact JIP60 (Van Damme et al., 2001).

Type 1 RIPs

Type 1 RIPs are single chain proteins consisting of a catalytically active domain of approximately 30kDa (Barbieri et al., 1993; Nielsen and Boston, 2001; Van Damme et al., 2001). Type 1 RIPs can be divided into three subgroups (Peumans and Van Damme, 2010): (i) the "classical" type 1 RIPs are synthesized on the rough endoplasmic reticulum (ER) and follow the secretory pathway to the vacuole/extracellular space. They were described in several dicotyledonous plant species. For example, saporin is found in the intercellular space and vacuole of the developing as well as mature seeds of soapwort (*Saponaria officinalis*), while it is only located in the extracellular space of young leaves (Carzaniga et al., 1994; Marshall et al., 2011). Another famous example, PAP (pokeweed antiviral protein) is located in the cell wall matrix in pokeweed (*Phytolacca americana*) leaves (Ready et al., 1986). (ii) A few type 1 RIP sequences from Poaceae (e.g. wheat and barley) lack a signal peptide, and hence are synthesized on free ribosomes and are located in the cytoplasm (Nielsen and Boston, 2001; Frigerio and Roberts, 1998; Leah et al., 1991). One example is tritin found in the germs of *Triticum aestivum* (wheat) (Coleman and Roberts, 1981). (iii) The third subgroup is found in *Zea mays* and related Panicoideae species. These type 1 RIPs are synthesized on free ribosomes as inactive precursors. Enzymatic activity of the protein is acquired only after proteolytic processing of the RIP precursor into two smaller polypeptides (e.g. the maize RIP b-32, Walsh et al., 1991).

Type 2 RIPs

Type 2 RIPs consist of an N-terminal domain with enzymatic activity (A chain) fused to a C-terminal carbohydrate binding domain (B chain). Type 2 RIPs are typically

3

described in terms of an AB structure, where the A chain is linked to the B chain through a disulphide bridge (Barbieri et al., 1993; Nielsen and Boston, 2001; Van Damme et al., 2001). Since type 2 RIP sequences contain a signal peptide, they follow the secretory route through the ER-Golgi pathway and finally end up in the vacuole or the intercellular space. The most famous type 2 RIP is ricin. Its biosynthesis and targeting in the plant cell have been studied in great detail: First, the preproricin polypeptide is translocated into the ER, where the signal peptide is cleaved. Second, the inactive single-chain precursor, referred to as proricin is transported via the ER and the Golgi apparatus to the protein storage vacuoles (PSV) of castor bean endosperm cells. There, an N-terminal propeptide and a linker peptide are proteolytically removed. The mature ricin consists of disulphide-linked A and B chains (Butterworth and Lord, 1983, Hiraiwa et al., 1997). The B chain of ricin is a lectin domain which specifically recognizes galactosylated carbohydrate structures and therefore ricin can also be considered as a galactose-binding lectin (Cummings and Etzler, 2009).

Type 3 RIP

Type 3 RIPs consist of an N-terminal RNA N-glycosidase domain fused to an unrelated domain with unknown activity (Chaudhry et al. 1994). At present a 60 kDa jasmonate-induced protein in barley, referred to as JIP60, is the only protein identified as a type 3 RIP. A recent study reported that the C-terminal domain of JIP60 is similar to the eukaryotic translation initiation factor 4E and plays a role in recruiting a subset of cellular messengers for translation when barley leaves are subjected to jasmonate and senescence stress (Rustgi et al. 2014). Microscopic observations allowed to show that JIP 60 is located in the cytoplasm (Feussner et al., 1995).

1.1.4   Occurrence of RIPs

RIPs are widely distributed in the plant kingdom and have been detected in Angiospermae (mono- and dicotyledons) or flowering plants from at least 14 families (Puri et al., 2012, Di Maro et al., 2014). However, RIPs are not ubiquitous in all plants. For example, the putative RIP domain is absent in the complete genome of *Arabidopsis thaliana* (Peumans and Van Damme, 2010). RIPs have been reported frequently in some plant families, particularly in Cucurbitaceae, Euphorbiaceae, Sambucaceae, Phytolaccaceae, Poaceae and Caryophyllaceae (Stirpe, 2014; Girbés et al., 2004). The Poaceae takes a special position in the whole group of RIPs, because this family contains both classical type 1 RIPs, two-chain type 1 RIPs and a type 3 RIP

(Van Damme et al., 2001). Hitherto, more than 50 RIPs have been purified and characterized from different plants. The expression level of RIPs is highly variable in plant tissues, ranging from traces of protein to hundreds of milligrams per 100 g fresh weight plant material (Szalai et al., 2005). RIPs are not associated with (a) particular tissue(s) but are found in virtually all plant parts (e.g. seeds, roots, leaves, bulbs, fruits and bark) (Szalai et al., 2005). Both the distribution over different tissues and the abundance are highly variable depending on the species. Often, different isoforms are found, sometimes even within the same tissue (e.g. pokeweed leaves, Parente et al., 2014; Jiménez et al., 2014). In addition, both type 1 and type 2 RIPs can occur within one plant species even in the same tissue (e.g. iris bulbs, Hao et al., 2001).

At present, besides plants, genuine RIPs have been purified exclusively from bacteria, e.g. shiga toxin (Obrig, 1997) and shiga-like toxin (Reisbig et al., 1981). It appears, however, that (expressed) RIP genes occur also in some fungi, algae and a few insects (Girbés et al., 2004; Stirpe 2004; Reyes et al., 2012; Lacadena et al., 2007).

1.2 Biological activities of RIPs

1.2.1 The enzymatic activity

1.2.1.1 The site-specific RNA N-glycosidase activity

RIPs are officially classified as proteins endowed with "rRNA N-glycosidase activity" (EC.3.2.2.22) (Fig. 1.2). Type 1 RIPs and the A chain of type 2 RIPs as well as the type 3 RIP can recognize a specific adenine residue (A_{4324} on rat liver 28S rRNA) and irreversibly cleave the nucleotide N-C bond between this specific adenine and the ribose (Fig. 1.2) (Endo, 2014; Puri et al., 2012). The depurination happens on the stem-loop of a GAGA sequence, known as the conserved α-sarcin/ricin loop, present in the large rRNA. This α-sarcin/ricin loop is highly conserved from *E.coli* to humans (Fig. 1.3) (Girbés et al., 2004) and plays important role in guanosine triphosphatase (GTPase) activation and hydrolysis in translational GTPase on ribosome (Voorhees et al., 2010). Furthermore, protein synthesis requires several GTPase factors, including the elongation factor 1 (EF1) and elongation factor 2 (EF 2) (Tumer and Li, 2012). The irreversible depurination of the α-sarcin/ricin loop by RIPs renders the ribosomes incapable of binding EF-2 (Montanaro et al., 1975) and interferes with the delivery of the EF1-dependent aminoacyl-tRNA to the ribosome and prohibits EF2-dependent

5

GTPase activities, causing protein synthesis inhibition (Wong et al., 2012; Mansouri et al., 2006).

Different RIPs may also show a diverse ribosome substrate specificity (Fig. 1.3) (Domashevskiy and Goss, 2015; Van Damme et al., 2001). For example, PAP deadenylates ribosomes from plants, yeasts, bacteria, and lower as well as higher animals. In contrast, ricin has a preference for mammalian and yeast ribosomes, and shows no or low activity on plant and *E. coli* ribosomes (Domashevskiy and Goss, 2015).
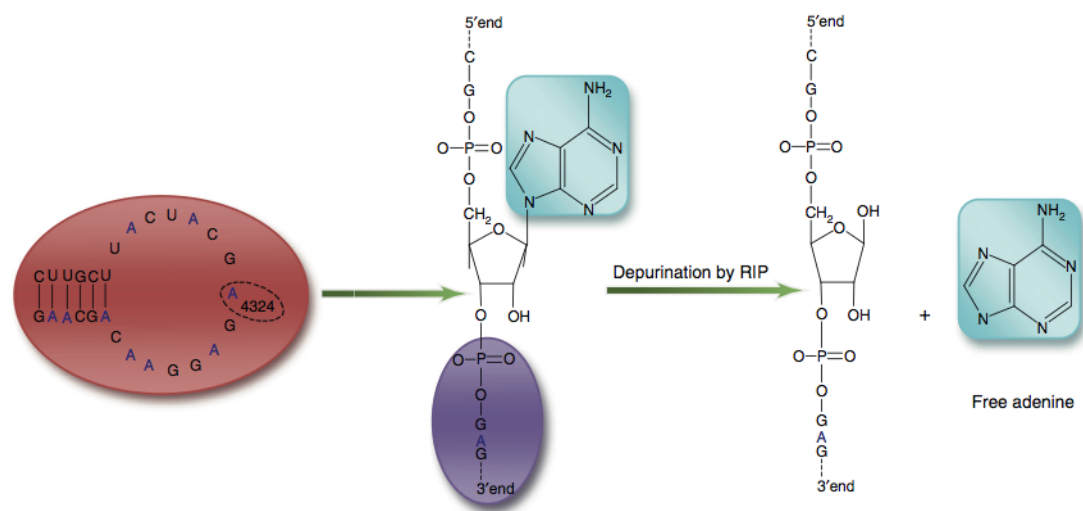
Figure 1.2 Model showing the RNA N-glycosidase activity of the ricin A chain. The specific N-glycosidase activity cleaves adenine (A_{4324}), which is located in the sarcin-ricin loop of the 28S rRNA of the 60S ribosomal subunit (Puri et al., 2012).
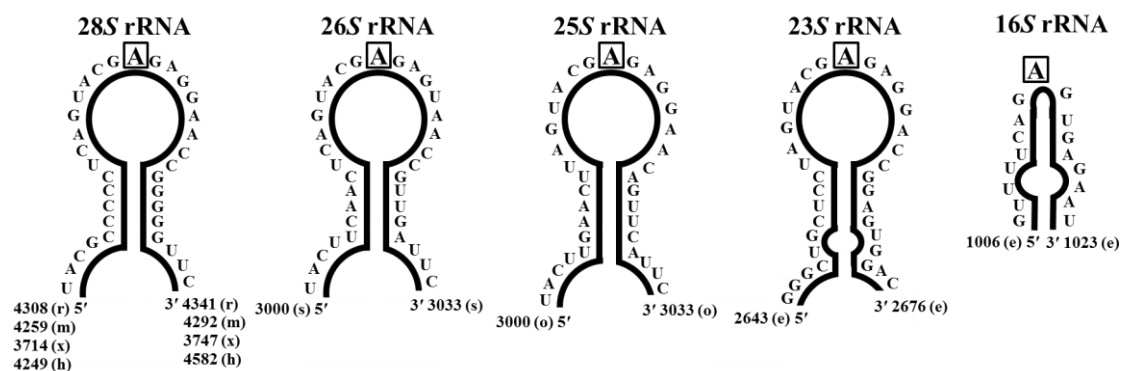
Figure 1.3 Structure of rRNA substrates for *N*-glycosidase activity of RIPs in *E. coli* (e); *Homo sapiens* (h); *Mus musculus* (m); *Oryza sativa* (o); *Rattus rattus* (r); *Saccharomyces cerevisiae* (s); *Xenopus laevis* (x) (Domashevskiy and Goss, 2015).

6

1.2.1.2   The polynucleotide: adenosine glycosidase activity

RIPs do not only depurinate the highly conserved sequence of the α-sarcin/ricin loop within the rRNA, but can also act on naked RNA at multiple sites (Tan et al., 2009; Domashevskiy et al., 2012; Domashevskiy and Goss, 2015). It has been demonstrated that some RIPs can remove multiple adenine residues from various polynucleotides (e.g. tobacco mosaic virus RNA), which is defined as polynucleotide: adenosine glycosidase (PAG) activity (Van Damme et al., 2001; Barbieri et al., 1997, 2000a).

1.2.1.3   DNA lyase activity

Next to the "classical" enzymatic activities including the RNA N-glycosidase activity and the PAG activity (Van Damme et al., 2001), some researchers also reported other unrelated enzymatic activities for RIPs. These "novel" activities include DNA lyase activity (de Benito et al., 1998), ribonuclease activity (Barbieri et al., 1997), phosphatase activities on nucleotides (Chen et al., 1996) as well as lipids (Helmy et al., 1999), chitinase activity (Remi Shih et al., 1997), and superoxide dismutase (SOD) activity (Li et al., 1996; Park et al., 2004b, Day et al., 1998). However, these "novel" activities are controversial since some of these activities are possibly caused by contaminants in the sample preparations (Endo, 2014).

For example, some studies reported that RIPs are able to cleave DNA (remove the base from damaged DNA), and therefore possess DNA lyase activity in addition to the depurination activity. E.g. Supercoiled DNA acts as a substrate and was cleaved into relaxed-circle and linear DNA (de Benito et al., 1998; Wang and Tumer, 1999; Meng et al., 2014). Since the activity was only detected at high RIP concentrations, the DNase activity associated with ricin, saporin and possibly with other type 1 RIPs is considered to be the result of nuclease contamination (Lombardi et al., 2010; de Virgillio et al., 2010; Barbieri et al., 2000b).

1.2.2   Role of RIPs in plant defense

RIPs are widely distributed in the plant kingdom, but certainly do not occur in all plant species. This indicates that RIPs do not play a universal role in the growth, development, or defense of plants. At present, RIPs have been studied primarily for their toxicity and their unique biological activities which can be exploited in medical applications, such as the antitumor and antiviral activities. Some questions remain: why do some plants produce and accumulate RIPs? Are the RIPs also toxic to plant cells?

Several evidences demonstrated that RIPs have evolved as plant defense proteins against pathogens or predators, such as fungi, bacteria (Tan et al., 2009), viruses and insects (Stirpe 2004; Stirpe and Battelli, 2006; Jiang et al., 2008). E.g. the highly toxic ricin is responsible to protect the seeds from invading pests and pathogens (Nielsen and Boston, 2001; Barnes et al., 2009). Although, most type 2 RIPs show a much lower toxicity for animal cells compared to ricin, the accumulation of such less toxic type 2 RIPs can also play an important role in plant defense (Peumans et al., 2001). A clear distinction should be made between different types of RIPs: only type 2 RIPs can interact with cells and get into the cytoplasm by binding to suitable glycan receptors on the cell surface (Sandvig and van Deurs, 2000). Theoretically, type 2 RIPs are toxic to all organisms once they gain entry to the cytoplasm of cells via the receptor-lectin-mediated uptake process. However, their action spectrum is probably restricted to animal cells because bacteria and fungi are protected by an impenetrable cell wall (Van Damme, 2001). It was considered that the inhibition of protein synthesis is the primary role for RIPs in plant defense.

In the general introduction, we focus only on the biotic stresses (aphids, viruses and fungi) that were also studied in this PhD thesis. More extensive information about the effects of biotic and abiotic stresses and RIP expression can be found in some reviews and book chapters (Van Damme et al., 2001; Peumans et al., 2001; Nielsen and Boston, 2001; de Virgilio et al., 2010; Stirpe and Lappi, 2014; Lord and Hartley, 2010; Tejero et al., 2015; Dang and Van Damme, 2015).

1.2.2.1 Pathogens and insects

Plants have developed a wide variety of constitutive and inducible defenses to protect themselves from damage. Most biotic (living) agents provoking plant disease are pathogenic microorganisms such as viruses, fungi and bacteria, and Metazoa such as parasitic nematodes and herbivorous insects (Freeman and Beattie, 2008).

Pathogens

Based on their different life styles, pathogens can be divided into biotrophic and necrotrophic pathogens. Biotrophic pathogens such as *Sphaerotheca pannosa* (a powdery mildew fungus) need living host tissues to obtain nutrients for growth and reproduction, usually through specialized feeding structures. In contrast, necrotrophic pathogens such as *Botrytis cinerea* kill the host tissues at the beginning of the infection by secreting phytotoxins and cell wall degrading enzymes, which allows them to feed on the dead tissues (Mengiste 2012). Hemi-biotrophic

pathogens such as *Pseudomonas syringae* have both biotrophic and necrotrophic stages in their life cycle (Pieterse et al., 2012). In general, viruses need nutrition from living tissues, whereas biotrophic and necrotrophic strategies can be observed in fungi and bacteria (Berger et al., 2007). Salicylic acid (SA) and Jasmonic acid (JA) are considered as major plant defense hormones. SA-dependent responses and signaling pathways are more effective against biotrophic pathogens (Glazebrook, 2005), while, the JA/ethylene pathway plays an important role in defense against necrotrophic pathogens and insect herbivores (Kazan and Manners, 2012) and is often associated with the wound response (Seo et al., 2007).

Insects

Insects can be found in almost all terrestrial and freshwater habitats, and are considered to represent a vast majority of all animal species on earth. Hemiptera, known as true bugs, represent the largest and most heterogeneous order of exopterygots. Many species from the Hemiptera such as aphids are definitely pests of crops and garden plants. Almost every plant is suffering from one or more aphid species, causing crop yield reduction. At the same time, there is a risk for aphids to transmit viruses (Hogenhout et al., 2008). The pea aphid, *Acyrthosiphon pisum*, is a parthenogenetic and non-host-alternating aphid, and as a consequence is an important migratory pest. This aphid can directly insert the stylet into the phloem tissue of host plants and consume the nutritive fluid (Losey and Eubanks, 2000).

1.2.2.2 Antiviral activity of RIPs

The first discovery of antiviral proteins came from the observation that transmission of tobacco mosaic virus (TMV) in plants can be inhibited by crude extracts of pokeweed leaves (Duggar and Armstrong, 1925). Afterwards, the active protein was isolated and identified as pokeweed antiviral protein (PAP), a type 1 RIP from *Phytolacca americana*. Although, there is no doubt about the antiviral activity of RIPs, the mode of action has not been elucidated and the antiviral activity of RIPs does not depend on the ribosomal inactivation. With respect to the RIP activity, three mechanisms are hypothesized (Vandenbussche et al., 2004b; Parente et al., 2014) (Fig. 1.4). (i) The RIPs can directly work on virus nucleic acids by their N-glycosidase activity or PAG activity (de Benito et al., 1997). Subsequently, the viral protein synthesis is inhibited and the production of virus will be decreased. (ii) RIPs directly inactivate host ribosomes to limit pathogen spreading by inhibition of translation (Taylor et al., 1994; Tumer et al., 1997). The lack of plant ribosomes will shut down the virus production. (iii) RIPs act indirectly by triggering activation of the

9

plant defense system. An overview of published data reporting the *in vitro, in vivo* and *in planta* antiviral activities of RIPs is summarized in Table 1.1. An overview of several isoforms and mutations of pokeweed antiviral protein from *Phytolacca americana* is shown in Table 1.2.
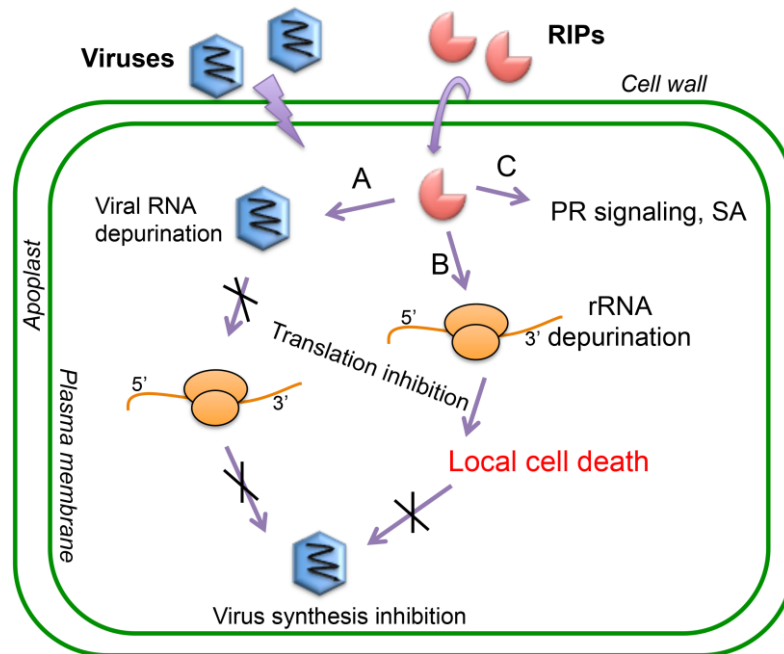
Figure 1.4 Schematic representation of some possible mechanisms for the antiviral activity of RIPs. (A) Direct effect of RIPs on viral RNA. Subsequently, the viral protein synthesis was inhibited and the virus production was decreased. (B) Local suicide model: upon entry of the virus, the plant cell becomes accessible for the (extracellularly located) RIP. After their entry into the cytoplasm the RIPs inactivate the ribosomes and eventually cause cell death. The lack of plant ribosomes will shut down the virus production (C) Defense proteins are up-regulated by RIPs, independent of rRNA depurination (Van Damme et al., 2001; Krivdova et al., 2014)

SNA-I, SNA-I', Nigrin b (SNA-V) and SNLRP, type 2 RIPs from *S. nigra*, showed the potential to protect transgenic tobacco plants against TMV infection (Chen et al., 2002a; Vandenbussche et al., 2004b). Furthermore, SNA-I, Nigrin b (SNA-V) and SNLRP exhibit a potent N-glycosidase activity on tobacco mosaic virus (TMV) RNA by multi depurination of the RNA chain (Vandenbussche et al., 2004b; Tejero et al., 2015). These antiviral activities possibly rely on direct depurination of the viral genomic RNA, since the expression of SNA-V did not induce the production of pathogenesis-related (PR) proteins. Similarly, type 1 and type 2 RIPs from *Iris* showed antiviral activity to TMV and tobacco etch mosaic virus, but the experiment also showed that PR gene expression was not changed (Vandenbussche et al., 2004a; Desmyter et al., 2003).

Table 1.1 Overview of antiviral activity of RIPs.

RIP	Species and tissue	Antiviral activity [a]			Reference
		In vitro	*In vivo*	*In planta*	
Type 1 RIP					
Agrostin	*Agrostemma githago* seeds	n.d.[b]	+	n.d.	Stirpe et al., 1983
Basella rubra RIP	*Basella rubra* seeds	+	+	n.d.	Bolognesi et al., 1997
Bouganin	*Bougainvillea spectabilis*	+	+	n.d.	
Bryodin-R	*Bryonia dioica* roots	-	+	n.d.	Barbieri et al., 1997; Stirpe et al., 1986
Dianthin	*Dianthus caryophyllus* leaves	-	+	+	Barbieri et al., 1997; Stirpe et al., 1981; Hong et al., 1996
Gelonin	*Gelonium multiflorum* seeds	-	+	n.d.	Barbieri et al., 1997; Stevens et al., 1981
Momordin	*Momordica charantia* seeds	-	+	n.d.	
Iris type 1 RIP (IRIP)	*Iris hollandica* bulbs	+	n.d.	+	Desmyter et al., 2003; Vandenbussche, 2004a
Mirabilis antiviral protein (MAP)	*Mirabilis jalapa* root tubers	+	+	n.d.	Bolognesi et al., 2002
Pokeweed antiviral protein (PAP)	*Phytolacca americana* spring leaves	+	+	+	Barbieri et al., 1997; Duggar and Armstrong, 1925; Lodge et al., 1993
PAP-II	*Phytolacca americana* early summer leaves	n.d.	n.d.	+	Wang et al., 1998
PhRIP1	*Phytolacca heterotepala*	+	n.d.	+	Corrado et al., 2008
Phytolacca insularis antiviral protein (PIP)	*Phytolacca insularis*	n.d.	+	+	Moon et al., 1997
Saporin-S	*Saponaria officinalis* seeds	+	+	n.d.	Bolognesi et al., 1997
Saporin-L	*Saponaria officinalis* leaves	+	n.d.	n.d.	
Trichosanthin	*Trichosanthes kirilowii* roots	-	+	+	Bolognesi et al., 1997; Lam et al., 1996
Alpha-momorcharin (α-MMC)	*Momordica charantia* seeds	n.d.	n.d.	+	Zhu et al., 2013
Beetin	*Beta vulgaris* leaves	+	n.d.	n.d.	Iglesias et al., 2005
Type 2 RIP					
Abrin	*Abrus precatorius* seeds	n.d.	+	n.d.	Stevens et al., 1981
EHL	*Eranthis hyemalis* tubers	n.d.	+	n.d.	Kumar et al., 1993
Modeccin	*Modecca digitata* roots	n.d.	+	n.d.	Stevens et al., 1981

Ricin	*Ricinus communis* seeds	-	+/-	+	Barbieri et al., 1997; Stevens et al., 1981; Taylor et al., 1994
Sambucus nigra agglutinin I (SNA-I)	*Sambucus nigra* bark	+	n.d.	+/- Some lines	Vandenbussche et al., 2004b
SNA-I'		n.d.	n.d.	+	Chen et al., 2002a
SNA-V		+	n.d.	+/-	Vandenbussche et al., 2004b
SNLRP		+	n.d.	+/- Some lines	
Iris agglutinin b (IRAb)	*Iris hollandica* bulbs	+	n.d.	+	Vandenbussche, 2004a

[a] *In vitro:* PAG activity assay on viral genomic RNA; *In vivo*: bioassay using virus/RIP solution; *In planta*: bioassay using RIP-expressing transgenic plants
[b] n.d.: not determined

Table 1.2 Isoforms of pokeweed antiviral protein (Domashevskiy and Goss, 2015).

Isoform	Source	Number of amino acid residues	MW (kDa), mature protein	Ref
PAP-I, simple PAP	Spring leaves	262	29	Irvin and Uckun, 1992
PAPx	PAP-I, point mutation in the active site (Glu176Val)-abolishing the RIP activity	262	29	Hudak et al., 2000a
PAP-II	Early summer leaves	285	30	Irvin and Uckun, 1992
PAP-III	Late summer leaves	285	30	Kurinov and Uckun et al., 2003
PAP-S	Seeds	262	29	Barbieri et al., 1982; Honjo et al., 2002
PAP-R	Roots	271	29.8	Bolognesi et al., 1990
PAP-H	Hairy roots	268	29.5	Park et al., 2002b
PAP-Culture	Tissue culture	262	29	Barbieri et al., 1989

Interestingly, alpha-momorcharin (α-MMC), a type 1 RIP isolated from the seeds of *Momordica charantia* shows distinct antiviral activity (Zhu et al., 2013). Quantitative real-time PCR analysis revealed that the SA-responsive defense-related genes [non-expressor of pathogenesis-related genes 1 (*NPR1*), *PR1*, *PR2*] were up-regulated in the α-MMC treated plants after inoculation with virus. Detection of Nitro blue tetrazolium, extinction of H_2O_2 and absorbance changes indicated that the activities of some antioxidant enzymes [superoxide dismutase, catalase, peroxidase] were increased after the α-MMC treatment.

Grafting experiments (both transgenic scions grafted onto wild type rootstocks and the reverse) showed that PAP can enhance resistance to TMV infection (Smirnov et al., 1997). The levels of SA and PR proteins were up-regulated in transgenic grafts expressing PAP, but not in wild type portions. SA, as a plant defense hormone, plays an important role in disease resistance signaling pathways (Vlot et al., 2009) against biotrophic pathogens (Glazebrook, 2005). It can trigger PR proteins resulting in systemic resistance to pathogens. No resistance was observed in transgenic tobacco expressing the inactive site mutant PAPx, suggesting that the enzymatic activity is required for antiviral activity. Besides depurination of TMV RNA, PAP also programs systemic protection in tobacco by triggering other defense signaling pathways. PAP expression resulted in basic as well as acidic isoforms of PR proteins and also induced the wound-inducible protein kinase (WIPK, a marker of SA-independent signal pathogen response), and the proteinase inhibitor PI-II, (a typical maker of wound response) (Van Damme et al., 2001).

1.2.2.3 Antifungal activity of RIPs

Many fungal ribosomes are highly susceptible to RIPs compared to plant ribosomes (Park et al., 2002a; Girbés et al., 2004). There have been many studies describing the antifungal activity of RIPs (particularly for type 1 RIPs), although RIPs are less potent than other antifungal proteins (Ng, 2004; Nielsen and Boston, 2001). For instance, some antifungal proteins such as chitinases and β-1,3-glucanases can easily hydrolyze the fungal cell wall consisting of chitin or β-1,3-glucans, but this is not possible for RIPs. An overview of published data reporting the *in vitro* and *in planta* antifungal activities of RIPs is summarized in Table 1.3.

Table 1.3 Overview of antifungal activity of RIPs.

RIPs	Species	Fungal species	*in vitro/in planta*	IC50	Reference
Type 1 RIP					
Hispin	Hairy melon seeds	*Coprinus comatus* *Fusarium oxysporum* *Physalospora piricola* *Mycosphaerella arachidicola* **NOT:** *Botrytis cinerea*	*In vitro* (plate assay)		Ng and Parkash, 2002
Luffacylin	*Luffa cylindrica* seeds	*Mycosphaerella arachidicola* *Fusarium oxysporum*	*In vitro* (plate assay)		Parkash et al., 2002
Panaxagin	*Panax ginseng* (Chinese ginseng root)	*Coprinus comatus* *Fusarium oxysporum* **NOT:** *Rhizoctonia solani*	*In vitro* (plate assay)		Ng and Wang, 2001
Hypsin	*Hypsizigus marmoreus* (mushroom)	*Mycosphaerella arachidicola* *Physalospora piricola* *Fusarium oxysporum* *Botrytis cinerea*	*In vitro* (plate assay)	2.7 μM 2.5 μM 14.2 μM 0.06 μM	Lam and Ng, 2001a
Lyophyllin	*Lyophyllum shimeji* (mushroom)	*Physalospora piricola* *Coprinus comatus*	*In vitro* (plate assay)	2.5 μM	Lam and Ng, 2001b
Alpha-momorcharin (α-MMC)	*Momordica charantia* (bitter melon)	*Sclerotinia sclerotiorum* *Fusarium graminearum* *Bipolaris maydis, Aspergillus niger, Aspergillus oryzae*	*In vitro* (plate assay)		Zhu et al., 2013
		Magnaporthe grisea	Transgenic rice		Qian et al., 2014
Mirabilis expansa protein (ME)	*Mirabilis expansa*	*Rhizoctonia solani* *Alternaria alternata* **NOT:** *Trichoderma reesei* *Candida albicans*	*In vitro* (fungal ribosomes and plate assay)		Park et al., 2002a
RTA (ricin toxin A chain)	*Ricinus communis*	*Rhizoctonia solani* *Alternaria alternata* *Trichoderma reesei* **NOT:** *Candida albicans*	*In vitro* (fungal ribosomes)		Park et al., 2002a

Sporin S-6	*Saponaria officinalis*	*Rhizoctonia solani* *Alternaria alternata* *Trichoderma reesei* *Candida albicans*	*In vitro* (fungal ribosomes)		Park et al., 2002a
C. moschata RIP	*Cucurbita moschata* (pumpkin)	*Phytopthora infestans*	*In vitro* (microtiter plate assay)		Barbieri et al., 2006
b-32	*Zea mays* (maize)	*Rhizoctonia solani, Aspergillus flavus, Aspergillus nidulans*	*In vitro* (microtiter plate assay)		Nielsen et al., 2001 Lanzanova et al., 2009 Lanzanova et al., 2011
		Fusarium culmorum *Fusarium verticillioides*	Transgenic wheat Transgenic maize		
PAP, PAPII	*Phytolacca americana* (pokeweed)	*Rhizoctonia solani*	Transgenic tobacco		Zoubenko et al., 1997 Wang et al., 1998
PAP-H	*Phytolacca americana* (pokeweed)	*Trichoderma reesei* *Rhizoctonia solani*	Pokeweed hair root *In vitro: no activity*		Park et al., 2002b
PhPAP I	*Phytolacca heterotepala* (Mexico pokeweed)	*Alternaria alternata* *Botrytis cinerea*	Transgenic tobacco		Corrado et al., 2005
Curcin 2	*Jatropha curcas*	*Rhizoctonia solani*	Transgenic tobacco		Huang et al., 2008
Trichosanthin	*Trichosanthes kirilowii*	*Pyricularia oryzae*	Transgenic rice		Yuan et al., 2002
		Erysiphe graminis	Transgenic wheat		Bieri et al., 2000
Barley type 1 RIP	*Hordeum vulgare* (barley)	*Blumeria graminis f. sp. tritici* (powdery mildew)	Transgenic wheat plants (detached leaf)		Bieri et al., 2003
		Alternaria brassicae	Transgenic Indian mustard		Chhikara, et al., 2012
		Rhizoctonia solani	Transgenic tobacco		Longemann et al., 1992
Dianthin, type 1 RIP	*Dianthus caryophyllus*	*Rhizoctonia solani*	Transgenic rice		Shah and Veluthambi, 2010
Type 2 RIP					
Lyophyllum antifungal protein (LAP)	*Lyophyllum shimeji* (mushroom)	*Physalospora piricola* **NOT:** *Rhizoctonia solani, Colletotrichum gossypii, Coprinus comatus.*	*In vitro* (plate assay)	70 nM	Lam and Ng, 2001b

15

(Transgenic) plant models

Most studies reporting the *in vivo* antifungal activity of RIPs were performed using transgenic tobacco plants and infection assays with fungal pathogens (Table 1.3). The wound inducible expression of PhPAP I, a type 1 RIP from *Phytolacca heterotepala* in transgenic tobacco plants demonstrated enhanced resistance against the fungal pathogens *Alternaria alternata* and *Botrytis cinerea* (Corrado et al., 2005). Expression of the type 1 RIP from barley in transgenic tobacco under the control of wound-inducible promoter revealed a potent antifungal activity against *Rhizoctonia solani* infection (Logemann et al., 1992). Transgenic rice plants expressing trichosanthin, a type 1 RIP from *Trichosanthes kirilowii*, enhanced the resistance to the major rice pathogen *Pyricularia oryzae* (Yuan et al., 2002). The type 1 RIP from maize endosperm, b-32, shows *in vitro* antifungal activities inhibiting the growth of *Rhizoctonia solani* (Lanzanova et al., 2011), *Aspergillus nidulans* and *Aspergillus flavus* (Nielsen et al., 2001). Transgenic wheat expressing the unprocessed b-32 displayed reduction of head blight symptoms caused by *Fusarium culmorum*- one major wheat fungal pathogen (Lanzanova et al., 2011). Maize b-32 RIP also increased the resistance to *Fusarium verticillioides* in an *in vitro* leaf disk assay (Lanzanova et al., 2009). These results suggest that b-32 protects fungal invasion.

***In vitro* models**

Next to the transgenic plant models, the antifungal properties of RIPs were also demonstrated in many studies using *in vitro* models. *In vitro* biological assays are useful, but the results are dependent on the purity of the RIPs. Sometimes, the co-purifying compounds from plant extracts might also show antifungal activities (Leah et al., 1991), indicating the necessity of highly purified recombinant proteins for *in vitro* assays. The *in vitro* antifungal activity has been described for several type 1 RIPs: luffacylin *from Luffa cylindrical* seeds (Parkash et al., 2001), panaxagin from the roots of Chinese ginseng (*Panax ginseng*) (Ng and Wang, 2001), hispin from hairy melon seeds (Ng and Parkash, 2002) and Hypsin from mushroom fruits (*Hypsizigus marmoreus*) (Lam and Ng, 2001a). Next to antiviral activity (Zhu et al., 2013), alpha-momorcharin (α-MMC), a type 1 RIP isolated from the seeds of *Momordica charantia* also possesses antifungal activity (Qian et al., 2014). It was observed that 50–67% of phytopathogenic fungal growth and spore germination were inhibited by the α-MMC tested at 500 µg/mL (Zhu et al., 2013). RTA (ricin toxin A chain), saporin S-6 and ME (a type 1 RIP from *Mirabilis expansa*) showed enzymatic activity to the ribosomes from *Rhizoctonia solani* and *Alternaria alternata* in *in vitro* depurination

assays (Park et al., 2002a). Moreover, ME failed to depurinate *Trichoderma reesei* ribosomes, while both RTA and saporin S-6 possess this activity. Interestingly, neither RTA nor saporin S-6 showed antifungal activity in a plate diffusion assays. In contrast, ME effectively inhibited the growth of *Rhizoctonia solani*, but not of *Trichoderma reesei.* It was also reported that entry of ME in the fungal cells is more important than its depurination activity. Microscopic analysis revealed that ME could get into fungal hyphae, but this was not shown for saporin S-6.

Mode of action

(i) Direct inhibition of fungal ribosomes via RIP activities

Antifungal activities of RIPs are enhanced together with defense proteins such as chitinases, β-1,3-glucanases or thaumatins. These PR proteins could facilitate the entry of RIPs into fungi by lysing the fungal cell walls (Zhu et al., 2013). Once the natural fungal defense-cell wall is destroyed, RIPs can depurinate fungal ribosomes to cause fungal death.

PAP-H in combination with chitinase, β-1,3-glucanase, and protease inhibited the growth of soil-borne fungi (*Trichoderma reesei* and *Rhizoctonia solani*), while only purified PAP-H did not show *in vitro* antifungal activity (Park et al., 2002b). The depurination of fungal ribosomes by PAP-H *in vitro* and *in vivo* suggests that PAP-H is able to penetrate fungal cells with the help of other PR proteins.

Transgenic wheat plants expressing an apoplastic type 1 RIP from barley seeds exhibited increased resistance to *Blumeria graminis* f.sp. tritici (powdery mildew) in a detached leaf infection assay (Bieri et al., 2003). Transgenic *Brassica juncea* expressing the combination of a barley type 1 RIP and a class II chitinase showed resistance to *Alternaria brassicae* with up to 44% of reduction of hyphal growth in *in vitro* antifungal assays (Chhikara et al., 2012).

(ii) Up-regulated endogenous host defenses against fungi

It was reported that antifungal effect of PAP against *Rhizoctonia solani* was distinctly associated with SA-independent induction of PR genes in transgenic tobacco, instead of depurination activity of PAP (Zoubenko et al., 1997). The inhibitory effects of PAP-II on *Rhizoctonia solani* infection were concentration dependent. Similar to previous studies, the SA-independent induction of PR genes was detected (Wang et al., 1998).

1.2.2.4 Insecticidal activity of RIPs

Plants have evolved a variety of defense mechanisms to protect themselves from insect herbivores such as physical barriers (trichomes, thorns and cuticles), secondary metabolites (glucosinolates, benzoxazinoids, alkaloids and phenolics), defensive proteins and toxic compounds (Howe and Jander, 2008). Ricin and saporin were the first RIPs which were shown to be toxic to insect larvae (Gatehouse et al., 1990). It was suggested that type 1 and type 2 RIPs are possibly involved in defense against insect herbivores, as well as herbivorous animals such as rabbits. Subsequently, RIPs (in particular type 2 RIPs) received a lot of attention for their potential insecticidal activities (Walski et al., 2014). An overview of the entomotoxic activity of RIPs is given in table 1.4.

Insecticidal activity of type 2 RIPs

Feeding assays with ricin and cinnamomin (isolated from seeds of *Cinnamomum camphora* tree) first described the insecticidal activity of type 2 RIPs. Ricin demonstrated strong toxicity to several insects including cow pea weevil (*Callosobruchus macultatus*), cotton boll weevil (*Anthonomus grandis*), housefly (*Musca domestica*), and larvae of the silkworm *Bombyx mori* (Wei et al., 2004; Gatehouse et al., 1990). Cinnamomin exhibited toxicity towards insect larvae. Cinnamomin (LD50 is 16599 mg/kg) was less toxic than ricin (LD50 is 489 mg/kg) in the feeding of the silkworm (*Bombyx mori*) (Table 1.4). The LC50 to bollworm (*Helicoverpa armigera*) larvae fed on diet containing cinnamomin was 1839 mg/kg and the LC50 to mosquito (*Culex pipines pallens*) larvae was 168 mg/kg (Zhou et al., 2000). For comparison, the LC50 for inhibition of protein synthesis by cinnamomin was approx. 14 nM when tested in an *in vitro* translation system of bollworm larvae (Zhou et al., 2000).

Since numerous lectins are also toxic to insects (Carlini and Grossi-de-Sá, 2002), it is possible that the insecticidal activity of type 2 RIPs should not be attributed to their enzymatic activity but rather could be related to their carbohydrate binding properties (Lannoo and Van Damme 2014). SNA-I isolated from the bark of elderberry exhibits specific binding to Neu5Acα(2,6)GalNAc/Gal. Shahidi-Noghabi et al. (2009) reported that the transgenic tobacco plants overexpressing SNA-I or its isoform SNA-I' enhanced the plants resistance to different insect species such as aphids and caterpillars. Mutation of the SNA-I B chain in one carbohydrate binding site reduced the insecticidal activity, while mutation of both carbohydrate binding sites completely abolished the toxic effect. Therefore, the insecticidal properties of

Table 1.4 Overview of published data on the entomotoxic activity of RIPs - updated from Vargas and Carlini, 2014.

RIP	Dose-effect	Insect species	Order	Administration	Reference
Type 1 RIP					
Saporin, from *Saponaria officinalis* seeds	LD_{50} 3X 10^{-3}% (dry wt)	*Callosobruchus maculatus*	Coleoptera	Artificial diet	Gatehouse et al., 1990
	LD_{50} 5X 10^{-2}% (dry wt)	*Abies grandis*	Coleoptera		
	No effect	*Spodoptera littoralis*	Lepidoptera		
	No effect	*Heliothis virescens*	Lepidoptera		
Saporin and momordin (from *Momordica charantia* seeds)	20 and 40 µg (reduced weight)	*Anticarsia gemmatalis*	Lepidoptera	*Phaseolus vulgaris* foliar disks containing air-dried RIPs	Bertholdo-Vargas et al., 2009
	40 µg (induced DNA damage)	*Spodoptera frugiperda*	Lepidoptera		
PAP-S Lychnin (from *Lychnis chalcedonica* seeds) Gelonin (from *Gelonium multiflorum* seeds)	20 and 40 µg (reduced weight); 40 µg (induced DNA damage and diminished lipid oxidative damages)	*Anticarsia gemmatalis*	Lepidoptera	*Phaseolus vulgaris* foliar disks containing air-dried RIPs	Bertholdo-Vargas et al., 2009
	20 and 40 µg (reduced weight); 40 µg (induced DNA damage and induced activity)	*Spodoptera frugiperda*	Lepidoptera		
Restrictocin (produced by *Aspergillus restrictus*)	1000 mg/kg kill 38.5%	*Carpophillus freeman*	Coleoptera	Artificial diet	Brandhorst et al., 1996
	1000 mg/kg kill 62.5%	*Spodoptera frugiperda*	Lepidoptera		
	No effect	*Helicoverpa zea*	Lepidoptera		
Unprocessed b-32 Papain-activated	10% mortality (pro-RIP)	*Helicoverpa zea*	Lepidoptera	Dried diet 1mg/g of diet	Dowd et al., 1998
	70% mortality (activated RIP)	*Trichoplusia ni*	Lepidoptera		
	39% mortality (activated RIP)	*Spodoptera frugiperda*	Lepidoptera		
	No effect	*Ostrinia nubalis*	Lepidoptera		
	No effect	*Plodia interpunctella*	Lepidoptera		
	No effect	*Carpophillus freeman*	Coleoptera		
Maize active b-32	20% mortality at day 1 (WT 4.3%)	*Helicoverpa zea*	Lepidoptera	Transgenic tobacco	Dowd et al., 2003 Dow et al., 2012
	28% mortality at day 4 (WT 18.8%)	*Lasioderma serricorne*	Coleoptera	Transgenic maize	
Maize RIP2 - Isoform from b-32	26% (reduced weight)	*Spodoptera frugiperda*	Lepidoptera	Dried diet 0. 8ng /mg of diet	Chuang et al., 2014
IRIP, from bulbs of *Iris hollandica*	22% mortality at 15 days, 78% mortality at 23 days	*Myzus nicotianae*	Hemiptera	Transgenic tobacco	Shahidi-Noghabi et al., 2006
	No reduction at 7-8 days	*Spodoptera exigua*	Lepidoptera		

Type 2 RIP					
Ricin, from seeds of (*Ricinius communis*)	LD$_{50}$ 5X 10^{-4}% (dry wt)	*Callosobruchus maculatus*	Coleoptera	Artificial diet	Gatehouse et al., 1990
	LD$_{50}$ 5X 10^{-3}% (dry wt)	*Abies grandis*	Coleoptera		
	No effect	*Spodoptera littoralis*	Lepidoptera		
	No effect	*Heliothis virescens*	Lepidoptera		
	LD$_{50}$ 489 mg/kg	*Bombyx mori*	Lepidoptera	Air-dried onto mulberry leaves	Wei et al., 2004
Sambucus nigra agglutinin I (SNA-I), from bark of *Sambucus nigra*	LD$_{50}$ 374 µg/ml	*Acrythosiphon pisum*	Hemiptera	Artificial diet	Shahidi-Noghabi et al., 2008
	Delayed development and reduced adult survival and fertility	*Myzus nicotianae*	Hemiptera	Transgenic tobacco	
	12% reduction of larval biomass at 3 days (DNA damage)	*Spodoptera exigua*	Lepidoptera	Artificial diet- larvae 5mg/g SNA-I	Shahidi-Noghabi et al., 2010a
	LD$_{50}$ 0.5 µg/ml	*Tribolium castaneum*	Coleoptera	*In vitro* assay with cells	Walski et al., 2014
	20% mortality feeding diet containing 2% SNA-I			Artificial diet- larvae	
SNA-I mutation at (Asp231ΔGlu) in B chain	Reduced the insecticidal activity of SNA-I	*Myzus nicotianae*	Hemiptera	Transgenic tobacco	Shahidi-Noghabi et al., 2008
SNA-I mutation at two position (Asn48ΔGlu and Asp231ΔGlu) in B chain	Completely abolished the SNA-I effect on tobacco aphids	*Myzus nicotianae*	Hemiptera	Transgenic tobacco	
SNA-I'- isoform SNA-I, from bark of *Sambucus nigra*	Reduction in adult aphid survival	*Myzus nicotianae*	Hemiptera	Transgenic tobacco	Shahidi-Noghabi et al., 2009
	Reduction in survival and weight of larvae and pupae	*Spodoptera exigua*	Lepidoptera	Transgenic tobacco	
Cinnamomin, from seeds of (*Cinnamomum camphora*)	LD$_{50}$ 1839 mg/kg	*Helicoverpa armigera*	Lepidoptera	Artificial diet	Zhou et al., 2000
	LD$_{50}$ 168 mg/kg	*Culex pipiens pallens*	Diptera		
	LD$_{50}$ 16,599.4 mg/kg	*Bombyx mori*	Lepidoptera	Oral feeding	Wei et al., 2004
IRA, from bulbs (*Iris hollandica*)	33% mortality at 15 days, 100% mortality at 23 days	*Myzus nicotianae*	Hemiptera	Transgenic tobacco	Shahidi-Noghabi et al., 2006
	Reduced 31%-33% at 7-8 days	*Spodoptera exigua*	Lepidoptera		

20

SNA-I can be linked to its carbohydrate binding activity (Shahidi-Noghabi et al., 2008).

So far, few studies investigated the mechanism of RIP toxicity to insects. SNA-I showed toxicity to *T. castaneum* cells as well as larvae (Walski et al., 2014) and caused cell apoptosis in the gut tissues of *Acyrthosiphon pisum* and *Spodoptera exigua* (Shahidi-Noghabi et al., 2010a). SNA-I also induced caspase-3 like activity in the midgut cell line of Lepidoptera (CF-203) (Shahidi-Noghabi et al., 2010b). In 2011, the same group also detected the internalization of the fluorescein isothiocyanate-labeled SNA-I into midgut cells CF-203 using confocal microscopy. It was also demonstrated that pre-exposure of insect midgut cells with specific inhibitors of clathrin- and caveolae-mediated endocytosis inhibited uptake as well as caspase-mediated cytotoxicity induced by SNA-I. The uptake mechanism(s) for both lectins required phosphoinositide 3-kinases, but did not depend on the actin cytoskeleton (Shahidi-Noghabi et al., 2011).

Insecticidal activity of type 1 RIPs

Due to the lack of carbohydrate binding domain in type 1 RIPs the question arises how type 1 RIPs exert their toxicity to insects? These RIPs could bind to specific sites/ receptors on the cell surfaces, and provoke toxicity to the cells once the RIPs enter in the cytosol.

Feeding on a diet containing micrograms amounts of the type 1 RIPs saporin, PAP-S, lychnin, gelonin and momordin affected the survival and developmental rate of *Anticarsia gemmatalis* and *Spodoptera frugiperda* (Bertholdo-Vargas et al., 2009). These type 1 RIPs also induce DNA damage (Bertholdo-Vargas et al., 2009).

Dowd and co-workers reported that transgenic tobacco lines (*Nicotiana tabacum*) expressing the active maize (*Zea mays*) RIP-b-32 exhibit resistance to larvae of corn earworm (*Helicoverpa zea*) (Dowd et al., 2003) resulting in increased mortality and reduced weights. It was also found that maize leaves expressing the endogenous maize RIP b-32 enhanced resistance to various insect pests (Dowd et al., 2012).

1.2.2.5 Indirect evidence for the involvement of RIPs in plant defense

Some plant RIP genes are regulated by biotic stresses, such as viral infections (Iglesias *et al.*, 2005), insect herbivory (Zhou *et al.*, 2000; Bertholdo-Vargas *et al.*, 2009) and fungal infections (Xu *et al.*, 2007), and by abiotic stresses such as heat and osmotic stress (Stirpe *et al.*, 1996), senescence (Stirpe *et al.*, 1996), salinity (Rippmann *et al.*, 1997), drought (Bass *et al.*, 2004), mechanical injury (Song et al., 2000; Tartarini et al., 2010) and oxidative stress (Iglesias *et al.*, 2005, 2008). It was reported that RIP expression patterns can also be modulated by plant hormones such as JA (Reinbothe *et al.*, 1994a,b; Xu *et al.*, 2007), abscisic

acid (ABA) (Xu *et al.*, 2007; Müller et al., 1997), gibberellic acid (Ishizaki *et al.*, 2002) and ethylene (Park *et al.*, 2002b). For example, JIP60 is produced in both methyl JA (MeJA) treated and senescent barley leaves and plays a role in the reprogramming of the translational machinery (depurination of 28S rRNA or dissociation of ribosome) in response to stress (Rustgi et al., 2014). Maize b-32 is induced by methyl jasmonate (Chaudhry et al., 1994; Müller et al., 1997). Transcript levels of PIP2 from *Phytolacca insularis* are up-regulated by both MeJA and ABA treatments (Song et al., 2000). The accumulation of toxic unprocessed maize protein RIP2 (73% sequence similarity to unprocessed b-32) is triggered by caterpillar attack and wounding in combination with MeSA, MeJA, ethephon as well as ABA treatment (Chuang et al., 2014). PAP-II expression is environmentally regulated. Enhanced activity of PAP-II was reported in senescent and stressed leaves (Park et al., 2002b; Domashevskiy and Goss, 2015). Curcin 2, a type 1 RIP from *Jatropha curcas* was induced in leaves after fungal infections with *Pestsalotia funereal*, *Curvularia ljunata* (walk) Boed and *Gibberella zeae* (Schw) Petch, but not by *Rhizoctonia solani* (Qin et al., 2005). In rice (*Oryza sativa*), 31 genes encoding type 1 RIPs are expressed in various tissues and associated with abiotic stress such as cold, salinity and drought, as well as biotic stresses, such as fungal (*Magnaporthe grisea*) and bacterial (*Xanthomonas oryzae* pv *oryzae*) infections (Jiang et al., 2008). Overexpression of one of these RIPs resulted in plants with enhanced resistance to drought and salinity (Jiang et al., 2012).

1.2.3 Animal studies

The toxic effects of different type 2 RIPs on laboratory animals have been tested by Barbieri and his colleagues (1993). They reported that the RIPs end up in the gut of the animals, when the animal ingests plants containing RIPs. Due to the toxicity of the RIPs, the endothelial cells will be damaged and lesions are formed in the gut wall. Eventually, ricin can reach the blood system, causing death through damage to major tissues. Rabbit treated with a high dose of ricin (100 μg) showed blood vessel congestion in most examined organs (e.g. eye, liver and kidneys) (Gareth 2014). The lethal doses (LD50s) (μg/kg) for several type 2 RIPs tested in mice have been reported: 2.6 (ricin), 0.56 (abrin), 2.3 (modeccin), 1.4 (volkensin) and 2.4 (viscumin) (Griffiths 2014). The toxicity of the same RIP for different animals may vary. The LD50 of volkensin to rat is 50-60 ng/kg, which is ~20-fold lower than in mice. Administering large parenteral doses of RIP per kg of body weight of either nigrins or ebulins to mice triggered toxicity when administered in the range of 2–12 mg (Tejero et al. 2015). Histological analysis showed that the intestine was highly damaged after injection of nigrin b and ebulin f. The CC531-lacZ colorectal cancer rat metastasis model was used to determine the *in vivo* antineoplastic efficacy of the purified riproximin (type 2 RIP from *Ximenia americana*) (Voss et al., 2006; Bayer et al., 2012). It was suggested that riproximin has

significant anticancer activity at total dosages of 100 (perorally) and 10 (intraperitoneally) pmol riproximin/kg. It is worth to mention that if type 2 RIPs are inhaled and enter the lungs or enter the blood stream through damaged skin or by injection, RIPs are extremely toxic. For instance, ricin is around 1000-fold more toxic after inhalation compared to uptake by the oral route, because in the latter case part of ricin will be degraded in the intestinal tract (Alexander et al., 2008).

1.2.4 Effects of RIPs on mammalian cells

1.2.4.1 Cytotoxicity of RIPs on mammalian cells

Hitherto, both type 1 and type 2 RIPs from many plants have been well studied for their cytotoxicity towards mammalian cells (Puri et al., 2012). Already in the early days of RIP research, it was reported that type 2 RIPs are more toxic to cancer cells than to normal cells (Lin et al., 1970; Stirpe, 2014). As a consequence RIPs attracted a lot of attention as potential antitumor therapeutic medicines. Some highly toxic type 2 RIPs (such as ricin, abrin and volkensin) show potent cytotoxicity towards mammalian cells. Although some type 2 RIPs have strong protein synthesis inhibition activity *in vitro*, they are 10^3-10^5 less toxic than ricin in animal cells (Ferreras et al., 2011), such as e.g. the type 2 RIPs from *Sambucus* species (Table 1.5). Although not all the mechanisms of cytotoxicity induced by RIPs are entirely understood, at least, the well-studied RIPs can provide some ideas about the physiological activities of RIPs on mammalian cells.

Table 1.5 Cytotoxicity of interesting type 2 RIPs

RIPs	Tissue	Sugar Specificity	Rabbit Lysate IC50 (nM)	HeLa Cells IC50 (nM)
Ricin	Seeds (*Ricinius communis*)	Gal/GalNAc	0.1	0.67×10^{-3}
Abrin	Seeds (*Abrus precatorius*)	Gal	0.5	3.7×10^{-3}
Volkensin	Roots (*Adenia volkensii*)	Gal	0.37	0.3×10^{-3}
Ebulin f	Fruits (*Sambucus ebulus*)	Gal	0,03	17
Ebulin l	Leaves (*Sambucus ebulus*)	Gal	0.15	64.3
Nigrin b	Bark (*Sambucus nigra*)	Gal/GalNAc	0.1	27.6
Nigrin f	Fruits (*Sambucus nigra*)	Gal	0.03	2.9
Sieboldin	Bark (*Sambucus sieboldiana*)	Neu5Ac-Gal/GalNAc	0.9	11.8

IC50: concentration required to inhibit translation for 50%; unless indicated translation was assayed with reduced RIPs in rabbit reticulocyte lysates. Gal: D-galactose; GalNAc: N-acetylgalactosamine; Neu5Ac: N-acetyl-neuraminic acid (sialic acid) (Tejero et al., 2015; Ferreras et al., 2011).

1.2.4.2 Interaction of RIPs with cells: endocytosis and intracellular trafficking

At present only a few RIPs have been investigated for their binding, uptake, intracellular trafficking and processing in cells. These studies of the intracellular pathway of RIPs provided very important evidence to explain the different mechanisms of toxicity for different RIPs.

The intracellular pathway of type 2 RIPs

The less toxic RIP nigrin b and the highly toxic RIP ricin are two good examples that provide some general ideas about the intracellular journey of type 2 RIPs in a cell (Fig. 1.5). Furthermore, the internalization and uptake of these RIPs provide a possible explanation for the lower toxicity of nigrin b compared to ricin in HeLa cells. Initially, nigrin b and ricin follow a similar pathway to reach the endosomes (Jiménez et al., 2014). The lectin chains of ricin or nigrin b recognize and bind to glycoproteins and glycolipids that are present on the surface of cells. These glycoproteins and glycolipids can be different for ricin and nigrin b (Ferreras et al., 2011). Subsequently, ricin and nigrin b are internalized into the cell and reach the endosomes. From this point onwards, a small number of ricin molecules follows the trans-Golgi network (TGN) to the ER, where the disulphide bridge between A and B chain is reduced (Battelli et al., 2004). Afterwards, the RIP domain will be transported to the cytosol and will reach the ribosomes via the endoplasmic reticulum-associated degradation (ERAD) pathway (Lord et al., 2005; Spooner et al., 2008). Due to the low lysine residue content, the RIP domain can escape from the proteolytic degradation after translocation from ER to cytosol during this ERAD pathway (Deeks et al., 2002). In the cytosol, the RIP domain blocks the ribosomes causing protein synthesis inhibition and cell death. This pathway is sensitive to brefeldin A and low temperature (Mayerhofer et al., 2009). A comparison between ricin and nigrin b shows that 79% of ricin and 94% of nigrin b molecules are degraded in the lysosomal compartment and the resulting products are expelled from the cell (Battelli, et al., 1997a; Spooner and Lord, 2012; Sandvig and van Deurs, 2005). The translocation of nigrin b to the cytosol is concentration dependent. When the extracellular concentration of nigrin b is high, the endosomes saturated with nigrin b will release the nigrin b into the cytosol and subsequently cause ribosome inactivation without passing of the RIP via the TGN-ER pathway (Citores et al., 2003; Battelli et al., 1997a and 2004a). In contrast to ricin, the pathway of nigrin b is insensitive to low temperature and brefeldin A treatment.
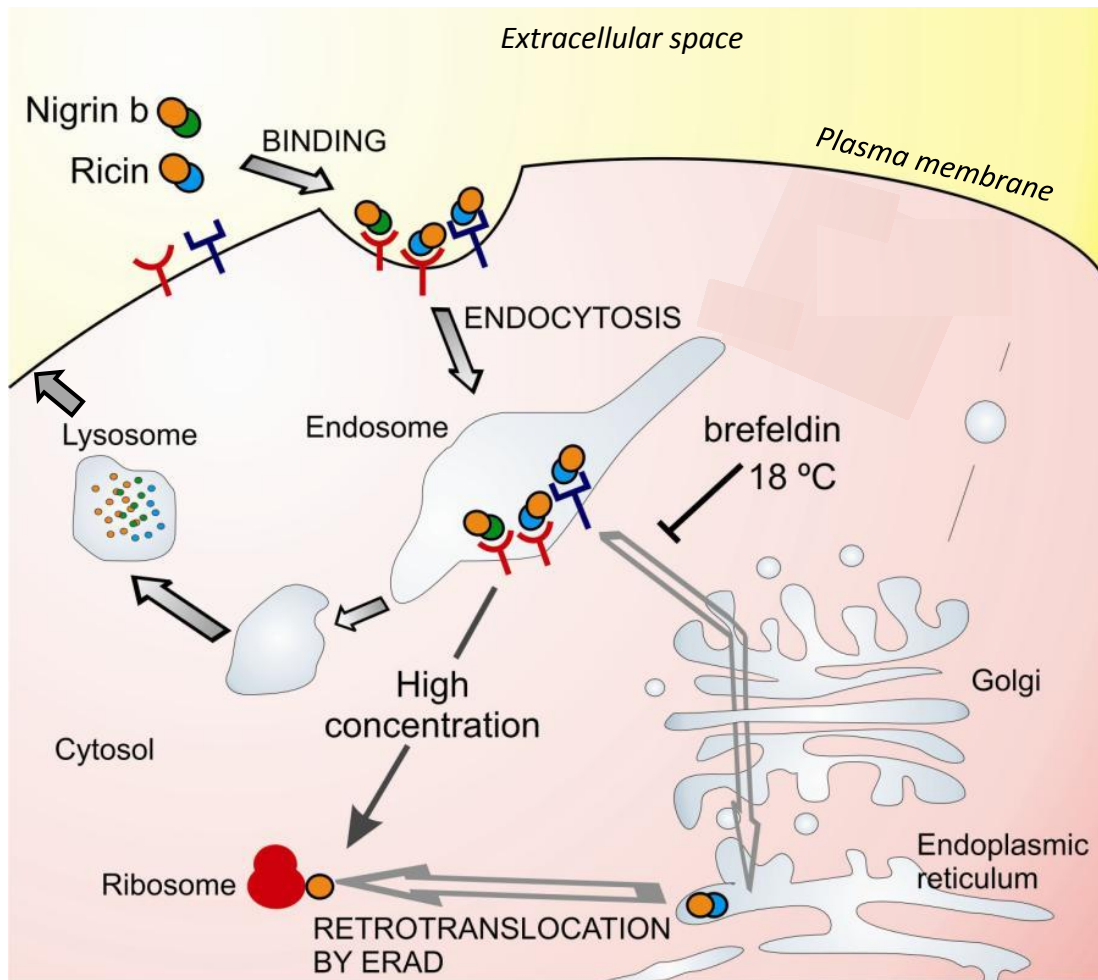
Figure 1.5 Intracellular trafficking of ricin and nigrin b (Ferreras et al., 2011; Jiménez et al., 2014).

Nigrin b and the highly toxic type 2 RIP volkensin (isolated from seeds of *Adenia volkensii*) bind to HeLa cells with the same affinity (approx. 10^{-10}M) and have a similar number of binding sites (2 X 10^{-5}/cell), two-log lower than for ricin (Battelli et al., 2004). Nigrin b accumulates between cytoplasmic dots and the Golgi compartment, which is in contrast to volkensin and ricin stacking in the perinuclear region (Battelli et al., 2004). For the toxicity, the amount of RIP that is degraded and excreted is important. E.g. one reason why nigrin b is less toxic to cells than ricin is that nigrin b is more rapidly degraded and excreted during the endosomal pathway (Ferreras et al., 2011). Nigrin b is completely inactive after excretion to the extracellular space, while this is not the case for volkensin and ricin (Battelli et al., 2004). The receptors on the cell surface are also important, and probably decide about the intracellular pathway for the different type 2 RIPs (Ferreras et al., 2011). E.g. ricin is targeted to the ribosomes in the cytosol via the TGN-ER pathway, while the nigrin b enters cytosol from endosomes without trafficking to the TGN-ER. Some receptors might carry ricin and the related highly toxic type 2 RIPs (e.g., viscumin, abrin, modeccin, and volkensin, but not nigrin

b) to TGN and subsequently are retrogradely transported to the ER (Mayerhofer et al., 2009). The receptors internalized with nigrin b don't deliver it to TGN. The number of lysines in a protein is another important factor for their toxicity. Volkensin is excreted by cells faster than ricin, but, possibly, the lower amount of lysine residues in ricin protects it from protein degradation. As a consequence, excreted but non-degraded proteins can be taken up by the cells again (Battelli et al., 2004).

The intracellular pathway of type 1 RIPs

Unlike type 2 RIPs, in which the lectin domain facilitates the endocytosis mechanism, type 1 RIPs enter the cells via different internalization pathways and the efficiency is low. The mechanism of uptake followed by type 1 RIPs is not well understood. Some investigations of the internalization of type 1 RIPs (e.g. saporin and trichosanthin) suggested different mechanisms for cellular uptake (Fig. 1.6). Type 1 RIPs are proposed to gain entry to the cells via fluid-phase endocytosis or macro-pynocytosis (Vago et al., 2005). But, some evidence also indicated that specific binding to a receptor for the type 1 RIP on the cell surface may occur.

Some observed intracellular pathways for type 1 RIPs are shown in Fig. 1.6. Saporin binds to low-density lipoprotein receptor-related proteins (LRP)/α2-macroglobulin receptor (α2MG-R) on the cell surface in a variety cell types. After being endocytosed, the toxin reaches the cytosol delivered from the endolysosomal compartment. This delivery pathway has not yet been identified, but does not occur via the Golgi apparatus (a different intracellular route compared to ricin) (Vago et al., 2005). Recently, it has been reported that saporin locates to the nucleus (Bolognesi et al., 2012). However, in some cell types, saporin can enter the cells according to a α2MG-R-independent pathway, because the level of this receptor is not in agreement with the amount of saporin taken up by the cell (Bagga et al., 2003; Ippoliti and Fabbrin, 2014).

Trichosanthin binding to the cell surface can also be assisted by lipoprotein receptor-related protein members (Jiao and Liu, 2010) and can be transported to multivesicular bodies (MVB) (de Virgilio et al., 2010) in Jurkatt-T cells. Some trichosanthin can escape from the endosome under the condition of low pH. Upon lowering of the pH, trichosanthin is partly incorporated into the intraluminal vesicles of this organelle with a semi-denatured state (Fang et al., 2011). Subsequently, the MVB fuses to the plasma membrane and releases the intraluminal vesicles into the extracellular space. There, they diffuse and can reach other syngeneic or allogeneic Jurkatt-T cells by unknown mechanism(s).
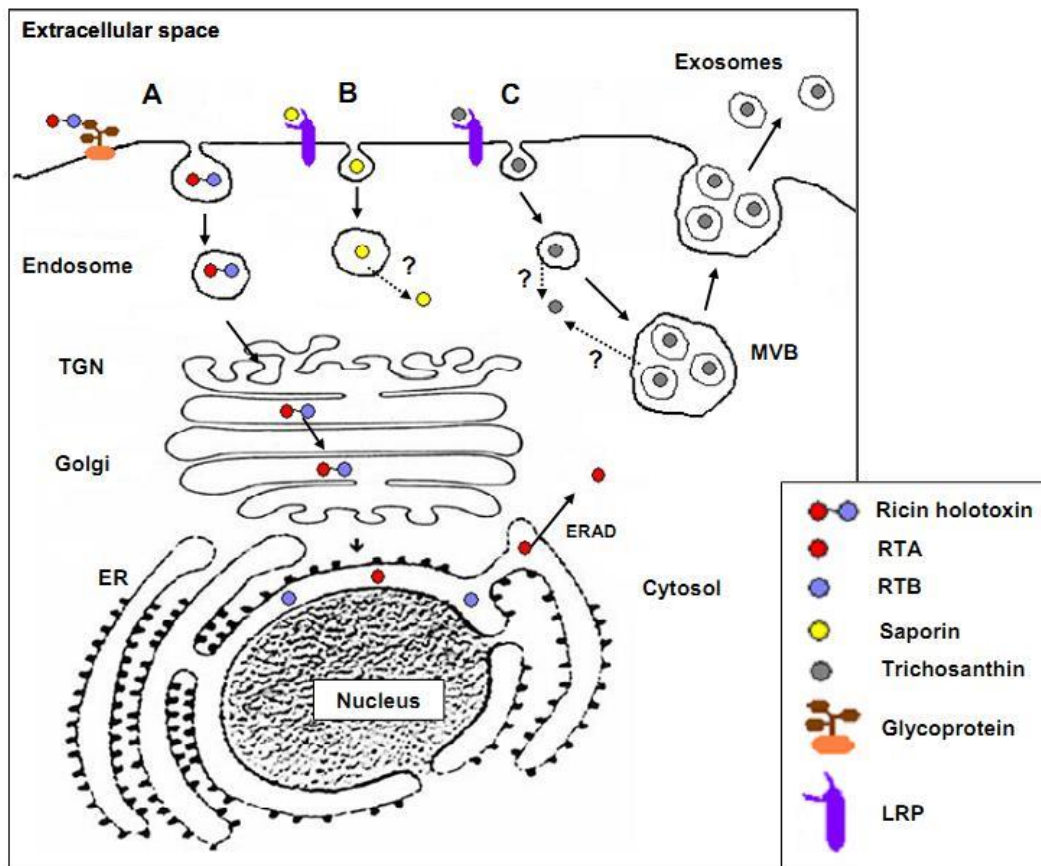
Figure 1.6 Schematic representation of the intoxication pathways followed by Ricin (A), Saporin (B) and Trichosanthin (C) (de Virgilio et al., 2010).

1.2.4.3 Mechanisms of cell death induced by RIPs

Apoptosis induced by RIPs

Apopotosis, or energy-dependent programmed cell death, is essential for maintaining cell populations in tissues (Sevrioukova 2011). The morphological changes of apoptosis like cell shrinkage, membrane blebbing, nuclear fragmentation, irreversible chromatin condensation (pyknosis), complete dissolution of the chromatin (karyolysis), disruption of the cytoskeleton, and formation of small apoptotic bodies have been observed. Apoptosis can be induced by: (1) an extrinsic pathway involving an extracellular death receptor (tumor necrosis factor), (2) an intrinsic pathway or intracellular mitochondrial-initiated events, and (3) the perforin/granzyme pathway: cell–cell interactions that result in delivery of the transmembrane pore-forming molecule perforin and serine proteases granzymes into the target cell (Elmore, 2007).

It has been reported that RIPs induce apoptotic cell death via different mechanisms: downstream of mitochondrial activation, regulation of apoptotic proteins, activation of caspases, induction of unfolded protein response and inhibition of antioxidant proteins and

others (Fig. 1.7) (Das et al., 2012; Narayanan et al., 2005; Sikriwal and Batra, 2010). A comparison of the various pathways of apoptosis that are triggered by RIPs reveals that mitochondria play an important role in cellular stress and cell death (Narayanan et al., 2005). The loss of mitochondrial membrane potential will damage mitochondria, and will irreversibly activate caspases, triggers release of cytochrome c and will increase the production of reactive oxygen species (ROS). Any or all of these events can cause cell death. Nevertheless, these processes of programmed cell death induced by RIPs are not entirely understood. With the classical mechanism of RIP induced cell death, it is considered that the N-glycosidase activity causes apoptosis. However, the mechanism of protein synthesis inhibition programming cell death provoked by RIPs is still an enigma. The question is whether protein synthesis inhibition is essential for RIP induced apoptosis. Three different hypotheses have been pointed out by Das et al. (2012). The translation inhibition activity of RIPs is (i) necessary and sufficient, (ii) necessary but not sufficient, (iii) neither necessary, nor sufficient.

First, the translation inhibition activity of RIPs is an essential factor for inducing apoptosis. Experiments with protein synthesis inhibitors (such as cycloheximide or anisomycin) inducing apoptosis suggest inhibition of protein synthesis is leading to apoptosis (Martin et al., 1990; Kageyama et al., 2002). Another evidence showed that the inhibition of protein translation by RIPs inhibits the pathway downstream of caspase activation and causes apoptosis (Olmo et al., 2001). In addition, Ghosh and Batra (2006) found that an isoform of saporin (with a mutation in the active site) has less RIP activity in a cell free system and shows less cytotoxicity. Furthermore, the apoptosis induced by ricin in HeLa cells causes DNA fragmentation, activation of caspase 3, numbers of apoptotic cells, induction of ROS, changes in the mitochondrial membrane potential and reduction of intracellular glutathione (Rao et al., 2005; Liao et al., 2012; Tesh, 2012). Protein translation inhibition is considered to be associated to mitochondrial stress (Narayanan et al., 2005). For example, abrin was reported to trigger the mitochondrial pathway of apoptosis in Jurkat cells. Following protein synthesis inhibition, a series of event happened: loss of mitochondrial membrane potential, caspase-3 activation and DNA fragmentation.

 Second, protein synthesis activity is not the sole factor for the induction of apoptosis by RIPs. The studies of PAP mutants show that certain RIP mutants lose their ability to induce the apoptosis process without possessing N-glycosidase activity (Hur et al., 1995). It was also demonstrated that although the depurination activity of PAP mutants was not sufficient, it was required for the induction of apoptotic cell death (Hudak et al., 2000b). By inactivating a thiol specific antioxidant protein (AOP), an abrin A chain mutant (lack of N-glycosidase activity) triggers cell death (Shih et al., 2001). AOP-1 was found to interact with the abrin A

chain mutant in a yeast two-hybrid system. Mitochondrial AOP-1 maintains the intracellular the level of ROS, and obstructs the release of cytochrome c from the mitochondria to the cytosol. The abrin A chain mutant blocks AOP-1 via directly binding to it. Subsequently, intracellular cytochrome c levels are increased, which activates the mitochondrial caspase pathway, eventually resulting cellular apoptosis. Due to the absence of N-glycosidase activity, the apoptosis triggered by the abrin A chain mutant is independent of enzymatic activity. Also in bacteria the level of depurination by Shiga toxin was not correlated with the level of cytotoxicity, as reported by Di et al. (2011).

Third, the inhibition of protein translation is neither required, nor sufficient for inducing apoptosis. The type 2 RIPs ricin, volkensin, and riproximin are able to induce apoptosis and depurinate ribosomes at different concentrations (Horrix et al., 2011). At the same time, the unfolded protein response is also induced by type 2 RIPs at concentrations below the level triggering the ribosomal inactivation. This accumulation of unfolded proteins in the ER is able to trigger apoptosis or autophagy (Malhotra and Kaufman, 2007; Verfaillie et al., 2010; Kim et al., 2008). A mutant form of abrin (absence of N-glycosidase activity) can also trigger programmed HeLa cell death (Sikriwal et al., 2008). Other studies have reported that induction of apoptosis by RIPs is independent of inhibition of protein translation (Das et al., 2012).
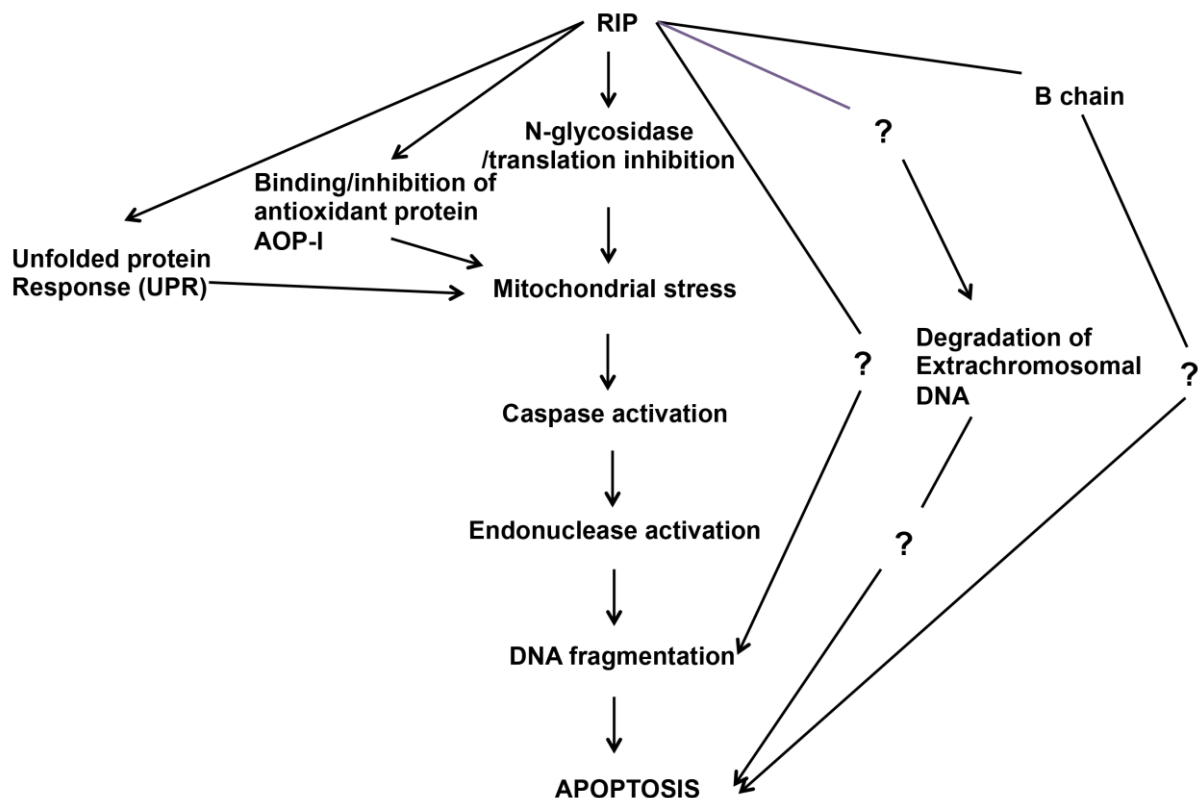
Figure 1.7 Possible mechanisms of RIPs to bypass the translation inhibition step to induce apoptosis (Das et al., 2012).

Role of type 2 RIP B chains

Many studies reported that type 2 RIPs are involved in the apoptosis by triggering extrinsic pathways or/and intrinsic pathways. Furthermore, proteins consisting only the lectin domain are also able to program cell death via apoptotic or/and autophagic pathway (Fu et al., 2011; Liu et al., 2010). Although the mechanisms of induction of cell death by lectins are well studied, the functions of the B chain apart from the A chain in type 2 RIP are poorly understood except for their role in assisting the entry into cells.

Necrosis induced by RIPs

In contrast to apoptosis (energy-dependent programmed cell death), the cell death of necrosis does not require new energy production but requires minimal energy, and is mainly induced by mitochondrial stress (Zong and Thompson, 2006). The morphological changes observed from necrotic cell death are distinct from that of apoptosis. Necrosis leads to cell swelling, membrane rupture and release of intracellular contents, and thus is associated with an inflammatory response. The RIPs not only induce apoptosis, but also trigger necrosis. However, apoptosis is still the major mechanism for the cell death induced by RIPs. Abrin showed inhibition of protein synthesis activity in all tested cell types and displayed different forms of cell death. In the human Jurkat cells (T-cell line), abrin induces apoptosis via mitochondrial stress resulting in the activation of caspases-3/9 and DNA fragmentation (Narayanan et al., 2004). However, abrin triggers necrosis in U266B1 cells (human B cell line) under a similar treatment (Bora et al., 2010). Mirabilis antiviral protein (MAP), a type 1 RIP isolated from the leaves of *Mirabilis jalapa*, causes apoptotic cell death in HeLa cells but necrosis in Raji cells (lymphoblasts from a case of Burkitt lymphoms), which also demonstrates that it is more toxic to HeLa cells than to Raji cells (Ikawati et al., 2003).

1.3 Distribution and evolution of RIPs

1.3.1 Distribution

1.3.1.1 Plant RIPs

Although RIPs are widely distributed in the plant kingdom, the N-glycosidase domain is not ubiquitous in plants (Peumans and Van Damme, 2010) as shown by the absence of a RIP domain from the first completed plant genome of *Arabidopsis thaliana*. In the meantime numerous genomes of species covering all major plant taxa have been completed, which now allows getting a better overview of the occurrence and overall structure of genes with an N-glycosidase domain by a silico approach that does not depend on the availability of "protein data".

What can be learned from analyses of completed plant genomes?

To identify RIP genes in the (nearly) completed plant genomes extensive screenings based primarily on BLASTp and tBLASTn searches of genomic (nucleotide) sequences were set up.

The results of this extensive *in silico* screening covering a total number of 42 plant genomes are summarized in Figure 1.8, showing a phylogenetic tree of plant species with indication of the RIP gene complement. For most species the RIP genes (if present) could readily be identified. However, for the Poaceae species the outcome of the screening is still preliminary because of the complexity of the RIP gene complement and the occurrence of (multiple) introns in some RIP genes. Apart from the identification of the genes the *in silico* analysis revealed the occurrence of several yet unknown chimeric RIPs (type 3 RIP) as well as type 1 RIPs. These latter type 1 RIPs, most probably are derived by domain deletion events from the type 2 RIPs. At present it is not clear how the multiple type 1 RIPs found in Poaceae species have to be classified.

Several important conclusions can be drawn from Figure 1.8. First, RIP genes are apparently absent from 24 out of completed 42 genomes. Even within the group of flowering plants more than half of all species investigated (20 out of the 38) lack RIP gene(s). Second, there are striking differences between the RIP gene complement of the different species ranging from a single gene to a complex set of genes. In addition, the identification of several novel chimeric forms implies that the heterogeneity of RIP genes in terms of domain architecture is no longer covered by the classical plant type 1, type 2 and type 3 RIPs, and argues for a novel classification system. Extended RIP gene families are apparently common in Poaceae species but there are striking interspecific differences with respect to both the gene number and the domain architecture. Third, in some families (e.g. Euphorbiaceae and Poaceae) RIP genes are found in all sequenced genomes whereas in others (e.g. Rosaceae) RIP genes occur in some genomes (*Malus domestica* and *Prunus persica*) but are absent from others (*Fragaria vesca*). It is interesting to report that RIP sequences are found in the transcriptome of several important fruit producing species. Apple (*Malus domestica*) expresses both type 1 and type 2 RIPs, whereas *Prunus persica* (e.g. apricot and peach) expresses a complex set of type 1 RIPs. These observations are of great interest for two reasons. (i) The presence of ricin-like proteins in common daily consumed fruits like apple and peach/apricot raises important questions with respect to food safety. (ii) The available expression data are indicative for a specific role of the RIPs. In this PhD project, apple was used as a model system for an in-depth study of the physiological role of both type 1 and type 2 RIPs.

31
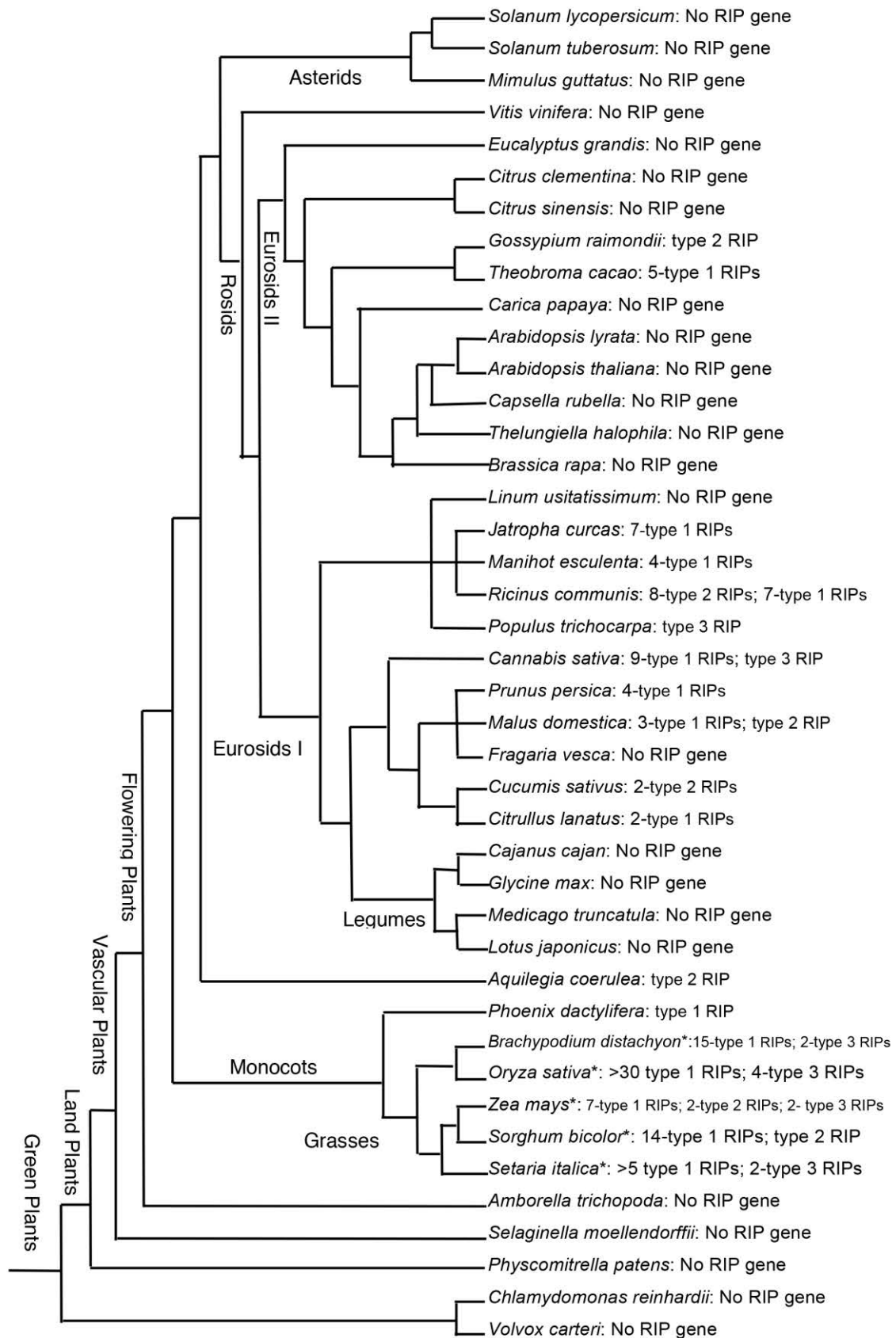
Figure 1.8 Schematic overview of the presence/absence of RIP genes in the currently completed plant genomes. The dendrogram reflects only the overall phylogeny of the species listed. The presence or absence of RIP genes is indicated. *Denotes preliminary results.

1.3.1.2 Bacterial, fungal and insect RIPs

RIP genes are widespread in plants. In contrast they are confined to a few bacterial, fungal and insect taxonomic groups, as shown by the *in silico* analysis (Shang et al., 2014). At present, RIP genes can be identified in only 16 bacterial species belonging to the families Actinobacteria, Gammaproteobacteria, Betaproteobacteria and Bacteroidetes. The best known and until recently the only identified group of bacterial RIPs are the so-called Shiga and Shiga-like toxins. Genuine Shiga and Shiga-like toxins and/or their genes have been identified in five different bacterial species all of which are classified in the family Enterobacteriaceae (Gammaproteobacteria) (Girbés et al., 2004; Stirpe 2004; Reyes et al., 2012). However, *in* silico analyses provide evidence for the presence of genes with an N-glycosidase domain in a few fungi. Type 3 RIP genes of fungi were identified in 8 Ascomycota species, all of which belong to the Sordariomycetes. Hitherto, no RIP has been isolated from an animal species. However, *in silico* analyses of the genome and transcriptome databases revealed that a RIP gene occurs in the genome of *Culex quinquefasciatus* (southern house mosquito), whereas three paralogs are found in *Aedes aegypti* (yellow fever mosquito). The presence of perfectly matching (partial) EST sequences indicates that all four insect RIP genes are expressed.

1.3.2 Molecular evolution of RIP genes

The novel insights in the taxonomic distribution and overall phylogeny resulted recently in a proposed model (Peumans and Van Damme, 2010) of the molecular evolution of the plant RIP gene family (Peumans et al., 2014; Lapadula et al., 2013; Di Maro et al., 2014).

At present there is a two-step hypothesis that tries to explain the molecular evolution of RIP genes (Fig. 1.9). First, it was suggested that the RIP domain itself developed in plants at least 300 million years (Myr) ago (Palmer et al., 2004). Type 1 RIPs directly evolved from this ancestor, ancestral type 2 RIPs were formed after a fusion of the enzymatic domain with a carbohydrate binding (lectin) domain that might be acquired by lateral transfer from a bacterium. This hypothesis is supported for two reasons: (i) the B chain of the firstly discovered type 2 RIP ricin shows a high similarity with the carbohydrate binding part of a β-glycosidase-like glycosyl hydrolase and an α-L-arabinofuranosidase B family protein from the *Actinomycete Catenulispora acidiphila*, and (ii) the cysteines (important for the formation of disulphide bond function) are also found in the bacterial sequences (Peumans and Van Damme, 2010).

The resulting ancestral type 2 RIP gave rise (through vertical inheritance) to the modern type 2 RIPs and by B domain deletion/gene truncation events to multiple lines of secondary type

1 RIP genes. In addition, deletion of the A domain resulted in the generation of lectin (B chain) genes. This hypothesis is based on a phylogenetic analysis suggesting that most type 1 RIPs found in dicots are derived from type 2 RIPs.
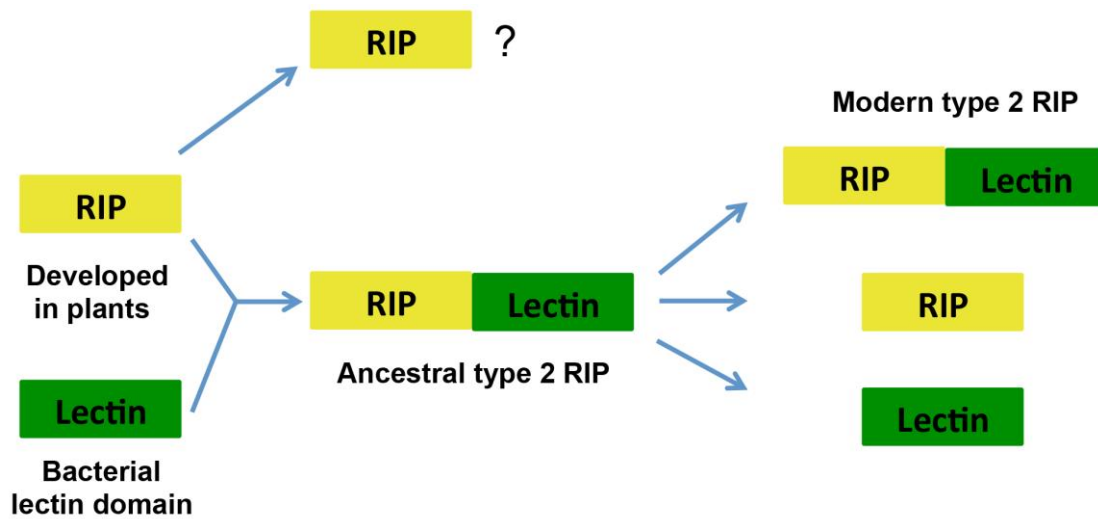
Fig 1.9 Hypotheses to explain the molecular evolution of RIP genes. The result of fusion of a RIP gene and a lectin gene is leading to an ancestral type 2 RIP. The resulting ancestral type 2 RIP gave rise to modern type 2 RIPs and by domain deletion/ gene truncation, to multiple lines of secondary type 1 RIPs and lectins.

The evolutionary link between plant and the non-plant RIPs

The most plausible explanation is that RIP genes in bacteria and fungi were acquired by a horizontal gene transfer of a RIP gene from a plant (e.g. RIP from fungi possibly obtained from a host-parasite relationship). It was reported that the sequence similarity between the fungal and plants RIPs amounts to approximately 50% (at the amino acid level) leaving no doubt that they are related evolutionary. This striking sequence similarity as well as the very narrow taxonomic distribution of the fungal RIPs are difficult to explain in terms of a classical vertical inheritance from a common ancestor that predates the separation of fungi and plants approximately 1200 Myr ago (Berbee and Taylor, 2010). A more likely –but still speculative- explanation is that the fungal RIP genes were acquired by lateral transfer from a plant (within a host-parasite relationship). Such a transfer can explain why RIP genes are confined to a dozen or so typical plant parasites. A similar conclusion holds true for the RIP genes found in bacteria but in this case the polyphyletic nature of the RIP gene family requires multiple independent lateral gene transfers from a plant into a prokaryote.

1.4 Applications of RIPs

Ricin was involved in some famous incidents. In the First World War, ricin was first investigated as a potential biological weapon. In 1978, the Bulgarian secret police used a modified umbrella with a tiny pellet containing ricin to murder the Bulgarian dissident Georgi Markov on a London street, which is now referred to as the "umbrella murder". The LD50 of this highly toxic type 2 RIP ricin for an average adult is 1.78 mg. Ricin has been in the list of schedule 1 controlled substance since 1972 Biological Weapon Convention and 1997 Chemical Weapon Convention. Of course, not all the RIPs are as toxic as ricin. Mostly, the applications of RIPs are considered in agriculture and in medicine.

1.4.1 RIPs in agriculture

RIPs can have practical application because of their antiviral, antifungal and insecticidal activities. The importance of RIPs in plant defense has been well documented. RIP genes can be transferred to plants with low or no expression of RIPs to enhance the plant resistance to predators and/or pathogens. Mostly, the transgenic plants overexpressing RIPs do not show any morphological changes. Nevertheless, the expression of some RIPs is toxic to the transgenic plants. For example, the expression of IRAb (type 2 RIP from iris bulbs) in tobacco plants resulted in the plants that were fertile but with impaired root development and stunted growth (Vandenbussche et al., 2004a). These phenotypical changes are controlled by the expression level of IRAb. Interestingly, the IRIP (type 1 RIP from iris bulbs) possibly evolutionary derived from IRAb (Van Damme et al., 2001), was not toxic for transgenic tobacco plants (Desmyter et al., 2003).

1.4.2 RIPs in medicine

For centuries, RIPs have already been applied for medical application through the use of medicinal plants. The most famous application for RIPs concerns its use as an abortifacient protein. For example, the trichosanthin, type 1 RIP from *Trichosanthes kirilowii*) has been used to induce abortion in China since ancient time (Chan et al., 2014). An important potential application of RIPs in medicine is their use in the battle against human immuno-deficiency virus (HIV). Some RIPs can inhibit the replication of HIV, such as trichosanthin, PAP and *Momordica* antiviral protein (MAP30) (Krivdova et al., 2014). Trichosanthin was the first RIP reported as anti-HIV protein *in vitro*. Its inhibition of HIV proliferation in cells led to Phase I/II clinical trials (Puri et al., 2012). Modified PAP has also been tested on HIV patients (Puri et al., 2012). Although not successful, the clinical trials presented the potential of RIPs for treating HIV positive patients.

So far, the construction and use of immunotoxins (RIPs linked to antibodies or other carriers) and other conjugates got a lot of attention. Compared to type 2 RIPs, the immunotoxins provide a better way to more specifically target and kill certain cell type, especially cancer cells (Kreitman, 2006). Immunotoxins can drive the RIPs in a selective way towards the cells to be eliminated. A variety of immunotoxins have been synthesized and tested towards several malignancies in cell cultures, animal models or patients. Gilabert-Oriol et al. (2014) summarized more than 450 RIP-based immunotoxins in his review. Saporin linked to antibody is a good example to show the cell death mechanism triggered by immunotoxins (Polito et al., 2013a)(Fig. 1.10). Normally, the targeted toxins are constructed by using type 1 RIPs or the A chain of type 2 RIPs. Due to the effect of the type 2 RIP B chains on the specific delivery of the toxins, whole type 2 RIPs can only be used after modification of the protein (Becker and Benhar, 2012). Experiments with the RIP-based toxins yielded promising results *in vitro* and in experimental animals (Fracasso et al., 2010). An immunotoxin based on bouganin induced little formation of antibodies in patients (Cizeau et al., 2012). However, patients suffered from vascular leak syndrome, fever, fatigue, hepatotoxicity and recurrence of the disease. These side effects could possibly be reduced by the use of mutant RIPs (Smallshaw et al., 2003). Nevertheless, there are also other hurdles to the use of the immunotoxins. For instance, the immunotoxins are recognized as foreign proteins, and thus antibodies will be formed, which might trigger an immunological response and prevents their repeated use. This phenomenon is an important problem of using immunotoxins. A possible way to reduce the immunogenicity of the proteins is to use humanized antibodies, rotate immunologically different RIPs, make PEGylation modification or deplete the immunodominant epitopes of RIPs (Lorberboum-Galski, 2011; Meng et al., 2012). Other obstacles including the expensive production, protein instability, short biological half-life and insufficient endosomal escape, can hopefully be solved in the future (Gilabert-Oriol et al., 2014).

Though there is still some distance between the laboratory studies and applications on the market or in clinical trials, all the knowledge of RIPs is necessary and important for the development of future applications. We believe that "First rate fundamental research, sooner or later, leads to important practical applications" (Krebs 1981; Stirpe 2014).
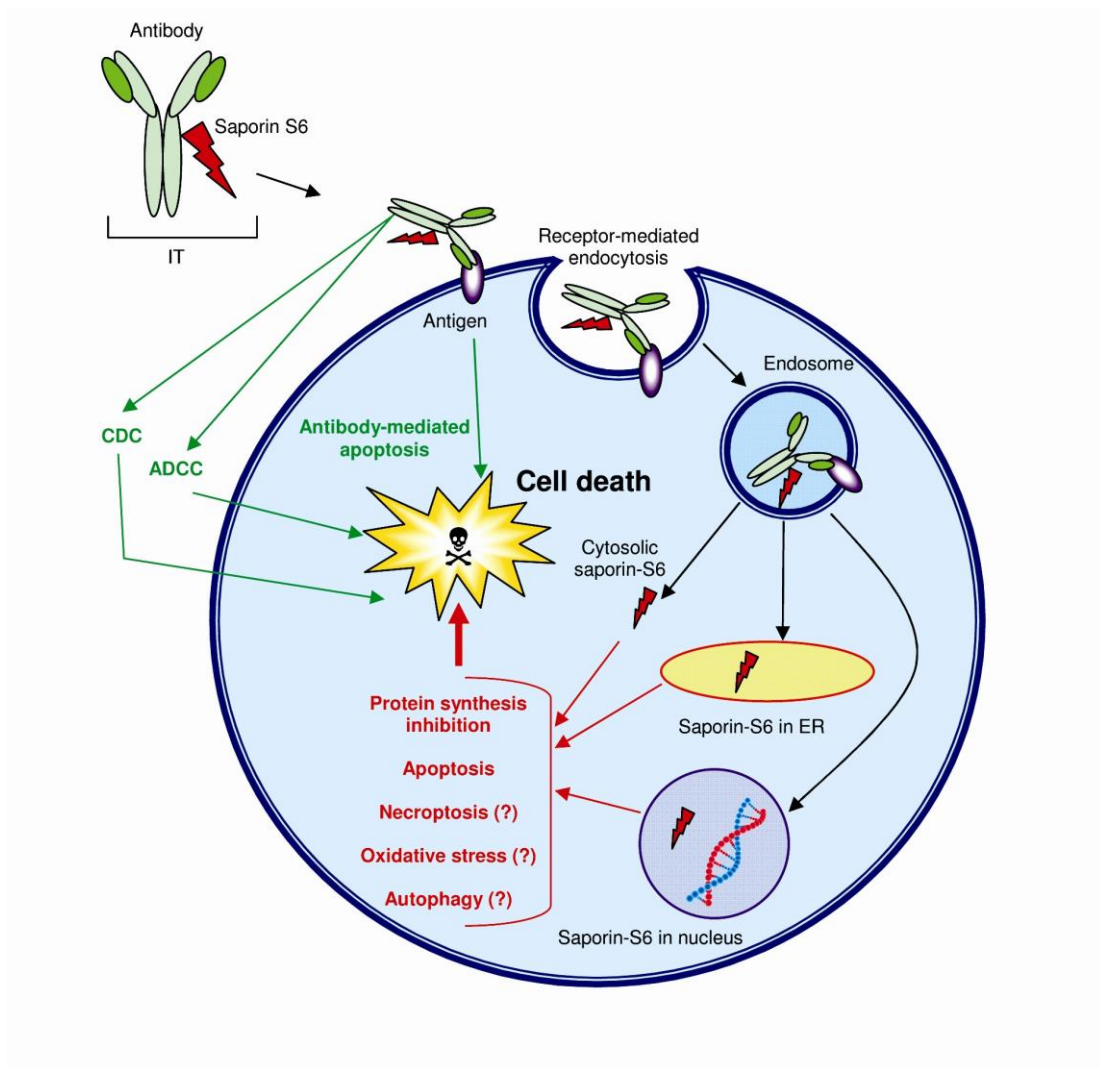
Figure 1.10 Multiple cell death pathways induced by saporin-S6 containing immunotoxins (ITs). The scheme shows the broad range of cell death mechanisms triggered by ITs. Once Saporin-S6 reaches the cytosol or ER or nucleus it can cause apoptosis activation (both caspase-dependent or -independent apoptosis), autophagy, necroptosis, oxidative stress and the inhibition of protein synthesis (in red). Moreover, cell death can also be activated by the antibody (in green) occurring through apoptosis or, when full-length antibodies are used through complement-dependent cytotoxicity (CDC) and antibody-dependent cellular cytotoxicity (ADCC) (Polito et al., 2013a).

Chapter 2

Characterization of a type 1 RIP and a type 2 RIP from *Malus domestica*

2.1 Abstract

The aim of this study was to identify and characterize the type 1 and type 2 RIPs from apple (*Malus domestica*). The RIP sequences from apple were successfully cloned from the apple genome, expressed in a heterologous system (in particular *Pichia pastoris* for type 1 RIP and tobacco BY-2 cells for type 2 RIP) and purified by affinity chromatography. SDS-PAGE revealed that the recombinant type 1 RIP polypeptide has a molecular mass of 38.8 kDa whereas the recombinant type 2 RIP consists of an AB structure of approximately 65.5 kDa. The IC50 values for *in vitro* protein synthesis inhibition by the recombinant apple type 1 and type 2 RIPs correspond to 186.6 and 300.7 nM, respectively. Screening of the recombinant apple type 2 RIP on a glycan array indicated that this type 2 RIP strongly reacts with terminal sialic acid residues. The cytotoxicity of the apple RIPs towards to mammalian cells revealed that the type 2 RIP from apple was toxic to human cells, whereas the type 1 RIP did not show any effect.

2.2 Introduction

Ribosome-inactivating proteins are a large family of enzymes comprising an N-glycosidase domain that is capable of catalytically inactivating eukaryotic ribosomes through the removal of a specific adenine residue from a highly conserved α-sarcin/ricin loop of the large rRNA (Peumans et al., 2001; Stirpe and Battelli, 2006). Though RIPs are classically associated with plants there is ample evidence now that RIP genes occur also in bacteria as well as in some fungi and invertebrates. However, apart from the bacterial shiga and shiga-like toxins and a single fungal protein (Reyes et al., 2010) virtually all research was concentrated on RIPs from flowering plants (Angiosperms). Due to the occurrence in some plants of large quantities of RIPs these proteins could readily be purified and studied in great detail with respect to their biochemical properties, biological activities and possible applications in medicine (antitumor and antiviral therapy) and agriculture (plant defense against fungi, viruses, bacteria and insects) (Stirpe and Lappi, 2014).

Plant RIPs are classically subdivided into two main groups namely type 1 RIPs consisting of an N-glycosidase domain and type 2 RIPs, which are chimeric proteins built up of an N-terminal N-glycosidase domain fused to a C-terminal carbohydrate binding domain (corresponding to a duplicated ricin B domain). However, this classification is too restrictive because genome and transcriptome analyses provided ample evidence for the occurrence in numerous plant species of RIP sequences with a completely different and often fairly complex domain architecture. However, the classification system with type 1 and type 2 RIPs is still practical because it allows to classify –apart from a single type 3 RIP from barley (Peumans et al.,

2001)- all plant RIPs purified thus far. *In silico* analyses of plant genomes/transcriptomes not only allowed identifying novel types of RIPs but yielded also a fairly detailed overview of the occurrence of the classical type 1 and type 2 RIPs in flowering plants and generated new insights in the molecular evolution of this protein family. Furthermore, it became evident that orthologs/homologs of the highly toxic type 2 RIPs are far more widespread in flowering plants than was previously documented and also occur in several food plants. Evidently, the (unexpected) occurrence of type 2 RIPs in food plants is of a great concern because the idea of eating homologs of some extremely toxic proteins like ricin and abrin is certainly not reassuring. This issue became a particularly hot item after the release of the apple genome sequence and transcriptome data (Velasco et al., 2010) revealed that this major fruit crop apparently expresses a ricin homolog (Shang et al., 2014). To answer the critical question whether the predicted ricin homolog might be of any concern from the point of view of food safety it seemed worthwhile to corroborate the biochemical properties and biological activities of the apple type 2 RIP as well as the expression of the corresponding gene. The *in silico* analyses further revealed that the apple genome comprises also a set of genes encoding type 1 RIPs. Though type 1 RIPs are usually not considered toxins the possible presence of such proteins in an edible fruit justifies a detailed study of their biological activities in general and cytotoxicity in particular. To achieve these goals recombinant type 1 and type 2 RIPs from apple were produced in an eukaryotic expression system and characterized for what concerns their biochemical properties and RNA N-glycosidase activity *in vitro*. In addition, the carbohydrate binding properties of the type 2 RIP were analyzed in detail using glycan arrays. Cytotoxicity studies with HeLa and NHDF cells further indicated that the apple type 2 RIP is moderately toxic whereas the type 1 RIP exhibits a low cytotoxicity, at least *in vitro*.

2.3   Materials and methods

2.3.1   Cell culture

Nicotiana. tabacum cv Bright Yellow-2 (BY-2) cells were grown in 250 ml Erlenmeyer flasks filled with 40 ml of liquid Murashige and Skoog (MS) medium on an orbital shaker (25°C, 150 rpm, constant darkness). The MS medium (adjusted to pH 5.7 with 1M KOH) contained 4.3 g/L MS micro and macro nutrients (Duchefa, Haarlem, The Netherlands), 30 g/L sucrose, 0.2 g/L KH_2PO_4 and 40 µl of a 1000-fold concentrated vitamin/hormone stock (containing per ml: 0.4 mg 2.4-D dissolved in ethanol, 1 mg thiamine and 100 mg myo-inositol). Cells were subcultured weekly by pipetting 1 ml of a dense culture into 40 ml fresh MS medium.

HeLa (Cervix carcinoma) and NHDF (human dermal fibroblasts, passage 9) cell cultures were grown in advanced DMEM (Life Technologies, Merelbeke, Gent) supplemented with 2% fetal

calf serum (Life Technologies) and 1% L-glutamine Penicillin-Streptomycin-Glutamin solution (Life Technologies) in an incubator set at 37°C and 5% CO_2.

2.3.2 Expression of type 1 RIP in *Pichia pastoris*

Expression of the type 1 RIP sequence was conducted following the EasySelect *Pichia* Expression Kit from Invitrogen (Invitrogen, Carlsbad, CA USA). To allow the secretion of the recombinant protein into the culture medium, the *E. coli/P. pastoris* shuttle vector pPICZαA containing an upstream α-mating sequence from *Sacharomyces cerevisiae* and a downstream polyhistidine tag was used. Therefore, the coding sequence of the type 1 RIP gene was amplified by PCR using genomic DNA extracted from the bark of *Malus domestica* cv 'Jacques Lebel' using the Fast DNA SPIN Kit (Qbiogene, USA). PCR was done using the specific primers EVD 578 and EVD 580 (Table 2.1) corresponding to the 5' and 3' region of the coding sequence. The PCR reactions were as follows: 2 min 94°C, 30 cycles (15s 94°C, 30s 55°C, 1 min 72°C), 5 min 72°C. The amplified type 1 RIP sequence was cloned as a EcoRI/NotI fragment in the shuttle vector pPICZαA and transformed into *E.coli* Top 10 cells via heat shock. Transformed clones were grown on LB agar plates with zeocin (25 µg/ml) at 37°C. Plasmid DNA was purified using the GeneJET™ Plasmid Miniprep Kit (Fermentas, St Leon-Rot, Germany) and sequenced by LGC Genomic (Berlin, Germany) using 5' and 3' AOX1 primers (EVD 21 and EVD 22, Table 2.1).

2.3.3 Transformation of *Pichia pastoris*, selection, and expression analysis

Electrocompetent cells of *P. pastoris* strain X-33 were prepared according to Invitrogen protocols. Before electroporation, the DNA construct was linearized using the restriction enzyme Sac I (Fermentas, St Leon-Rot, Germany) and incubated at 37°C overnight. 10 µg of linearized expression vector was transformed into *P. pastoris* strain X-33 using a Bio-Rad Gene pulser apparatus (Bio-Rad, Hercules, CA, USA) using the settings as described by Al Atalah et al. (2011). The transformants were selected on YPDS agar plates (1% yeast extract, 2% peptone, 2% dextrose, 1 M sorbitol, 1.5% agar) containing 200 µg/ml zeocin (Invitrogen). To analyse the expression, several colonies were inoculated in 5 ml BMGY medium (1% yeast extract, 2% peptone, 100 mM phosphate buffer, pH 6.0, 1.34% yeast nitrogen base with ammonium sulfate and without amino acids, $4x10^{-5}$% biotin, and 1% glycerol) at 30°C in a shaker incubator at 200 rpm for 24 h. Afterwards, *Pichia* cells were washed with sterilized water and resuspended in 5 ml of BMMY (BMGY containing 2% methanol instead of 1% glycerol). Cultures were treated with 2% methanol for 72 h at 22 °C with shaking at 250 rpm. Samples of the medium were analyzed by Western blots after trichloroacetic acid (TCA)

Table 2.1 Overview of PCR primer pairs used in this research

Amplified sequence	Primer name	5'-3' sequence
Specific gene amplification primers: type 1 RIP	EVD 578	AATATGGCACTATCCTTCTC
	EVD 580	AGTGGGCCGTCTATTTCTTC
AOX1-sequencing primer for Pichia vectors	EVD 21	GACTGGTTCCAATTGACAAGC
	EVD 22	GCAAATGGCATTCTGACATCC
Adding the non-complete *attB* sequences: type 2 RIP	EVD 607	AAAAAGCAGGCTTCACCATGACGAGAGTGTTAGCAATATAC
	EVD 713	AGAAAGCTGGGTGACGACCTTCGATGAAGAACGGCAGCCATTGCTGGTTGGG
Completing the *attB* sequences	EVD 2	GGGGACAAGTTTGTACAAAAAAGCAGGCT
	EVD 4	ACCACTTTGCTCAAGAAAGCTGGGT
Sequencing MultiSide LR reaction product from type 2 RIP	EVD 472	GAAACCTCCTCGGATTCCAT
	EVD 634	AACGGAGTCTTCAGTAAGTC

precipitation. For medium-scale cultures, *P. pastoris* X-33 colonies were inoculated into 10 ml BMGY medium and grown for 24 h at 30°C in a shaker incubator at 200 rpm. Afterwards, 10 ml preculture was subcultured into 50 ml BMGY medium in 250 ml Erlenmeyer flasks and incubated at 200 rpm for 24 h at 30°C. Cells were centrifuged at 3000 g for 10 min at room temperature and resuspended in 100 ml BMMY in 500 ml flasks after washing with sterilized water. After 24 h, 100% methanol (2% final concentration) was added to the culture twice per day. After 3 days, the yeast cell culture was centrifuged at 3000 g for 10 min. Solid ammonium sulfate (80% final concentration) was added to the supernatant and the proteins were allowed to precipitate at 4°C. Precipitated proteins were collected by centrifugation (14,600 g for 30 min at 4 °C), dissolved in 50 mM sodium acetic acid (pH 5), and dialysed against 50 mM sodium acetic acid (pH 5) for 24 h. After dialysis the protein solution was cleared by centrifugation (3000 g for 10 min) and the supernatant (adjusted to pH 3) used for the purification of the RIP.

2.3.4   Purification of recombinant type 1 RIP

Purification of recombinant type 1 RIP was achieved in three successive chromatographic steps. The proteins recovered from the medium were loaded onto a column (2 cm x 22 cm; 20 ml bed volume) of S Fast Flow equilibrated with 50 mM sodium acetate (pH 3). After washing the column with 50 mM sodium acetate (pH 3), the bound proteins were eluted with a solution of 0.5 M NaCl in 100 mM Tris/HCl (pH 8.7). The eluate was brought to a final concentration of 25 mM imidazole and loaded onto a column (1 cm x 22 cm; 5 ml bed volume) of Ni-Sepharose equilibrated with starting buffer (0.1 M Tris pH 7 containing 0.5 M NaCl and 25 mM imidazole). After washing with starting buffer, the proteins were eluted using a buffer (0.1 M Tris pH 7 containing 0.5 M NaCl) with increasing concentrations of imidazole (50, 175, 250 mM). Pure type 1 RIP eluted at a concentration of 175 mM imidazole. Finally, the eluate from the Ni-Sepharose column was diluted five times with 50 mM sodium acetic acid, adjusted to pH 3 and concentrated on a column (1 cm x 22 cm; 5 ml bed volume) of S Fast Flow using the same procedure as during the first chromatography step. The purity of the protein in the eluate was assessed by SDS-PAGE.

2.3.5   Construction of the binary vector for expression of type 2 RIP in BY-2 cells

To construct a binary vector that will allow the 35S Cauliflower Mosaic virus promoter-driven expression of the type 2 RIP from *Malus domestica*, the Gateway™ cloning technology of Invitrogen (Carlsbad, CA, USA) was used. The coding sequence of the complete type 2 RIP gene from apple was amplified as an *attB* product by PCR, using genomic DNA extracted from the bark of *Malus domestica* cv 'Jacques Lebel' and gene-specific primers EVD 607 and EVD 713 (Table 2.1) containing part of the *attB* sites in the first PCR. The construct was

completed with the *attB* sites using primers EVD2/EVD4 (Table 2.1). Cycling parameters for the PCR reactions were: 2min 94°C, 25 X (15s 94°C, 30s 55°C, 1 min 72°C), 5min 72°C. Subsequently, all *attB* PCR products were homogeneously recombined in the entry vector pDONR221 (Invitrogen). Using heat shock transformation, the entry clones were subsequently transferred into *E. coli* strain Top10 cells. Transformants were selected by colony PCR. The plasmid DNA extracted from the colonies was sent for sequencing (performed by LGC Genomics, Berlin, Germany) using the primers Donr-F and Seql-E (Table 2.1). Tobacco Bright Yellow (BY)-2 cells were transformed using the fusion construct containing the type 2 RIP sequence cloned behind the 35S CaMV promoter and C-terminally fused to a $(His)_6$ tag. These additional sequences were added by Gateway MultiSite recombination cloning techniques (Petersen and Stowers, 2011). Finally, the LR reaction was performed with a selected entry clone containing the type 2 RIP sequence, pEN-L4-2-R1, 0 and pEN-His(6) entry vectors in the pKCTAP destination vector containing the EGFP sequence using LR Clonase^{TM} II Plus Enzyme Mix (Invitrogen). The result of the LR reaction was verified by sequencing (LGC Genomics) using primers EVD 472 and EVD 634 (Table 2.1). The final construct was used for transformation of *Agrobacterium tumefaciens* strain LBA4404 by tri-parental mating a described by Hoekema et al., (1983).

2.3.6   Stable transformation of BY-2 cells and expression analysis

A three day old BY-2 cell culture was cocultivated with *A. tumefaciens* cells harboring the expression vector as previously described (Delporte et al., 2014). After 3 days cocultivation, transformed BY-2 cells were selected on MS agar plates containing antibiotics (500 mg/L carbenicillin, 100 mg/L kanamycin) and BY-2 vitamins for 3-4 weeks until resistant calli became visible. The transgenic calli were detected by the Fujifilm FLA-5100 Fluorescent Image Analyzing System (Tokyo, Japan) based on the expression of the EGFP sequence located on the vector. Fluorescent calli were used to start a BY-2 liquid cell culture by transferring a 1 cm homogenous appearing callus into 20 ml BY-2 cell medium in a 40 ml Erlenmeyer flask. For the purification of recombinant proteins the cell cultures were grown in 600 ml cultures in large Erlenmeyer flasks. After seven days, the medium was harvested using a sintered glass pore filter with a filter disc paper. Afterwards, the medium was adjusted to 1.5 M ammonium sulfate (by adding the solid salt) at pH 7.0 for the purification of type 2 RIP.

2.3.7   Purification of recombinant type 2 RIP

Purification of the recombinant type 2 RIP from apple was achieved in three consecutive chromatographic steps. The BY-2 medium (pH 7) was cleared by vacuum filtration and loaded onto a column (5 cm x 30 cm; 80 ml bed volume) of Phenyl Sepharose (GE

Healthcare, Uppsala, Sweden) equilibrated with 1.5 M ammonium sulfate (pH 7). After washing the column with 1.5 M ammonium sulfate (pH 7), the bound protein fraction was eluted with a solution of 20 mM 1,3 diaminopropane. The eluted fraction was brought at 1.5 M ammonium sulfate with the solid salt, the pH adjusted to 7 and applied onto a column (2 cm x 22 cm; 20 ml bed volume) of Fetuin-Sepharose 4B equilibrated with 1.5 M ammonium sulfate (pH 7) and washed with 1.5 M ammonium sulfate (pH 7). Bound proteins were eluted with a solution of 20 mM 1,3 diaminopropane and concentrated by a second chromatography on a small column (1 cm x 22 cm; 5 ml bed volume) of Fetuin-Sepharose 4B using the same procedure as for the first affinity chromatography step. Following this procedure the type 2 RIP fraction was eluted in a few ml of 20 mM 1,3 diaminopropane.

2.3.8   N-terminal sequence analysis

Purified type 1 and 2 RIPs were analyzed by SDS-PAGE, electroblotted onto a Problot [TM] polyvinylidene fluoride (PVDF) membrane (Applied Biosystems, Foster City, CA, USA) and the blot stained using 1:1 mix of Coomassie Brilliant Blue and methanol to visualize the protein. The bands of interest were cut and used for N-terminal sequencing by Edman degradation using a capillary Procise 491cLC protein sequencer without alkylation of cysteines (Applied Biosystems).

2.3.9   Agglutination assay

For testing the lectin activity of the purified recombinant type 2 RIP, trypsin-treated rabbit red blood cells (Bio-Mérieux, Marcyl'Etoile, France) were used. Assays were performed as described by Al Atalah et al. (2011).

2.3.10 Carbohydrate inhibition test

To determine the overall carbohydrate binding specificity of the recombinant type 2 RIP, hapten inhibition assays were carried out with a series of glycoproteins (thyroglobulin, fetuin, ovomucoid, asialomucin and mucin) and carbohydrates (mannose, methyl mannopyranoside, and galactose). Aliquots of 5 μl purified type 2 RIP (0.3 mg/mL) were mixed with 5 μl of a serially diluted carbohydrate or glycoprotein solution (in glass tubes) and incubated for 10 min at room temperature before adding 10 μl 1 M ammonium sulfate and 30 μl of a 10% (v/v) suspension of trypsin-treated erythrocytes. Agglutination activity was assessed visually after 1 h incubation at room temperature.

2.3.11 Glycan microarray screening assay

Glycan microarrays were printed as described previously (Blixt et al., 2004). The printed glycan array contains a library of natural and synthetic glycan sequences representing major glycan structures of glycoproteins and glycolipids. Array version 5.0 with 611 glycan targets, was used for the analyses with recombinant type 2 RIP (http://www.functionalglycomics .org/glycomics/publicdata/selectedScreens.jsp). The purified recombinant type 2 RIP was labeled using the Alexa Fluor® 488 Protein Labeling Kit (Invitrogen, California, USA) following the manufacturer's instructions. The labeled proteins were applied to separate microarray slides and incubated for 60 min under a cover slip in a dark, humidified chamber at room temperature. After incubation, the cover slips were gently removed in a solution of Tris-buffered saline containing 0.05% Tween 20 and washed by gently dipping the slides 4 times in successive washes of Tris-buffered saline containing 0.05% Tween 20, Tris-buffered saline, and deionized water. After the last wash, the slides were spun in a slide centrifuge for approximately 15s to dry and immediately scanned in a PerkinElmer ProScanArray MicroArray Scanner using an excitation wavelength of 488 nm and ImaGene software (BioDiscovery, El Segundo, CA, USA) to quantify fluorescence. The data are reported as average relative fluorescence units (RFU) of six replicates for each glycan present on the array after removing the highest and lowest values.

2.3.12 Protein deglycosylation

Recombinant proteins (type 1 RIP and type 2 RIP) were digested with N-glycosidase F (PNGase F) as described by Al Atalah et al. (2014a). Briefly, 2 µg of recombinant proteins were mixed in a volume of 10 µl denaturation buffer (0.5% SDS and 0.04 M dithiothreitol). The samples were boiled at 100°C for 10 min and cooled down to room temperature. To the denatured samples 2 µl of 10x reaction buffer (0.5 M sodium phosphate pH 7.5), 2 µl 10% NP-40 and 5.5 µl distilled water were added to reach a total volume of 20 µl. The samples were incubated at 37°C for 4 h after adding 0.5 µl of PNGase F (1000 U/µl) to each sample. RNAse B (2 µg) was used as a positive control. Finally, protein samples were analyzed by SDS-PAGE.

2.3.13 Protein synthesis inhibition activity

The protein synthesis inhibition activity of the recombinant proteins (type 1 RIP and type 2 RIP) and positive and negative controls (SNA-I and BSA, respectively) was determined using the TnT® T7 Quick Coupled Transcription/Translation System Kit (Promega, Mannheim, Germany) based on a cell-free system derived from rabbit reticulocytes (Voss et al., 2006). According to the manufacturer's instructions, the prepared mixture was incubated at 30°C

for 10 min and chilled on ice. Afterwards, 2 µl PBS or PBS containing different concentrations of proteins were added to the reaction mixture and incubated for 30 min at 30°C. After addition of 35 µl nuclease-free water at room temperature, the reaction samples were transferred to a luminometer plate (Greiner Labortechnik, Frickenhausen, Germany) containing 5 µl luciferase assay reagent at 25°C. The relative luciferase activities of the samples were determined at 562 nm for 10s using a microtiter top plate reader (Infinite 200, Tecan, Mannedorf, Switzerland) with an initial delay of 2s.

2.3.14 Cytotoxicity assay

To study the effect of recombinant RIPs from apple on cell viability and proliferation, a total of 3,000 HeLa or NHDF cells were seeded in a 96-well plate (Greiner Labortechnik) and incubated at 37 °C and 5% CO_2 for 24 h. Subsequently, the medium was exchanged with medium supplemented with various concentrations of apple RIPs (ranging from 0.05 to 2 µM), and incubated at 37°C and 5% CO_2 for 2 time points (24 h and 48 h), respectively. Phosphate buffered saline (Life Technologies) with/without 2 µM BSA was used in the control treatments (Oliveira et al., 2011). Four technical replicates were performed for each concentration, and each experiment was repeated three times.

Cell viability was determined by means of (resazurin-based) Presto Blue spectrophotometric assays (Life Technologies) according to manufacturer's instructions. In brief, the culture medium of each well was replaced with fresh culture medium containing 10% final concentration of Presto blue reagent. After incubation for 20 min in the dark at 37 °C and 5% CO_2 the fluorescence intensity of reduced resazurin was measured at 560/600 nm in a plate reader (Infinite 200, Tecan, Mannedorf, Switzerland).

Cell morphology was assessed using an inverted transmitted light microscope (Ti Eclipse, Nikon Instruments, Paris, France), with a 10x dry objective (Numerical aperture 0.5). Cells were imaged using the software package NIS-Elements (Nikon) and analyzed using Fiji (http://fiji.sc/Fiji).

2.3.15 Preparation of crude extracts from apple tissue

Crude extracts were prepared from apple (*Malus domestica* cv 'Golden delicious') fruits 10 days post pollination by homogenizing the tissue in 20 mM 1,3 diaminopropane (0.5 ml buffer per gram of fresh weight (FW)) with mortar and pestle. After centrifugation (10 min, 3000 g), the supernatant was adjusted to 1.5 M ammonium sulfate at pH 7.0 and loaded onto a column (1 cm x 10 cm; 4 ml bed volume) of Phenyl Sepharose (GE Healthcare, Uppsala, Sweden) equilibrated with 1.5 M ammonium sulfate (pH 7). After washing the

column with 1.5 M ammonium sulfate (pH 7), the bound protein fraction was eluted with a solution of 20 mM 1,3 diaminopropane, and analyzed by SDS-PAGE. The apple type 2 RIP was detected by western blot analysis.

2.3.16 Analytical methods

The total protein content of the extracts from apple tissue was estimated using the Coomassie (Bradford) Protein Assay Kit (Thermo Fischer Scientific, Rockford, IL USA). SDS-PAGE was performed in 15% polyacrylamide gels under reducing/non-reducing conditions (with/without betamercaptoethanol treatment). Proteins were visualised by staining with Coomassie Brilliant Blue R-250. For western blot analysis, samples were separated by SDS-PAGE and proteins transferred onto a PVDF membrane (Bio Trace^{TM} PVDF, PALL, Gelman Laboratory, Ann Arbor, MI, USA). First, the blots were blocked in blocking buffer, consisting of 5% milk powder dissolved in Tris buffered saline (TBS: 10 mM Tris, 150 mM NaCl and 0.1% (v/v) Triton X-100, pH 7.6). After blocking, blots were incubated for 1 h in TBS supplemented with the following primary antibodies: (i) for recombinant type 1 RIP purified from *Pichia pastoris* medium: mouse monoclonal anti-His (C-terminal) antibody (1:5000, Invitrogen; (ii) for recombinant type 2 RIP purified from tobacco cells: rabbit polyclonal anti-type 1 RIP antiserum (1:1500, produced by Thermo scientific by injecting two rabbits with recombinant type 1 RIP from apple). The secondary antibody was a 1:1000 diluted rabbit anti-mouse IgG (Dako Cytomation, Glostrup, Denmark) or a 1:5000 diluted horseradish peroxidase-coupled goat anti-rabbit IgG (Sigma-Aldrich, St. Louis Missouri, USA), respectively. Immunodetection was achieved by a colorimtric assay using 3,3'-diaminobenzidine tetrhydrochloride (Sigma-Aldrich) as a substrate. All washes and incubations were conducted at room temperature with gentle shaking. For sequence analysis, ClustalW was used for alignment of the apple RIPs, elderberry RIP (SNA-I) and A chain of ricin protein sequences. The signal peptide sequences were predicted by SignalP (http://www.cbs.dtu.dk/services/SignalP/).

2.3.17 Statistical analyses

Statistical analyses were performed using Prism version 5 (GraphPad, La Jolla, CA). One-way ANOVA (Dunnett's Multiple Comparison Test) was performed at the level of significance (*: $p < 0,05$; **: $p < 0,01$; ***: $p < 0,001$). The 50% lethal concentration (LC50) was determined using the non-linear regression analysis. Data are represented as means ± standard error (SE).

2.4   Results

2.4.1   Identification and sequence analysis of RIP genes in the apple (*Malus domestica*) genome

A detailed screening of the apple genome revealed the presence of three type 1 RIP genes located on different contigs and a single type 2 RIP gene located on still another contig. In addition to the genuine RIP genes the apple genome contains several pseudogenes: (i) one pseudogene covering most of the B chain of the type 2 RIP (comprises no ORF due to the presence of multiple stop codons) and (ii) three type 1 RIP pseudogenes.

Analysis of the apple type 1 RIP genes indicated that they encode three closely related proteins (The Apple Gene Function & Gene Family DataBase v1.0; >MDP0000918923, >MDP0000223290, >MDP0000134012 further referred to as type 1 RIP genes A-B-C) (Fig. 2.1) that share a high sequence similarity with the classical type 1 RIPs from e.g. Cucurbitaceae species. However, there is a major difference because the apple type 1 RIPs are apparently synthesized without a signal peptide whereas all other type 1 RIPs found in dicotyledonous plants are synthesized with a leader sequence. Evidently, the loss of the signal peptide has profound consequences because the apple type 1 RIPs are presumably synthesized in the cytoplasm, which raises the question how the cells can cope with the presence of a type 1 RIP in the cytoplasmic/nuclear compartment.

Only one of the three type 1 RIP genes was selected for the further study (The Apple Gene Function & Gene Family DataBase v1.0; >MDP0000918923, gene A). Of all type 1 RIPs identified thus far it shares the highest sequence identity with the *Bryonia cretica ssp dioica* (Cucurbitaceae) type 1 RIP bryodin (57% sequence identity and 67% sequence similarity). This apple gene encodes a 301 AA polypeptide and has a calculated molecular weight of 33 kDa (Fig. 2.2A). The deduced sequence comprises five putative N-glycosylation sites but the native protein is unlikely to be N-glycosylated because it is synthesized on free polysomes. The sequence of type 1 RIP gene-A is very similar to that of the apple type 1 RIP genes B and C (>MDP0000223290 (gene B): 48% sequence identity and 64% sequence similarity; >MDP0000134012 (gene C): 48% sequence identity and 63% sequence similarity). Residues that built up the core catalytic site of N-glycosidase domain are highly conserved when compared to ricin (Fig. 2.2A).

The apple type 2 RIP (The Apple Gene Function & Gene Family DataBase v1.0; >MDP0000711911) resembles the classical type 2 RIPs found in other plant species. Of all type 2 RIPs identified thus far it shares the highest sequence identity to the *Sambucus nigra* type 2 RIP SNA-I (48% sequence identity and 62% sequence similarity). An analysis of the

deduced amino acid sequence indicates that the apple type 2 RIP is synthesized with a 22 AA residue signal peptide (Fig. 2.2B). Cotranslational removal of this signal peptide yields a 526 AA polypeptide with seven putative N-glycosylation sites (Fig. 2.2B). Most amino acid residues that built up the catalytic site are conserved (Fig. 2.2A). Sequence alignment with ricin revealed a single AA substitution in the active site of the apple type 2 RIP (Tyr[80] of ricin is replaced by Ser[71]) (Fig. 2.2A). Alignment with SNA-I further indicates that all four intra-chain disulfide-bridges that stabilize the B chain (cys[24]-cys[43], cys[65]- cys[77], cys[147]- cys[162], cys[198]-cys[205]) are conserved in the apple RIP (Fig. 2.2B) and that the AAs that built the two carbohydrate binding domains are highly conserved between the apple type 2 RIP on the one hand and the SNA-I on the other hand (Fig. 2.2B) (Van Damme et al., 1996a; Kaku et al., 2007; Hu et at., 2012).

```
Gene B  MSIPFTLIDATPDSYSRFIDQLRARLTFG-TTSQGIRVLPPSRQVGNNARFIYVDLTNYD 59
Gene C  MSISFTLIGATPDSYSTFINQLRDRLTFG-TTSQGIPVLPSSRQVGNNDRFIYVNLTNYD 59
Gene A  MALSFSIKNATTTTYRTFIEALRAQLTAGGSTSHGIPVLRRRQDVKDDQRFVLVNLTNYD 60
        *::.*:: .**. :*   **: ** :** * :**:** **   ::* :: **: *:*****

Gene B  GVTVTIGIDVVNAYVMGYEQGEQNYPLQ-TLPDDPAPVELLFPNTRSAGELPFTGHYASL 118
Gene C  GVTVTIGIDVVNVYVMGYEQGGQNYLLGGTLPDEAA---TVFPNTRAAGELPFRADYGSL 116
Gene A  SYTITVAIDVVNAYVVGYCAGTRSYFLR-DPATHPPPLHRLFPGTTRT-TLPFAGDYLGL 118
        . *:*:.*****.**:** * :.* *     . ...   :**.*  :  *** ..* .*

Gene B  GEYARRMQNEQPNRRDQQALNRLSN--PMRQNIGLGPSSLHSAIDMLERAATPLSQAGAI 176
Gene C  GQYARGMPNEQPNRRDQQSVNRLRN--DMRENIALGPSSLHWAIHMLVHAAT-SSQASAI 173
Gene A  GRAAQEALQQNTNR-NRAAGSRIHENISMRERIPLGPGELDNAISQLRYAESASSQAAAF 177
        *. *:   :::.** :: : .*: :   **:.* ***..*. ** * * : ***.*:

Gene B  LVIIQMVSEAARYPYIERQVRESIQTGNSFLPDPRMLSLENNWSNLSRQIMGATRAGRES 236
Gene C  IVIIQMVSEAARYPYIERRVRESIQTANSFIPDPRMLTLENHWSTLSRQIMEATRAGRES 233
Gene A  IVIIQIVSEAARFRYIQGQVRDRIRDGTSAEPDPAMLSLENSWSNLSEQIQMVP-ANQLL 236
        :****:*****: **: :**: *: ..*   *** **:*** **.**.**   .. *.:

Gene B  FSTSVSLDDAYQSHGAPPLVVNSVRDSFIQDMEIALLLHDRGDDRGTDQGNDPENCTPGP 296
Gene C  FSTSVSLVDAYQSHGAPPLVVNSVRDSFVQDMEIALLLHDRGDDRGTDQGIDPKNCTAGP 293
Gene A  FINNGSVQIRKADN--SIVLVKSVDSDAVRGVAFLLYCGGNPPAPNSESARTSKVTVQKP 294
        * .. *:     .: . ::*:** .. ::.: : *   ..    .::.. .: . *

Gene B  SGSGIGRRGGKKPRRQHE 314
Gene C  SVSGRG----KKPHDEL- 306
Gene A  TLAKKK----K------- 301
        : :       *
```

Figure 2.1 Sequence alignments of the three type 1 RIP genes (A-MDP0000918923, B-MDP0000223290, C-MDP0000134012). '*' Means that the amino acids are identical in all sequences; ':' means conserved conversions (amino acids with the same shape, charge and other properties), and '.' semi-conserved substitutions (properties not the same but still similar).

```
                                                        1
Type 1  ------------------------------------MALSFSIKNATTTTYRTFI  19
Type 2  --------------------MTRVLAIYITLAFSLFLCGTECNISFSTSGATSNSYNTFI  18
Ricin   MKPGGNTIVIWMYAVATWLCFGSTSGWSFTLEDNNIFPKQYPIINFTTAGATVQSYTNFI  25
                                                        1      :.*:   .**  :* .**


Type 1  EALRAQLTAGGSTSHGIPVLRRRQDVKDDQRFVLVNLTNYDSYTITVAIDVVNAYVVGYC  79
Type 2  KALRAQLTNGATAIYDIPVLN--PSVPDSQRFLLVDLSNNGNNTITVAIDVVNASVVAYR  76
Ricin   RAVRGRLTTGADVRHEIPVLPNRVGLPINQRFILVELSNHAELSVTLALDVTNAYVVGYR  85
        .*:*.:** *.  . : ****     .:  .***:**:*:*  . ::*:*:**.** **.*


Type 1  A-GTRSYFLRDPATHPPPLHRLFPGTT-RTTLPFAGDYLGLGRAAQEALQQNTNRNRAAG  137
Type 2  ARAARPYFLADAP--DEALDILFNDTR-GFFLPFTSNYVDLEKAAEKS-----------  121
Ricin   AGNSAYFFHPDNQEDAEAITHLFTDVQNRYTFAFGGNYDRLEQLAGNL-----------  133
        *  :  :* *    .:   **  ..    :.* .:*  * : * :


Type 1  SRIHENISMRERIPLGPGELDNAISQLRYAESASS----QAAAFIVIIQIVSEAARFRYI  193
Type 2  ---------REKIPLGLTPLHNAITSLWNHESEE-----AAVSLLVIIQTVFEAARFRVI  167
Ricin   ---------RENIELGNGPLEEAISALYYSTGGTQLPTLARSFIICIQMISEAARFQYI  184
                 **.* **    *.:**: *    .:      * :::: ** : *****: *


Type 1  QGQVRDRIRDGTSAEPDPAMLSLENSWSNLSEQIQMVPANQLLFINNGSVQIRKADNSIV  253
Type 2  EQRVRNSISSKANFIPDPAMLSLENNWLAISWETQHALNG----VFSKSIQLRSTNNNLF  223
Ricin   EGEMRTRIRYNRRSAPDPSVITLENSWGRLSTAIQESNQG----AFASPIQLQRRNGSKF  240
        :  .:*   *       ***:::****.*  :*   *   .        .:*:: :... .


Type 1  LVKSVDSDAVRGVAFLLYCGGNPPAPNSESARTSKVTVQKPTLAKKKK-----------  301
Type 2  LVDSVSSSIMAGVAFLFYN--CVTFPNIIKMPVNVV-----------MGKEIDNEICAV  269
Ricin   SVYDVS-ILIPIIALMVYRCAPPPSSQFSLLIRPVVPNFNADVCMDP------------  291
         *  .*.   :   :*::.*    . .:            *


Type 2  QNRTTHISGLEGLCVDVKNGLDSDGNLVQIWPCGQ--QRNQKWTFQPDETIRSMEKCMTA  327
Ricin   -EPIVRIVGRNGLCVDVRDGRFHNGNAIQLWPCKSNTDANQLWTLKRDNTIRSNGKCLTT  350
        :   .:* * :*******::*     :** :*:*** .  : ** **:: *:**** **:*:


Type 2  YSTSSPENYVMIYNCTTAVLEATKWALSTDGTITHRRSGLVLTAHEATRGTTLTIATNSH  387
Ricin   YG-YSPGVYVMIYDCNTAATDATRWQIWDNGTIINPRSSLVLAATSGNSGTTLTVQTNIY  409
        *. ** *****:*.**. :**:* :  :*** : **.***:* ... *****: ** :


Type 2  SPKQGWRVADDVEPTVTSIIGYNDMCLTANDDKSRVWMEYCVPSKNQQQWALYSEGTIRV  447
Ricin   AVSQGWLPTNNTQPFVTTIVGLYGLCLQANS--GQVWIEDCSSEKAEQQWALYADGSIRP  467
        : .*** ::::.:* **:*:*  .:** **.  .:*:* * ..* :* *****:*:*:**


Type 2  NSDRTLCVTSNGHNSSNVIIILKCELKRGDQRWVFKTDGSILNPNAELVMDVKNSDVYLR  238
Ricin   QQNRDNCLTSDSNIRETVVKILSCGPASSGQRWMFKNDGTILNLYSGLVLDVRASDPSLK  224
        :.:*  *:**:.:  ..*: **.*    ..***:**.**:*** : **:**: **  *:


Type 2  QIILYPYYGTPNQQWLPFF  269
Ricin   QIILYPLHGDPNQIWLPLF  255
        ****** :* *** ***:*
```

Figure 2.2A Sequence alignment of the Ricin (acc. no. XP_002534649.1), apple type 1 and type 2 RIPs. '*' Means that the amino acids are identical in all sequences; ':' means conserved conversions (amino acids with the same shape, charge and other properties), and '.' semi-conserved substitutions (properties not the same but still similar). N-terminal signal peptide is shown in *gray*. The amino acids known to be important for the catalytic activity of the N glycosidase domain of ricin are highlighted in *yellow*. Amino acid residues known to be important for the carbohydrate binding activity in ricin are shown in *green.* Putative N-glycosylation sites are highlighted in *pink*.

```
                                              1
Type 2   ---MTRVLAIYITLAFSLFLCGTECN---------ISFSTSGATSNSYNTFIKALRAQL 25
SNA-I    MRLVAKLLYLAVLAICGLGIHGALTHPRVTPPVYPSVSFNLTGADT-YEPFLRALQEKV 30
         :::.* : :       .* : *: :    1          :**. :** :   *:.*::**: ::


Type 2   TNGATAIYDIPVLNP--SVPDSQRFLLVDLSNNGNNTITVAIDVVNASVVAYRARAARPY 83
SNA-I    ILGNHTAFDLPVLNPESQVSDSNRFVLVPLTNPSGDTVTLAIDVVNLYVVAFSS-NGKSY 89
          *  : :*:*****  .*.**:**:** *:* ..:*:*:****** ***: :  ..:*


Type 2   FLADAPDEALDILFNDTRGFFLPFTSNYVDLEKAAEKSREKIPLGLTPLHNAITSLWNH- 142
SNA-I    FFSGSTAVQRDNLFVDTTQEELNFTGNYTSLERQVGFGRVYIPLGPKSLDQAISSLRTYT 149
         *::.:.      * ** **     * **.**..**: .  .*  **** ..*.:**:** .:


Type 2   ----ESEEAAVSLLVIIQTVFEAARFRVIEQRVRNSISSKANFIPDPAMLSLENNWLAIS 198
SNA-I    LTAGDTKPLARGLLVVIQMVSEAARFRYIELRIRTSITDASEFTPDLLMLSMENNWSSMS 209
             ::: * .***:** * ****** ** *:*.**:. ::* **   ***:**** ::*


Type 2   WETQHALNG-VFSKSIQLRSTNNNLFLVDSVSSSIMAG-VAFLFYNCVTFPN-------- 248
SNA-I    SEIQQAQPGGIFAGVVQLRDERNNSIEVTNFRRLFELTYIAVLLYGCAPVTSSSYSNNAI 269
          * *:*   * :*:  :***. :** : * ..  :    :*.*:*.*.....


Type 2   ---IIKMPVNVVMGKEIDNEICAVQNRTTHISGLEGLCVDVKNGLDSDGNLVQIWPCGQQ 305
SNA-I    DAQIIKMPV--FRGGEYE-KVCSVVEVTRRISGWDGLCVDVRYGHYIDGNPVQLRPCGNE 326
            ******  . * * : ::*:* : * :*** :******: *   *** **: ***::


Type 2   RNQKWTFQPDETIRSMEKCMTAYSTSSPENYVMIYNCTTAVLEATKWALSTDGTITHRRS 365
SNA-I    CNQLWTFRTDGTIRWLGKCLTASSS------VMIYDCNTVPPEATKWVVSIDGTITNPHS 380
          ** ***:.* *** : **:** *:       ****:*.*.  *****.:* *****: :*


Type 2   GLVLTAHEATRGTTLTIATNSHSPKQGWRVADDVEPTVTSIIGYNDMCLTANDDKSRVWM 425
SNA-I    GLVLTAPQAAEGTALSLENNIHAARQGWTVG-DVEPLVTFIVGYKQMCLRENGENNFVWL 439
         ****** :*:.**:*:::  .* *:.:*** *.  ****  ** *:**::*** *.::.  **:


Type 2   EYCVPSKNQQQWALYSEGTIRVNSDRTLCVTSNGHNSSNVIIILKCELKRGDQRWVFKTD 485
SNA-I    EDCVLNRVQQEWALYGDGTIRVNSNRSLCVTSEDHEPSDLIVILKCEGS-GNQRWVFNTN 498
         * **  .: **:****.:*******:*:*****:.*:. *:.*::***** .  *:*****:*:


Type 2   GSILNPNAELVMDVKNSDVYLRQIILYPYYGTPNQQWLPFF--- 526
SNA-I    GTISNPNAKLLMDVAQRDVSLRKIILYRPTGNPNQQWITTTHPA 542
         *:* ****:*:*** : ** **:****   *.*****:.
```

Figure 2.2B Sequence alignment of apple type 2 RIP and SNA-I (acc. no. U27122). '*' Means that the amino acids are identical in all sequences; ':' means conserved conversions (amino acids with the same shape, charge and other properties), and '.' semi-conserved substitution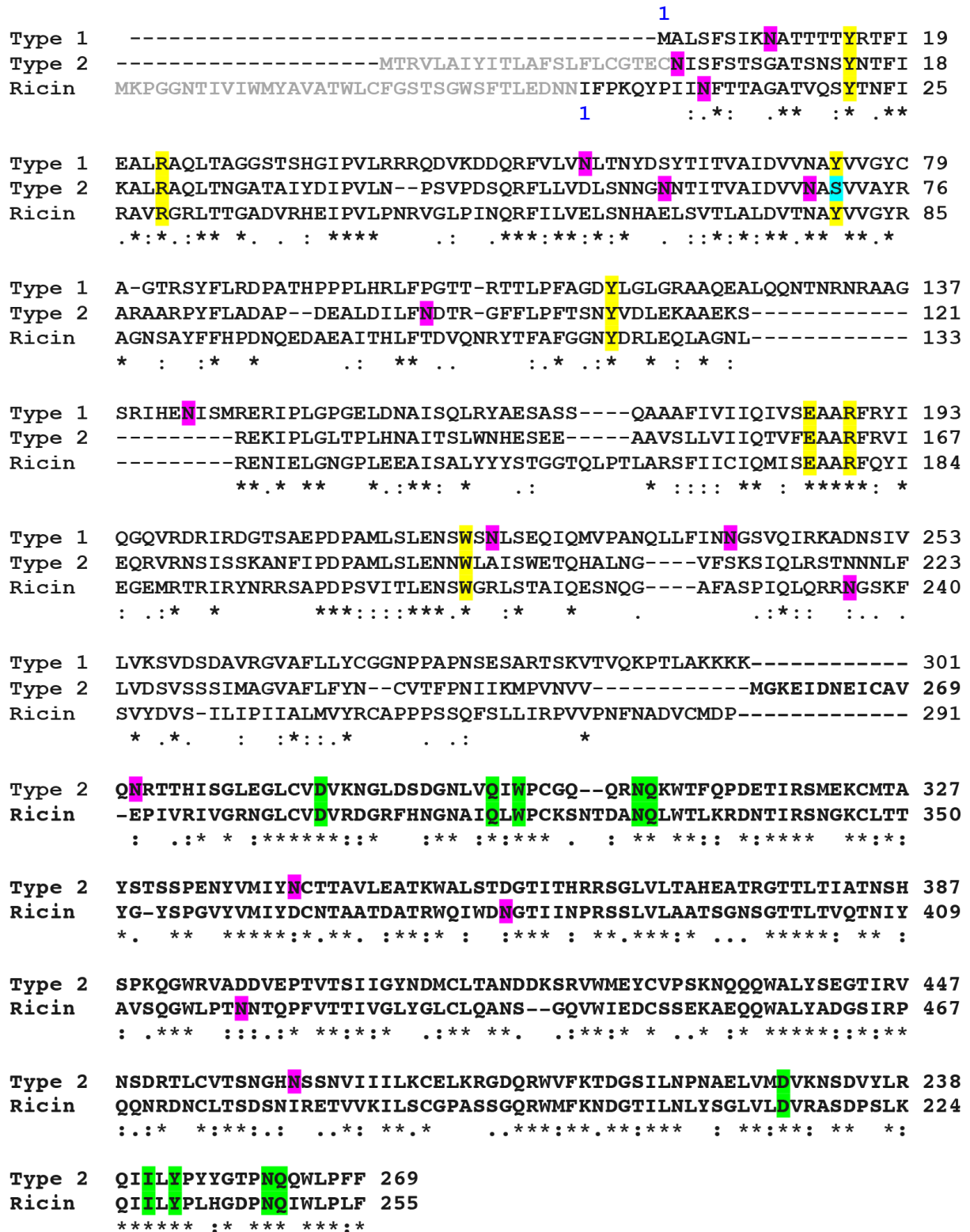s (properties not the same but still similar). The N-terminal signal peptide is shown in *gray*. Amino acid residues known to be important for the carbohydrate binding activity in ricin are shown in *green*; Residues reported to be critical for the binding to sialic acid in the Neu5Ac(α2-6)Gal/GalNAc sequence of 2-6-sialyllactose (according to Kaku et al., 2007) are indicated in *blue*. Basic residues for 6S-Gal binding according to Hu et al. (2012) are highlighted in *yellow*. Cys residues involved in disulfide bridges in SNA-I are shown in *red*. Putative N-glycosylation sites are highlighted in *pink*. The N-terminal sequence of the recombinant type 2 RIP determined by Edman degradation is underlined.

The *in silico* analysis allowed identifying the type 1 and type 2 RIP sequences in the apple genome but yielded apart from sequence data no information about the biochemical

properties and biological activities of the final protein products. Therefore the RIPs had to be purified and characterized. Since screening of the transcriptome database yielded only a few transcripts of the type 2 RIP gene and no transcript for the type 1 RIP gene it seemed likely that the expression level of these genes is (very) low and that accordingly it would be extremely difficult to purify the RIPs from apple tissue. Hence, both the type 1 and the type 2 RIP had to be produced as recombinant proteins. For the production of the apple type 1 RIP *P. pastoris* was chosen as an expression system whereas for the type 2 RIP tobacco BY-2 cells were used. The latter system was selected because it is known that tobacco cells are capable of correctly performing the rather complex co- and post-translational processing of the type 2 RIP (Buntru et al., 2014).

2.4.2 Purification and characterization of recombinant type 1 RIP from *P. pastoris*

The coding sequence of the apple type 1 RIP gene A (>MDP0000918923) was successfully cloned into the *E. coli*/*P. pastoris* pPICZαA shuttle vector and expressed into *P. pastoris* strain X-33. Because the expression vector contained the N-terminal α-mating sequence from *Sacharomyces cerevisiae* (for secretion) and C-terminal epitope tags (c-myc and His tag, Fig. 2.2C), the extracellular expression was detected by western blot analysis with an anti-His antibody. Subsequently, the recombinant type 1 RIP was purified using a combination of cation exchange chromatography and metal affinity chromatography. On average 2 mg recombinant type 1 RIP was purified from per liter medium of the *Pichia* culture.

MRFPSIFTAVLFAASSALAAPVNTTTEDETAQIPAEAVIGYSDLEGDFDVAVLPPFSNSTNNGLLFINTTIASIA AKEEGVSLEKRE^{86}**A**^{87}**EA**^{89}**EF**ALSFSIKNATTTTYRTFIEALRAQLTAGGSTSHGIPVLRRRQDVKDDQRFVLVN LTNYDSYTITVAIDVVNAYVVGYCAGTRSYFLRDPATHPPPLHRLFPGTTRTTLPFAGDYLGLGRAAQEALQQNT NRNRAAGSRIHENISMRERIPLGPGELDNAISQLRYAESASSQAAAFIVIIQIVSEAARFRYIQGQVRDRIRDGT SAEPDPAMLSLENSWSNLSEQIQMVPANQLLFINNGSVQIRKADNSIVLVKSVDSDAVRGVAFLLYCGGNPPAPN SESARTSKVTVQKPTLAKKKK*GLQKLISEEDLNSAVDHHHHHH*

Figure 2.1C Sequence of apple type 1 RIP construct expressed in *Pichia*. Note that the apple sequence is preceded by an N-terminal signal peptide from yeast (in bold) necessary for secretion and followed by a C-terminal tag containing a c-myc epitope and a (His)$_6$ tag (in bold and italic). The cleavage sites for the α-mating signal peptide sequence are indicated (Kex2 protease site at position 86 and Ste 13 protease sites at position 87 and 89). The N-terminal sequence of the recombinant type 1 RIP determined by Edman degradation is underlined. Putative N-glycosylation sites are highlighted in *gray*.

SDS-PAGE analysis revealed that the molecular mass of the recombinant type 1 RIP was approximately 38.8 kDa (Fig. 2.3A), which was ~ 2.7 kDa higher than the calculated

molecular mass of the recombinant type 1 RIP including the c-myc and $(His)_6$ tags (36.1 kDa). Western blot analysis with a monoclonal antibody directed towards the His tag (Fig. 2.3B) or antibody specifically directed against the type 1 RIP confirmed that the 38.8 kDa band corresponded to the recombinant RIP. Edman degradation of the recombinant type 1 RIP yielded the sequence EAEAEFALSFSI. Since the EA repeats in this sequence correspond to the *Pichia* α-mating sequence it can be concluded that the signal peptide sequence was not correctly cleaved by the Ste13 protease.
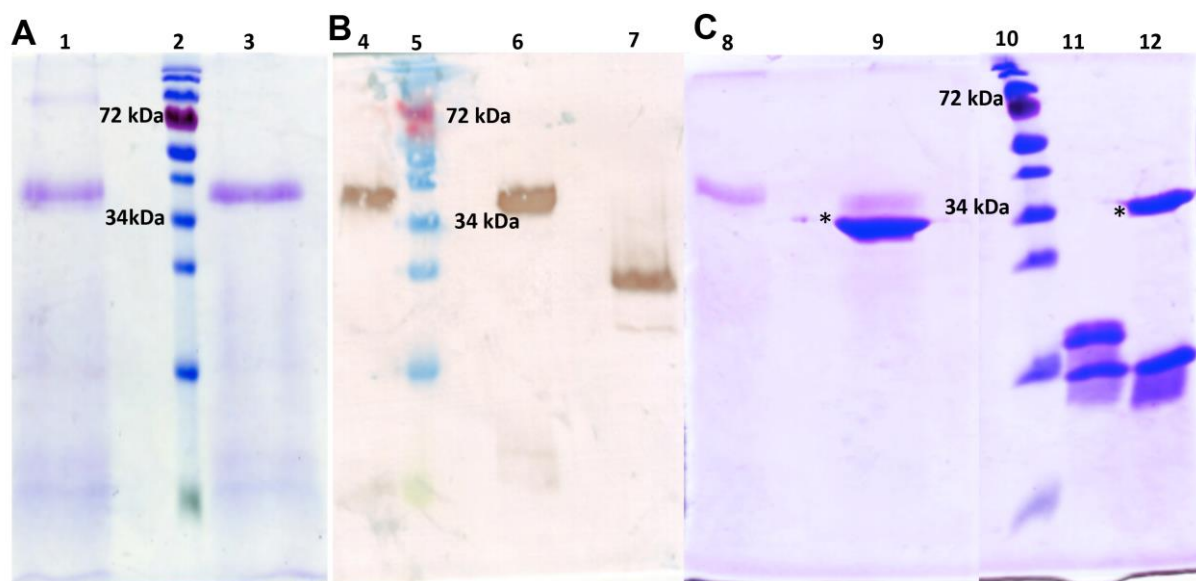

Figure 2.3 SDS-PAGE and Western blot analysis of recombinant type 1 RIP.

Panel A and B: SDS-PAGE and Western blot analysis with a monoclonal anti-His antibody, respectively of recombinant type 1 RIP; lanes 1 and 4 unreduced type 1 RIP, lanes 3 and lane 6: reduced type 1 RIP, lanes 3 and lane 6: reduced type 1 RIP treated with betamercaptoethanol, lane 7: positive control (S2, Al Atalah et al., 2011). Panels C: SDS-PAGE after PNGase F treatment of the recombinant type 1 RIP, lane 8: untreated type 1 RIP, lane 9: type 1 RIP treated with PNGase F, lane 11: untreated RNAseB, lane 12: RNAseB treated with PNGase F. Protein ladder (increasing molecular mass: 10, 15, 25, 35, 45, 55, 70, 100, 130, 170 kDa) (Fermentas) was run in lanes 2, 5 and 10. The position of the polypeptide corresponding to PNGase F is indicated with an asterisk.

2.4.3 Purification and characterization of recombinant type 2 RIP from *BY-2* cells

Cloning of the coding sequence of the type 2 RIP gene (>MDP0000711911) into the vector pKCTAP yielded a fusion construct with a C-terminal $(His)_6$ tag. The protein was expressed under the control of the 35S CaMV promoter. The transformed BY-2 cells were selected after microscopic detection of expressed EGFP signals. Only the positive colonies were transferred into the liquid culture. After growth of the cells for 6 weeks the fusion protein, the type 2 RIP

was purified from the medium using a combination of hydrophobic interactions chromatography and affinity chromatography. Approximately 10 mg of purified recombinant type 2 RIP was obtained per liter medium.

SDS-PAGE analysis (Fig. 2.4A) of reduced (with beta-mercaptoethanol) recombinant apple type 2 RIP yielded a major polypeptide band of 65.5 kDa and a minor band of ~80kDa while the unreduced protein yielded besides the major 65.5 kDa and minor bands of ~80kDa one additional minor bands of high molecular weight (~110 kDa). The size of the major 65.5 kDa polypeptide bands is approximately 4 kDa higher than the calculated molecular mass of the apple type 2 RIP (61. 5 kDa, A and B domain containing a $(His)_6$ tag). Western blot analysis using a polyclonal antibody against the apple type 1 RIP confirmed that the 65.5 kDa polypeptide reacts with the RIP antibody (Fig. 2.4B). Western blot analysis using a monoclonal anti-His antibody yielded no signal indicating that the C-terminal His tag in the recombinant type 2 RIP cannot be detected. Edman degradation of the 65.5 kDa polypeptide yielded the sequence of GATAXXDIXXL, which implies that besides the signal peptide an extra propeptide of 27 AA residues is cleaved at the N-terminus of the recombinant type 2 RIP secreted to the BY-2 cell medium.

The combined results of the SDS-PAGE and western blot analysis (Fig. 2.4B) indicate that the A and B chain are still located on a single polypeptide in the recombinant apple RIP, which implies that the processing step whereby the linker between the A and B chain is excised from the precursor protein does not take place. This observation was rather surprising because it is well known that –at least in transgenic plants- tobacco cells are fully capable of carrying out the "canonical" cleavage of the type 2 RIP precursors into the A and the B chain. To check whether the lack of processing is due to the incapability of the BY-2 cells to excise the linker sequence or is an inherent feature of the apple type 2 RIP a crude extract from very young (10 days post-pollination) apple (*Malus domestica* cv 'Golden delicious') fruits was analyzed by SDS-PAGE and subsequent western blot analysis. As shown in Fig. 2.4C the type 2 RIP present in the fruit tissue also yields a molecular mass of ~66 kDa corresponding to a polypeptide that was not cleaved into an A and a B chain. These data suggest that the apple type 2 RIP does -unlike all previously studied type 2 RIP not undergo the proteolytic removal of the linker between the A and the B chain.
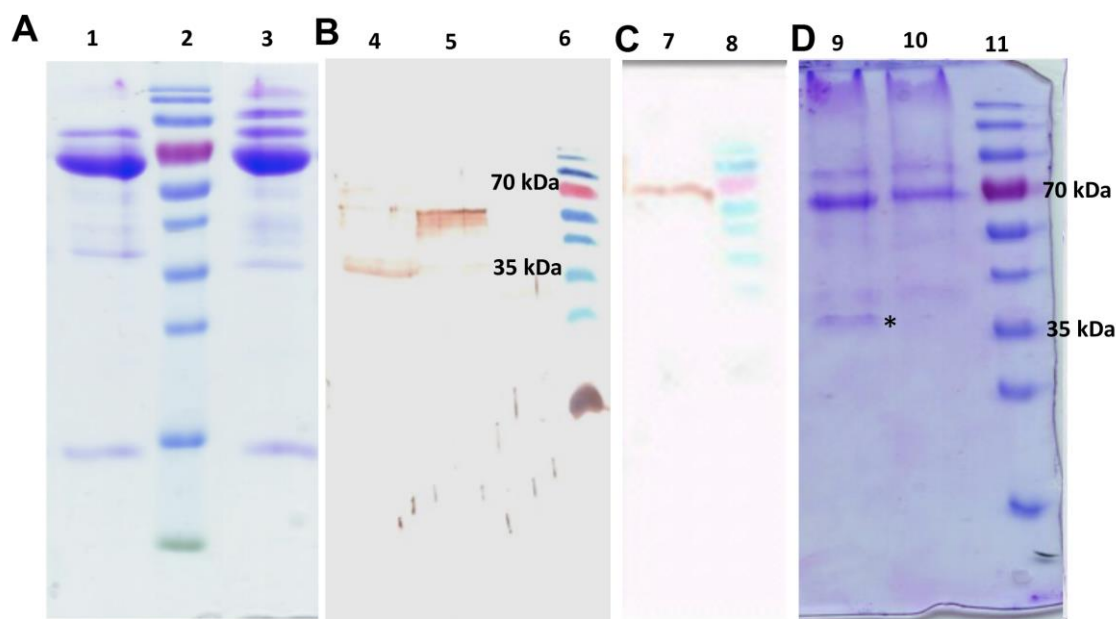
Figure 2.4 SDS-PAGE and Western blot analysis of recombinant type 2 RIP.
Panels A and B: SDS-PAGE and Western blot analysis with a polyclonal anti-type 1 RIP antibody, respectively, of recombinant type 2 RIP, lanes 1 and 5: reduced type 2 RIP, lane 3: unreduced type 2 RIP, lane 4: positive control (type 1 RIP). Panel C: Western blot analysis of a crude extract from apple with a polyclonal anti-type 1 RIP antibody. lane 7: reduced crude extract. Panels D: SDS-PAGE after PNGase F treatment of the recombinant type 2 RIP, lane 9: type 2 RIP treated with PNGase F, lane 10: untreated type 2 RIP. The position of the polypeptide corresponding to PNGase F is indicated with an asterisk. Protein ladder (increasing molecular mass: 10, 15, 25, 35, 45, 55, 70, 100, 130, 170 kDa) (Fermentas) was run in lanes 2, 5, 6, 8 and 11.

2.4.4 Glycosylation analysis

Since it could be inferred from the deduced sequences that both the type 1 and type 2 RIP sequences comprise multiple putative N-glycosylation sites (Fig. 2.3A and 2.4A) the recombinant proteins produced in *P. pastoris* and tobacco BY-2 cells, respectively, are in principle prone to glycosylation. To check the presence of N-glycans the recombinant proteins were digested with PNGase F. As shown in Fig. 2.3C and 2.4D PNGase F treatment of the type 1 and type 2 RIPs resulted in a shift of approximately 1.7 kDa and 2 kDa, respectively, indicating that both recombinant proteins are N-glycosylated.

2.4.5 Agglutination activity and carbohydrate binding properties of recombinant type 2 RIP

To check the carbohydrate binding activity, the recombinant apple type 2 RIP was tested for agglutination activity towards trypsin treated rabbit erythrocytes. The recombinant protein behaved as a genuine lectin, the minimal concentration required for agglutination being 1.55 µg/ml. Preliminary hapten inhibition assays indicated that galactose and the glycoproteins

fetuin and thyroglobulin (Table 2.2) inhibited the agglutination activity of the recombinant type 2 RIP. A more detailed analysis of the carbohydrate binding specificity was carried out using glycan microarray v5.0 (Fig. 2.5). A summary of the most strongly interacting glycans is presented in Table 2.3. The same table also includes a comparison to the sugar-binding properties of SNA-I. It appears that the apple type 2 RIP reacts preferentially with Neu5Ac (glycan #11) and glycans carrying at least one terminal Neu5Ac residue as well as with KDNα2-6Galβ1-4GlcNAc (glycan #357) (Table 2.3). Furthermore, the apple type 2 RIP interacted also with Neu5Gc (glycan #286) but less strongly than with Neu5Ac.

Table 2.2 Carbohydrate binding specificity of recombinant type 2 RIP expressed in BY-2 cells.

		Inhibitory activity
Glycoprotein	Thyroglobulin	0.06 mg/ml
	Fetuin	0.06 mg/ml
	Ovomucoid	0.5 mg/ml
	Mucine	0.5 mg/ml
	Asialoimucin	1 mg/ml
Sugar	Mannose	0.05 M
	Galactose	0.0125 M
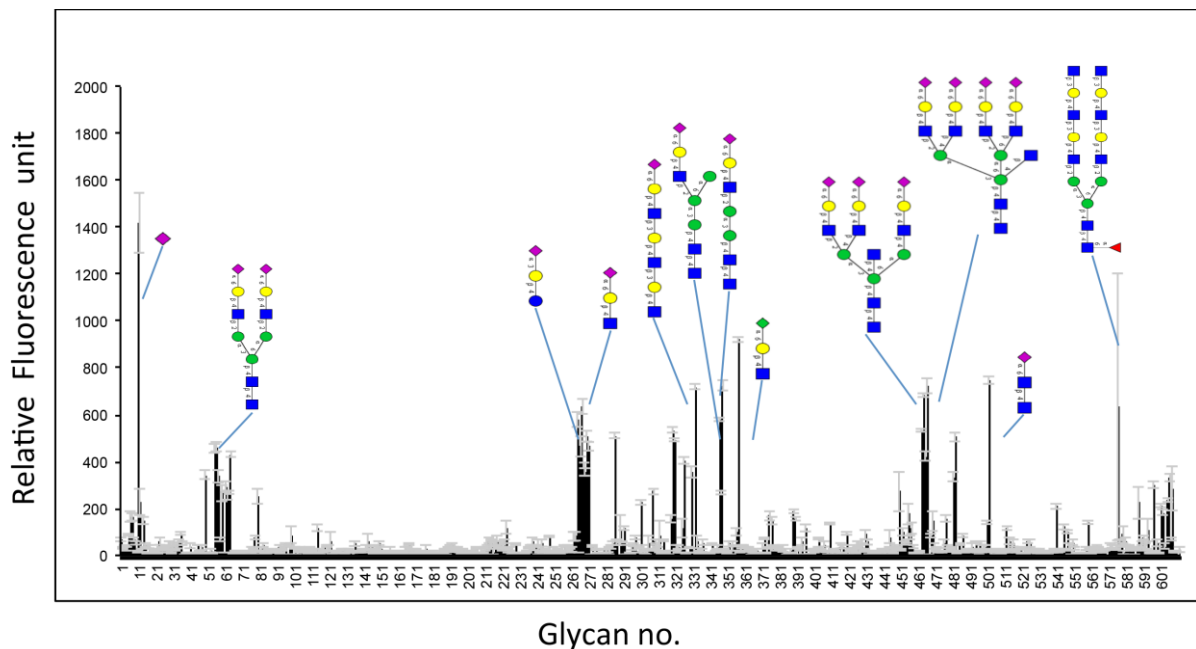
Figure 2.5 Glycan array analysis of recombinant type 2 RIP from apple (*Malus domestica*) at 300 µg/ml. The Consortium for Functional Glycomics website (http://www.functionalglycomic. org) supports the complete raw data for all the proteins. Sugar code used: green circles represent mannose residues, yellow circles indicate Gal, blue squares indicate GlcNAc residues, red triangles show fucose, purple diamonds indicate NeuAc and green diamonds indicate Kdn.

Table 2.3 Overview of the top 30 glycans interacting with the apple type 2 RIP and comparative analysis with SNA-I. The glycan with the highest relative fluorescence unit (RFU) is assigned a value of 100. The rank is the percentile ranking. NA: not available in this glycan array version.

Glycan no	Structure	Apple type 2 RIP 300µg/ml		SNA-I 0.1µg/ml	
		RFU	Rank	RFU	Rank
11	Neu5Acβ-Sp8	1421	100	25	0.09
357	KDNα2-6Galβ1-4GlcNAc-Sp0	922	64.9	30	0.11
502	Neu5Acα2-6GalNAcβ1-4(6S)GlcNAcβ-Sp8	746	52.5	NA	NA
348	Neu5Acα2-6Galβ1-4GlcNAcβ1-2Manα1-3Manβ1-4GlcNAcβ1-4GlcNAc-Sp12	724	51.0	17952	65.01
466	Neu5Acα2-6Galβ1-4GlcNAcβ1-6(Neu5Acα2-6Galβ1-4GlcNAcβ1-2)Manα1-6(GlcNAcβ1-4)(Neu5Acα2-6Galβ1-4GlcNAcβ1-4(Neu5Acα2-6Galβ1-4GlcNAcβ1-2)Manα1-3)Manβ1-4GlcNAcβ1-4GlcNAcβ-Sp21	721	50.8	NA	NA
332	Neu5Acα2-6Galβ1-4GlcNAcβ1-3Galβ1-4GlcNAcβ1-3Galβ1-4GlcNAcβ-Sp0	719	50.6	24563	88.95
464	Neu5Acα2-6Galβ1-4GlcNAcβ1-4Manα1-6(GlcNAcβ1-4)(Neu5Acα2-6Galβ1-4GlcNAcβ1-4(Neu5Acα2-6Galβ1-4GlcNAcβ1-2)Manα1-3)Manβ1-4GlcNAcβ1-4GlcNAcβ-Sp21	683	48.1	NA	NA
267	Neu5Acα2-6Galβ1-4(6S)GlcNAcβ-Sp8	638	44.9	14288	51.74
576	GlcNAcβ1-3Galβ1-4GlcNAcβ1-3Galβ1-4GlcNAcβ1-2Manα1-6(GlcNAcβ1-3Galβ1-4GlcNAcβ1-3Galβ1-4GlcNAcβ1-2Manα1-3)Manβ1-4GlcNAcβ1-4(Fucα1-6)GlcNAc-Sp24	633	44.6	NA	NA
264	Neu5Acα2-3Galβ1-4Glcβ-Sp8	582	40.9	18033	26.30
346	Manα1-6(Neu5Acα2-6Galβ1-4GlcNAcβ1-2Manα1-3)Manβ1-4GlcNAcβ1-4GlcNAc-Sp12	581	40.9	NA	NA
319	Galβ1-4GlcNAcβ1-2Manα1-6(Neu5Acα2-6Galβ1-4GlcNAcβ1-2Mαnα1-3)Manβ1-4GlcNAcβ1-4GlcNAcβ-Sp12	533	37.5	22956	83.13
463	Neu5Acα2-6Galβ1-4GlcNAcβ1-2Manα1-6(GlcNAcβ1-4)(Neu5Acα2-6Galβ1-4GlcNAcβ1-2Manα1-3)Manβ1-4GlcNAcβ1-4GlcNAcβ-Sp21	533	37.5	NA	NA
286	Neu5Gcα2-6Galβ1-4GlcNAcβ-Sp0	510	35.9	13790	49.94
270	Neu5Acα2-6Galβ1-4GlcNAcβ1-3Galβ1-4(Fucα1-3)GlcNAcβ1-3Galβ1-4(Fucα1-3)GlcNAcβ-Sp0	510	35.9	20964	75.91
482	Neu5Acα2-6Galβ1-4GlcNAcβ1-2Manα1-6(Neu5Acα2-6Galβ1-4GlcNAcβ1-2Manα1-3)Manβ1-4GlcNAcβ1-4(Fucα1-6)GlcNAcβ-Sp24	504	35.5	NA	NA
320	GlcNAcβ1-2Manα1-6(Neu5Acα2-6Galβ1-4GlcNAcβ1-2Manα1-3)Manβ1-4GlcNAcβ1-4GlcNAcβ-Sp12	493	34.7	14464	52.38
271	Neu5Acα2-6Galβ1-4GlcNAcβ1-3Galβ1-4GlcNAcβ-Sp0	467	32.9	25668	92.95
266	Neu5Acα2-6GalNAcβ1-4GlcNAcβ-Sp0	466	32.8	29	0.11
56	Neu5Acα2-6Galβ1-4GlcNAcβ1-2Manα1-6(Neu5Acα2-6Galβ1-4GlcNAcβ1-2Man-α1-3)Manβ1-4GlcNAcβ1-4GlcNAcβ-Sp21	462	32.5	NA	NA
55	Neu5Acα2-6Galβ1-4GlcNAcβ1-2Manα1-6(Neu5Acα2-6Galβ1-4GlcNAcβ1-2Manα1-3)Manβ1-4GlcNAcβ1-4GlcNAcβ-Sp12	458	32.3	18898	66.44
64	Fucα1-2Galβ1-3GalNAcβ1-4(Neu5Acα2-3)Galβ1-4Glcβ-Sp9	429	30.2	19	0.07
465	Neu5Acα2-6Galβ1-4GlcNAcβ1-6(Neu5Acα2-6Galβ1-4GlcNAcβ1-2)Manα1-6(GlcNAcβ1-4)(Neu5Acα2-6Galβ1-4GlcNAcβ1-2Manα1-3)Manβ1-4GlcNAcβ1-4GlcNAcβ-Sp21	424	29.8	NA	NA
326	Neu5Acα2-3Galβ1-4GlcNAcβ1-2Manα1-6(Neu5Acα2-6Galβ1-4GlcNAcβ1-2Manα1-3)Manβ1-4GlcNAcβ1-4GlcNAcβ-Sp12	406	28.5	10	0.04

268	Neu5Acα2-6Galβ1-4GlcNAcβ-Sp0	370	28.6	27613	100
269	Neu5Acα2-6Galβ1-4GlcNAcβ-Sp8	355	26.0	14288	51.74
330	Neu5Acα2-6Galβ1-4GlcNAcβ1-3Galβ1-3GlcNAcβ-Sp0	353	25	21014	76.10
49	Neu5,9Ac2α2-6Galβ1-4GlcNAcβ-Sp8	344	24.9	21953	79.50
57	Neu5Acα2-6Galβ1-4GlcNAcβ1-2Manα1-6(Neu5Acα2-6Galβ1-4GlcNAcβ1-2Manα1-3)Manβ1-4GlcNAcβ1-4GlcNAcβ-Sp24	339	24.2	NA	NA
481	Neu5Acα2-6Galβ1-4 GlcNAcβ1-6(Neu5Acα2-6Galβ1-4GlcNAcβ1-3)GalNAcα-Sp14	334	23.9	NA	NA

2.4.6   Apple RIPs inhibit protein synthesis *in vitro*

To check the N-glycosidase activity a eukaryotic cell free translation system (based on a rabbit reticulocyte lysate) was challenged with the recombinant apple RIPs. As shown in Fig. 2.6 both the type 1 and type 2 RIPs exhibited a concentration-dependent translation-inhibiting activity, the IC50 value being 186.6 nM and 300.7 nM, respectively. These values are 30 to 50-fold higher than the IC50 determined for SNA-I (IC50=5.88 nM) in the same experiment (Fig. 2.6C). It can be concluded, therefore, that the apple RIPs possess N-glycosidase activity but are only moderately active as compared to e.g. SNA-I.
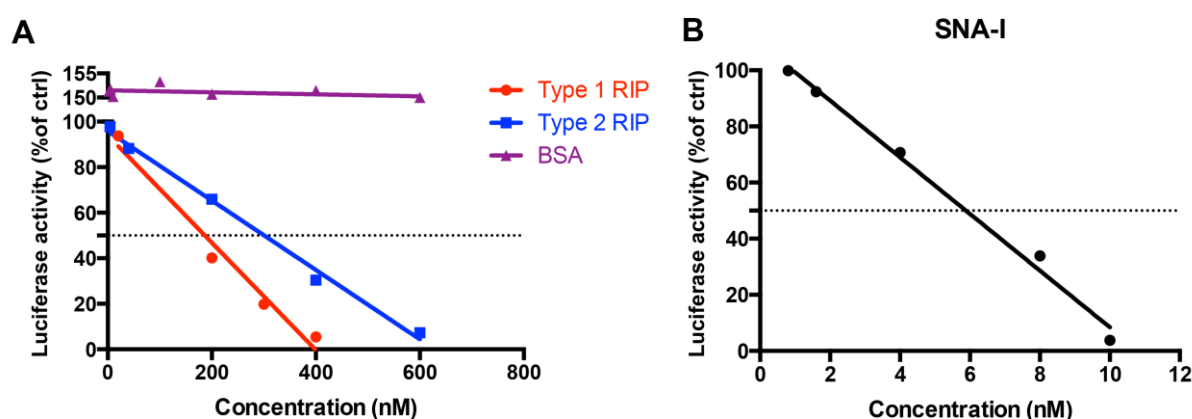

Figure 2.6 Effect of the apple RIPs on protein synthesis in a cell-free translation assay. Panel A: Luciferase activity as a function of the concentration of apple type 1 and type 2 RIPs. BSA was included as a negative control. Panel B: Luciferase activity as a function of the concentration of SNA-I (type 2 RIP, positive control).

2.4.7   Cytotoxicity of apple RIPs to mammalian cells

To assess the cytotoxicity/antiproliferative activity of the apple RIPs HeLa and NHDF cells were challenged with increasing concentrations (0.05-2 µM) of the recombinant apple RIPs and cell viability was followed by spectrophotometric assays. As shown in Fig. 2.7A the type 1 RIP had no effect at all on HeLa and NHDF cell viability and proliferation after incubation of the cells and the RIP for 24 h and 48 h. Surprisingly, the value for the NHDF cells incubated with type 1 RIP for 48 h was much higher than that of the control (1x PBS), suggesting that the type 1 RIP might stimulate cell growth. In contrast, the apple type 2 RIP caused a significant ($p<0.05$) cytotoxicity towards both cell lines. There was a clear dose- and time-dependent effect, indeed, for the type 2 RIP on HeLa and NHDF cell lines. After 24 h and 48 h incubation, a significant effect on cell viability was observed for the type 2 RIP ($p<0.05$) at a concentration of 0.6 µM. The cytotoxic effect on HeLa cells was accompanied by clear

morphological changes such as cell rounding and blebbing (Fig. 2.7C). The LC50 values for the type 2 RIP on HeLa cells were 1.13 µM and 0.84 µM after 24h and 48h incubation, respectively. For comparison, the LC50 values for the type 2 RIP on NHDF cells were 0.86 µM and 0.66 µM after 24h and 48h incubation, respectively. As evidenced by the marginally increased LC50 values, NHDF cells were slightly more susceptible to the recombinant type 2 RIP than HeLa cells.
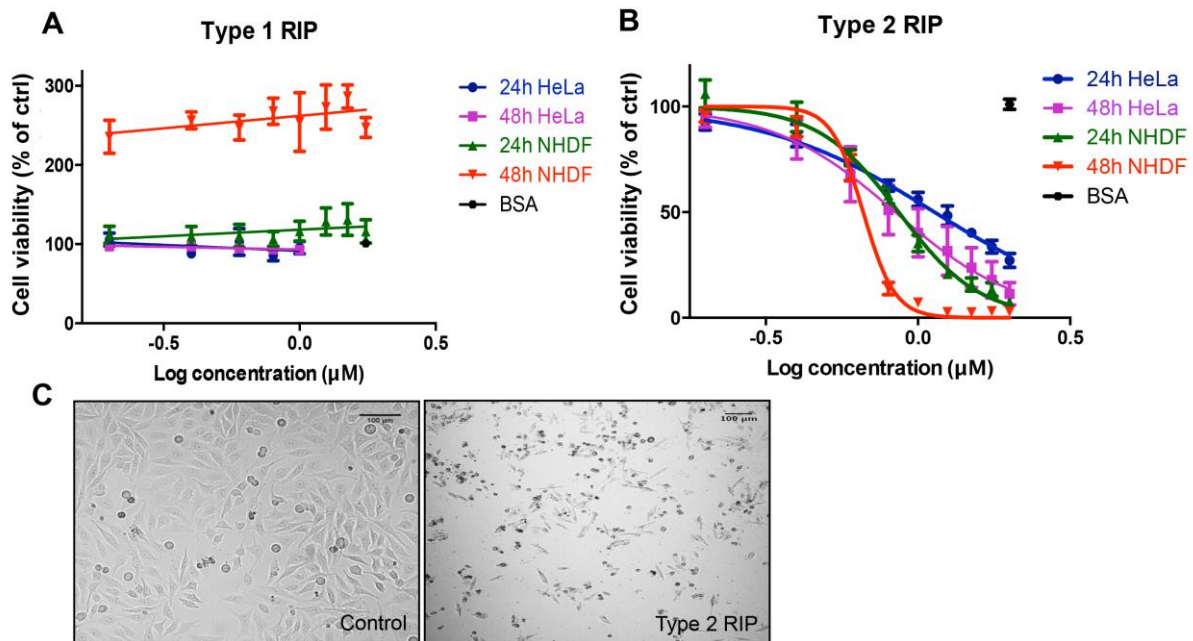

Figure 2.7 Effect of recombinant apple RIPs on HeLa cervix carcinoma and NHDF cell viability after incubation for 24 and 48 h. Panels A and B: Viability of HeLa and NHDF cells upon incubation for 24 and 48h in the presence of increasing concentrations of apple type 1 and type 2 RIPs, respectively. Results are expressed as % ctrl (treated/control X 100) = ratio of surviving treated cells/ surviving cells percent in control. All data are expressed as means ± SE of 3 biological replicates in 4 technical replicates (n=12). Panel **C**: Transmission light microscopy images of HeLa cells grown in the absence (control) and presence of 2 µM type 2 RIP for 24h. Scale bars represent 100 µm.

2.5 Discussion

This present chapter deals with a biochemical/functional study of the proteins encoded by the type 1 and type 2 RIP genes identified in the apple *(Malus domestica)* genome. Due to the very low expression levels the purification of mg quantities of the native type 1 and type 2 RIPs starting from apple tissues was impractical. Therefore the RIP genes were expressed in a heterologous system and the recombinant proteins purified by conventional protein purification techniques. Recombinant type 1 RIP was successfully expressed in the cell medium of *P. pastoris* (strain X-33) cells. The yield was approximately 2 mg per liter medium, which is rather low as compared to the yields reported for other proteins in the same expression system (6-8 mg/L) (Al Atalah et al., 2011). *P. pastoris* was not retained as an

expression system for the apple type 2 RIP since this organism is most likely not capable of properly performing the complex co- and translational processing required to convert the primary translation product of a type 2 RIP sequence into the mature biologically active protein. Therefore tobacco BY-2 cells were chosen as an expression system because as can be concluded from previously reported experiments with transgenic plants tobacco cells are capable of producing correctly processed recombinant type 2 RIP (Chen et al., 2002a). As was expected BY-2 cells express and secrete the apple type 2 RIP in the BY-2 medium, the final concentration exceeding 10 mg per liter.

SDS-PAGE and Western blot analysis allowed determining the molecular structure of the recombinant RIPs. The type 1 RIP purified from *P. pastoris* behaves as a single polypeptide of approximately 38.8 kDa on SDA-PAGE. Enzymatic deglycosylation reduces the apparent Mr by 1.7 kDa suggesting that 1 out of 4 potential N-glycosylation sites carry an N-glycan. Though the protein is secreted by the *P. pastoris* cells Edman degradation of the recombinant type 1 RIP revealed that the processing of the α-mating sequence from *Saccharomyces cerevisiae* was not correctly performed by the Ste13 protease. Problems with correct processing of this α-mating sequence have been reported before at several occasions (Al Atalah et al., 2011; Oliveria et al., 2008; Lannoo et al., 2007). Despite the incorrect/incomplete processing of the N-terminal α-mating sequence and the presence of a His tag at the C-terminus the recombinant type 1 RIP is catalytically active (see below). It should be emphasized here that the native type 1 RIP produced by the apple cells is synthesized without a signal peptide and accordingly is presumably not N-glycosylated since it does not enter the secretory pathway.

Recombinant type 2 RIP produced by BY-2 cells yielded a major polypeptide band of ~65.5 kDa upon SDS-PAGE both in its reduced and unreduced form. This implies that unlike all other type 2 RIPs studied thus far the processing step whereby the linker between the A and B chain is excised does not take place in the recombinant apple type 2 RIP. Since the latter processing step does also not take place in the apple tissue itself, one can only conclude that there is some particularity in the sequence of the apple type 2 RIP that renders it insensitive to the "canonical" proteolytic cleavage of the linker sequence between the A and B chain. N-terminal sequence analysis of recombinant apple type 2 RIP suggests that not only the signal peptide but also a 27 AA propeptide is cleaved at the N-terminus. Moreover, the His tag artificially added at the C-terminus of the coding sequence of the type 2 RIP sequence was never detected by a monoclonal antibody directed towards the polyhistidine tag (data not shown). These findings suggest that some undefined proteases present in the medium of the BY-2 cells do modify the secreted type 2 RIP, which is not surprising since several reports

describe similar proteolytic modifications of other proteins expressed in this system (Yang et al., 2012; Magy et al., 2014; Mandal et al., 2014). Most probably, the proteolytic modifications in the medium do not affect the biological activity of the recombinant type RIP since it exhibits both N-glycosidase and carbohydrate binding activity (see below).

The apparent Mr of the recombinant apple type 2 RIP (Fig. 2.4A) is considerably higher than the Mr calculated from the deduced AA sequence. Taking into account that the AA sequence comprises seven putative N-glycosylation sites the recombinant protein was treated with PNGase F SDS-PAGE indicated that there was 2 kDa was shift after PNGase treatment, suggesting that one N-glycosylation site was probably glycosylated.

Translation inhibition experiments with a cell-free system derived from rabbit reticulocytes confirmed that both recombinant apple RIPs possess N-glycosidase activity. However, the catalytic activity of the type 1 RIP (IC50= 186.6 nM) and the type 2 RIP (IC50= 300.7 nM) is much lower than that of SNA-I (included in the same experiment as a positive control) and four orders of magnitude inferior to the values reported for ricin (IC50= 100 pM, Ferreras et al., 2011). According to previous work (Kim and Robertus, 1992) the replacement of Tyr[80] of ricin by Ser[71] accounts for a 160-fold reduction in the catalytic activity. Hence this AA substitution in the apple type 2 RIP sequence can explain the higher IC50 value. However this reasoning does not hold true for the apple type 1 RIP in which the Tyr[80] of ricin is conserved. Therefore, it is likely that residues other than those involved in the canonical active site also influence the catalytic properties of the apple RIPs. The value of BSA (negative control) is 50% higher than we expected (Fig 2.7A), suggesting BSA does not inhibit protein synthesis and even enhances cell viability. This is consistent with the reports of BSA increasing transcription and translation (Li et al., 2014) and luminescence intensity (He and Ma, 2013).

The apple type 2 RIP not only exhibits N-glycosidase activity but also behaves as a genuine lectin with a well-defined carbohydrate binding activity and specificity. Glycan microarray assays revealed that the recombinant type 2 RIP preferentially interacts with Neu5Ac and glycans carrying at least one terminal Neu5Ac(α2-6)Gal/GalNAc residue, and also strongly interacts with 2-keto-3-deoxy-D-glycero-D-galactononic acid (KDN). In addition, the type 2 RIP reacted with a non sialylated complex glycan. Though the preferential interaction with Neu5Ac and glycans carrying terminal Neu5Ac(α2-6)Gal/GalNAc residue is reminiscent of the carbohydrate binding specificity of SNA-I the results summarized in Table 2.3 leave no doubt that there are major differences between both lectins. For example the apple RIP has a much higher affinity for Neu5Ac than for Neu5Ac(α2-6)Galβ1-4GlcNAc whereas for SNA-I this is the

reverse. Though still speculative the latter observation might indicate that the binding site of the apple type 2 RIP is less extended compared to that of SNA-I.

Viability assays with HeLa and NHDF cells indicated that the apple type 1 RIP is virtually devoid of cytotoxicity. In contrast, the type 2 RIP reduced the viability of both HeLa and NHDF cells in a dose- and time-dependent manner, and also provoked morphological changes such as cell rounding and shrinking. It should be emphasized, however, that the cytotoxicity of the apple type 2 RIP is several orders of magnitude lower than that of a genuine toxin like ricin. The latter observation is rather trivial within the context of a comparative study of the toxicity of type 2 RIPs but is of paramount interest for what concerns the possible food safety related issues raised by the predicted occurrence of a ricin homolog in apple.

Chapter 3

Subcellular and tissue localization of ribosome-inactivating proteins from apple (*Malus domestica*)

3.1 Abstract

Sequence analysis indicated that the apple type 1 RIP sequence does not contain a signal peptide sequence, and revealed the presence of a nuclear localization targeting signal (NLS) ^{298}KKKK^{301}. In contrast, the type 2 RIP sequence possesses a 22 amino acid N-terminal hydrophobic signal peptide (SP). These differences in their sequences suggested that these two proteins will be synthesized in different cellular compartments, resulting in a different subcellular localization for the two RIPs. In this study, three transient transformation systems as well as stable transformation in Arabidopsis plants have been performed to investigate the subcellular localization of fusion proteins for (part of) the RIP sequences coupled to enhanced green fluorescent protein (EGFP). Confocal microscopy revealed that the type 1 RIP fusion with N- and C-terminal EGFP located to the nucleus and the cytoplasm. All fusion proteins containing the SP from the type 2 RIP coding sequence followed the secretory pathway. The construct of SP::EGFP was targeted to the vacuole and fluorescence also appeared in some vesicles. Furthermore, fusion proteins for the type 2 RIP were secreted into intercellular space without any evidence that these fluorescent proteins also pass by the vacuole. Quantitative analysis of the transcript levels demonstrated that the type 2 RIP is present during the early stages of development, being abundant especially in young tissues. Unfortunately no transcripts were detected for the type 1 RIP in any of the tissues tested. These data on the subcellular and tissue specific localization of the RIPs will contribute to a better understanding of the physiological role of these RIPs in the plant cell.

3.2 Introduction

Ribosome-inactivating proteins accumulate in different plant organs of many plant species (Marshall et al., 2011; de Virgilio et al., 2010). Some RIPs are highly abundant in a single tissue, while others have been identified in different plant tissues (roots, leaves, stems, bark, flowers, fruits, seeds, latex) (Stirpe, 2004). In some cases there is also evidence for developmental regulation of RIP expression, or even stress inducible expression of RIPs (Chaudhry et al., 1994; Rustgi et al., 2014, Xu et al., 2007; Song et al., 2000; Reinbothe et al., 1994a,b; Müller et al., 1997).

Previous molecular and biochemical studies indicated that RIPs can be divided into two major groups. One group comprises the type 1 RIPs, consisting of one single enzymatic chain (Van Damme et al., 2001) and the second group contains all type 2 RIPs, composed of an A chain and a B chain, linked by a disulfide bridge (de Virgilio et al., 2010). Most type 2 RIP sequences contain a N-terminal signal peptide. These proteins are synthesized following the secretory pathway (including biosynthesis and sorting) starting with protein synthesis on ER

associated ribosomes, transport through the Golgi complex, and eventually targeting to the vacuole/protein bodies or secretion to the intercellular space (Rojo and Denecke, 2008; De Marcos et al., 2012). In recent years the biosynthesis of type 2 RIPs was studied in great detail, with special focus on ricin. It was shown that targeting of the ricin precursor to its final destination in the cell is associated with processing of the RIP precursor polypeptide, in particular the processing of the linker peptide located between the A and B chain, the latter processing step being important for generating a fully functional and toxic ricin (Frigerio and Roberts, 1998).

Compared to type 2 RIPs, the biosynthesis of type 1 RIP got much less attention. Similar to type 2 RIPs most type 1 RIPs are also synthesized as precursors containing a signal peptide, and hence they are translocated to the ER and follow the secretory route, with final targeting to the vacuole or the intercellular space, as demonstrated for saporin and pokeweed antiviral protein, respectively (Marshall et al., 2011). However, some cereal type 1 RIPs are also known as cytosolic proteins (Nielsen and Boston, 2001; Frigerio and Roberts, 1998), such as the maize kernel RIP (b-32) (Walsh et al., 1991) and the barley RIP (RIP 30) (Leah et al., 1991). In particular the type 1 RIPs from Poaceae are synthesized without a signal peptide and hence are translated on free ribosomes in the cytoplasm, and finally presumably locate to the cytoplasm and nucleus. At present, there are no microscopical data for the nuclear localization of type 1 RIPs.

The subcellular localization of eukaryotic proteins is crucial for the proteins to execute their biological functions (Xiang et al., 2013). Proteins must be targeted to or retained in the correct subcellular compartment(s) or organelle(s) at the right time during plant development. To obtain some first indications on the subcellular localization of the apple RIPs, we used sequence analysis tools to check for the presence of signal peptides and possible targeting peptides. In addition, transient transformation assays (*N. benthamiana* plants, *Arabidopsis* protoplasts and *Arabidopsis* cells) combined with stable transformation of *Arabidopsis* plants allowed to investigate the subcellular localization of the apple RIP sequences fused to EGFP. To gain better insights in the tissue-specific expression of RIPs, a quantitative analyses was performed to study the transcript levels of apple RIPs in different tissues from three different varieties of apple, in particular 'Golden Delicious', 'Jonagold' and 'James Grieve', throughout development.

3.3   Materials and methods

3.3.1   *In silico* analysis

The tools Phobius (http://www.ebi.ac.uk/Tools/pfa/phobius/, Käll et al., 2007) and target P (http://www.cbs.dtu.dk/services/TargetP/, Emanuelsson et al., 2000) were used to predict whether the RIP sequences are synthesized with a SP. A transcriptome analysis was performed by searching type 1 or type 2 RIP sequences from apple in the translated Expressed Sequence Tags (EST) database (tBLASTn) from the National Center for Biotechnology Information (NCBI).

3.3.2   Plant materials

Seeds of *N. benthamiana* and *A. thaliana* ecotype Columbia (Col-O) were supplied by Dr. Verne A. Sisson (Oxford Tobacco Research Station, Oxford, NC USA) and Lehle Seeds (Round Rock, Texas, USA), respectively. To establish an in vitro culture, dry seeds were surface sterilized with 70% ethanol (v/v) for 2 min and then with 7% NaOCl (v/v) for 10 min. After thorough rinsing with sterile distilled water, the sterilized seeds were sown on Murashige and Skoog (MS) medium (4.3 g/L MS micro and macro nutrients containing vitamins (Duchefa, Haarlem, The Netherlands), 30 g/L sucrose, pH 5.7 (adjusted with 0.5 M NaOH), and 8 g/L plant agar (Duchefa) in glass jars (Murashige et al., 1962). *Arabidopsis* seeds were imbibed for 2 days at 4°C in the dark before they were transferred to a growth chamber at 21°C with a 16/8 h (floral dip) or 12/12 h (protoplasts isolation) light/dark photoperiod. *Arabidopsis* plantlets were transferred to artificial soil (Jiffy-7, columnar diameter 44 mm, AS Jiffy Products, Drobak, Norway) to grow adult plants. Tobacco seeds were incubated directly in a growth chamber at 25°C with a 16/8 h light/ dark photoperiod.

A. thaliana cell suspension cultures were cultured as described in Van Hove et al. (2011). Apple (*Malus domestica*) trees from the cultivars 'Golden Delicious', 'Jonagold' as well as 'James Grieve', and pear (*Pyrus* sp.) trees from 'Conference' are grown on the campus of the Faculty of Bioscience Engineering (Ghent University) under natural conditions. Samples were collected from April to September 2013: leaf buds, young leaves (1 cm), old leaves, unopened flower buds, unopened flowers, opened flowers, fruits 10 day after anthesis (DAA) (fruits 10 DAA), fruits 35 days after anthesis (fruits 35 DAA), seeds, spring bark (collected in May). Flower buds were stripped of petals and petioles. Whole 10 day old fruits were sampled with only the stalk removed. Only the fruit part was taken for the fruit samples collected at 35 DAA. Seeds were collected from mature fruits. For each sample

material was pooled from at least 10 tissues from at least 5 individual trees. All samples were frozen in liquid nitrogen at the time of harvest and stored at -80°C until use.

3.3.3 EGFP fusion constructs

To construct a binary EGFP fusion vector that will allow the 35S Cauliflower Mosaic Virus promoter-driven expression of the type 1 RIP and type 2 RIP from *Malus domestica*, the Gateway™ cloning technology of Invitrogen (Carlsbad, CA, USA) was used. An overview of all expression constructs is shown in Figure 3.1. The coding sequences for the type 1 RIP and type 2 RIP sequences from apple were amplified as *attB* products by PCR, using genomic DNA extracted from the bark of *Malus domestica* cv 'Jacques Lebel' and gene-specific primers [EVD 697/EVD 606 (with stop codon) and EVD 605/EVD 695 (without stop codon) for type 1 RIP, EVD 607/EVD 696 (without stop codon) for type 2 RIP, Table 3.1]. The coding sequence of EGFP was coupled to the C-terminus of the SP of the type 2 RIP using overlap PCR as described in Vallejo et al., (1994). Specific primers (EVD 607/EVD 704, EVD 705/ EVD 806, Table 1) were used to amplify SP and EGFP fragments for overlapping extension PCR, respectively.   The SP-type 1 RIP fusion was constructed by overlap PCR using primers (EVD 607/EVD 633, EVD 632/EVD 695, Table 3.1). Control constructs contained the EGFP sequence alone. All constructs were completed with the *attB* sites using primers EVD2/EVD4 (Table 1). Cycling parameters for the PCR reactions were: 2 min 94°C, 25 X (15s 94°C, 30s 55 °C, 1 min 72°C), 5 min 72°C for all PCR reactions. Subsequently, all *attB* PCR products were homogeneously recombined in the entry vector pDONR221 (Invitrogen). Using heat shock transformation, the entry clones were subsequently transferred into *E. coli* strain Top10 cells. Transformants were selected by colony PCR. The plasmid DNA extracted from the colonies was sent for sequencing (performed by LGC Genomics, Berlin, Germany) using the primers Donr-F and Seql-E (Table 3.1). Finally, the LR reaction was done with the plasmids pK7FWG2, pK7WGF2 (Karimi et al., 2002) and pK7WG2.0. The results of the LR reaction were verified by sequencing (LGC Genomics) using gene specific primers EVD 605/EVD 606/EVD 607 and EGFP primers EVD 594/EVD 595.

Table 3.1 PCR primer pairs used in this research.

| Amplified sequence	Name	5'-3' sequence
Forward primer to add the non-complete *attB* sequences: type 1 RIP	EVD 605	AAAAAGCAGGCTTC ACCATGGCACTATCCTTCTCCATTAAG
Adding the non-complete *attB* sequences for type 1 RIP fused with N-terminal EGFP	EVD 697	AAAAAGCAGGCTTCACCGCACTATCCTTCTCCATTAAG
	EVD 606	AGAAAGCTGGGTGCTATTTCTTCTTCTTGGCGAGGGTTGG
Adding the non-complete *attB* sequences for type 1 RIP fused with C-terminal EGFP	EVD 606	AAAAAGCAGGCTTCACCATGGCACTATCCTTCTCCATTAAG
	EVD 695	AGAAAGCTGGGTGTTTCTTCTTCTTGGCGAGGGTTGG
Adding the non-complete *attB* sequences for type 2 RIP fused with C-terminal EGFP	EVD 607	AAAAAGCAGGCTTCACCATGACGAGAGTGTTAGCAATATAC
	EVD 696	AGAAAGCTGGGTGGAAGAACGGCAGCCATTGCTGGTTGGG
Primer for overlapping extension PCR: fusion of EGFP part to SP	EVD 704	TCCTCGCCCTTGCTCACCATGCACTCGGTGCCACAGAGAA
Forward primer for overlapping extension; fusion of SP to type 1 RIP	EVD 632	CTCTGTGGCACCGAGTGCATGGCACTATCCTTCTCCATT
Reverse primer for overlapping extension; fusion of type 1 RIP to SP	EVD 633	GGAGAAGGATAGTGCCATGCACTCGGTGCCACAGAGAA
Primer for overlapping extension; fusion of SP part to EGFP	EVD 806	AGAAAGCTGGGTGTTACTTGTACAGCTCGTCCATGCC
Completing the *attB* sequences: forward and reverse primer	EVD 2	GGGGACAAGTTTGTACAAAAAAGCAGGCT
	EVD 4	ACCACTTTGCTCAAGAAAGCTGGGT
Reverse primer to amplify EGFP	EVD 594	CTTGTACAGCTCGTCCATGC
Forward primer to amplify EGFP	EVD 595	CTCGTGACCACCCTGACCTA
qPCR reference gene: 18S ribosomal RNA gene from apple: forward and reverse primer	P 35	AGAGGGAGCCTGAGAAACGG
	P 36	CAGACTCATAGAGCCCGGTATTG
qPCR reference gene: Glyceraldehyde 3-Phosphate Dehydrogenase from apple: forward and reverse primer	P 52	CCAGGGGAGCAAGACAGTTGGT
	P 53	TCATTCTCTGCCCCCAGTAAGGATG
qPCR target gene: type 1 RIP: forward and reverse primer	P 66	TGTCGCGTTCCTGCTTTACT
	P 67	CGAGGGTTGGCTTCTGAACA
qPCR target gene: type 2 RIP: forward and reverse primer	P 57	AAAGCACTGCGAGCCCAA
	P 58	AGAGGAAGCGTTGTGAGTCC
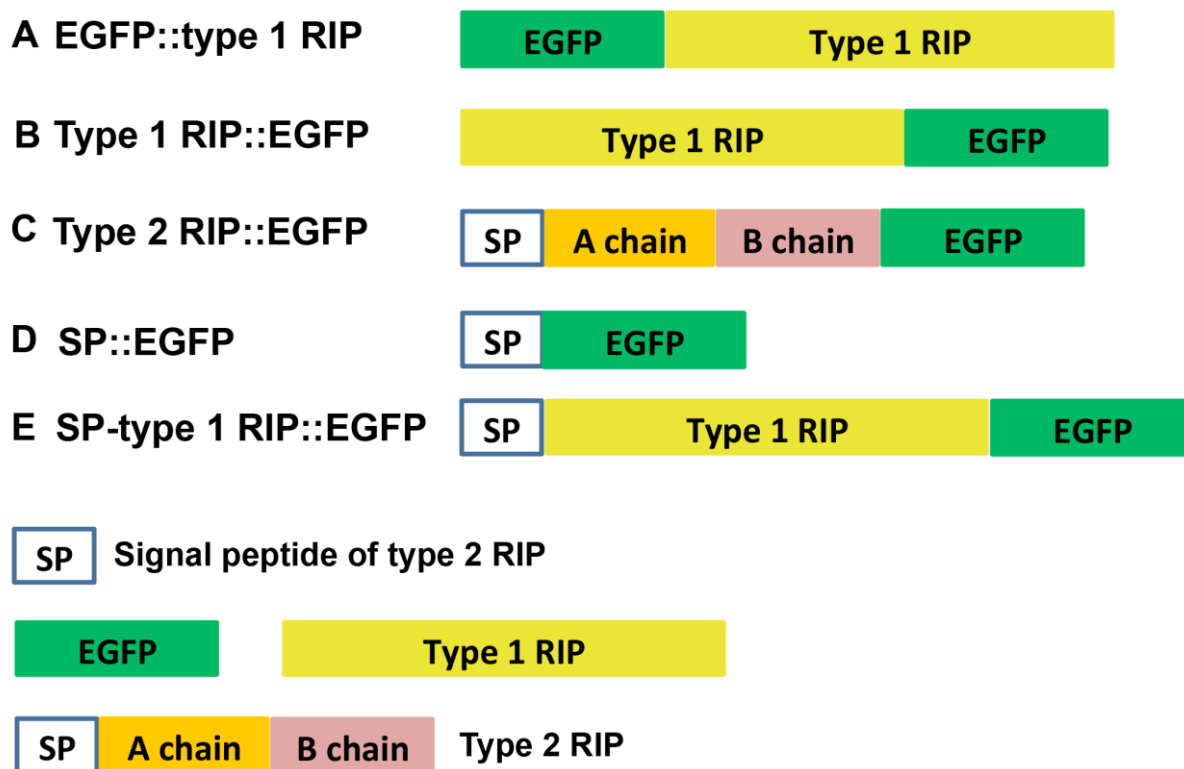
Figure 3.1 Schematic overview of different EGFP fusion constructs used in this study. All coding sequences were cloned under the control of the 35S CaMV promoter.

3.3.4 Transient expression of EGFP fusion proteins

All expression constructs were transferred to *A. tumefaciens* strain C58C1PMP90 by triparental mating. For transient expression of RIPs in leaf epidermal cells, suspensions of *A. tumefaciens* strain C58C1PMP90 at a bacterial optical density (OD600) of 0.1 were infiltrated into 6 week-old leaves of *N. benthamiana* as previously described by Delporte et al. (2014). Transient transformation of a two-day old *Arabidopsis* cell culture was achieved by cocultivation of the cells with suspensions of *A. tumefaciens* C58C1PMP90 as described by Van Leene et al., (2007). The fluorescence of transformed cells was analyzed after 3 days incubation on a rotary shaker. The expression constructs were also transiently transformed into *Arabidopsis* protoplasts as described by Yoo et al., (2007) and Xiang et al., (2011). Subsequently, after 16 h incubation under low light, the fluorescence of the transformed protoplasts was captured by confocal microscopy (Nikon instruments, Paris, France).

3.3.5 Stable expression of EGFP fusion proteins

The binary vectors containing EGFP fusion constructs were transformed into *A. tumefaciens* GV3101 by electroporation. Subsequently, these agrobacteria were used to transform *A. thaliana* ecotype Columbia plants using the floral dip method described by Clough et al.,

(1998). T0 seeds were selected on MS medium containing kanamycin (50 µg/ml) following the procedure described by Harrison et al., (2006) and afterwards several independent lines were tested by confocal microscopy (Nikon). To allow a better visualization of the localization of the type 2 RIP, protoplasts from stably transformed *A. thaliana* were isolated as described by Yoo et al. (2007).

3.3.6   RNA extraction and cDNA synthesis

Total RNA was extracted from all apple and pear samples using the RNeasy Plant Mini Kit (Qiagen, Valencia, CA USA) following the manufacturer's instructions, with an additional sonication step after addition of buffer RLT/RLC (Qiagen). Subsequently, the remaining DNA was removed by DNase I treatment (ThermoScientific, Erembodegem, Belgium). cDNA synthesis was performed using the M-MLV Reverse Transcripase Kit (Invitrogen). cDNA quality was checked using two pairs of reference gene primers P 35/P 36 and P 51/P 52 (Table 1) to amplify the sequence encoding the 18S ribosomal RNA gene (18S rRNA, Schaffer et al., 2007) and Glyceraldehyde 3-Phosphate Dehydrogenase (GAPDH, Foster et al., 2006. In total 40 ng cDNA was used as the template for the reverse transcription-PCR (RT-PCR) reaction, which was performed using the following parameters: 45X (2 min 95°C, 25s 58°C, 20s at 72°C), 5 min 72°C. The PCR products were visualized on a 2.5% agarose gel (Invitrogen).

3.3.7   Analysis of RIP expression in apple tissues by quantitative real-time PCR

qRT-PCR was performed on a CFX96™ Real-Time PCR Detection system using the iQ™ SYBR® Green Supermix kit (Bio-Rad, California, USA). The amplification specificity of the primers was checked by sequencing of RT-PCR products and analysis of the dissociation curve after qRT-PCR. To determine the efficiency of corresponding primer amplification, a serial dilution of cDNA mixed from different tissues was used to obtain standard curves. In each reaction, 10 µl of 2X supermix, 2 µl cDNA (40 ng/µl), 1 µl of 10 µM from each primer and 6 µl water were mixed in a total volume of 20 µl. The thermal profile consisted of 10 min at 95°C as a pre-denaturation step, followed by 45X (25s 96°C, 25s 60 °C, 20s at 72°C). The stability M values for the different reference genes were calculated by GeNorm Plus (Hellemans et al., 2007), after the quantification cycle (Cq) values processed into qBase[PLUS]. The relative expression level of the target genes was normalized against the reference genes *Malus domestica* 18S ribosomal RNA gene (18S rRNA) (Schaffer et al., 2007) and GAPDH (Foster et al., 2006) (Table 1) using qBase[PLUS]. Target primers (P 66/P 67 for type 1 RIP, P 57/P 58 for type 2 RIP, Table 1) for qRT-PCR were designed by primer 3.0 software

http://frodo.wi.mit.edu/ to amplify <120 bp amplicons. Each reaction was performed in triplicate. One biological replicate was performed in this expression analysis experiment.

3.3.8 Confocal microscopy

Confocal images were acquired with a Nikon A1R confocal system, mounted on a Nikon Ti microscope body using a 40× Plan Apo objective lens (Numerical aperture 0.75) or 60× oil immersion lens (NA 1.4) appropriate filters. Images were analyzed with Fiji (http://fiji.sc/Fiji).

3.4 Results

3.4.1 Sequence analysis

To obtain a primary indication of the subcellular localization, the tools Phobius (Käll et al., 2007) and TargetP (Emanuelsson et al., 2000) were used to predict whether the RIP sequences are synthesized with a signal peptide (SP). According to the tool Phobius, both type 1 and type 2 RIPs are predicted as non-cytoplasmic proteins. Both bioinformatics tools agree that the amino acid sequence of the type 2 RIP precursor contains a 22 amino acid signal peptide (MTRVLAIYITLAFSLFLCGTEC) at its N terminus. According to TargetP the probability for a SP in the type 2 RIP sequence is estimated as 0.946 (close to 1), indicating that the presence of a SP is very likely. Most probably this SP is important for targeting of the polypeptide to the secretory pathway and protein synthesis on ER associated ribosomes. Since the probability for the occurrence of a SP sequence in the type 1 RIP sequence is close to 0 (0.058), a signal peptide is probably absent from this sequence. Interestingly, the presence of a typical nuclear localization signal (NLS) (^{298}KKKK^{301}) at the C- terminus of in the type 1 RIP sequence demonstrated that the type 1 RIP may be located in the nucleus. Analysis of the apple type 2 RIP sequences for the presence of vacuolar targeting sequences, such as the sequence LLIRP reported for ricin (Jolliffe, et al., 2003) and the sequence NPIRL found in saporin (Matsuoka and Nakamura, 1991) did not yield any such protein motifs.

3.4.2 Transient expression and localization of the RIP-EGFP fusion proteins in *N. benthamiana* epidermal leaf cells

To study the subcellular localization of apple RIPs in living cells, EGFP was used as a reporter tag. Several fusion constructs between (part of) RIP sequences and EGFP were generated according to Figure 3.1 (A-E). Subsequently, these constructs were transiently expressed in *N. benthamiana* epidermal leaf cells. The EGFP fluorescence in the cells was captured by a confocal laser scanning microscope. A construct for free EGFP was used as a control, and yielded fluorescence in the cytoplasm and the nucleus (Fig. 3.2A).

Using *Agrobacterium* mediated transformation fusion constructs for the type 1 RIP sequence either N-terminally or C-terminally linked to EGFP (Fig. 3.1A and B) were introduced in *N. benthamiana*. Confocal microscopy of leaf samples at two days after transformation revealed fluorescence in the nucleus and cytosolic compartment of tobacco epidermal cells (Fig. 3.2B and C). Z-stack analysis confirmed the presence of the EGFP fluorescence signal throughout the nucleus.

The construct for type 2 RIP composed of the complete type 2 RIP sequence (including the SP) C-terminally fused to EGFP (Fig. 3.1C) yielded fluorescence around the nucleus and at the edge of the cells (Fig. 3.2E). Very similar fluorescence patterns were observed for the fusion construct consisting of the SP (from the type 2 RIP) linked to the type 1 RIP sequence and the fusion between SP and the EGFP sequence (Fig. 3.2D and F).
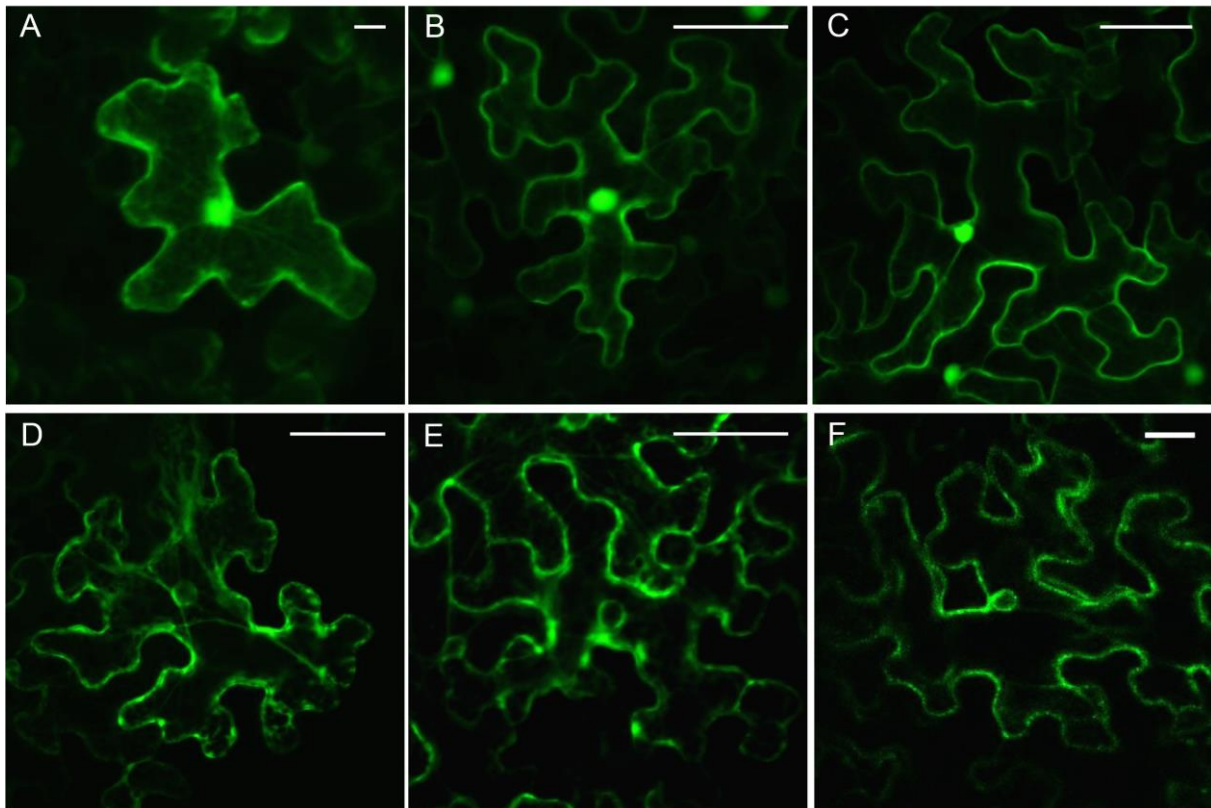

Figure 3.2 Confocal microscopy images of RIP fusion constructs with EGFP expressed in *N. benthamiana* epidermal leaf cells. (A) EGFP control (B) EGFP::Type 1 RIP (C) Type 1 RIP::EGFP (D) SP::EGFP (E) Type 2 RIP::EGFP (SP-A chain-linker-B chain-EGFP) (F) SP-Type 1 RIP::EGFP (SP-Type 1 RIP-EGFP). Scale bars represent 25 μm.

3.4.3 Transient expression and localization of the RIP-EGFP fusion proteins in *Arabidopsis* protoplasts

To confirm the localization results obtained from the tobacco leaf infiltration and further determine in which organelles and subcellular compartments the RIPs were localized, we transiently transformed the RIP constructs in *Arabidopsis* protoplasts. Due to lack of cell wall, the protoplasts are unstable and vulnerable. All the protoplast cells expressing type 2 RIPs or SP were observed as undergoing morphological changes. For instance all cell organelles are located on one side of the protoplast (Fig. 3.3F, Fig. 3.5 E), the cells are shrinking (Fig. 3.3D, Fig. 3.5F), the cell membrane is not sharp (Fig. 3.5 D and E). Both the N-terminal and C-terminal EGFP fusion to the type 1 RIP sequence (Fig. 3.1A and B) clearly accumulated in the cytoplasm and the nucleus (Fig. 3.3A, B and C). All constructs containing the SP sequence of the type 2 RIP (Fig. 3.1D and E) revealed expression in the vacuole (Fig. 3.3D and G) and some small punctate structures at the edge of protoplast or in between the chloroplasts (Fig. 3.3E, F and G). In addition, the SP::EGFP fusion protein also clearly marked the ER network (Fig. 3.3F). Despite several repetitions of the experiment, no fluorescence was detected for the constructs of type 2 RIP::EGFP (Fig. 3.1C) in this transient expression system.

3.4.4 Transient expression and localization of the RIP-EGFP fusion proteins in *Arabidopsis* suspension cell cultures

Neither the transient transformation of tobacco leaf tissue nor the transient transformation in *Arabidopsis* protoplasts allowed to unambiguously show the localization of the type 2 RIP in the cell. Therefore, we also transiently expressed the RIP-EGFP fusion proteins in *Arabidopsis* suspension cell cultures. Free EGFP was used as a control and yielded fluorescence in the cytoplasm and the nucleus of the plant cells/protoplasts, including the nucleolus (Fig. 3.4A). Fluorescence for both N- and C-terminal EGFP fusions to the type 1 RIP was detected in the cytoplasm and the nucleus (Fig. 3.4B and C). The fusion construct encoded by SP-EGFP and SP-type 1 RIP::EGFP yielded fluorescence in the vacuolar compartment as well as some bright fluorescent vesicles at the edge of the cell (Fig. 3.4D and F). Fluorescence from the construct with the type 2 RIP fused C-terminally to EGFP was visualized in clear vesicles or punctate bodies surrounding the cells (Fig. 3.4E), but was never detected inside the vacuole.
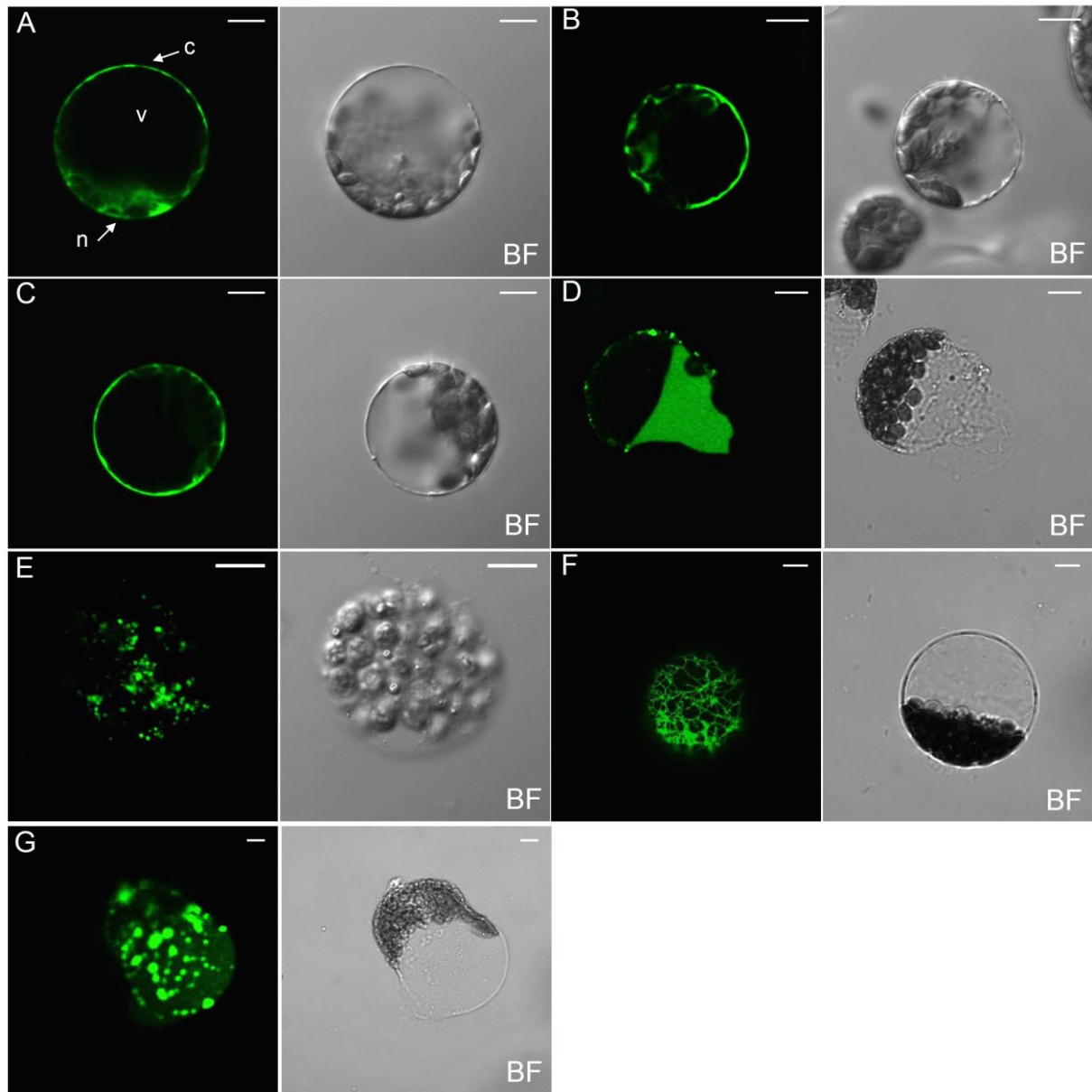
Figure 3.3 Confocal images of transiently transformed *Arabidopsis* protoplasts expressing fusion proteins. (A) EGFP fluorescence and bright field (BF). (B) EGFP fluorescence and BF of EGFP::type 1 RIP fusion protein. (C) EGFP fluorescence and BF of type 1 RIP::EGFP fusion protein. (D, E, F) EGFP fluorescence and BF of SP::EGFP fusion protein. (G) EGFP fluorescence and BF of SP-type 1 RIP::EGFP fusion protein. Scale bars represent 10 μm. Cell compartment: n, nucleus; c, cytoplasm; v, vacuole
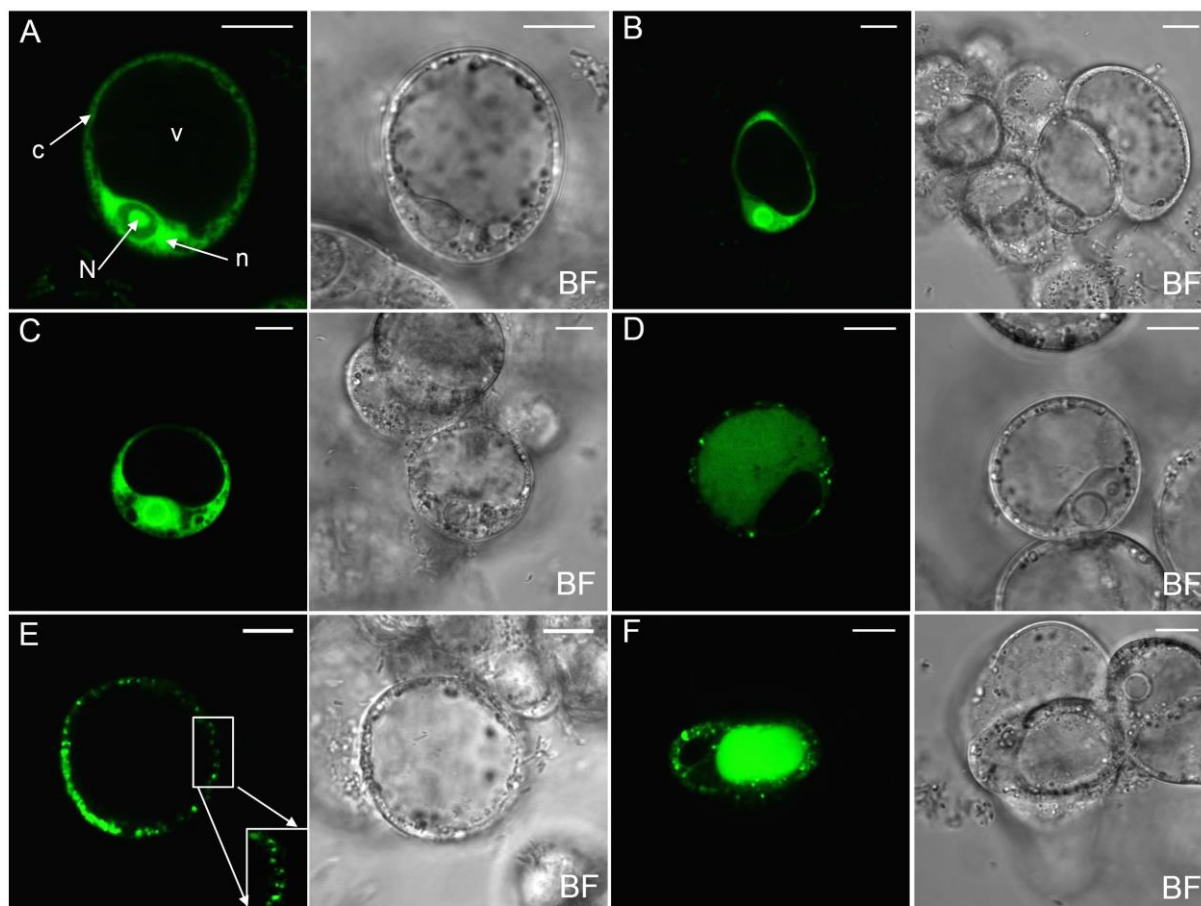
Figure 3.4 Confocal images showing transient expression of fusion proteins in *Arabidopsis* suspension cells. (A) EGFP fluorescence and bright field (BF). (B) EGFP fluorescence and BF of EGFP::type 1 RIP fusion protein. (C) EGFP fluorescence and BF of type 1 RIP::EGFP fusion protein. (D) EGFP fluorescence and BF of SP::EGFP fusion protein. (E) EGFP fluorescence and BF of type 2 RIP::EGFP fusion protein. (F) EGFP fluorescence and BF of SP-type 1 RIP::EGFP fusion protein. Scale bars represent 10 µm. Cell compartment: N, nucleolus; n, nucleus; c, cytoplasm; v, vacuole

3.4.5 Stable expression and localization of the RIP-EGFP fusion proteins in *Arabidopsis* plants

To prove the results obtained from the transient transformation experiments in the tobacco leaf, *Arabidopsis* protoplasts and cells, the RIP constructs were also used for stable transformation of *Arabidopsis* plants. Microscopic analysis of *Arabidopsis* leaves stably transformed with a construct expressing a fusion protein of the type 1 RIP and EGFP indicated that the type 1 RIP located to the nucleus and the cytoplasm (Fig. 3.5A and B). In contrast, a dotted fluorescent pattern was detected at the edge of the leaf cells for the construct type 2 RIP::EGFP (Fig. 3.5C). To gain better insight into the localization pattern observed for the type 2 RIP, protoplasts were prepared from leaf tissue with stable expression of the type 2 RIP. Within the protoplasts the fluorescence signal was clearly

visualized in the ER network (Fig. 3.5E), in small punctate structures in between chloroplasts (Fig. 3.5F) and in larger punctate spots/vesicles in the cells (Fig. 3.5D), but fluorescence was never detected in the vacuole.
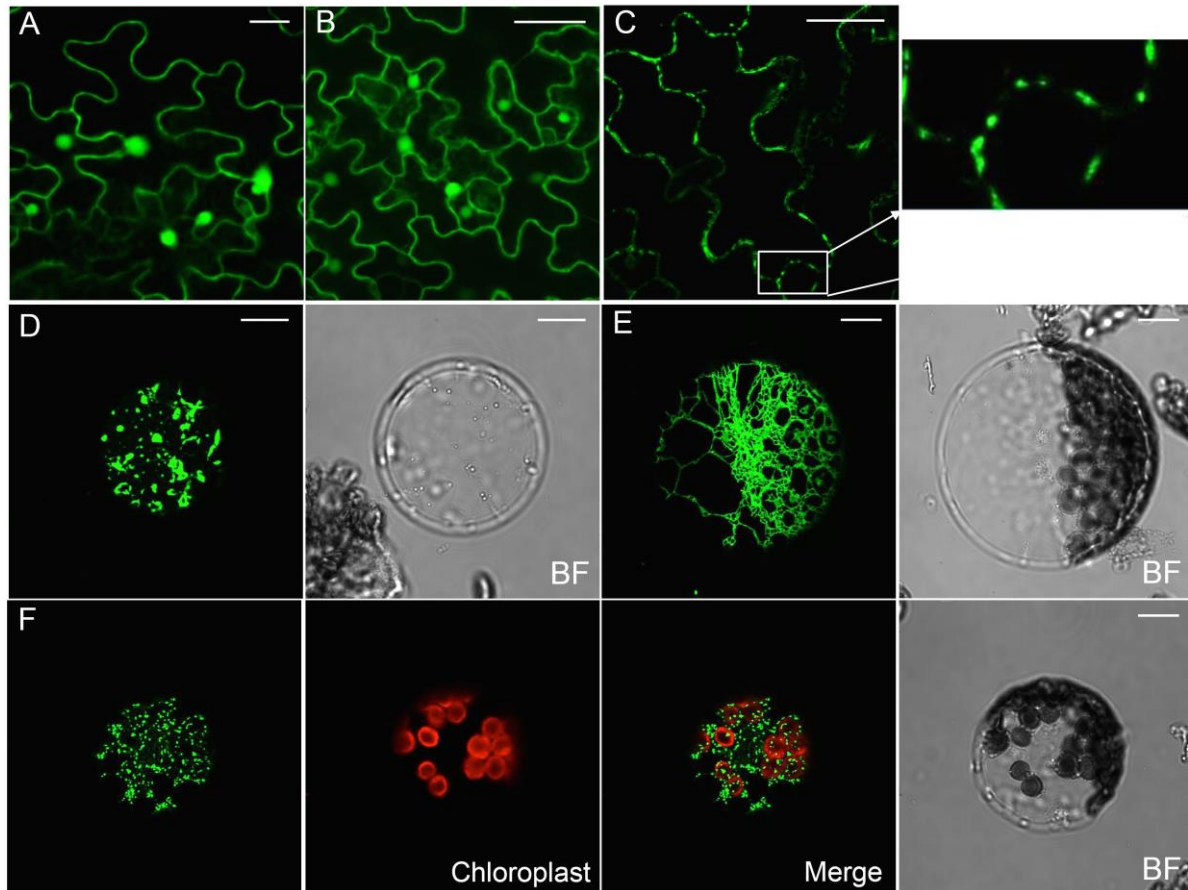

Figure 3.5 Confocal images showing stable expression of fusion proteins in *Arabidopsis* plants (A, B, C) and protoplasts isolated from stably transformed *Arabidopsis* leaves. (A, B) EGFP fluorescence of type 1 RIP fused with N- and C- terminal EGFP, respectively. (C) Fluorescence of EGFP coupled with type 2 RIP. (D, E, F) EGFP fluorescence and BF of protoplasts obtained from stably transformed type 2 RIP::EGFP fusion protein. Scale bars represent 25 μm and 10 μm in images of plant leaf cells and protoplasts, respectively.

3.4.6 Analysis of apple RIP gene expression in different tissues

Transcriptome analyses of EST obtained for different apple cultivars revealed that ESTs encoding the type 2 RIP are most abundant in the young tissues, including ESTs for spur buds (cv Pacific Rose), young shoots, pre-opened flower buds and 10 DAA fruits (cv Royal Gala). No EST sequences were retrieved for the type 1 RIP sequence from apple.

To investigate the tissue-specific expression of the apple RIPs we analyzed the transcript levels for type 1 and type 2 RIPs from apple in different tissues from a tree and throughout

development of the fruit. Analyses were done for three different cultivars of apple, in particular 'Golden Delicious', 'Jonagold' and 'James Grieve'. For comparison the same analysis was also performed for one pear tree (cv 'Conference'). In total ten different tissues (leaf buds, young leaves, old leaves, unopened flower buds, unopened flowers, opened flowers, fruits 10 DAA, fruits 35 DAA, seeds, spring bark) were sampled (Fig. 3.6). RNA was extracted and analyzed by qRT-PCR.

Quantitative analysis of the type 2 RIP transcript levels in the different apple cultivars and tissues showed that the type 2 RIP was expressed, albeit with strongly varying mRNA levels depending on the tissues under study (Fig. 3.7). All relative expression levels were normalized to the expression of two reference genes (18S rRNA and GAPDH). The relative expression level for the type 2 RIP was high in leaf buds and unopened flower buds for all different cultivars. Furthermore, the accumulation of the type 2 RIP mRNAs in young apple leaves is also high, except for 'James Grieve'. Furthermore, the relative expression level of the type 2 RIP decreased considerably during development, e.g. during maturation from young leaves to old leaves. It is worthy to note that the relative expression level for the type 2 RIP was also high in bark from 'Golden Delicious'. Unfortunately, no data are available for the bark samples from 'James Grieve' and 'Jonagold' because analyses on these tissues failed probably due to the bad RNA quality. Type 2 RIP transcripts were detected in unopened flowers and opened flowers, though transcript levels were considerably lower than in young leaves. The lowest expression levels for the type 2 RIP were observed in fruits (10 DAA and 35 DAA) and seeds for all three apple cultivars, with decreasing levels during fruit maturation.

Similar as for apple, quantitative analysis of the type 2 RIP expression in pear revealed that the relative expression levels for the type 2 RIP are high in leaf buds, young leaves and unopened flower buds. Moreover, the type 2 RIP expression levels were clearly down regulated during flower and fruit development (unopened flower buds compared to unopened flowers and opened flowers / fruit 10 DAA compared to fruit 35 DAA) as well as during leaf development (young leaves compared to old leaves). Interestingly type 2 RIP transcript levels were higher in the seeds compared to those in the fruit samples.

Transcripts for the type 1 RIP could not be detected in any of the apple and pear tissues under study, suggesting that the type 1 RIPs are expressed at a very low level (data not shown).
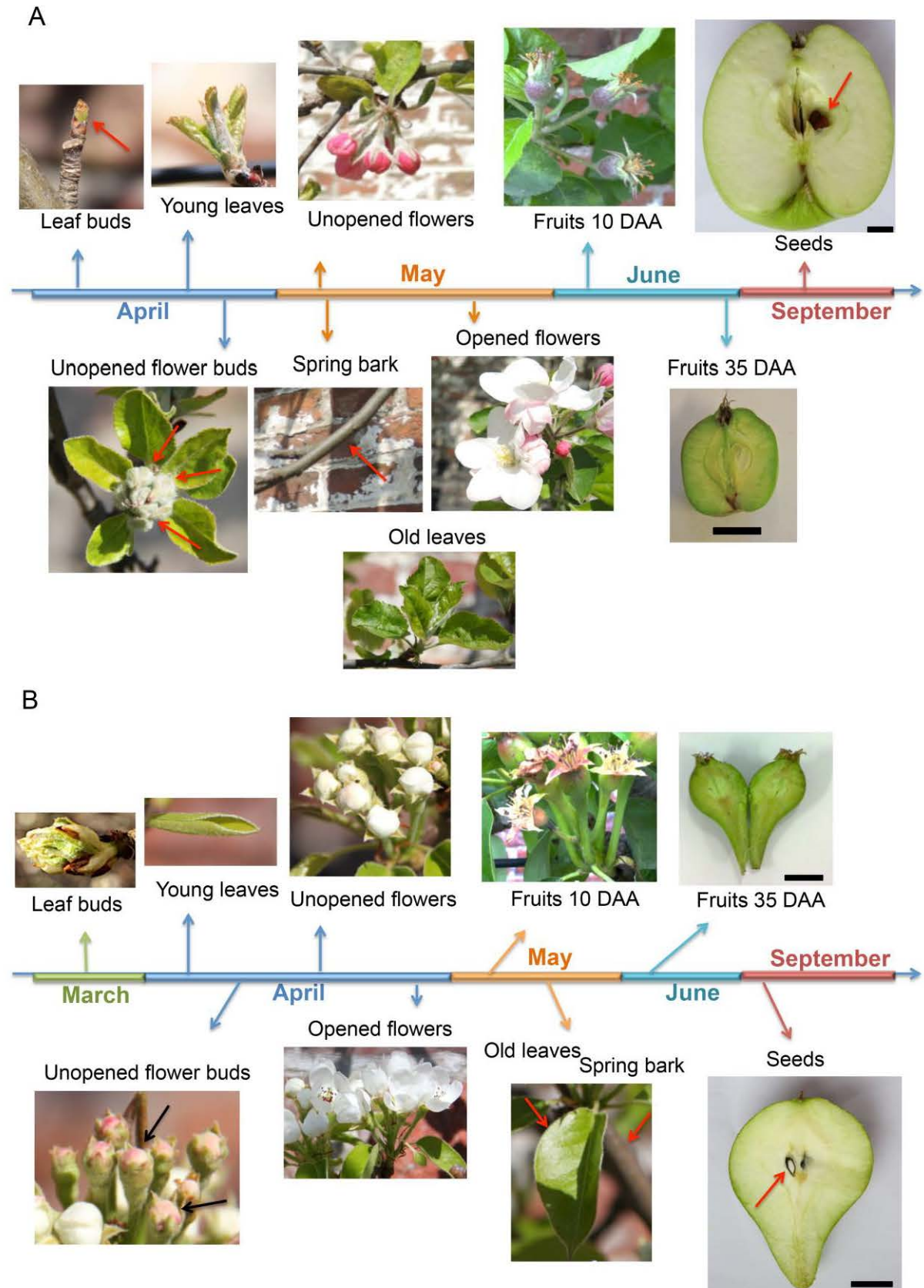
Figure 3.6 Overview of the timing for the collection of the different tissues from apple cv 'Golden Delicious' (A) and pear cv 'Conference' (B). Arrows indicate the sampled tissue. Scale bars represent 1 cm.
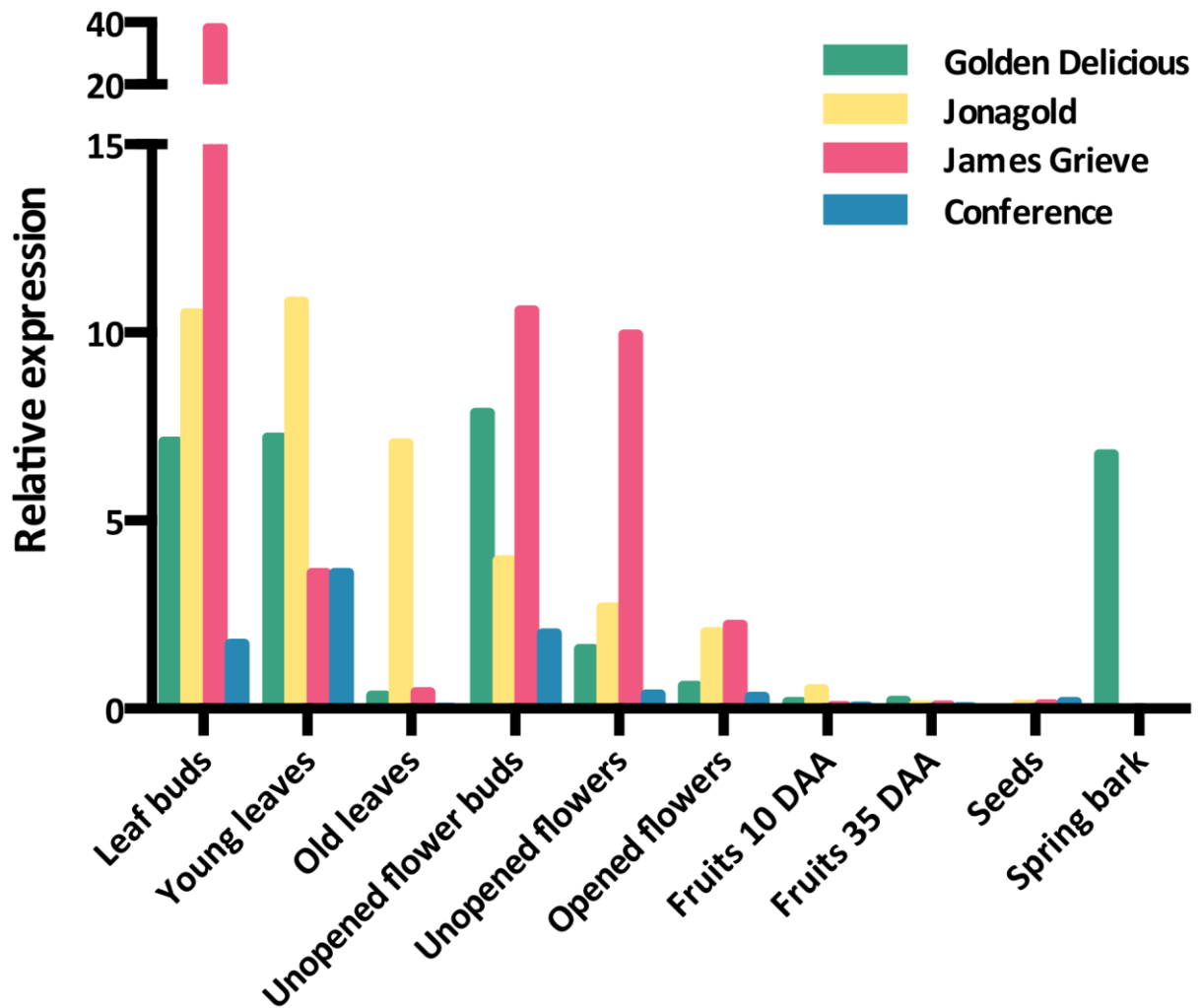
Figure 3.7 Quantitative RT-PCR analysis of the expression of the type 2 RIP genes in different tissues from three apple cultivars: 'Golden Delicious', 'Jonagold' and 'James Grieve' and one pear cultivars: 'Conference'. Transcript levels were normalized to the expression of 18S rRNA and GAPDH.

3.5 Discussion

The subcellular localization of apple RIPs was investigated using confocal microscopy of fusion proteins tagged by EGFP (Brandizzi et al., 2004) and expressed in different cell systems, namely transient transformations (tobacco epidermal cells, *Arabidopsis* protoplasts, *Arabidopsis* suspension cells) and a stable transformation (*Arabidopsis* plants). The transient transformation of *N. benthamiana* plants is widely accepted due to its ease, high efficacy and consistency of operation (Yang et al., 2000). However, it is difficult to distinguish some compartments (e.g. plasma membrane, cell wall, cytoplasm and tonoplast…), therefore this method is not optimal to investigate the localization of a protein that follows the secretory pathway to be secreted outside the cell. Denecke et al. (2012) suggested to use a variety of experimental systems to investigate the subcellular localization of secretory proteins. Recently, protoplast transformation has been suggested as a versatile

cellular system that allows rapid transient gene expression (Yoo et al., 2007, Xiang et al., 2011). Nevertheless, it is important to realize the limitations of this expression system. After transformation of the construct into the protoplast, expression can be observed only up to 30 h (Denecke et al., 2012). Although stable transformation in *Arabidopsis* plants is labor-intensive and time-consuming being a major disadvantage of the method, the EGFP signal detection is not time-dependent. Furthermore, protoplast isolation from stably transformed Arabidopsis leaves can yield additional information on protein synthesis and trafficking in the cell.

All the transient transformation assays with tissues and protoplasts as well as the stable transformation of plant cells, revealed that the type 1 RIP sequence fused to EGFP located to the nucleus and the cytoplasm. These data are in agreement with the observation that the RIP sequence lacks a SP –resulting in the synthesis of the protein on free ribosomes in the cytoplasm. Furthermore the presence of a basic NLS (^{298}KKKK^{301}) at the C-terminus of the type 1 RIP sequence supports targeting of the protein to the nuclear compartment. These data provide evidence that the apple type 1 RIP is a cytosolic protein, similar to cereal type 1 RIPs (Frigerio and Roberts, 1998).

Confocal microscopy revealed that the expression patterns detected for the fusion proteins with the type 2 RIP sequence were very different compared to the data obtained for the type 1 RIP. Fluorescence of type 2 RIP was observed in the cytoplasm in the *N. benthamiana* transient transformation system (Fig. 3.2 DEF). Probably, some type 2 proteins are remaining in the cytoplasm due to the high expression under 35S promotor. In the expression system of protoplasts and *Arabidopsis* cells, all fusion proteins containing the SP sequence from the type 2 RIP followed the secretory pathway. Fusion of the signal peptide taken from the type 2 RIP sequence to EGFP or type 1 RIP::EGFP clearly yielded expression of these constructs in the vacuole. In contrast C-terminal fusion of EGFP to the type 2 RIP sequence (also containing the SP) resulted in targeting of the fusion protein directly to the intercellular space. No evidence was obtained for transport of the fusion protein through the vacuole. It is unclear at present why the type 2 RIP constructs and the constructs containing the SP coupled with other proteins (type 1 RIP/EGFP) follow a different route.

It was reported that type 2 RIP sequences such as ricin contain an internal vacuolar targeting signal sequence containing a LLIRP motif (Frigerio et al., 2001; Jolliffe, et al., 2003), resembling the vacuolar target sequence NPIRL necessary for sorting of sporamin (Matsuoka and Nakamura, 1991). The conserved Ile residue within this motif is essential for the vacuolar targeting of proricin, since modification of Ile^{271} into Gly resulted in secretion of

proricin into the medium (Frigerio et al., 2001). The isoleucine residue was also found in the sequence [274]IKMPV[278] present in the linker sequence between the A and B chain of SNA-I (Chapter 2, Fig. 2.2B), suggesting SNA-I can behave as vacuolar storage protein. Furthermore, immunofluoresce microscopy confirmed that SNA-I is located in protein bodies in the phloem parenchyma of *S. nigra* bark (Van Damme et al., 1996a, Greenwood et al., 1986). Previous reports indicated that most type 2 RIPs accumulate in the storage vacuole due to the presence of sequence-specific vacuolar sorting signals (ssVSS)-mainly located at N terminus, C-terminal signals (ctVSS) and protein structure dependent signal (psVss; Frigerio et al., 2001) (Xiang et al., 2013). Without these propeptides, the vacuolar proteins are secreted (Vitale and Raikhel, 1999). Although the apple type 2 RIP sequence contains the same vacuolar targeting sequence ([250]IKMPV[254]) as in SNA-I, our data provide no evidence that this sequence serves as a vacuolar targeting signal.

Expression of a ricin mutant lacking the lectin chain in tobacco protoplasts revealed that the construct consisting of SP and A chain was synthesized on the ER and translocated into cytosol. Since the A chain contains a low amount of lysine residues, the protein can escape proteasomal degradation (Ceriotti and Roberts, 2006, Di Cola et al., 2001, 2005). Within the cytoplasm the ricin A chain will inactivate the host cell ribosomes (Nicholas et al., 2003, Di Cola et al., 2001, 2005). In contrast, the final destination of the protoplast-synthesised saporin completely differs from that of ricin A chain: the protein is synthesized on the ER, is transported from ER to the Golgi and is finally secreted into the protoplast culture medium (Marshall et al., 2011). Unlike the A chain of ricin, the fusion construct SP-type 1 RIP::EGFP followed the secretory pathway from the ER to the Golgi, and ended up in the vacuole. Most probably, part of the protein was also secreted into the medium/intercellular space similar to saporin.

Analysis of the expressed sequence tags (ESTs) available for apple RIPs revealed that type 2 RIP sequences are expressed in spur buds, young shoots, young flower buds and young immature fruits, but yielded no information for the expression of type 1 RIP sequences from apple. Considering this result the apple type 2 RIP is most abundant during the early growth stages. These data were confirmed by qPCR analyses on different tissues sampled during development of apple and indicated that type 2 RIP expression is decreasing during growth of leaves and flowers, as well as during fruit development, since almost no RIP expression was detected in fruits sampled 35-days after anthesis. Surprisingly, the expression of the type 2 RIP in seeds from mature apple fruit is quite low. This is unlike many other type 2 RIPs (e.g. ricin) which are highly expressed in the developing seeds, especially in the stages when

the endosperm is fully expanded (Loss-Morais et al., 2013).

The expression of type 2 RIP showed some variability between different apple cultivars. (i) Plausibly, this is due to some major differences between the cultivars (Table 3.2). 'Jonagold' and 'Golden Delicious' are belonging to group of 'Jonagold', whereas 'James Grieve' belongs to group of 'Delikates'. 'Golden Delicious' and 'James Grieve' are diploid, whilst 'Jonagold' is triploid (a cross of 'Golden Delicious' and 'Jonathan'). In addition, the timing of fruit harvest and bloom is also different among these apple cultivars. (ii) For practical reasons all tissues were collected at specific time points which were identical for all trees, whilst, the different apple cultivars were not always in the same developmental stage. To reduce the differences among different trees (with slight differences in their developmental stage), tissue samples from several trees were mixed. Since the timing for the collection of the different tissues was not optimal, this could also be the cause of some variability with RIP expression between different cultivars.

In this study, the subcellular localization of apple RIPs was investigated using confocal microscopic analysis of EGFP fusion constructs with the RIP sequences expressed in different cell systems. Taken together all the data from these transient and stable gene expressions, it was demonstrated that the apple type 2 RIP is synthesized in the ER and secreted into the intercellular space. In contrast, all the evidence showed that the apple type 1 RIP is synthesized on free ribosomes and is targeted to the nucleus and the cytoplasm. Furthermore, the results of transcriptome analysis and the qPCR analysis provided evidence for differential transcript accumulation of apple type 2 RIPs in different tissues from apple. The results of the subcellular localization study, taken together with the fact that type 2 RIP transcript levels reach the highest levels in young tissues might be relevant from the point of view of the physiological importance of the RIP, e.g. a role in (crop) plant protection as part of plant defense.

Table 3.2 Some important differences between apple cultivars (Smolik and Krzysztoszek, 2010; Pereira-Lorenzo et al., 2009).

James Grieve	Jonagold	Golden Delicious
Cluster I	Cluster II	
Diploid (2n=34)	Triploid (2n=51) a cross of non-reduction diploid Golden Delicious x diploid Jonathan	Diploid (2n=34 chromosomes)
Early apples, harvested at the end of July and available until the end of September	Winter apples, harvested at the beginning of October and available until the end of May.	
Midseason bloom		Late bloom

3.6   Supplemental data

Type 1 RIP deduced AA sequence:

MALSFSIKNATTTTYRTFIEALRAQLTAGGSTSHGIPVLRRRQDVKDDQRFVLVNLTNYDSY
TITVAIDVVNAYVVGYCAGTRSYFLRDPATHPPPLHRLFPGTTRTTLPFAGDYLGLGRAAQE
ALQQNTNRNRAAGSRIHENISMRERIPLGPGELDNAISQLRYAESASSQAAAFIVIIQIVSE
AARFRYIQGQVRDRIRDGTSAEPDPAMLSLENSWSNLSEQIQMVPANQLLFINNGSVQIRKA
DNSIVLVKSVDSDAVRGVAFLLYCGGNPPAPNSESARTSKVTVQKPTLAKKKK

Type 2 RIP deduced AA sequence:

MTRVLAIYITLAFSLFLCGTECNISFSTSGATSNSYNTFIKALRAQLTNGATAIYDIPVLNP
SVPDSQRFLLVDLSNNGNNTITVAIDVVNASVVAYRARAARPYFLADAPDEALDILFNDTRG
FFLPFTSNYVDLEKAAEKSRDKIPLGLTPLHNAITSLWNQESEEAAVSLLVIIQTVFEAARF
RVIEQRVRNSISSKANFIPDPAMLSLENNWLAISWETQHALNGVFSKSIQLRSTNNNLFLVD
SVSSSIMAGVAFLFYNCVTFPNIIKMPVNVVMGKEIDNEICAVQNRTTHISGLEGLCVDVKN
GLDSDGNLVQIWPCGQQRNQKWTFQPDETIRSMEKCMTAYSTSSPENYVMIYNCTTAVPEAT
KWALSTDGTITHRRSGLVLTAHEATRGTTLTIATNSHSPKQGWRVADDVEPTVTSIIGYNDM
EYCVPSKNQQQWALYSEGTIRVNSDRTLCVTSNGHNSSNVIIIKCELKRGDQRWVFKTDGSI
LNPNAELVMDVKNSDVYLRQIILYPYYGTPNQQWLPFF

Figure S3.1 The RIP sequences cloned from pear (*Pyrus* sp.) cv 'conference'

Chapter 4

Ribosome-inactivating proteins from apple (*Malus domestica*) possess antifungal, antiviral and insecticidal activities

4.1 Abstract

Genes encoding ribosome-inactivating proteins have been identified in the genome/transcriptome of several edible fruits. In this study the involvement of type 1 RIP and type 2 RIP from apple (*Malus domestica*) in plant defense was investigated. The antiviral and antifungal activities of RIPs from apple were studied *in planta* using transgenic tobacco (*Nicotiana tabacum* L. cv Samsun NN) plants. Although the expression of apple RIPs under the control of the 35S cauliflower mosaic virus promoter causes morphological changes in some plants the majority of the transgenic lines exhibited a normal phenotype. Bioassays with a series of transgenic lines demonstrated that both type 1 and type 2 RIPs offer the plants an enhanced resistance against *Botrytis cinerea* and tobacco mosaic virus. In addition, feeding trials with an artificial diet supplemented with purified recombinant proteins revealed that the RIPs are toxic to the aphid *Acyrthosiphon pisum*. These findings indicate that the apple RIPs exhibit an unusually broad spectrum of defense activities and accordingly might be involved in defense related processes.

4.2 Introduction

Plants are continuously threatened by diseases and infection by plant viruses, phytopathogenic fungi and bacteria, as well as by damage caused by phytophagous insects (Dangl et al., 2013; Dodds and Rathjen, 2010). To resist pathogen infections and insect herbivory, plants developed a number of sophisticated mechanisms to cope with these biotic stress factors. More specifically, plants are capable of rapidly recognizing harmful pathogens and trigger an efficient defense response (Muthamilarasan and Prasad, 2013; Wirthmueller et al., 2013; Lannoo and Van Damme, 2014). Furthermore DNA recombinant technology now enables the engineering and/or introduction into crop species of plant defense genes that confer disease resistance in plants or direct the synthesis of compounds exhibiting toxicity towards e.g. fungi, bacteria, insects or herbivores, which eventually yields transgenic lines with enhanced plant growth and performance (Galvez et al., 2014).

Ribosome-inactivating proteins are a family of enzymes with a unique N-glycosidase activity that enables them to remove a specific adenine from the highly conserved sarcin-ricin loop of the large ribosomal RNA resulting in the catalytic inactivation of the ribosomes and a rapid arrest of cellular protein synthesis (Peumans et al., 2001; Stirpe and Battelli, 2006). The (super)family of RIPs is classically divided into type 1 RIPs consisting of an N-glycosidase domain of approximately 30 kDa, and type 2 RIPs,

which are in fact chimeric proteins built up of an N-terminal N-glycosidase domain fused to a C-terminal carbohydrate binding domain of approximately 30 kDa corresponding to a duplicated ricin-B domain. Though most research efforts have been concentrated on the classical type 1 and type 2 RIPs the wealth of sequence data generated by genome and transcriptome analyses demonstrated that the RIP superfamily is far more complex than previously believed and comprises a broad range of chimeric forms with an unusually broad range of domain architectures. In addition the genome/transcriptome analyses revealed that RIPs are far more widespread among higher plants than was previously inferred from the research with the proteins themselves. Interestingly, the genome/transcriptome based approach also allowed identifying the presence and expression of RIP genes in numerous crop plants, fruits and vegetables that until now were not suspected to contain RIPs such as sugar beet (*Beta vulgaris*), cannabis (*Cannabis sativa*), spinach (*Spinacia oleracea*), peach (*Prunus persica*), plum (*Prunus domestica*), apple (*Malus domestica*), strawberry (*Fragaria × ananassa*), and pumpkin (*Cucurbita moschata*) (Barbieri et al., 2006; Polito et al., 2013b; Peumans et al., 2014). Despite the tremendous amount of research devoted to a multidisciplinary study of numerous RIPs no clear answers can be given yet to the question why at least some plants synthesize and accumulate proteins with N-glycosidase activity.

During an in-depth *in silico* screening of the genome/transcriptome of different edible plant species our attention was drawn to the presence of both type 1 and type 2 RIP genes in the apple (*Malus* sp.) genome (see chapter 2). Since apple is a major fruit crop it seemed worthwhile to corroborate the biological activities and physiological importance of apple RIPs. To gain better insight into the physiological role of the apple RIPs, transgenic tobacco plants were constructed expressing the apple RIP sequences under the control of the 35S cauliflower mosaic virus promoter. Expression of the RIP sequences in transgenic tobacco plants was analyzed by quantitative real-time reverse transcription polymerase chain reaction (qRT-PCR), activity assays and western blots. Subsequently the transgenic tobacco plants were tested for disease resistance to tobacco mosaic virus (TMV) and infection by the fungus *Botrytis cinerea*. In addition, the recombinant proteins were added to an artificial diet to determine the insecticidal activity of apple RIPs against pea aphids (*Acyrthosiphon pisum*). Our results showed that the apple RIPs exert a pronounced effect on disease development and therefore can be involved in plant defense against viruses, fungi and insects.

4.3   Materials and methods

4.3.1   Plant materials

To establish an *in vitro* culture of tobacco (*Nicotiana tabacum* L. cv Samsun NN) seeds were first surface sterilized with 80% ethanol (v/v) for 5 min and then with 5% NaOCl (v/v) for 15 min. After thorough rinsing with sterile distilled water, the sterilized seeds were sown in glass jars containing Murashige and Skoog (MS) medium (4.3 g/L MS micro and macro nutrients containing vitamins (Duchefa, Haarlem, The Netherlands), 30 g/L sucrose, pH 5.7 (adjusted with 0.5 M NaOH), and 8 g/L plant agar (Duchefa)) (Murashige et al., 1962). Four to five week old plants were used for the leaf disc transformation.

For the *Botrytis cinerea* and TMV bioassays sterilized seeds of wild type plants or transgenic tobacco lines (T1 generation) were germinated on MS medium (containing 100 mg/L kanamycin for the selection of the transgenic lines). Two-week old seedlings were transferred into pot soil and grown for another four weeks under a photoperiod regime of 16/8 h light/dark at 25°C. For each line, 12 plants were used for the bioassays. All bioassays were performed in three independent replicates.

4.3.2   Construction of binary vectors

To construct a binary vector that will allow the 35S promoter-driven expression of the type 1 RIP and type 2 RIP from *Malus domestica*, the Gateway^{TM} cloning technology of Invitrogen (Carlsbad, CA, USA) was used. The coding sequences for the type 1 RIP and type 2 RIP from apple were amplified as *attB* products by PCR, using genomic DNA extracted from the bark of *Malus domestica* cv 'Jacques Lebel' and gene-specific primers (EVD 605/EVD 606 for type 1 RIP, EVD 607/ EVD 608 for type 2 RIP) containing part of the *attB* sites in the first PCR and primers EVD2/EVD 4 for the second PCR (Table 4.1). Tobacco Bright Yellow (BY)-2 cells were transformed using the type 2 RIP sequence as well as fusion constructs for the type 1 RIP and the B chain of type 2 RIP linked with the signal peptide (5'ATGACGAGAGTGTTAGCAATATACATTACTCTCGCATTTAGCCTCTTTCTCTGTGGCACCG AGTGC3') from the type 2 RIP sequence and a His tag (6 x histidine) at the N- and C-terminus, respectively. These additional sequences were added by PCR using specific primers. Finally, the constructs were completed with the *attB* sites using primers

92

Table 4.1 List of PCR primer pairs used in this research

Amplified sequence	Primer name	5'-3' sequence
Adding the non-complete *attB* sequences : type 1 RIP	EVD 605	AAAAAGCAGGCTTC ACCATGGCACTATCCTTCTCCATTAAG
	EVD 606	AGAAAGCTGGGTGCTATTTCTTCTTCTTGGCGAGGGTTGG
Adding the non-complete *attB* sequences : type 2 RIP	EVD 607	AAAAAGCAGGCTTCACCATGACGAGAGTGTTAGCAATATAC
	EVD 608	AGAAAGCTGGGTGTTAGAAGAACGGCAGCCATTGCTGGTT GGG
Completing the *attB* sequences	EVD 2	GGGGACAAGTTTGTACAAAAAAGCAGGCT
	EVD 4	ACCACTTTGCTCAAGAAAGCTGGGT
Sequencing	Donr-F	TCGCGTTAACGCTAGCATG
	Seql-E	GTTGAATATGGCTCATAACAC
Nictaba sequence, quality check of genomic DNA	EVD 1	AAAAAGCAGGCTTCACCATGCAAGGCCAGTGGATAGCCGC
	EVD 3	AGAAAGCTGGGTGTTAGTTTGGACGAATGTCGAAGCC
Tobacco ribosomal protein L25 (L18908)	EVD 282	TGCAATGAAGAAGATTGAGGACAACA
	EVD 283	CCATTCAAGTGTATCTAGTAACTCAAATCCAAG
qPCR reference gene: elongation factor 1α gene (EF1α)	P85	GATTGGTGG AATTGGTACTGTC
	P86	AGCTTCGTGGTGCATCTC
qPCR reference gene: Beta actin	P91	ATGCCTATGTGGGTGACGAAG
	P92	TCTGTTGGCCTTAGGGTTGAG
qPCR target gene: type 1 RIP	P55	AATCTGCATCCTCCCAAGCC
	P56	GCGGACTTGTCCCTGAATGT
qPCR target gene: type 2 RIP	P57	AAAGCACTGCGAGCCCAA
	P58	AGAGGAAGCGTTGTGAGTCC

EVD2/EVD4. Cycling parameters for the PCR reactions were: 2min 94°C, 25 X (15s 94°C, 30s 55 °C, 1 min 72°C), 5 min 72°C. Subsequently, all *attB* PCR products were homogeneously recombined in the entry vector pDONR221 (Invitrogen). Using heat shock transformation, the entry clones were subsequently transferred into *E. coli* strain Top10 cells. Transformants were selected by colony PCR. The plasmid DNA extracted from the colonies was sent for sequencing (performed by LGC Genomics, Berlin, Germany) using the primers Donr-F and Seql-E (Table 4.1). Finally, the LR reactions were performed with selected entry clones and enabled the cloning of the coding sequence for the type 1 RIP and the type 2 RIP in the pK7WG2.0 destination vector for tobacco plant transformation. Similarly the sequences encoding type 1 RIP, type 2 RIP and type 2 RIP B-chain were transferred into the pK7WG2D destination vector for BY-2 cell transformation.

4.3.3 Transformation of *Nicotiana tabacum* L. cv Samsun NN

The binary vectors carrying the type 1 or type 2 RIP sequence from *M. domestica* were introduced into *Agrobacterium tumefaciens* strain LBA4404 by tri-parental mating as described by Hoekema et al., (1983). Transformed cells were selected on YEB medium (consisting of 5 g/L beef extract, 5 g/L peptone, 5 g/L sucrose, 1 g/L yeast extract, and 15 g/L bacteriological agar) containing 50 mg/L spectinomycin and 20 mg/L gentamycin, and used for the transformation of *Nicotiana tabacum* L. cv Samsun NN following the leaf disc co-cultivation transformation procedure (Horsch et al., 1985). The transgenic plantlets were selected on MS medium containing kanamycin (300 mg/L) and carbenicillin (100 mg/L). The transformed tobacco plants were grown and seeds were harvested. The seeds were selected on MS agar plates containing 100 mg/L kanamycin. These plants from the T1 generation were used for the different experiments.

4.3.4 PCR analysis and RT-PCR

The integration of the T-DNA into the plant genome was checked by PCR on DNA extracted from tobacco leaves from plantlets of generation 0 and 1 (T0 and T1 generation). The cetyl trimethyl ammonium bromide (CTAB) method was used to extract the genomic DNA from tobacco leaves. The Nictaba (*Nicotiana tabacum* agglutinin; Chen et al., 2002b) sequence was amplified using the primers EVD 1 and EVD 3 (Table 4.1) to verify the quality of the genomic DNA. To check the presence of the type 1 and type 2 RIP sequences in the genomic DNA, PCR was performed using specific primers (EVD 605/EVD 606 for type 1 RIP, EVD 607/ EVD 608 for type 2 RIP,

Table 4.1). Cycling parameters for the PCR reactions were: 2 min 94°C, 25X (15s 94°C, 30s 55 °C, 1 min 72°C), 5 min 72°C. PCR analysis was used for the initial screening. Only the PCR positive plants were selected for further growing and collection of seeds.

Total RNA was isolated from transgenic tobacco leaves using Tri Reagent (Sigma-Aldrich, Bornem, Belgium) and the remaining DNA was removed by DNase I treatment (ThermoScientific, Erembodegem, Belgium). cDNA synthesis was performed using the M-MLV Reverse Transcripase Kit (Invitrogen). In total 40ng cDNA was used as the template for the RT-PCR reaction, which was performed using the same parameters as for the PCR amplification of genomic DNA. cDNA quality was checked using specific primers EVD 282 and EVD 283 (Table 4.1) to amplify the sequence encoding ribosomal protein L25.

4.3.5 Analysis of RIP expression in the transgenic plants by qRT-PCR

qRT-PCR was performed on a CFX96™ Real-Time PCR Detection system using the iQ™ SYBR® Green Supermix kit (Bio-Rad, California, USA). The amplification specificity of the primers was checked by sequencing of the RT-PCR products and analysis of the dissociation curve after qRT-PCR. To determine the efficiency of corresponding primer amplification, a serial dilution of cDNA was used to obtain standard curves. In each reaction, 10 μl of 2X supermix, 2 μl cDNA (40 ng/μl), 1 μl of 10 μM from each primer and 6 μl water were mixed in a total volume of 20 μl. The thermal profile consisted of 10 min at 95°C as a pre-denaturation step, followed by 45X (25s 96°C, 25s 60 °C, 20s at 72°C). The stability M values for the different reference genes were calculated by GeNorm Plus (Hellemans et al., 2007), after the quantification cycle (Cq) values processed into qBase^{PLUS}. The relative expression level of the target genes was normalized against the reference genes elongation factor 1α gene (EF1α) (Genebank Acc No. AF120093, Schaart et al., 2010) and beta actin (Genebank Acc No. U60495, Zhang et al., 2011) (Table 4.1) using qBase^{PLUS}. Target primers for qRT-PCR were designed by primer 3.0 software http://frodo.wi.mit.edu/ (Table 4.1) to amplify <120 bp amplicons. Each reaction was performed in triplicate.

4.3.6 Preparation of crude extracts and western blot analysis

Total protein from tobacco leaves was extracted in phosphate buffered saline (1X PBS: 17.1 mM NaCl, 3.31 mM $Na_2HPO_4.2H_2O$, 0.58 mM $Na_2HPO_4.12H_2O$, 13.4 mM KCl, 7.35 mM KH_2PO_4) using 0.5 ml buffer per gram of fresh weight (FW) leaf material.

Afterwards, the protein concentration was determined by the Coomassie (Bradford) Protein Assay Kit (Thermo Fischer Scientific, Rockford, IL, USA) according to the Bradford dye-binding procedure (Bradford et al., 1976).

Crude extracts from transgenic lines and wild type plants were immunodetected by western blot analysis. Therefore, the samples were separated by SDS-PAGE on a 15% polyacrylamide gel and proteins were transferred onto a polyvinylidene fluoride (PVDF) membrane (Bio Trace™ PVDF, PALL, Gelman Laboratory, Ann Arbor, MI, USA). First, the blots were blocked in blocking buffer, consisting of 5% milk powder dissolved in Tris buffered saline (TBS: 10 mM Tris, 150 mM NaCl and 0.1% (v/v) Triton X-100, pH 7.6). After blocking, blots were incubated for 1 h in TBS supplemented with a 1/1500 dilution rabbit anti-SNA-I (Chen et al., 2002a) antiserum as primary antibody. The secondary antibody was a 1/5000 diluted horseradish peroxidase-coupled goat anti-rabbit IgG (Sigma-Aldrich). Immunodetection was achieved by adding a sufficient amount of enhanced chemiluminescence detection substrate (Clarity™ Western ECL Substrate, Bio-Rad). The ChemiDoc MP imaging system (Bio-Rad) was used for the visualization of the signals from the blots. All washes and incubations were conducted at room temperature with gentle shaking.

4.3.7 Semi-quantitative analysis of the type 2 RIP content in transgenic lines

To compare the expression level between the different transgenic lines, a semi-quantitative analysis of the type 2 RIP content was performed by agglutination assays using rabbit erythrocytes (BioMérieux, Marcy I'Etoile, France). Agglutination assays were done in small glass tubes by mixing 10 µl total protein extract from each transgenic line (or the wild type plant), 10 µl of 1 M ammonium sulfate and 30 µl of a 10% suspension of trypsin-treated rabbit erythrocytes. After 30 min at room temperature, the agglutination was assessed visually. During these assays, similar amounts of total protein were compared for different transgenic lines or wild type plants. The whole experiment was repeated twice with different batches of plants.

4.3.8 Stable transformation of BY-2 cells and expression analysis

A three day old BY-2 cell culture was cocultivated with *A. tumefaciens* cells harboring the expression vector as previously described (Delporte et al., 2014). After 3 days cocultivation, transformed BY-2 cells were selected on MS agar plates containing antibiotics (500 mg/L carbenicillin, 100 mg/L kanamycin) and BY-2 vitamins for 3-4

weeks until resistant calli became visible. The transgenic cell colonies were detected by the Fujifilm FLA-5100 Fluorescent Image Analyzing System (Tokyo, Japan) based on the expression of the EGFP sequence located on the vector. Fluorescent calli were used to start a BY-2 liquid cell culture by transferring a 1 cm homogenous appearing callus into 20 ml BY-2 cell medium in a 40 ml Erlenmeyer. For the purification of recombinant proteins the cell cultures were grown into large-scale (600 ml) cultures. After seven days, the medium was harvested using a sintered glass pore filter with a filter disc paper. Afterwards, the medium was adjusted to 1.5 M ammonium sulfate at pH 7.0 for the purification of type 2 RIP and type 2 RIP B-chain. For purification of type 1 RIP, the medium was adjusted to pH 3.0.

4.3.9 Purification of recombinant RIPs and lectin

Purification of the recombinant type 2 RIP was achieved in three consecutive chromatographic steps. The BY-2 medium (pH 7) was obtained by vacuum filtration and loaded onto a column (5 cm x 30 cm; 80 ml bed volume) of Phenyl Sepharose (GE Healthcare, Uppsala, Sweden) equilibrated with 1.5 M ammonium sulfate (pH 7). After washing the column with 1.5 M ammonium sulfate (pH 7), the bound protein fraction was eluted with a solution of 20 mM 1,3 diaminopropane. The eluted fraction was brought to 1 M ammonium sulfate with the solid salt, the pH adjusted to 7 and applied onto a column (2 cm x 22 cm; 20 ml bed volume) of Fetuin-Sepharose equilibrated and washed with 1.5 M ammonium sulfate (pH 7). Bound proteins were eluted with a solution of 20 mM 1,3 diaminopropane and concentrated by a second chromatography on a small column (1 cm x 22 cm; 5 ml bed volume) of Fetuin-Sepharose using the same procedure as for the first affinity chromatography step. Following this procedure the type 2 RIP fraction was eluted in a few ml of 20 mM 1,3 diaminopropane. The lectin B chain from the type 2 RIP was purified essentially as described for the type 2 RIP using hydrophobic interaction chromatography (HIC) combined with affinity chromatography.

To isolate the recombinant type 1 RIP a purification scheme was developed that included two consecutive chromatographic steps. First the cleared BY-2 medium (adjusted to pH 3) was loaded on a column (2 cm x 22 cm; 20 ml bed volume) of S Fast Flow equilibrated with 50 mM sodium acetate (pH 3). After washing the column with 50 mM sodium acetate (pH 3), the type 1 RIP fraction was eluted with a solution of 1 M NaCl in 20 mM 1,3 diaminopropane (pH 8.7). The eluted fraction was adjusted to pH 3.0 with 1 M HCl and concentrated on a small column (1 cm x 22 cm; 5 ml bed

volume) of S Fast Flow using the same procedure as during the first chromatography step. The purity of the protein in the second eluate was assessed by SDS-PAGE analysis.

4.3.10 Pathogens and infection method

The fungal and virus infection experiments were done in collaboration with the lab of Prof. Monica Höfte (Department of Crop Protection, Ghent University, Belgium).

Botrytis cinerea strain R16 (Faretra & Pollastro, 1991) was grown on PDA (Potato Dextrose agar, Lab M, Lancashire, UK) for 5 days in the dark at 18°C and 10 days under a light regime of UV/dark of 12h/12h at 21°C. The conidial inoculation suspension was prepared as follows: spores were washed from the plates with distilled water containing 0.01% (v/v) Tween 20. After removal of mycelial debris, the conidial suspension was centrifuged for 10 min at 4500 rpm at 14°C. The supernatant was removed and the conidia were resuspended in sterilized distilled water. The inoculation suspension containing 2 X 10^5 spores/ml was prepared in ¼ strength PDB (potato dextrose broth, Duchefa) (Audenaert et al., 2002; Asselbergh et al., 2007; Seifi et al., 2013).

Infection experiments with *B. cinerea* were performed as described by Audenaert et al., (2002). The petioles of detached tertiary leaves from 6-week-old tobacco plants were wrapped in wet cotton and placed on a plastic tray containing four layers of absorbent paper. A total of 12 leaves per line were inoculated by putting 6 droplets of 10 µl conidial inoculation suspension on each leaf surface. The trays were moisturized with approximately 400 ml of distilled water and closed with plastic folium to keep a relative humidity of 100% and incubated at 22 °C under dark condition. After two days, disease symptoms were evaluated by quantification of the lesion diameter by Image Analysis Software for Plant Disease Quantification: *Assess 2.0* (https://www.apsnet.org/apsstore/shopapspress/Pages/43696m5.aspx). Inoculation droplets were classified as non-spreading (the lesion area was not larger than the inoculation droplets), spreading (pale-brown, round-shaped dots; lesion area was much larger than inoculation droplets) or necrotrophic (dark-brown, irregularly- shaped dots) lesions (Supplementary Fig. S4.1).

4.3.11 Visualization of defense responses

In vivo assay

To observe the differences in defense responses between wild type and transgenic tobacco plants, leaf discs were inoculated with *B. cinerea* as described above and fungal growth analyzed after 16 h and 24 h. Infected leaf discs were fixed in 100% ethanol overnight. Fungal structures were stained with 0.1% trypan blue in 10% acetic acid for 60s followed by three rinsing steps in distilled water, using the trypan blue staining technique (Seifi et al., 2013). Afterwards, samples were mounted in 50% glycerol before microscopic observation. Images of the stained fungal structures were digitally acquired with an Olympus BX51 microscope equipped with an Olympus ColorView III camera (Tokyo, Japan).

In vitro assay

The *in vitro* microtiter-plate antifungal activity test was performed as described by Broekaert et al. (1990). Each well of a 96-well polypropylene U bottom plate (Bibby Sterilin Ltd. Stone, Staffs, U.K.) was filled with 20 µl of filter-sterilized recombinant purified protein (5 mg/L of type 1 RIP, type 2 RIP or type 2 RIP B-chain) and mixed with 80 µl ½ strength PDB containing 1.6×10^4 spores of *B. cinerea*. After 20 h incubation at 21°C, the images were digitally acquired with an Olympus BX51 microscope equipped with an Olympus ColorView III camera (Tokyo, Japan).

4.3.12 Virus material and infection method

Tobacco mosaic virus strain vulgare (*TMV-vulgare*) was purchased from Leibniz-Institut Deutsche Sammlung von Mikroorganismen und Zellkulturen GmbH, (DSMZ, Braunschweig, Germany). Inoculation of the tobacco plants with TMV was performed using the standard mechanical rubbing method (Vandenbussche et al., 2004a). To perform the inoculation, 0.05 g tobacco leaves fully infected with TMV were extracted in 1 ml of cooled 50 mM potassium phosphate buffer (pH 7.0). Fully expanded leaves of *N. tabacum* cv Samsun NN (6-week-old) were dusted with silicon carbide (mesh size 400, Sigma-Aldrich) and inoculated by gently rubbing the upper leaf surface with 200 µl of the viral suspension inoculum, followed immediately by rinsing with deionized water. Following inoculation, plants were maintained in a growth room at 25°C under a 16/8 h light/dark regime. The lesion diameter and the disease index of the infected leaves were examined three days after inoculation.

The TMV infection lesions were evaluated by scoring the infected leaves into six different groups according to the lesion symptoms as defined in supplementary Fig. S4.2 (Kanzaki et al., 2004, Seifi et al., 2013).

4.3.13   Insect bioassays on artificial diet

The insect bioassays were done in collaboration with the lab of Prof. Guy Smagghe (Department of Crop Protection, Ghent University, Belgium).

Pea aphids (*Acyrthosiphon pisum*) were maintained on young broad bean plants (*Vicia faba* L) (Sadeghi et al., 2009a). To synchronize the age of the nymphs, mature aphids were put on a bean plant. After 24 h, all neonate nymphs were used in the bioassay. Before and during the bioassays, all insects were maintained in growth chambers at 25 ± 2°C with 65 ± 5% relative humidity and a 16/8 h light/ dark photoperiod.

The basal food used for the aphids was developed from a standard diet for *A. pisum* (Febvay et al., 1998) as described in Sadeghi et al., (2009b) and Al Atalah et al., (2014b). A feeding sachet was constructed by putting 150 μl artificial diet in between two layers of parafilm under sterile conditions. To determine the effects of the proteins (type 1 RIP, type 2 RIP or type 2 RIP B-chain) on the neonate nymphs, several concentrations of the recombinant proteins (type 1 RIP: 80, 160, 320, 640, 960 mg/L; type 2 RIP: 17, 34, 68, 136, 204 mg/L; type 2 RIP B-chain: 30, 60, 120, 240, 360 mg/L) were tested. Since a solution of 20 mM un-buffered diaminopropane was used to dissolve the recombinant proteins, an artificial diet supplemented with equal volumes of this solution was used as a control. A total number of ten neonate nymphs was transferred onto the artificial diet containing the recombinant proteins. The mortality was determined and the dead insects were removed daily for three consecutive days. For each protein concentration, three replicates were carried out.

4.3.14   Statistics

Data were expressed as means ± standard error (SE). For the quantitative RT-PCR, three technical replicates were performed. In the agglutination activity assay, data from two biological replicates were averaged. All decimal percentages and numbers were rounded to the nearest integer. In the classification of the fungal infection lesion evaluation experiment, different letters represent significant differences (Duncan; $P < 0.05$) between different tobacco lines analyzed by IBM Statistical

Package for the Social Sciences Statistics (IBM SPSS Statistics, IBM, New York, US). In the Disease Index analysis, the infection differences between transgenic lines and wild type plants were statistically analysed using SPSS (Tuckey's b). Lesion diameters were compared between the transgenic lines and the wild type plants, using the one-way ANOVA (Dunnett's Multiple Comparison Test) test for the statistical analysis. The 50% lethal concentration (LC50) together with the 95% confidence limits and the R^2 of the sigmoid curve fitting were determined using the non-linear regression analysis in Prism version 5 (GraphPad, La Jolla, CA).

4.4. Results

4.4.1 Ectopic expression of type 1 and type 2 RIP sequences from apple in transgenic tobacco plants

The coding sequences of type 1 RIP or type 2 RIP from apple were cloned into a binary vector using the Gateway technology. Therefore, the RIP sequences were amplified from genomic DNA from apple (*Malus domestica* cv 'Jacques Lebel') and cloned behind the 35S cauliflower mosaic virus promoter sequence. Tobacco (*Nicotiana tabacum* L. cv Samsun NN) leaf discs were transformed with *Agrobacterium tumefaciens* LBA4404 harboring the destination vector pK7WG2.0 with the type 1 or type 2 RIP sequence. A total of 50 independent transgenic lines per construct were obtained after shoots and roots emerged from the transformed calli. After screening, only independent T0 lines (28 per construct) presenting the RIP sequence at DNA level were allowed to grow into adult plants and produce seeds. Once plantlets of the T1 generation were obtained, the expression of the type 1 or type 2 RIP gene was checked at the DNA, RNA and protein level by PCR analysis, quantitative RT-PCR and Western blot analysis, respectively. A total number of 16 plants were tested for each construct. Finally, five lines with the type 1 RIP gene and seven lines with the type 2 RIP gene were selected for the biotic stress experiments.

PCR analysis of both genomic DNA and RNA/cDNA yielded amplification products of 900 bp and 1641 bp, respectively, which demonstrated that the type 1 and the type 2 RIP sequences are (i) present in the tobacco and (ii) transcribed (Fig. 4.1A and B). Western blot analysis further demonstrated that both the type 1 RIP and the type 2 RIP are present in crude leaf extracts (Fig. 4.1C). Quantitative RT-PCR was applied for a more detailed analysis of the ectopic expression of the type 1 and type 2 RIP sequences in the transgenic tobacco plants. Thereby the expression of type 1 and type 2 RIP transcripts in each line was normalized against the reference genes (EF1α

and beta actin). This approach indicated that line 7 of the type 1 RIP series exhibited the highest type 1 RIP expression. Within the type 2 RIP series lines 11, 18, 27 and 44 exhibited the highest expression levels (Fig. 4.1D). For these lines the high expression of the type 2 RIP was confirmed by –on a biological activity based- semi-quantitative agglutination assays with rabbit erythrocytes. As shown in Table 4.2 crude extracts from leaves of lines 27 and 44 exhibited the highest agglutination activity followed by these from lines 11 and 18. Extracts from plants of lines 22, 25 and 28 were clearly less active in the agglutination assays.

A comparison of the quantitative RT-PCR results further indicated that the expression level of the type 2 RIP gene in tobacco plants was approximately ten-fold higher than that of the type 1 RIP gene (Fig. 4.1D).

Table 4.2 Agglutination activity of crude leaf extracts from transgenic tobacco plants expressing type 2 RIP and wild type plants. A, B and C refer to extracts prepared from three different batches of plants of each line. The protein concentration in the extracts of the series A, B and C amounted to 0.86, 1.72 and 3.44 µg, respectively. A type 2 RIP from elderberry (SNA-I) was used as a positive control. The buffer 1xPBS was used as negative control.

Transgenic line	Agglutination activity of protein extract*		
	A	B	C
T2-11	+	+	++
T2-18	+	+	++
T2-22	-	-	-
T2-25	+	+	+
T2-27	++	++	+++
T2-28	-	-	-
T2-44	++	++	+++
WT	-	-	-
PC (SNA-I)	++++	++++	++++
NC (1XPBS)	-	-	-

*: ++++, +++, ++ and + indicate very strong, strong, good and weak agglutination activity of rabbit red blood cells; –, designates lack of activity.
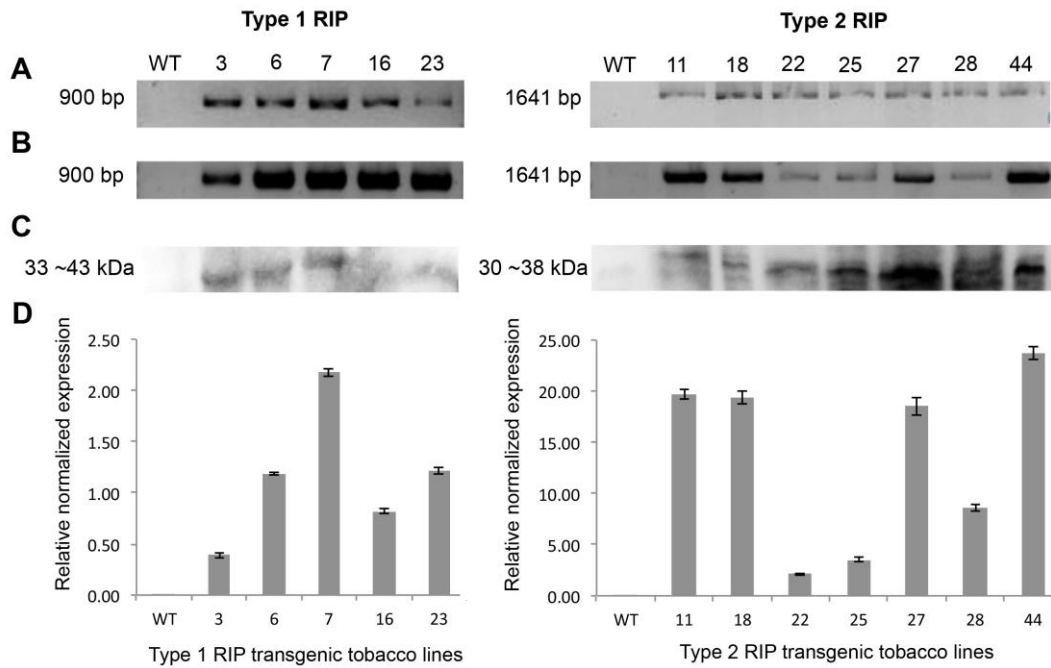
Figure 4.1 Overview of the analysis of the transgenic lines at DNA, RNA and protein level. Panel (A): Gel electrophoresis of PCR fragments amplified from genomic DNA extracted from the wild type and transgenic tobacco plants using RIP specific primers; panel (B): Gel electrophoresis of PCR fragments amplified from RNA extracted from the wild type and transgenic tobacco plants using RIP specific primers; panel (C): Western blot analysis of protein samples by ECL detection. Equal amounts (20 μg) of crude extracts were loaded on gel; panel (D): Quantitative RT-PCR analysis of the expression of the RIP genes. Transcript levels were normalized to the expression of EF1α and beta-actin. Numbers refer to the numbering of the transgenic lines.

4.4.2 Phenotypic changes in tobacco plants overexpressing RIP genes

Upon monitoring of the 56 transgenic lines of the T0 generation it was observed that approximately 3.6% of all the tobacco plants expressing the type 2 RIP gene developed abnormal flowers (characterized by double layers of incomplete flowers) (Supplementary Fig. S4.3). Since the yield of seeds for these flowers was very low, these plants were discarded from the selection of plants to be studied. Furthermore, approximately one third of the plants in the T1 generation displayed abnormal morphological phenotypes (Fig. 4.2A and B) and/or a reduced root system (Fig. 4.2D). Some plants from the T1 generation overexpressing the type 2 RIP had two shoots (8.03%) or a reduced amount of roots (41.1%). Similar observations were made for the T1 generation of type 1 RIP overexpressing plants in that approximately one third of the plants suffered an impaired root system (Fig. 4.2C and Supplementary Fig. S4.4). These observations indicate that (over)expression of either the type 1 or type 2 RIP genes from apple affects normal development in at least

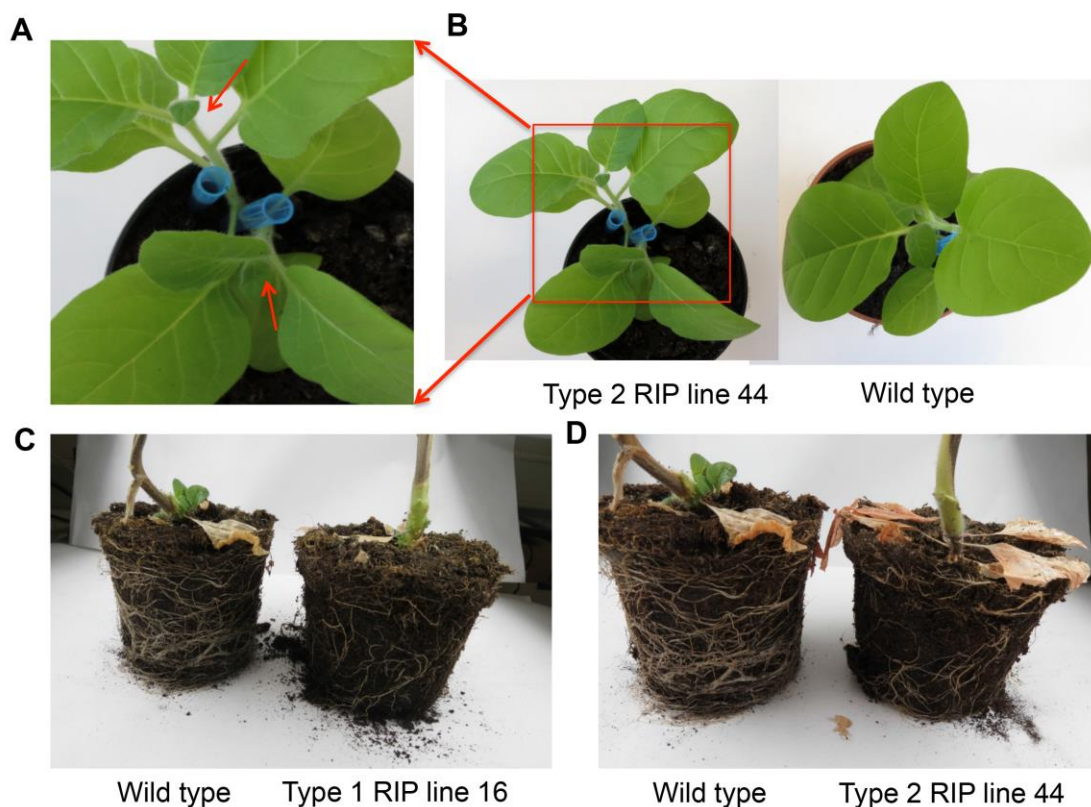part of the transgenic tobacco plants.

Figure 4.2 Pictures showing abnormal morphological phenotypes in the T1 generation of the transgenic tobacco plants overexpressing apple RIP sequences. Panel (A): Tobacco plant expressing type 2 RIP with two shoots; panel (B): Comparison of a wild type plant and a tobacco plant expressing type 2 RIP; panel (C and D): Comparison of root development in wild type and transgenic tobacco plants expressing type 1 and type 2 RIPs, respectively.

4.4.3 Antifungal activity of apple RIPs on *B. cinerea* with/without plant defense system

To investigate whether overexpression of the type 1 or type 2 RIP gene from apple possibly enhances the resistance of transgenic tobacco plants against fungi a series of bioassays was set up with *B. cinerea* strain R16, which is virulent to tobacco (Achuo et al., 2004). Plants generated from five and seven independent transformants expressing the type 1 RIP and the type 2 RIP, respectively, were inoculated with *B. cinerea* conidial spores. The first symptoms of fungal infection appeared between 24 h and 48 h after artificial inoculation of the leaves. Macroscopic disease symptoms were evaluated at 48 h post-inoculation (hpi) by classification of the lesion types and quantitative measurement of the spot diameter. The percentage of non-spreading lesions was higher in all transgenic lines when

compared to the wild type leaf tissue (Fig. 4.3A, B and C), suggesting that most wild type plants were more susceptible to *B. cinerea* than the transgenic lines. The graph showing the percentage of non-spreading lesions (Fig. 4.3D) suggests a difference between tobacco plants overexpressing the type 1 RIP and the type 2 RIP, respectively, indicating a higher antifungal activity for the type 2 RIP. It is also worth noting that the germination and development of the fungus on leaves of plants of lines 11, 18, 27 and 44 of the type 2 RIP series is slowed down significantly. Moreover, all the transgenic lines apparently exhibited a decreased spreading of *B. cinerea* as can be concluded from the reduction of the diameter of the lesions (Fig. 4.3 E, F and G). The inhibition of fungal germination at the early stage of leaf infection was further corroborated by microscopic analysis. Observations at 16 and 24 hpi clearly demonstrated that the fungus already infected the tobacco plants. However, the length of the fungal hyphae on the leaves of the transgenic lines was much shorter than in the wild type plants, which indicates that expression of type 1 and type 2 RIPs from *M. domestica* results in a clearly visible reduction of the development of Botrytis (Fig. 4.4).

To assess direct effects of the recombinant proteins on fungal growth, *B. cinerea* spores were germinated in the presence or absence of 100 ng purified recombinant type 1 and type 2 RIPs. As shown in Fig. 4.5 addition of both type 1 and type 2 RIPs resulted in a clear reduction of the germination of the fungal spores and development of the hyphae after 20 h. In contrast, addition of the recombinant protein corresponding to the B chain of the type 2 RIP did not affect spore germination and fungal growth.
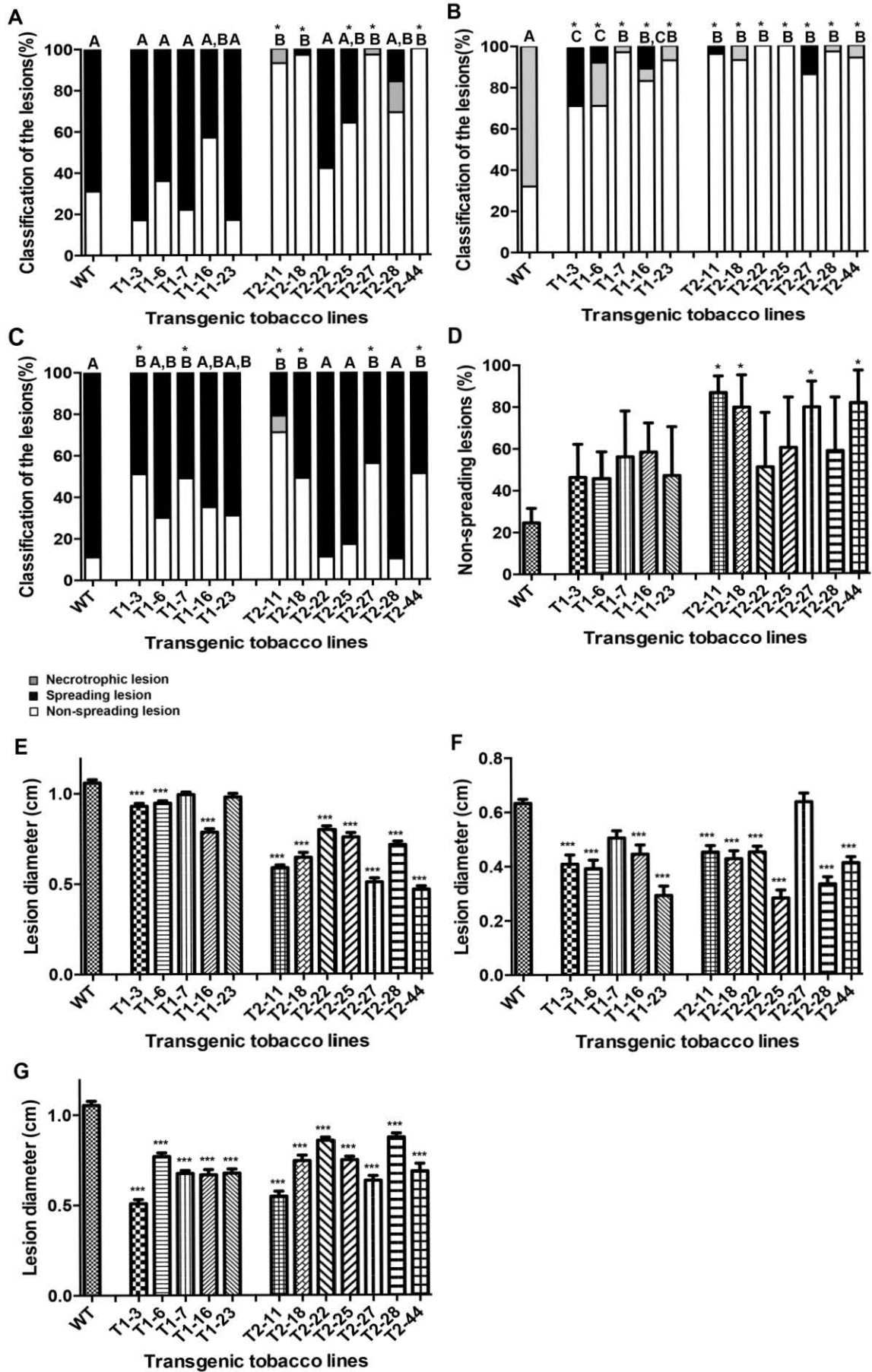
□ Necrotrophic lesion
■ Spreading lesion
□ Non-spreading lesion

Figure 4.3 Effect of *B. cinerea* infection on tobacco plants expressing type 1 and type 2 RIPs from apple*.* Panels (A, B and C): Distribution of the three classes of infection lesions (spreading lesion, necrotrophic lesion and non-spreading lesion) in wild type and transgenic tobacco lines. The three different panels show the results of three independent infection experiments. Panel (D): Percentage of non-spreading lesions in wild type and transgenic tobacco lines. Panels (E, F and G): Lesion diameter in wild type and transgenic tobacco lines. Twelve plants of each line were used in three independent replicate infection experiments. Data are means ±SE of at least twelve different plants (leaves). Numbers refer to numbering of transgenic lines. Asterisks denote values significantly different from the wild type (WT) (*: $p < 0.05$; **: $p < 0.01$; ***: $p < 0.001$).
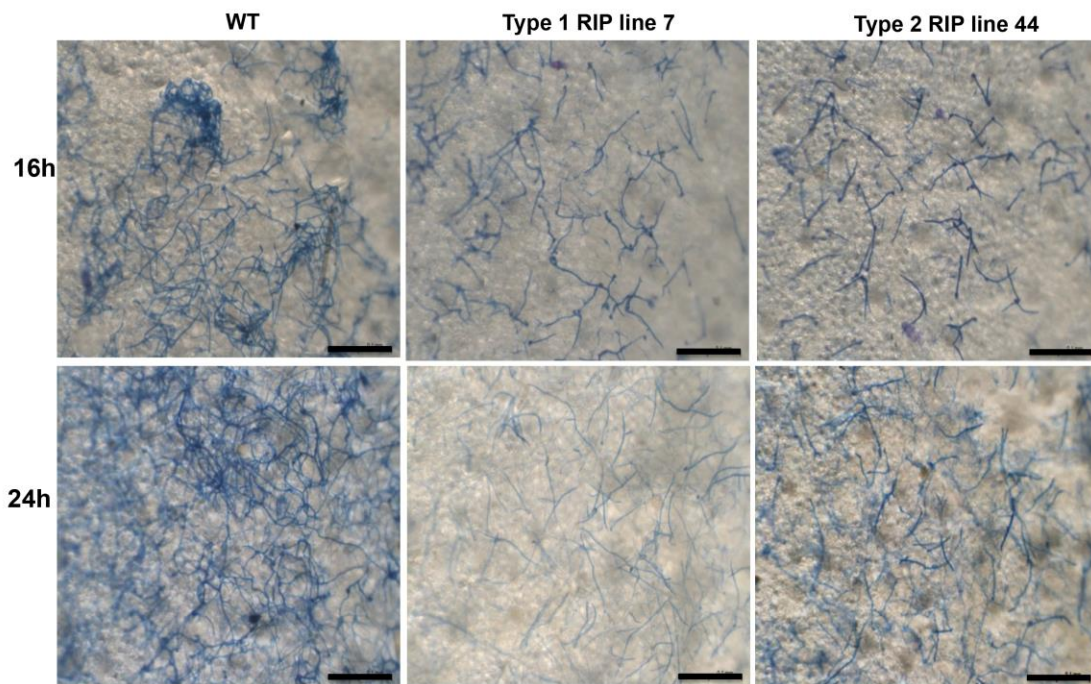

Figure 4.4 Microscopic analysis *B. cinerea* infection in wild type plants and tobacco plants expressing apple RIPs. Images show trypan blue staining of *B. cinerea* infecting the wild type and transgenic tobacco (type 1 RIP line 7 and type 2 RIP line 44) leaf tissue. Fungal growth was monitored 16h and 24h post-inoculation. Scale bars represent 0.2 mm.
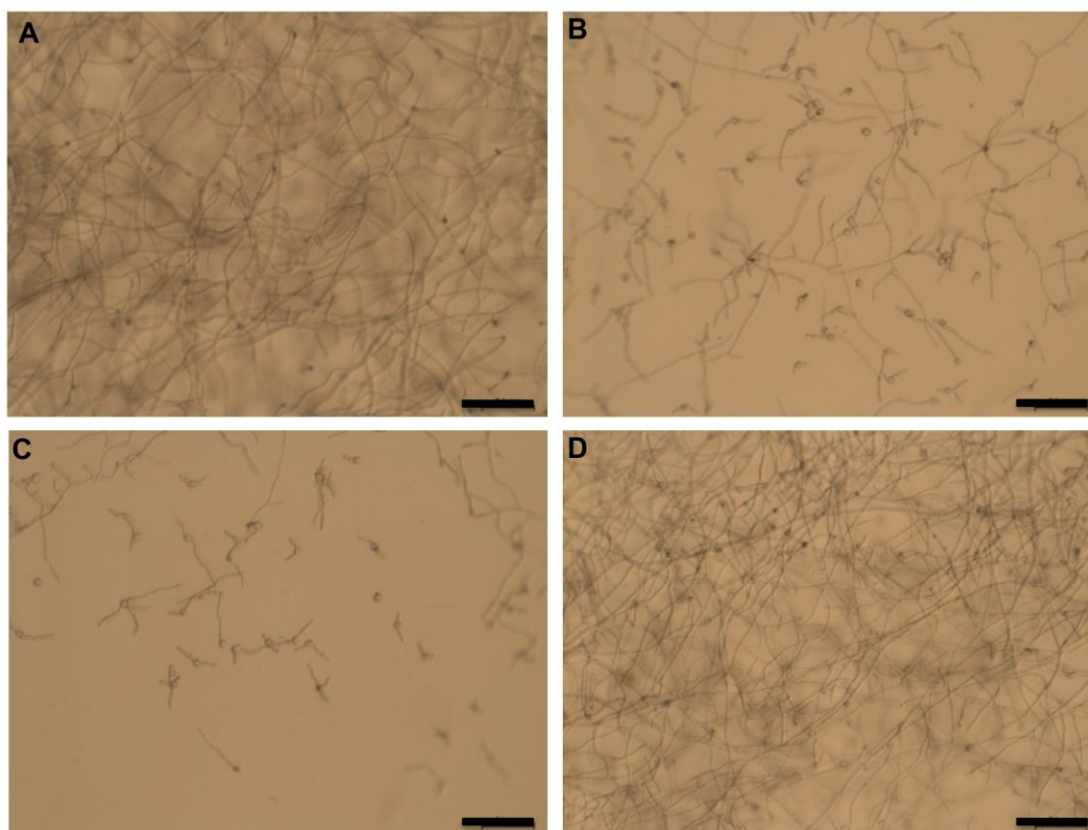
Figure 4.5 Microscopic visualization of the inhibitory effect of recombinant type 1 RIP, type 2 RIP and type 2 RIP B-chain on the *in vitro* growth and morphology of *B. cinerea*. Panel (A): *B. cinerea* grown in the control medium (1/2 strength PDB); panels (B, C and D): *B. cinerea* grown in 1/2 strength PDB supplemented with 1µg/ml recombinant type 1 RIP, type 2 RIP and type 2 RIP B-chain, respectively. Pictures were taken 20h after incubation. Scale bars represent 0.15 mm. Note the stunted growth and hyperbranching of the fungus grown in the presence of the recombinant proteins.

4.4.4 Antiviral activity of the apple RIPs

To assess the *in planta* antiviral activity of the apple type 1 and type 2 RIPs transgenic tobacco plants were constructed and challenged with TMV. For these experiments *Nicotiana tabacum* cv. Samsun NN was chosen because this genotype exhibits -due to the presence of the *N* gene- a hypersensitive necrotic reaction upon infection with TMV. As shown in Fig. 4.6 both the number of lesions and the lesion size were reduced in the transgenic lines as compared to the wild type plants, (Fig. 4.6). In wild type plants, lesions were more abundant and appeared as larger, dry, pale-brown, irregularly shaped dots, whereas in the transgenic lines, infection spots were small round-shaped, dark-brown dots. These observations clearly indicated that the expression of type 1 and type 2 RIPs slowed down the development of the viral infection symptoms.
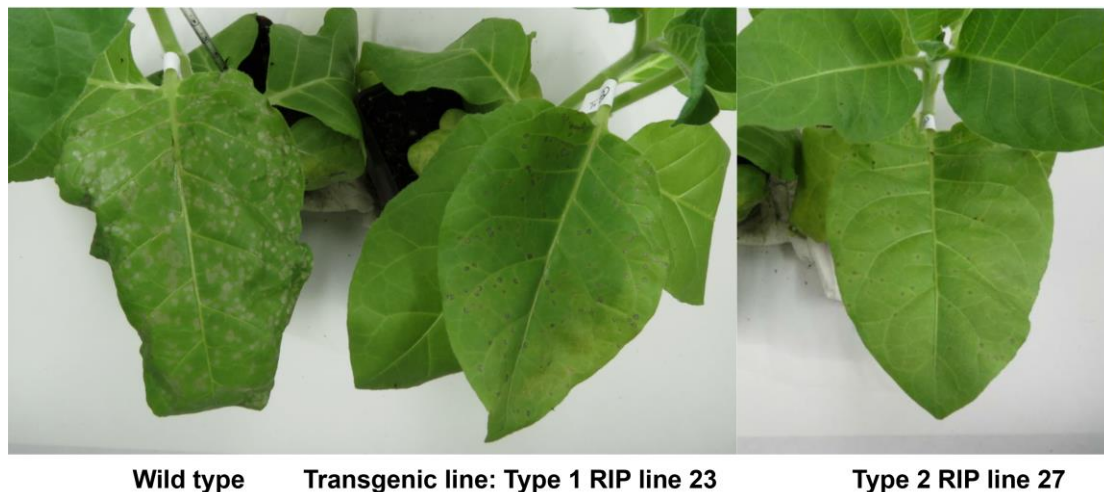
Figure 4.6 Photographs of the development of lesions on the leaves of wild type and transgenic tobacco plants upon infection with TMV. Pictures were taken 3 days post-infection and show a dramatic decrease in the appearance of symptoms in the transgenic plants expressing type 1 and type 2 RIPs from apple.

To quantify the antiviral activity in the transgenic lines, each infected leaf of the transgenic and wild type control plants was scored and evaluated as described in Materials and Methods. Compared to the wild type plants, all transgenic lines exhibited a clear reduction of both the disease index and the lesion diameter. Transgenic lines 16 and 23 of the type 1 RIP series and lines 27 and 44 of the type 2 RIP series displayed a statistically significant decrease, indeed, of the disease index in three biological replicates (Fig. 4.7A, B and C). Moreover, the lesion diameter in the leaves of the RIP overexpression lines was also significantly reduced as compared to that of the wild type plants (Fig. 4.7 A', B' and C'), which indicates that the ectopically expressed apple RIPs reduce spreading of the lesions. Though both type 1 and type 2 RIPs definitely affect spreading of the virus the type 2 RIP apparently performed better than the type 1 RIP.
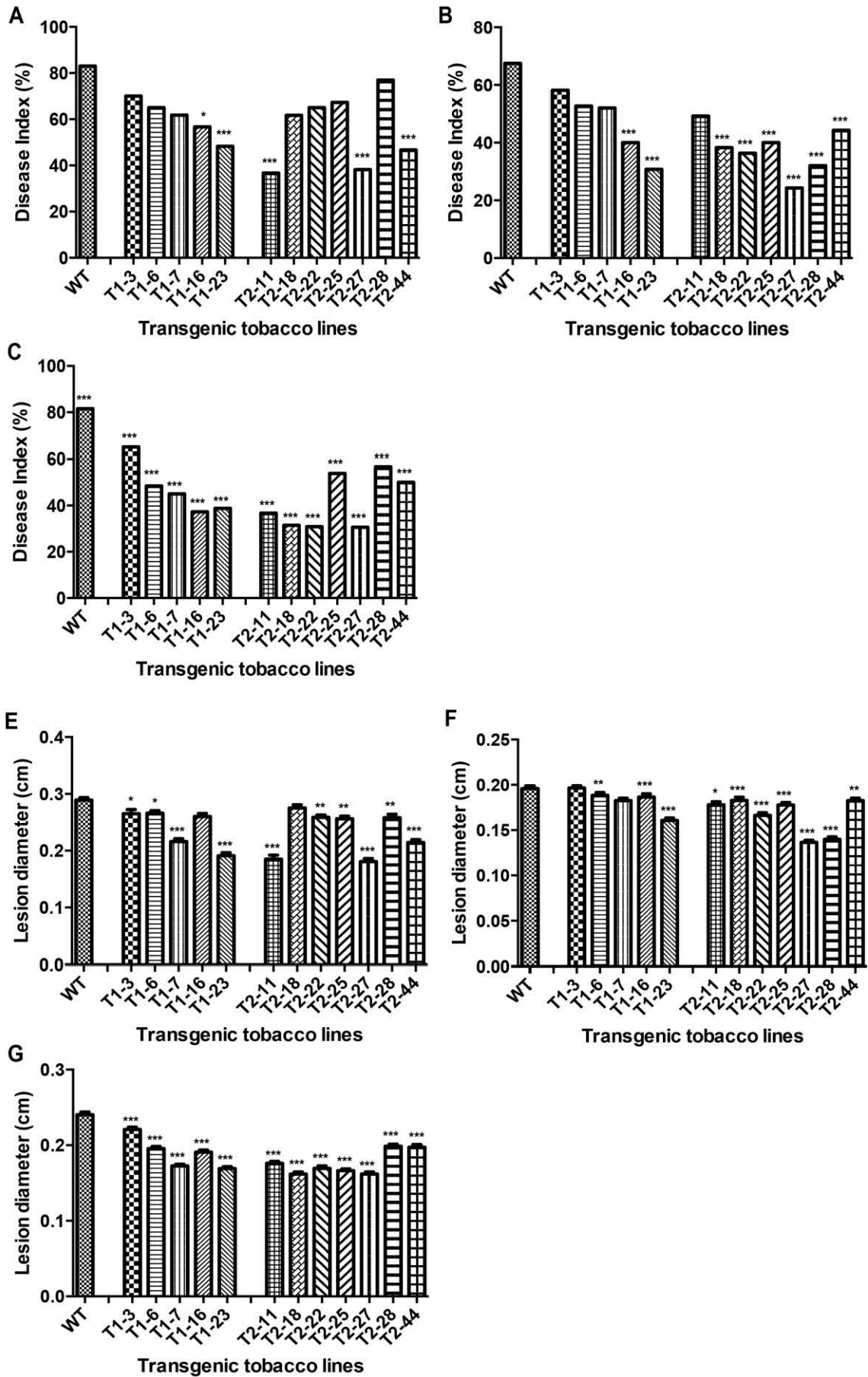
Figure 4.7 Quantitative analysis of the effect of ectopically expressed apple RIPs on the resistance of transgenic tobacco plants to TMV infection. Panels (A, B and C): comparison of the disease index in wild type and transgenic tobacco plants expressing apple type 1 and type 2 RIPs. Each panel represents the results of three independent infection experiments. The disease index was calculated from the number of lesions and the lesion size on the leaf according to the procedure described in Supplementary Fig. S4.2. Panels (A', B' and C'): comparison of the viral lesion diameter in wild type and transgenic tobacco plants expressing apple type 1 and type 2 RIPs. Each panel represents the results of three independent infection experiments. Data are means ±SE of at least twelve different plants (leaves). Asterisks denote values significantly different from the wild type (WT) (*: $p < 0.05$; **: $p < 0.01$; ***: $p < 0.001$).

4.4.5 Insecticidal activiy of recombinant apple proteins (type 1 RIP, type 2 RIP and type 2 B-chain) on *Acyrtosiphon pisum*

To assess the entomotoxic/insecticidal activity of the apple RIPs a series of feeding trials were set up. An artificial diet containing increasing concentrations of recombinant proteins (type1 RIP, type 2 RIP and type 2 RIP B-chain) was fed to neonate (<24h) nymphs of *A. pisum* to test the insecticidal activity and determine the 50% lethal concentration of the different proteins. The mortality of the neonate nymphs was determined 2 and 3 days after feeding, respectively (Fig. 4.8). Two days after feeding calculated LC_{50} values for the type 1 RIP, the type 2 RIP and the type 2 RIP B-chain were 566.1 mg/L (95% confidence limits: 468.5 to 684.0 mg/L and $R^2=0.89$), 84.09 mg/L (95% confidence limits: 69.77 to 101.4 mg/L and $R^2=0.89$) and 159.02 mg/L (95% confidence limits: 130.1 to 194.7 mg/L and $R^2=0.90$), respectively. After 3 days, the aphid mortality reached 100% at the highest concentration of the proteins tested and the LC_{50} value decreased to 340.5 mg/L (95% confidence limits: 270.6 to 428.5 mg/L and $R^2=0.87$) for type 1 RIP, 33.42 mg/L (95% confidence limits: 28.95 to 38.57 mg/L and $R^2=0.97$) for type 2 RIP and 105.9 mg/L (95% confidence limits: 94.02 to 119.3 mg/L and $R^2=0.95$) of type 2 RIP B-chain. It should be noted that the average mortality for nymphs in the control was 0% and 0.11% at day 2 and day 3, respectively.
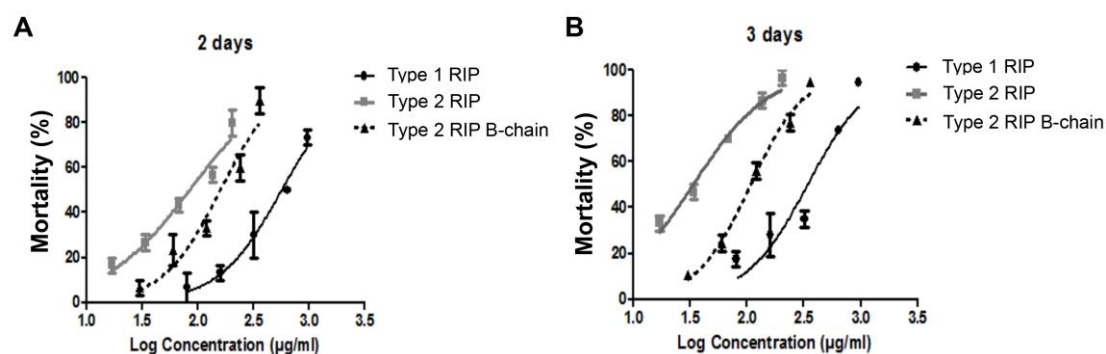
Figure 4.8 Effect of recombinant apple RIP on *A. pisum* in feeding trials with an artificial diet. Panels A and B show the dose response curves for apple type 1 RIP, type 2 RIP and type 2 RIP B-chain on the nymphal mortality of *A. pisum* after two and three days, respectively. Data are expressed as means ±SE based on three replicates with a total of 30 nymphs tested for each protein concentration.

4.5   Discussion

At present the physiological role of RIPs in plants is still poorly understood. Since genome sequencing programs leave no doubt that many plant species do not possess a RIP gene one can reasonably conclude that RIPs are not essential for normal growth and development of plants and accordingly can be considered as accessory proteins. However, this does not preclude that at least some RIPs contribute to some extent to the survival of plants in their natural environment. Experimental evidence is accumulating, indeed, for a defense-related role of several RIPs. For example, the extremely high toxicity of ricin, abrin and other type 2 RIPs certainly offers an efficient protection against herbivorous animals and invertebrates (Krivdova et al., 2014). Other less toxic type 2 RIPs as well as type 1 RIPs are believed to enhance the plant's defense potential against viruses and fungi (Chen et al, 2002a; Vandenbussche et al., 2004a,b, Corrado et al., 2005). However, since only a limited number of RIPs were involved in studies of defense-related processes no general conclusions can be drawn with respect to the contribution of RIPs to the plant's survival under natural conditions.

To broaden our insight in the biological defense-related activities it seemed worthwhile to make a detailed study of some "novel" RIPs that distinguish themselves in one way or another from the RIPs used in previous studies. During an *in silico* search for such a novel system our attention was drawn to apple. The genome of this fruit species comprises a gene for a type 2 RIP and several genes for a

type 1 RIP (see chapter 2). Interestingly, the type 2 RIP lacks (unlike the classical type 2 RIPs) an internal vacuolar targeting signal sequence containing a LLIRP motif (Frigerio et al., 2001) and accordingly is predicted to be secreted. Moreover, the type 1 RIPs are (unlike all other type 1 RIPs from dicots described thus far) apparently synthesized without a signal peptide and hence presumed to be retained in the cytoplasmic/nuclear cell compartment (see chapter 3). This particular feature of the apple type 1 RIP results from an evolutionary event whereby the lectin domain was deleted from a typical type 2 RIP gene and, in addition, the signal peptide was lost due a frame shift resulting from a single nucleotide deletion (Peumans et al., 2014). These considerations, taken together with the fact that the hitherto unsuspected occurrence of RIPs in apple might be of some concern from the point of view of food safety, justified to choose apple as a novel system to study the physiological role of RIPs.

To corroborate the protective activities of the apple RIPs a series of experiments were set up with both the purified recombinant proteins and transgenic tobacco plants overexpressing the RIP genes. Recombinant proteins were isolated by standard techniques from BY-2 cell cultures. Transgenic tobacco plants were constructed to express the type 1 and type 2 RIP genes under the control of the 35S cauliflower mosaic virus promoter and the actual expression of the transgenes was analyzed at the DNA, RNA and protein level. Fig. 4.1 reveals that the expression on mRNA level does not match with the detected protein level for several transgenic lines (Fig. 4.1), which is possibly due to differences on the transcriptional and translational level. Based on table 4.2, the transgenic type 2 RIP tobacco lines could be ordered by the degree of their agglutination activity as follows: line 27 ≅ line 44 > line 11≅ line 18 > line 25 > line 22≅ line 28. The agglutination activity of most tobacco lines expressing type 2 RIP correlates fairly well with the expression level of the RIP at transcript level (Fig. 4.1).

Visual inspection revealed that some transgenes exhibit a phenotype characterized by the occurrence of twin shoots and a reduced root development but in no case a dramatic growth inhibition was observed. Similar observations have been reported previously for tobacco plants expressing RIPs from *Iris* (Desmyter et al., 2003; Vandenbussche et al., 2004a). This suggests that RIPs have an indirect effect that results in the phenotypes described. Reduced capacity of translation may lead to side effects in disease development.

To check the antifungal activity leaves of transgenic tobacco plants were challenged with spores of *Botrytis cinerea*, a necrotrophic fungus that causes important losses in many crop plants and fruits, such as apple, strawberry, grape and tomato (Choquer et al., 2007), and is also a major threat in apple post-harvest storage. Ectopic expression of both type 1 and type 2 apple RIPs definitely resulted in a reduction of the growth rate and spreading of *B. cinerea* (Fig. 3 and 4). *In vitro* experiments confirmed that the purified proteins also slowed down spore germination and hyphal growth. A comparative analysis of the different transgenic lines further indicated that the antifungal activity is correlated with the expression level of the RIP. The differences between independent biological replicates are possibly due to the differences in environmental conditions during the infection experiment. At present it is still unclear how RIPs act on fungi. Fungal ribosomes are very susceptible to RIPs but in order to provoke an effect the RIP must enter the cytoplasm of the fungal cells (Krivdova et al., 2014). The type 2 apple RIP eventually ends up in the extracellular space (see Chapter 3), whereas the type 1 RIP accumulates in the nucleus and cytoplasm (see Chapter 3). When *B. cinerea* breaches the cell wall and infects the host cells both type 1 and type 2 RIPs can come in contact with the growing hyphae. The type 2 RIP might enter the fungal cell after binding of the B chain to the glycoconjugates in membrane and endocytosis but the type 1 RIP –if taken up at all- must enter by another mechanism (direct endocytosis?). Irrespective of the exact mode of action of the apple RIPs their antifungal activity is hardly comparable to that of genuine antifungal proteins (Selitrennikoff, 2001).

RIPs are often considered as antiviral proteins. Several type 1 RIPs (e.g. pokeweed antiviral protein) were demonstrated, indeed, to increase the plant's resistance to viruses. It is believed that upon infection with a virus the RIPs inactivate the host cell ribosomes, which results in cell death and stops further spread of the virus (Tumer et al., 1997). Type 2 RIPs were less intensively studied for what concerns their antiviral activity but experiments with transgenic plants revealed that also some type 2 RIPs offer protection against viruses (Chen et al., 2002a). The fortuitous occurrence of both type 1 and type 2 RIPs in apple offered a unique opportunity to corroborate and compare the antiviral activity of the two different types of RIPs within a single species. Bioassays with transgenic tobacco plants demonstrated that both ectopically expressed apple type 1 and type 2 RIPs reduce – in a statistically significant way- spreading of the lesions and lesion diameter upon infection with TMV. Quantitation of the antiviral activity revealed that the apple type 2 RIP

apparently performed better than the type 1 RIP. The latter observation is somewhat surprising because it is generally believed that type 1 RIPs are more potent antiviral proteins than type 2 RIPs (Krivdova et al., 2014).

Besides antifungal and antiviral activities some RIPs have been reported to exert toxic effects on insects both *in planta* and in artificial diets. Hitherto insecticidal activities have been reported almost exclusively for type 2 RIPs, which due to the presence of a lectin B chain are capable of entering the cells on the surface of the gastro-intestinal tract and fully exert their cytotoxicity (Vargas and Carlini, 2014). Thereby the insecticidal activity of the protein is not directly determined by the intrinsic cytotoxicity of the protein but depends for a great deal on the match between the carbohydrate binding activity and specificity of the lectin part of the type 2 RIP and the structure of the glycans exposed on the surface cells along the gastrointestinal tract (Shahidi-Noghabi et al., 2008; Mondal et al., 2011). Feeding trials with recombinant apple proteins revealed that both the type 1 and type 2 RIPs as well as the B chain of the latter exhibit toxicity towards *A. pisum* when added to an artificial medium. However, the type 2 RIP is approximately 10-fold more toxic than the type 1 RIP. Moreover, the B chain of the type 2 RIP alone is approximately 5 times more toxic than the type 1 RIP. These observations suggest that lectin-carbohydrate interactions contribute to the toxicity of the type 2 RIP.

Summarizing, the results presented in this chapter demonstrate that the apple RIPs exhibit a markedly broad range of defense-related activities, at least when tested *in planta* and/or *in vitro*. The observed combination of antifungal, antiviral and insecticidal activities is quite unique and might offer interesting perspectives for further research and practical applications in (crop) plant protection.

4.6 Supplemental data

Figure S4.1 Photographic illustration of the different types of lesions occurring on tobacco leaves after infection with *B. cinerea*. The three classes of lesions distinguished are: (1) non-spreading lesion, (2) necrotrophic lesion and (3) spreading lesion.
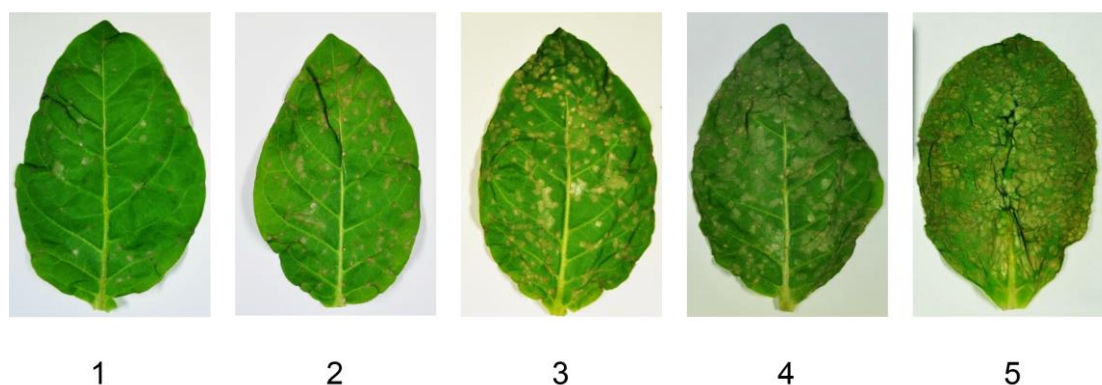

Figure S4.2 Photographic illustration of the method used to determine the disease index of tobacco leaves after infection with TMV. Evaluation of the infection lesions was based on a rating system consisting of the following six different scores (Kanzaki et al., 2004, Seifi et al., 2013): 0, Non-disease symptoms; 1, few small lesions with the lesion area covering less than 2% of the total leaf area; 2, either many small lesions, or a few larger lesions, with the lesion area accounting for 2%–5% of the total leaf area; 3, larger and more numerous lesions, with the lesion area accounting for 5%-10% of the total leaf area; 4, high amount of large lesions starting to fuse with each other, lesion area accounts for around 10-50% of the total leaf area; 5, large lesions linked to each other, the lesion area covering over 50% of the total leaf area, and the leaf was dying off.

Disease index (DI) =: [(0 x a) + (1 x b) + (2 x c) + (3 x d) + (4 x e) + (5 x f) / (a + b + c + d + e + f)] x 100/5, where a-f are the number of leaves examined with scores 0-5, respectively. Each transgenic line and wild type plant was evaluated and the disease level was used to calculate the disease index.
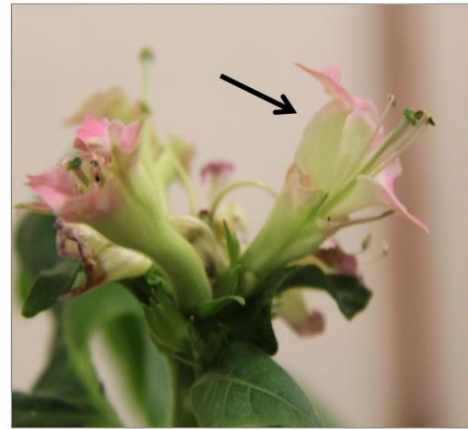
A

Wild type   Type 2 RIP line 50

B   **C**

Wild type   Type 2 RIP line 50

Figure S4.3 Pictures showing abnormal morphological phenotypes in the T0 generation of the transgenic tobacco plants overexpressing apple type 2 RIP sequences. Panel (A): Comparison of a wild type plant and a tobacco plant expressing type 2 RIP; panel (B): Wild type tobacco plant flowers; panel (C): Tobacco plant expressing type 2 RIP with abnormal flowers (double layers of incomplete flowers).
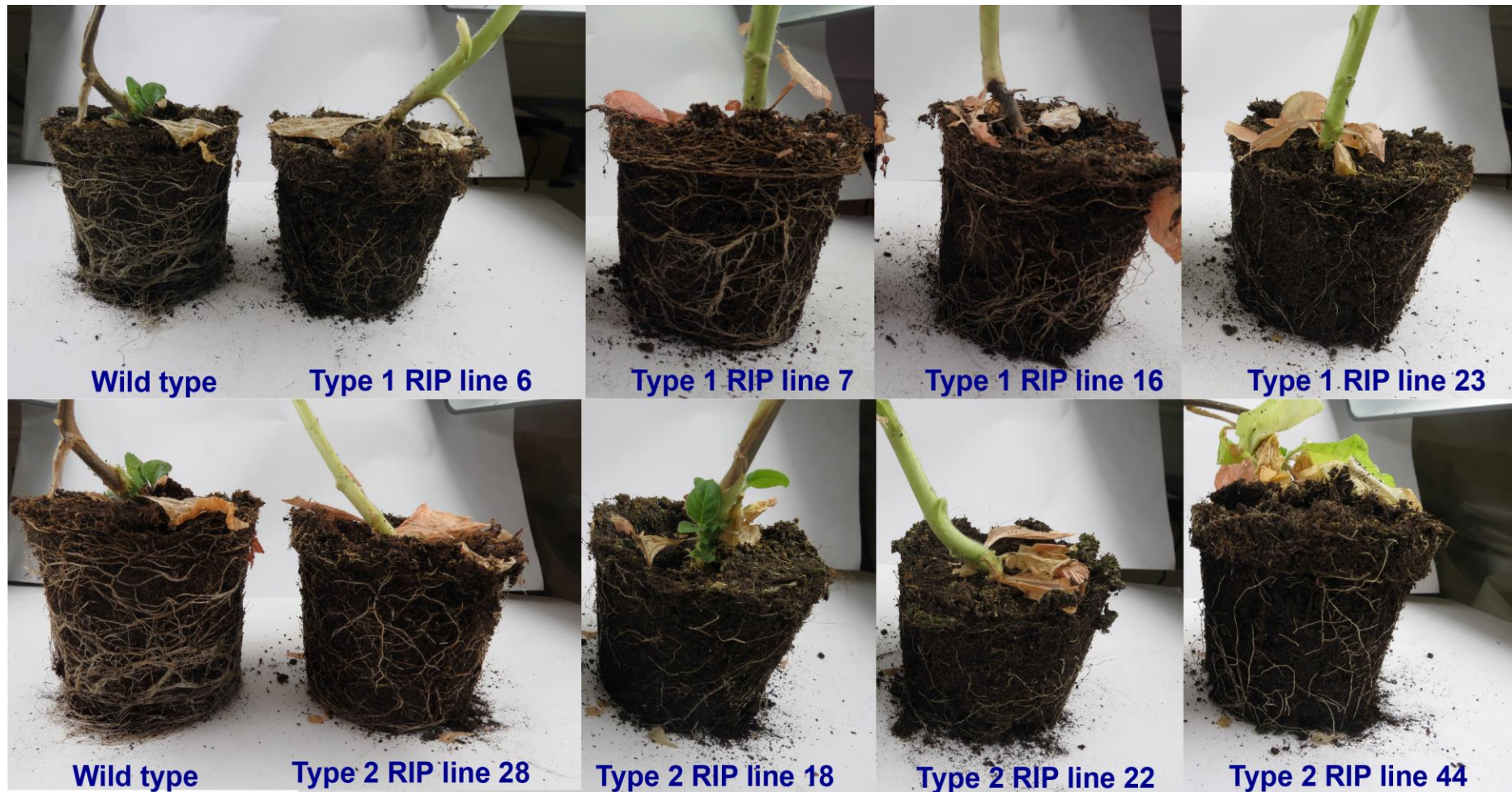
Figure S4.4 Pictures showing abnormal morphological phenotypes in the T1 generation of the transgenic tobacco plants overexpressing apple RIP sequences. Comparison of root development in wild type and transgenic tobacco plants expressing type 1 and type 2 RIPs, respectively.

Chapter 5

Comparative analysis of carbohydrate binding properties of *Sambucus nigra* lectins and ribosome-inactivating proteins

5.1 Abstract

In the past three decades a lot of research has been done on the extended family of carbohydrate binding proteins from *Sambucus nigra*, including several so-called type 2 RIPs as well as hololectins. Although all these proteins have been studied for their carbohydrate binding properties using hapten inhibition assays, detailed carbohydrate specificity studies have only been performed for a few *Sambucus* proteins. In particular SNA-I, has been studied extensively. Because of its unique binding characteristics this lectin was developed as an important tool in glycoconjugate research to detect sialic acid containing glycoconjugates.

At present much less information is available with respect to the detailed carbohydrate binding specificity of other *S. nigra* lectins and RIPs, and as a consequence their applications remain limited. In this paper we report a comparative analysis of several lectins from *S. nigra* using the glycan microarray technology. Ultimately a better understanding of the ligands for each lectin can contribute to new/more applications for these lectins in glycoconjugate research. Furthermore, the data from glycan microarray analyses combined with the previously obtained sequence information can help to explain how evolution within a single lectin family eventually yielded a set of carbohydrate binding proteins with a very broad specificity range.

5.2 Introduction

Elderberry species played an important role in studies related to the biochemistry, molecular biology and physiology of both plant lectins and ribosome-inactivating proteins (RIPs). The first report of an elderberry lectin describing the isolation and partial characterization of a lectin from bark tissue of *Sambucus nigra* dates back to 1984 (Broekaert et al., 1984). A few years later it turned out that this lectin (now referred to as SNA-I) exhibits a unique specificity towards NeuAc(α2-6)Gal/GalNAc (Shibuya et al., 1987) and accordingly can be used as a powerful tool in glycoconjugate research. Despite detailed biochemical studies the structure of SNA-I remained unclear until cloning of the corresponding cDNA revealed that the lectin is in fact a type 2 RIP structurally en evolutionary related to ricin (Van Damme et al., 1996).

In the meantime ample evidence has been presented for the occurrence of a fairly extended lectin/RIP family not only in *Sambucus nigra* but also in other elderberry

species like *Sambucus ebulus* L*., Sambucus sieboldiana Blume ex Graebn.,* and *Sambucus racemosa* L*.* (Girbés et al., 2003). Of all elderberry species, the lectin/RIP family from *S. nigra* is the best characterized. It includes several so-called type 2 RIPs as well as hololectins. For historical reasons the lectins are usually referred to by the abbreviation SNA (from *S. nigra* agglutinin) followed by Roman numbers attributed in chronological order of their discovery. Hitherto, SNA-I, SNA-II, SNA-III, SNA-IV and SNA-V have been described (Broekaert et al., 1984; Van Damme et al., 1996a, b and 1997a; Peumans et al., 1991 and 1998; Kaku et al., 1990; Mach et al., 1991). In addition to the genuine (i.e. agglutinating) lectins/RIP, a closely related type 2 RIP was identified in 1997 that exhibited no agglutination activity and did not bind to any immobilized carbohydrate or glycoprotein and accordingly was named SNLRP, which stands for *S. nigra* lectin related protein (Van Damme et al., 1997b). Lectins/RIPs occur in all tissues of elderberry but are particularly abundant in bark tissue, in which they represent >95% of the total protein content and are believed to play a role in defense against herbivores.

Analysis of the purified proteins revealed marked differences in the molecular structure of the different lectins. Some lectins (SNA-II, SNA-III and SNA-IV) are homodimeric proteins composed of identical subunits, whereas others (SNA-I, SNA-V and SNLRP) are built up of two different subunits (Table 5.1). Molecular cloning and sequence analyses eventually revealed the relationships between the different lectins at the genetic level, and allowed classifying the different lectins into the family of ricin-related lectins or type 2 RIPs. SNA-I, SNA-V and SNLRP are type 2 RIPs, which are basically chimeric proteins built up of an enzymatically active A chain and a lectinic B chain held together by an inter-chain disulfide bound. Both chains are derived from a single precursor by a complex post-translational processing involving several proteolytic events (Van Damme et al., 1996a, b and 1997b). In the case of the precursor of SNA-V an alternative processing takes place whereby not only the linker between the A and B chain but a sequence of 272 amino acid residues covering the complete A chain, the linker and the first 8 amino acids of the B chain are excised giving rise to a protein consisting solely of a slightly truncated B chain. SNA-V and SNA-II are a rare example of two plant proteins with a totally different molecular structure that are derived from the very same precursor through a differential post-translational processing (Van Damme et al., 1996b). SNA-IV closely resembles SNA-II for what concerns its molecular structure. However, the origin of the SNA-IV subunits is completely different because it is not derived from a type 2 RIP precursor

Table 5.1 Overview of type 2 RIPs and lectins (underline) from *Sambucus nigra*

Name	Source	Structure	Molecular weight	Reported carbohydrate binding specificity	Protein synthesis inhibition	Agglutination activity	Reference
SNA-I	Bark	Tetramer [A-s-s-B]$_4$	240 kDa (4 X 60 kDa)	Neu5Ac(α2-6)Gal/GalNAc	+	+++	Broekaert et al., 1984
SNA-I'	Bark	Dimer [A-s-s-B]$_2$	120 kDa (2 X 60 kDa)	Neu5Ac(α2-6)Gal/GalNAc	+	++	Kadirvelraj et al., 2011
SNA-V	Bark	Dimer [A-s-s-B]$_2$	120 kDa (2 X 60 kDa)	GalNAc >Gal	+	+	Van Damme et al., 1996b
SNLRP	Bark	Monomer [A-s-s-B]	62 kDa		+	-	Van Damme et al., 1997b
SNA-II	Bark	Dimer [B]$_2$	60 kDa (2 X 30 kDa)	GalNAc >Gal	-	+	Van Damme et al., 1996b
SNA-III	Seeds	Dimer [B]$_2$	60 kDa (2 X 30 kDa)	GalNAc >Gal	-	+++	Peumans et al., 1991
SNA-IV	Fruit	Dimer [B]$_2$	64 kDa (2 X 32 kDa)	Gal/GalNAc	-	+++	Mach et al., 1991 Van Damme et al., 1997a

*, results based on hapten inhibition assays

**, +++, ++ and + indicate very strong, strong and weak agglutination activity of rabbit red blood cells; -, designates lack of agglutination activity.

but from the primary translation product of a gene in which the complete A chain, the linker sequence and the first 8 amino acid residues of the B chain are deleted (Van Damme et al., 1997a). The final quaternary structure of the elderberry RIPs and lectins depends on the degree of oligomerization of the protomers. Like in all other plant lectins and type 2 RIPs non-covalent interactions mediate the oligomerization of the elderberry proteins except for SNA-I. In the latter type 2 RIP an extra Cys residue at position 47 of the B chain allows the formation of inter-protomer disulfide bonds (Van Damme et al., 1996a).

The availability of the purified proteins also allowed studying the biological activities of the elderberry type 2 RIPs (SNA-I, SNA-V and SNLRP) and lectins (SNA-II and SNA-IV). All three type 2 RIPs exhibit a high N-glycosidase activity *in vitro* demonstrating that they possess a catalytically active A chain. However, their cytotoxicity towards animal and human cells is rather low and can in no way be compared with that of the genuine toxic type 2 RIPs, like ricin (Girbés et al., 2003). Most probably the low cytotoxicity of the type 2 RIP from *S. nigra* (as well as these from other elderberry species) results from a low uptake/internalization, which itself might be linked to the cell-binding properties and eventually to the sugar-binding specificity. Apart from SNLRP all elderberry type 2 RIPs and lectins agglutinate human erythrocytes and can be purified by affinity chromatography on an immobilized carbohydrate or glycoprotein (Peumans et al., 1991). Hapten inhibition assays revealed the gross-specificity and allowed classifying the different *Sambucus* lectins according to their carbohydrate binding specificity. The hololectins SNA-IV and SNA-II, and the type 2 RIP SNA-V exhibited specificity towards Gal/GalNAc and Gal/GalNAc containing glycan structures (Kaku et al., 1990; Van Damme et al., 1996b; Mach et al., 1996) whereas binding assays with SNA-I revealed specificity for NeuAc(α2-6)Gal/GalNAc (Shibuya et al., 1987). Since until now SNA-I (and the nearly identical orthologs from *S. canadensis* and *S. sieboldiana,* Shibuya et al., 1989) is the only documented lectin that interacts exclusively with glycoconjugates carrying the Neu5Acα2-6Gal/GalNAc linkage SNA-I was developed into an efficient analytical reagent to detect sialic acid containing glycans. Much less information is available with respect to the detailed carbohydrate binding specificity of other *S. nigra* lectins and RIPs, and as a consequence their applications remain limited. It was reported that the Gal/GalNAc binding lectin SNA-II can recognize the carcinoma Tn epitope (Ser-O-GalNAc) (Maveyraud et al., 2009). Since galactose-containing glycans on the cell surface are important molecules e.g. for the interaction between cells, or between cells and

pathogens (Rhodes et al., 2008; Boscher et al., 2011), it is important to have some more detailed knowledge on the carbohydrate binding properties of the lectins. Therefore a comparative analysis was made of the glycan binding specificities of the type 2 RIP B chain and lectins from *S. nigra* using glycan arrays (Van Damme et al., 2011). A major advantage of the glycan microarray is the availability of many glycans that can be analysed in a single analysis using limited amounts of the immobilized glycans and of the fluorescently labelled carbohydrate binding proteins. Ultimately a better understanding of lectin ligands can also contribute to new applications for these lectins in glycoconjugate research. In addition, glycan microarray analyses combined with the previously obtained sequence information can help to explain how evolution within a single lectin family eventually yielded a set of carbohydrate binding proteins with such a broad specificity range.

5.3 Materials and methods

5.3.1 Lectins and RIPs

Apart from SNLRP all *S. nigra* proteins were purified by a combination of affinity chromatography and gel filtration as described previously (Broekaert et al., 1984; Mach et al., 1991; Van Damme et al., 1996b and 1997a). SNA-I SNA-II and SNA-V were isolated from lyophilized *S. nigra* bark whereas SNA-IV was purified from fruits. SNLRP was isolated from a lectin-depleted bark extract by ion-exchange chromatography and gel filtration (Van Damme et al., 1997b).

5.3.2 Glycan array screening

Glycan microarrays were printed as described previously (Blixt et al., 2004). The printed glycan array contains a library of natural and synthetic glycan sequences representing major glycan structures of glycoproteins and glycolipids. Array version 2.0 and 2.1 with 264 and 303 glycan targets, respectively, were used for the analyses with *S. nigra* RIPs and lectins (http://www.functionalglycomics.org/ glycomics/publicdata/selectedScreens.jsp). The purified *S. nigra* proteins were labeled using the Alexa Fluor® 488 Protein Labeling Kit (Invitrogen, California, USA) following the manufacturer's instructions. The labeled proteins were applied to separate microarray slides and incubated for 60 min under a cover slip in a dark, humidified chamber at room temperature. After incubation, the cover slips were gently removed in a solution of Tris-buffered saline containing 0.05% Tween 20 and washed by gently dipping the slides 4 times in successive washes of Tris-buffered

saline containing 0.05% Tween 20, Tris-buffered saline, and deionized water. After the last wash, the slides were spun in a slide centrifuge for approximately 15s to dry and immediately scanned in a PerkinElmer ProScanArray MicroArray Scanner using an excitation wavelength of 488 nm and ImaGene software (BioDiscovery, El Segundo, CA, USA) to quantify fluorescence. The data are reported as average relative fluorescence units (RFU) of six replicates for each glycan present on the array after removing the highest and lowest values.

5.3.3   Sequence alignment and phylogenetic analysis

ClustalW (Thompson et al., 1994) was used for alignment of the eldeberry lectins/RIP protein sequences. The phylogenetic tree of the sequences was constructed using the constraint-based alignment tool-COBALT (http://www.ncbi.nlm.nih.gov/tools/cobalt/) (Papadopoulos and Agarwala 2007).
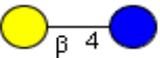
5.4   Results and Discussion
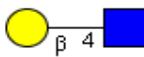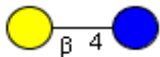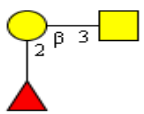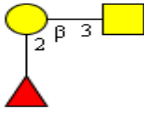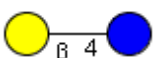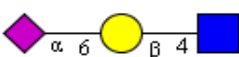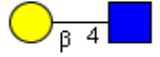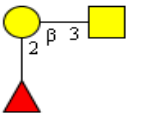
5.4.1   Carbohydrate binding properties of type 2 RIPs B chain and lectins from *S. nigra*

To corroborate the biological activity of the different *S. nigra* lectins and B chains of type 2 RIPs, detailed carbohydrate binding studies were performed using a screening of the lectins on a glycan array. As shown in Figure 5.1, all *S. nigra* proteins exhibited a strong reaction towards a well-defined set of carbohydrates/glycans of the glycan array. For each analysis the 30 most reactive glycans were analyzed in detail to determine the preferred glycan motifs for each protein (Table 5.2).

The glycan array result for SNA-I (Fig. 5.1a) showed strong binding to Neu5Ac (α2-6) Gal/GalNAc, which is in agreement with previous reported publications (Shibuya et al., 1987). All strongly interacting glycans contain at least one terminal sialic acid residue bound in the α2-6 configuration. Recent reports also showed a comparative analysis of SNA-I and several sialic acid binding proteins using a specific array containing sialylated glycans (Smith et al., 2010; Song et al., 2011; Padler-Karavani eta l., 2012). These data also clearly indicated that SNA-I is unique with respect to its carbohydrate binding properties. SNA-I showed stronger binding to 2-keto-3-deoxy-D-glycero-D-galactononic acid (Kdn) and Kdn derivatives than the derivatives of more common Neu5Ac and Neu5Gc (Song et al., 2011). Of all *Sambucus nigra* lectins under study SNA-I showed the strongest binding to the glycan array which is in agreement with its very strong interaction with cells and glycoproteins.

In contrast to SNA-I none of the other *S. nigra* lectins tested exhibited any preference for sialic acid containing glycans. SNA-II, SNA-IV and SNA-V all clearly interacted with Gal/GalNAc containing glycans as well as with the single GalNAc residue. In the case of SNA-II and SNA-V all reactive glycans possess a terminal Gal or GalNAc residue, but substitution with α1-2 Fuc is tolerated. Unlike SNA-II and SNA-V, SNA-IV also recognizes Gal residues in sialylated complex glycans. This sialic acid residue can occur in the α2-6 as well as α2-3 configuration. Furthermore, SNA-IV is the only protein tested that reacted with N-glycolylneuraminic acid (Neu5Gc) α2-6-linked to GalNAc[NeuGc (α2-6)GalNAc]. Although Gal and Neu5Gc are also present on the array they do not show up as interactors with any of the lectins under study.

Table 5.2 Glycan array data analysis. Top three glycan motifs that reacted with *S. nigra* type 2 RIPs and lectins.

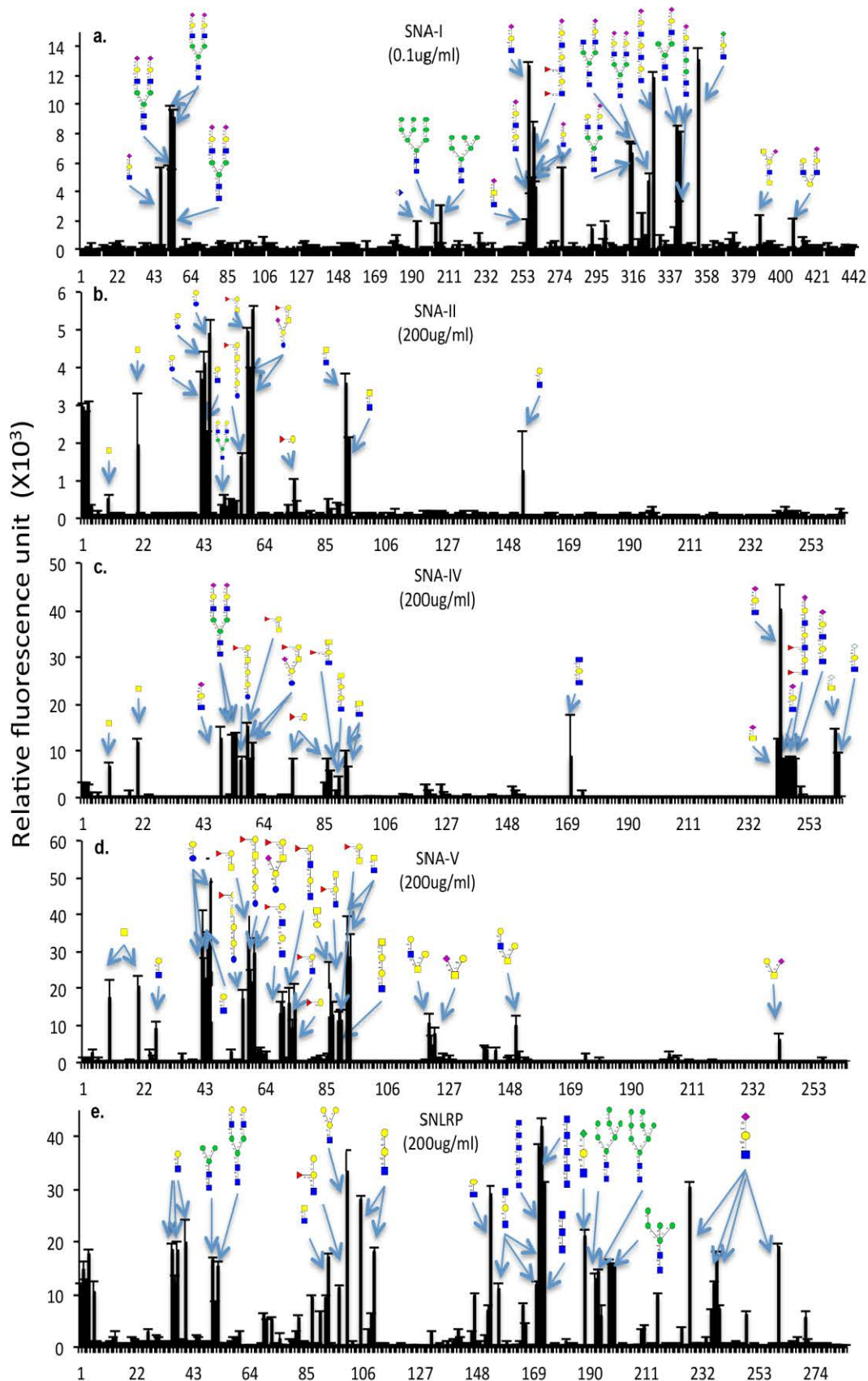| Protein		1. Glycan motifs	2. Glycan motifs	3. Glycan motifs
Type 2 RIP	SNA-I	Neu5Ac(α2-6)-Galβ1-4GlcNAc	Gal (β1-4)GlcNAcβ	Gal(β1-4)-Glcβ
	SNA-V	Gal(β1-4)-Glcβ	Fuc(α1-2)Gal(β1-3)GlcNAcβ	GalNAc(β1-4)GlcNAcβ
	SNLRP	GlcNAc(β1-4)GlcNAcβ	Gal (β1-4)GlcNAcβ	
Lectin	SNA-II	Fuc(α1-2)Gal(β1-3)GalNAcβ	Gal(β1-4)-Glcβ	GalNAc(β1-4)GlcNAcβ
	SNA-IV	Neu5Ac(α2-6)-Galβ1-4GlcNAc Neu5Ac(α2-3)-Galβ1-4GlcNAc	Gal(β1-4)GlcNAcβ	Fuc(α1-2)Gal(β1-3)GalNAcβ

Figure 5.1 Legend on next page

Figure 5.1 The Consortium for Functional Glycomics website (http://www.functionalglycomic.org) supports the complete raw data for all the proteins. Sugar code used: green circles represent mannose residues; yellow circles and squares indicate galactose and *N*-Acetylgalactosamine residues, respectively; blue squares indicate GlcNAc residues, red triangles show fucose, purple diamonds indicate NeuAc and white diamonds indicate NeuGc.

Though the glycan array analyses of SNA-I, SNA-II, SNA-IV and SNA-V revealed previously unknown carbohydrate binding properties there was no conflict with the "old" results based on hapten-inhibition assays. In contrast, analysis of SNLRP on the glycan array revealed that this protein can no longer be considered a "carbohydrate-binding-defective lectin related protein" since it strongly interacts with GlcNAc-oligomers (pentamer, hexamer, trimer with decreasing affinity) as well as with many glycan structures containing GlcNAc residues substituted with Gal residues. Taken into account that SNLRP reacts with GlcNAc oligomers as well as both high mannose and complex N-glycans it seems likely that SNLRP reacts with the core structure of N-glycans. Apparently the protein does not require oligomers of GlcNAc since also glycan structures containing a single GlcNAc residue (e.g. Galβ1-4GlcNAc) are recognized. However, the monomeric GlcNAc was not reactive on the array.

A comparison of the glycans reacting with SNA-I, SNA-IV and SNLRP revealed that they all interact preferentially with type 2 lactosamine structures (Galβ1-4GlcNAc) (Table 5.2), located internally or at the terminal branches of the glycans, some of which are also sialylated. These glycan motifs are responsible for blood group determination, cell-cell recognition and adhesion processes in the higher animals (Stanley et al. and Cummings 2009).

Based on the results of the glycan array results and in particular on the top 30 most reactive glycans the *Sambucus* lectins can be divided into three specificity groups (Table 5.2). The first group comprises the lectins that recognize Gal/GalNAc containing glycans, being SNA-II, SNA-V and SNA-IV. SNA-I forms the second group and specifically reacts with glycans containing terminal sialic acid residues (α2-6) linked to Gal/GalNAc. Finally, SNLRP can be considered a GlcNAc binding lectin, representing a third specificity group.

Two other *S. nigra* lectins, which have been isolated in the past (namely SNA-III and SNA-I') were not analyzed on the glycan microarrays because the purified proteins were no longer available. However, the results of preliminary specificity studies

indicate that the specificity of SNA-III is similar to that of SNA-IV whereas SNA-I' exhibits the same exclusive specificity towards Neu5Ac(α2-6)Gal/GalNAc as SNA-I.

5.4.2 Carbohydrate binding sites within the ricin B domain

Lectins of the ricin B chain type consist of two β-trefoil domains, which are binding domains found in various kinds of proteins and show a pseudo threefold symmetry formed by an α, β and γ-subdomain. It is commonly accepted that triplication of an ancestral gene (Hazes, 1996) encoding a conserved amino acid sequence gave rise to the β-trefoil domains composing the ricin B chain (Robertus and Ready, 1984; Rutenber et al., 1987). The specific amino acid residues that form the actual sugar-binding site in ricin have been determined by cocrystalization of ricin with several carbohydrate and glycan structures (Montfort et al., 1987). It has been reported that both the α-subdomain of the first β-trefoil domain and the γ-subdomain of the second domain can interact with glycans. No interaction with carbohydrate molecules has been shown for the β-subdomain of the β-trefoil (Rutenber and Roberus, 1991)

Sequence alignment of the full-length amino acid sequences deduced from the cDNA clones encoding lectins and the B chains of the type 2 RIPs from *S. nigra* revealed a considerable degree of sequence conservation. Furthermore alignment with the ricin sequence also enabled a comparative analysis of the amino acid residues in the carbohydrate binding sites (Figure 5.2, Table 5.3).

Table 5.3 Comparative analysis of the residues forming the carbohydrate binding sites of ricin and the type 2 RIP B chains and lectins from *S. nigra*.

RIP - B chain/lectin	Subdomain- Iα	Subdomain - IIγ
SNA-I	Asp26, Gln39, Arg41, Asn48, Gln49	Asp231, Ile243, Tyr245, Asn252, Gln253;
SNLRP	Asp23, Gln36, Leu38, Ser45, Gln46	Glu230, Ile242, Tyr244, Asn251 , Gln252
SNA-II	Asp16, Gln29, Trp31, Asn38, Gln39	Asp227, Ile239, Phe241, Asn248, Gln249
SNA-V	Asp24, Gln37, Trp39, Asn46, Gln47	Asp235, Ile247, Phe249, Asn256, Gln257
SNA-IV	Asp18, Gln31, Trp33, Asn40, Gln41	Asp229, Ile241, Phe243, Asn250, Gln251
Ricin	Asp15, Gln27, Trp29, Asn39, Gln40	Asp227, Ile238, Tyr241, Asn248, Gln249

Subdomain Iα

```
SNA-IV    ---------DGEPITGNIIGRDGLCVDVRNGYDTDGTPLQLWPCGT--QRNQQWTFYTDD
SNA-V     ---DGETCTLRTSFTRNIVGRDGLCVDVRNGYDTDGTPLQLWPCGT--QRNQRWTFDSDD
Ebulin    ---DGETCAIPAPFTRRIVGRDGLCVDVRNGYDTDGTPIQLWPCGT--QRNQQWTFYNDK
SNA-I     -GGEYEKVCSVVEVTRRISGWDGLCVDVRYGHYIDGNPVQLRPCGN--ECNQLWTFRTDG
SNA-Im    -GGEYEKVCSVVEVTRRISGWDGLCVDVRYGHYIDGNPVQLRPCGN--ECSQLWTFRTDG
SSA-I     -GGEYEKVCSVVEVTRRISGWDGLCVDVRGGHYIDGNPVQLRPCGN--ECNQLWTFRTDG
SNA-I'    GGEDEERCSVVEEVTRRIGGRDGFCAEVKNGDEKDGTPVQLSSCGE--QSNQQWTFSTDG
SNLRP     ----DDEKCTVVDVTRRISGRDGLCVDVRDGLAKDGNPVQLLSCGQ--QSSQQWTFRTDG
Ricin     -----------EPIVRIVGRNGLCVDVRDGRFHNGNAIQLWPCKSNTDANQLWTLKRDN
           .* *  :*:*..:*: *    :*..::** .*     : .* **:    *
```

Subdomain Iβ / Subdomain Iγ

```
SNA-IV    TIRSMGKCMTANGLSNGSNIMIFNCSTAVENAIKWEVTIDGSIINPSSGLVMTAPSAASF
SNA-V     TIRSMGKCMTANGLNNGSNIVIFNCSTAAENAIKWEVPIDGSIINPSSGLVMTAPRAASR
Ebulin    TIRSMGKCMTANGLNSGSYIMITDCSTAAEDATKWEVLIDGSIINPSSGLVMTAPSGASR
SNA-I     TIRWLGKCLTASSS-----VMIYDCNTVPPEATKWVVSIDGTITNPHSGLVLTAPQAAEG
SNA-Im    TIRWLGKCLTASSS-----VMIYDCNTVPPEATKWVVSIDGTITNPHSGLVLTAPQAAEG
SSA-I     TIRWLGKCLTTSSS-----VMIYDCNTVPPEATKWVVSIDGTITNPRSGLVLTAPQAAEG
SNA-I'    TIQSLGKCLTTSSS-----VMIYNCKVVPPESTKWVVSIDGTITNPRSGLVLTAPKAAEG
SNLRP     TIRSLGKCLTNSGDSSGNYAMIYNCDTAIRDATKWVLSIDGTITHRLSGLVLTAPQAAQG
Ricin     TIRSNGKCLTTYGYSPGVYVMIYDCNTAATDATRWQIWDNGTIINPRSSLVLAATSGNSG
          **:   ***:*    .      :* :*...  :: :* :  :*:* :  *.**::*.  . .
```

Subdomain IIα

```
SNA-IV    TILLLQNNIYAASQGWTVSNDVQPIVALIVGYNEMCLQSNGENNGVWMEDCEAT---SLQ
SNA-V     TILLLEDNIYAASQGWTVTNNVKPIVASIVGYKEMCLQSNGENNGVWMEDCEAT---SLQ
Ebulin    TTLLLENNIHAASQGWTVSNDVQPIATLIVGYNEMCLQANGENNNVWMEDCDVT---SVQ
SNA-I     TALSLENNIHAARQGWTVG-DVEPLVTFIVGYKQMCLRENGENNFVWLEDCVLN---RVQ
SNA-Im    TALSLENNIHAARQGWTVG-DVEPLVTFIVGYKQMCLRENGENNFVWLEDCVLN---RVQ
SSA-I     TALSLEKNIHAARQGWTVG-DVEPLVTFIVGYKQMCLRENGENNFVWLEDCVLN---RVE
SNA-I'    TLVSLEKNVHAARQGWIVG-NVEPLVTFIVGYEQMCLETNPGNNDVSLGDCSVKSASKVD
SNLRP     TTLLLQKNIHAASQGWIVG-NVVPLVTFIVGYNQMCLRANTQNNPLWLEDCVLN---RTE
Ricin     TTLTVQTNIYAVSQGWLPTNNTQPFVTTIVGLYGLCLQANSGQ--VWIEDCSSE---KAE
          * : :: *::*. ***      :. *:.: ***     :**. *   :  : : **        :
```

Subdomain IIβ / Subdomain IIγ

```
SNA-IV    QQWALFGDRTIRVNSDRGLCVTTNGYNSKDLIIILQCQGLPS-QRWFFNSNGAIVNPNST
SNA-V     QQWALYGDRTIRVNSTRGLCVTTNGYNSKDLIIILKCQGLPS-QRWFFNSDGAIVNPKSR
Ebulin    QQWALFDDRTIRVNNSRGLCVTSNGYVSKDLIVIRKCQGLAT-QRWFFNSDGSVVNLKST
SNA-I     QEWALYGDGTIRVNSNRSLCVTSEDHEPSDLIVILKCEGSGN-QRWVFNTNGTISNPNAK
SNA-Im    QEWALYGDGTIRVNSNRSLCVTSEDHEPSDLIVILKCEGSGN-QRWVFNTNGTISNPNAK
SSA-I     QEWALYGDGTIRVNSNHSLCVTSEDHEPSDLIVILKCEGSGN-QRWVFNTNGTISNPNAK
SNA-I'    QKWALYGDGTIRVNNDRSLCVTSEGKSSNEPIIILKCLGWAN-QRWVFNTDGTISNPDSK
SNLRP     QMWALYGDGTIRVNSDRSLCVS---HSSSDLIIILKCQGSSN-QRWVFNTNGTISNPNAK
Ricin     QQWALYADGSIRPQQNRDNCLTSDSNIRETVVKILSCGPASSGQRWMFKNDGTILNLYSG
          * ***: *  :**  :. :.  *::           .   : * .*     . ***.*::*:: *  :
```

Subdomain IIγ

```
SNA-IV    LVMDVKESDVSLREIIIFPYHGDPNQQWVTQVLPS
SNA-V     HVMDVRASNVSLREIIIFPATGNPNQQWVTQVLPS
Ebulin    RVMDVKESDVSLQEVIIFPATGNPNQQWRTQVPQI
SNA-I     LLMDVAQRDVSLRKIILYRPTGNPNQQWITTTHPA
SNA-Im    LLMEVAQRDVSLRKIILYRPTGNPNQQWITTTHPA
SSA-I     LVMDVAQHDISLRKIILYRPTGNSNQQWITTTQPA
SNA-I'    LVMHVDQNDVPLRKIILSHPSGTSNQQWIASTHPA
SNLRP     LVMEVRQSDVSLRQIIIYHPTGNLNQQWITDTDPV
Ricin     LVLDVRASDPSLKQIILYPLHGDPNQIWLPLF---
          ::.*     : .*:::*:      *  ** *  .
```
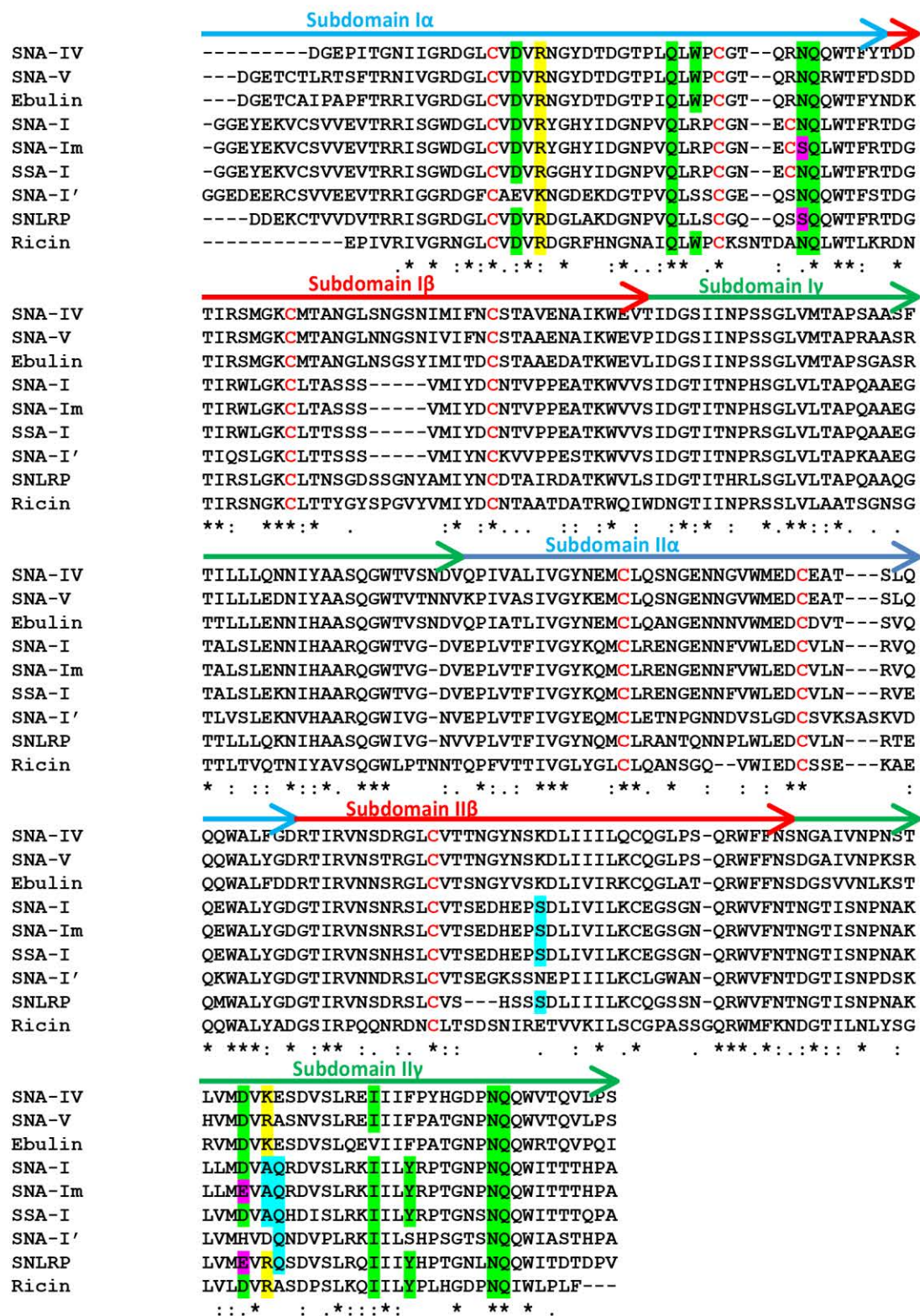
Figure 5.2 Sequence alignment of the B chains of the *S. nigra* type 2 RIP/lectins and ricin. '*' Means that the amino acids are identical in all sequences; ':' means conserved conversions (amino acids with the same shape, charge and other properties), and '.' semi-conserved substitutions (properties not the same but still similar). X: Amino acid residues forming the binding sites in ricin; X: Amino acid residues replaced in SNA-I by site-directed mutagenesis

130

to mimic the conversion of the highly active B chain of SNA into the completely inactive B chain of SNLRP; X: Residues reported to be critical for the binding to the sialic acid in Neu5Aα2-6Gal/GalNAc sequence of 2-6-sialyllactose (according to Kaku et al. 2007). X: Basic residue for 6S-Gal binding according to Hu et al. 2012. Cys residue involved disulphide bridges are shown in bold. Homologous subdomains (α, β, γ) are indicated by arrows.

Three out of five residues (corresponding to Asp15, Gln27 and Gln40 in ricin) forming the carbohydrate binding site in the α-subdomain of the β-trefoil of ricin are conserved between ricin and all *Sambucus* lectins under study. Trp residue 29 in the first binding site of ricin is also present in the Gal/GalNAc binding proteins SNA-II, SNA-IV and SNA-V but has been replaced by an Arg residue in SNA-I and a Leu in SNLRP (Table 5.3). In addition, residue Asn39 of the ricin binding site was replaced in SNLRP, but was conserved in all other *Sambucus* proteins.

Similarly three out of five amino acids (Ile238, Asn248 and Gln249 in ricin) in the carbohydrate binding site of the γ-subdomain of the β-trefoil of ricin are conserved among all sequences shown in Figure 5.2. Asp227 from ricin is also present in all *Sambucus* lectins, except for SNLRP where it is replaced by a Glu residue. Tyr241 is conserved between ricin, SNA-I and SNLRP, but was replaced by a Phe residue in the Gal/GalNAc binding proteins SNA-II, SNA-IV and SNA-V.

At present SNA-II is the only lectin from *S. nigra* for which information with respect to its three-dimensional structure is available. In 2009 Maveyraud et al. reported the X-ray structure of SNA-II in complex with Gal and five Gal-related saccharides (GalNAc, lactose, alpha1-methylgalactose, fucose, and the carcinoma-specific Tn antigen) at 1.55 Å (Maveyraud et al., 2009). These structural data confirm that the Gal/GalNAc-binding residues of SNA-II are present around the conserved Asp16 in subdomain I α and Asp227 in subdomain II γ. Three-dimensional structures have also been reported for the SNA-V ortholog found in *S. ebulus* (called ebulin-I) (Pascal et al., 2001). The structures of both SNA-II and the B chain of ebulin-I appear to be identical.

At present no structural data are available for SNA-I. However, based on the results of mutational analysis of SSA-I (the SNA-I ortholog from *S. sieboldiana*), which shares 94% sequence identity with SNA-I and exhibits the same specificity) it was concluded that Ser197, Ala 233 and Gln234 in the B chain of SSA-I are crucial for binding to the Neu5Acα2-6Gal/GalNAc sequences (Kaku et al., 2007). If so, one has to conclude that

this binding site is not confined to the γ-subdomain of the second ricin domain but covers also (part of) the β-subdomain (harboring Ser197). Though the conclusions drawn for SSA are supported by the presence of the very same amino acid residues in the sequence of the B chain of SNA-I (being Ser 197, Ala 233 and Gln234) they are contradicted by the fact that in SNA-I', which binds Neu5Acα2-6Gal/GalNAc almost equally well as SNA-I (Van Damme et al., 1997c), the presumed critical residues Ser 197 and Ala 233 are replaced by an Asn and Asp residue, respectively. Irrespective of these contradictory results the Neu5Acα2-6Gal/GalNAc binding site can be localized with certainty at the C-terminus of the B chain because it has been demonstrated that a 22 kDa polypeptide corresponding to the C-terminal part of the B chain exhibits the same binding properties as the parent type 2 RIP (Peumans et al., 1998).

At present only few sialic acid binding lectins of plant origin have been reported. A ricin-like lectin specific for glycans terminating with the sequence Neu5Acα2-6Gal was also purified from the fruiting bodies of *Polyporus squamosus* (Kadirvelraj et al., 2011; Mo et al., 2000). Similar to SSA-I a Serine residue was shown to be a key residue for the interaction between the lectin and the Neu5Ac residue. Interestingly a novel sialic acid binding lectin was created from a naturally occurring Gal binding ricin-like lectin designated EW29Ch (C-terminal domain of earthworm 29-kDa lectin). Using random mutagenesis by error-prone PCR the lactose binding pocket of the scaffold protein EW29Ch was modified into an extended binding site for α2-6 sialic acid, confirming the close relationship between Gal binding and sialic acid binding lectin of the ricin type (Yabe et al., 2007).

Another interesting observation from the glycan array data is that the different *Sambucus* lectins react with sulfated glycans, mainly 6-O-sulfated galactoses. Recently a few papers have shown that some basic amino acids in the ricin-like lectins are crucial for the recognition of 6-O-sulfated glycans. Wang et al. have shown that modification of the terminal Galβ has a significant effect on the interaction with the *Ricinus communis* agglutinin 120, RCA120 (Wang et al., 2011). Sulfation at the 6-O- or 2-O- positions of the terminal Galβ enhanced the binding activity of RCA120 whereas sulfation at the 4-O- position abolished the activity when compared with the non-sulfated residues. Similarly, Hu et al. have shown that mutants of EW29Ch in which a Glu residue at position 20 was replaced by an Arg or Lys residue acquired the ability to recognize 6-O-sulfated galactose (Hu et al., 2012). Sequence alignment of all *Sambucus* lectin sequences (Fig. 5.2) indicated that basic amino acids (Arg or Lys, corresponding to Arg 17 in ricin) are present in subdomain

Iα of all *Sambucus* lectins under study. In addition, these basic residues are also present in subdomain II γ of most *Sambucus* lectins (except SNA-I, SNA-I' and SSA). These data are in good agreement with the observation that all *Sambucus* lectins analysed on the glycan array reacted with sulfated glycans. SNA-I, SNA-II, SNA-IV and SNA-V showed good interaction with 6-O-sulfated galactose residues whereas SNLRP showed interaction with 6-O- sulfated, 4-O-sulfated as well as 3-O-sulfated galactoses.

5.4.3 The complex mixture of type 2 RIP and related lectins covers an unsually broad and unique range of carbohydrate binding specificities

Though the occurrence of multiple type 2 RIP genes within a single plant species is the rule rather than the exception, the RIP/lectin family in elderberry species seems to be unique for several reasons. First, even in the absence of a completed genome sequence the total number of documented protein and cDNA sequences of *S. nigra* exceeds that found in any other species. Secondly, *S. nigra* is the only species identified thus far in which both type 2 RIPs and lectins built up of subunits sharing a very high sequence identity with the B chain of the type RIP have been identified. Third, the documented range of carbohydrate binding specificities covered by the mixture of *S. nigra* RIP/lectins is much broader than that of any set of type 2 RIPs from any other species (e.g. *Ricinus communis*, *Viscum album*). This taken together with the availability of ample sequence information and detailed specificity analyses using glycan microarrays raised the question how evolution of a gene family within a single species eventually resulted in a battery of proteins capable of interacting with an extended range of carbohydrate structures.

Sequence alignments revealed a high degree of sequence identity between the B chains of the different elderberry RIP/lectins leaving no doubt that they are all members of a single protein family. Moreover, the elderberry proteins share also a high sequence identity with ricin, and according to X-ray crystallographic studies and molecular modelling have a nearly identical overall fold. Accordingly, the very detailed information at the atomic level of the structure of the carbohydrate binding sites in ricin was exploited to explain and interpret the results of the specificity studies of the elderberry lectins obtained by hapten inhibition assays. Though this approach was perfectly applicable to the Gal/GalNAc-binding properties of e.g. SNA-II, SNA-IV, SNA-V and ebulin-I, as well as for the apparent lack of sugar-binding activity of SNLRP it failed to explain the Neu5Ac (α2-6) Gal/GalNAc binding

133

properties of SNA-I and SSA-I. Moreover, the introduction of the highly performing glycan microarray technique revealed that the specificity of ricin is not primarily directed against Gal or GalNAc but against more complex glycan structures, which implies that the fine specificity (especially in terms of recognition of complex glycans) of ricin homologs can hardly been inferred from the conservation of the "canonical" residues occurring in the two binding sites of the ricin B chain. This limitation is clearly illustrated by the differences in specificity between SNA-II/SNA-V and SNA-IV. Though these proteins share all "canonical" amino acid residues in both the α-subdomain of the first β-trefoil domain and the γ-subdomain of the second domain SNA-IV is capable of interacting with Gal residues in sialylated complex glycans and [NeuGc(α2-6)GalNAc], whereas SNA-II/SNA-V is not. Most probably these obvious differences in specificity rely on differences in the amino acid sequence in the respective γ-subdomains of the second domain.

SNLRP represents another example of the limitations inherent to predictions made on the basis of the presence/absence of presumed critical residues in the binding sites. Molecular modelling and docking studies with Gal and GalNAc confirmed that the presumed inactive B chain of this type 2 RIP possessed only defective binding sites (Van Damme 1997b). However, glycan microarray analysis revealed that SNLRP strongly interacts with GlcNAc-oligomers as well as with the core structure of N-glycans, and accordingly should be considered a genuine lectin with a specificity unprecedented among type 2 RIPs.

Since it is evident that the carbohydrate binding properties of the different elderberry lectins are determined by the atomic structure of the binding sites and thus eventually rely on the amino acid sequence of the B chains it seemed worthwhile to check whether and if so to what extent differences in specificity are reflected in the overall phylogeny of the RIP/lectin family. Analyses of the B chain of the *S. nigra* type 2 RIPs and lectins allowed to investigate the sequence similarity and evolutionary relationships between the proteins under study. Furthermore it allowed checking whether the grouping of the *Sambucus* lectins in different clades could also be correlated with their carbohydrate binding properties. Therefore, a phylogenetic tree was built of the sequences of the *S. nigra* RIP/lectins. Besides the RIP/lectins discussed here a few more *Sambucus* type 2 RIP as well as ricin were included. As shown in Figure 5.3 the dendrogram yields two major clades for the *Sambucus* protein. The first clade groups the Gal/GalNAc specific binding lectins SNA-V and SNA-IV whereas the second comprises SNA-I, SNA-Im (an inactive mutant

of SNA-I in which two amino acid residues were replaced Chen et al., 2002c), SSA-I, SNA-I' (a paralog of SNA-I missing the Cys residue involved in the inter-protomer disulfide bond formation) (Van Damme 1997b, c) and SNLRP (Van Damme 1997b). Ricin forms a separate branch.
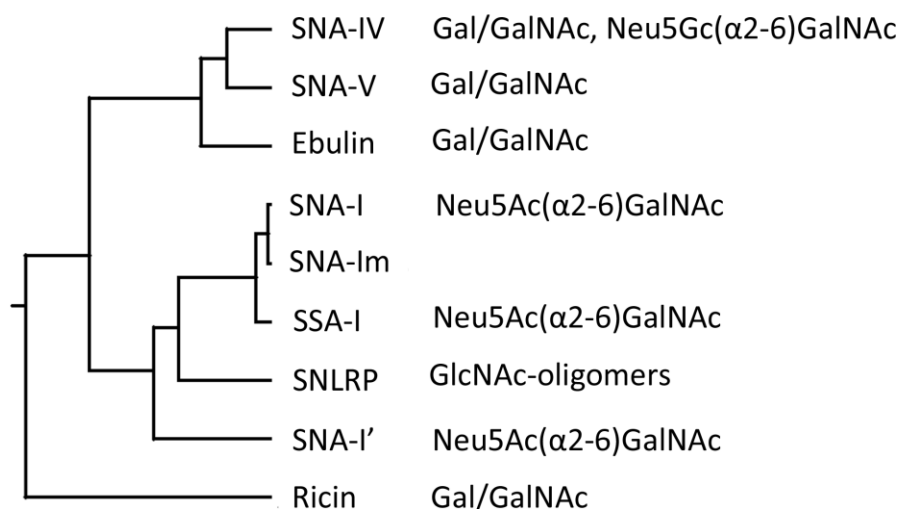

Figure 5.3 Phylogenetic tree of sequences encoding type 2 RIPs and lectins from *S. nigra* and ricin. The dendrogram was made by using constraint-based alignment tool (COBALT). Accession numbers: Ricin (XP_002534649.1), SNA-I (U27122), SNA-I' (U66191), SNA-II (U41299), SNA-IV (U76523), SNA-V (U41299), SNLRP (U58357), SSA-I (D25317), Ebulin (AJ400822).

Two major conclusions can be drawn from the dendrogram. First, there is no straight forward relationship between sequence identity/similarity and carbohydrate binding specificity. This can easily be explained by the fact that replacement of one or two amino acids within a binding site can profoundly alter the activity and specificity of a lectin but has little consequences for its phylogeny, as is illustrated by SNA-I/SNA-Im. Secondly, the sequence of the B chain of ricin forms a separate branch indicating that all elderberry sequences represent a monophyletic group and thus evolved from a single ancestral gene through multiple gene duplication events. It is most likely that gene duplication and/or excision events have occurred in the ancestral lectin gene. In addition amino acid changes in the carbohydrate binding sites resulted in differences in the carbohydrate binding specificity for the different *Sambucus* lectins (Van Damme et al., 1998; Ferreras et al., 2010). Our data also agree with the hypothesis that sialic acid binding lectins have emerged during evolution from the

135

Gal binding lectins, as evidenced by the fact that some trace features of Gal recognition still remain in the sialic acid binding lectins such as SNA-I (Yabe et al., 2007).

Since no complete genome sequences are available the exact composition of the *S. nigra* RIP/lectin gene family cannot be determined yet. However, cDNA sequencing revealed that most -if not all- of the currently identified genes occur in multiple copies, and provided also indications for the occurrence of RIPs and lectins that have not been identified yet. Though only a preliminary analysis can be made of the phylogeny and the evolution it seems likely that (as was suggested previously by Kaku et al. 2007) a gene encoding a Gal/GalNAc-binding lectin was at the basis of the current elderberry RIP/lectin gene family. Genome and transcriptome sequencing programs provided evidence for the occurrence of (extended) type 2 RIP gene families in other species (e.g. *Ricinus communis*, *Viscum album*). However, the range of carbohydrate binding specificities covered by the whole set of type 2 RIP and related lectins is apparently far more narrow than in elderberry.

Evidently, the simultaneous occurrence of large amounts of three different type 2 RIPs raises the question of the physiological importance of these proteins for elderberry. At present, one can only speculate about the evolutionary advantage of possessing such a mixture of carbohydrate binding proteins. Most likely, a synergistic effect between the different RIP/lectins eventually results in an increased resistance to phytophagous insects and/or herbivorous animals. Indeed, over the years several experiments have shown that several RIPs and lectins from *S. nigra* play an important role in plant defense against pathogens (Chen et al., 2002a) and insects (Shahidi-Noghabi et al., 2008, 2009), or show a more or less selective cytotoxicity towards tumor cells (Battelli et al., 1997a). Mutational analysis with SNA-I have shown that especially the B chain of the protein, and thus the carbohydrate binding properties of the protein play an important role in the toxicity to cells and organisms. The variety of glycan-binding specificities from B chains of type 2 RIPs and lectins from *S. nigra* indicates that they will play an important role in the protein-carbohydrate recognition taken place at the surface of cells. For instance first evidence already showed interaction of different *Sambucus* lectins with insect and animal cells (Shahidi-Noghabi et al., 2011; Shang et al., 2013) and proved the importance of the carbohydrate binding activity in the interaction with the cell surface (Shahidi-Noghabi et al., 2008, chapter 7). More research is needed to identify the interacting proteins for the *Sambucus* lectins on the cell and unravel how the

lectins are internalized. Surely, a better knowledge of the glycans interacting with the proteins will enable to decipher the biological activity of these proteins and will contribute to future applications of the lectins in glycoconjugate research.

Chapter 6

The cytotoxicity of elderberry ribosome-inactivating proteins is not solely determined by their protein translation inhibition activity.

Chapter 6 The cytotoxicity of elderberry ribosome-inactivating proteins is not solely determined by their protein translation inhibition activity

6.1 Abstract

Although the protein translation inhibition activity of ribosome inactivating proteins (RIPs) is well documented, little is known about the contribution of the lectin chain to the biological activity of these proteins. In this study, we compared the *in vitro* and intracellular activity of several *S. nigra* (elderberry) RIPs and non-RIP lectins. Our data demonstrate that RIPs from elderberry are much more toxic to HeLa cells than to primary fibroblasts. Differences in the cytotoxicity between the elderberry proteins correlated with differences in glycan specificity of their lectin domain, cellular uptake efficiency and intracellular destination. Despite the fact that the bulk of the RIPs accumulated in the lysosomes and partly in the Golgi apparatus, we could demonstrate effective inhibition of protein synthesis *in cellula*. As we also observed cytotoxicity for non-RIP lectins, it is clear that the lectin chain triggers additional pathways heralding cell death. Our data suggest that one of these pathways involves the induction of autophagy.

6.2 Introduction

Plant ribosome-inactivating proteins (RIPs) possess highly specific rRNA *N*-glycosidase activity and are capable of catalytically inactivating eukaryotic ribosomes. This inactivation occurs through the removal of a specific adenine residue from a highly conserved (sarcin/ricin) loop of the large ribosomal RNA (Peumans et al., 2001; Stirpe et al., 2006). Based on their domain architecture, RIPs can be divided into two main categories. Type 1 RIPs such as saporin and trichosanthin represent a group of single-chain proteins with enzymatic activity. The type 2 RIPs are chimeric proteins composed of an A-chain with protein synthesis inhibition activity and a B-chain with carbohydrate-binding/lectin activity (Van Damme et al., 2001). Infamous type 2 RIPs are ricin and abrin, potent toxins that are present in the seeds from *Ricinus communis* (castor bean) and *Abrus precatorius* (jequirity bean), respectively. Some well-known type 2 RIPs (such as ricin, abrin and volkensin) have been shown to exert anti-tumor activity (Puri et al., 2012). This has sparked interest in their use for potential therapeutic applications. However, there are major differences between the cytotoxicity of different type 2 RIPs, and while some type 2 RIPs (e.g. from *Sambucus nigra* (Ferreras et al., 2011)) exhibit strong protein synthesis inhibition activity *in vitro*, they can be as much as 10^3-10^5 less toxic than ricin when administered to animal cells. Possible explanations for this discrepancy include differential cellular uptake efficiency and/or intracellular trafficking of the proteins.

It has been shown that the cytotoxicity of certain type 2 RIPs relies on the binding of the B-chain to glycoconjugates at the cell surface, as such facilitating cellular uptake of the ribosome-inactivating proteins (Sandvig et al., 1978). Incubation of mammalian cells with ricin results in its endocytosis and subsequent transport to the TGN, followed by retrograde transport from the Golgi apparatus to the ER (Lord et al., 2005; Spooner et al., 2008), where the disulphide bridge between the A- and B-chain is cleaved. Finally, the A-chain enters the cytoplasm where it exerts its N-glycosidase activity (Sandvig et al., 1991; Lord et al., 1998; Yoshida et al., 1991). Volkensin, follows a similar internalisation pathway as ricin (Barbieri et al., 2004). In contrast, nigrin b, which has comparable plasma membrane binding affinity to volkensin (approx. 10^{-10}M), enters the cytosol without passing the TGN and ER (Barbieri et al., 2004; Jiménez et al., 2014; Battelli et al., 1997a). These data show that the intracellular trafficking pathway (co-)determines cytotoxicity. However, for many RIPs, information on the internalisation kinetics is lacking or incomplete.

As for their cytotoxic activity, it has been reported that RIPs induce apoptotic cell death through different mechanisms, often involving the induction of the unfolded protein response and mitochondrial dysfunction (Das et al., 2012; Narayanan et al., 2005; Sikriwal et al., 2010). One of the pending questions is whether protein synthesis inhibition is the sole responsible for this RIP-induced apoptosis. The contribution of a lectin domain could modulate RIP activity *in vivo*, either in an antagonistic or synergistic manner. Providing support for the latter, various lectins have been shown to induce cytotoxicity (Fu et al., 2011; Liu et al., 2010).

Studies to evaluate the cytotoxicity and/or internalization of type 2 RIPs have mainly focused on proteins with similar, fairly generic carbohydrate recognition domains (mostly galactose-binding) (Barbieri et al., 2004; Narayanan et al., 2005; Fang et al., 2012; Gadadhar and Karande, 2013; Voss et al., 2006). However, other specific sugar-binding domains may bear more potential for selective targeting of certain (e.g. cancer) cell types. Elderberry (*Sambucus nigra*) produces several type 2 RIPs (SNA-I, SNA-V and SNLRP) and lectins (SNA-II and SNA-IV), with a variety of carbohydrate binding properties, which form an ideal model system to investigate their differential cytotoxicity towards mammalian cells. Glycan array analyses revealed that SNA-I shows strong binding to Neu5Ac(α2-6)Gal/GalNAc, while SNA-II (corresponding to the lectin domain of SNA-V), SNA-IV and SNA-V exhibit clear interaction with Gal/GalNAc residues. Furthermore, SNA-IV is able to recognize Gal residues in sialylated complex glycans occurring in the α2-6 as well as the α2-3

linkage. In contrast to the other *S. nigra* proteins, which interact with terminal residues from glycans, SNLRP recognizes the core N-glycan structure since it shows reactivity towards GlcNAc oligomers as well as N-glycans (Shang and Van Damme, 2014). At present, mostly SNA-I and SNA-V have been studied for their biological properties (Shang and Van Damme, 2014; Battelli et al., 1984; Citores et al., 2002; Ferreras et al., 2011; Tejero et al., 2015).

Since all type 2 RIPs show a clear protein translation inhibition activity *in vitro* (Battelli et al., 1984; Svinth et al., 1998), but exhibit clear differences in cytotoxicity, it is conceivable that the B-chain has an important modulatory role. However, at present the exact working mechanisms are unresolved. To enhance insight in the mode of action of the different *S. nigra* type 2 RIPs (SNA-I, SNA-V and SNLRP) and non-RIP lectins (SNA-II and SNA-IV), we investigated their behaviour *in vitro* and *in cellula*. Our data confirmed that the elderberry RIPs are much less toxic than the classical RIPs from *Ricinus* and *Abrus*, but also showed that mortal cell cultures (fibroblasts) were less susceptible to the elderberry proteins than HeLa cell lines. In addition, our results revealed that differences among the elderberry proteins correlate with uptake efficiency and the glycan specificity of their lectin domains.

6.3 Materials and methods

6.3.1 RIPs and lectins

All proteins from *Sambucus nigra* were purified by affinity chromatography and gel filtration as described previously (Broekaert et al., 1984; Mach et al., 1991; Van Damme et al., 1996b; Van Damme et al., 1997b). SNA-I, SNA-II, SNA-V and SNLRP were isolated from lyophilized *S. nigra* bark and SNA-IV from fruits. *S. nigra* RIPs (SNA-I, SNA-V and SNLRP) were reduced by incubation with 0.025 M dithiothreitol (DTT) at 37 °C for 1 h as described by Emmanuel et al. (1998).

6.3.2 Cell culture

HeLa (Cervix carcinoma, American Type Culture Collection, Manassas, Virginia, USA), NHDF (human dermal fibroblasts, passage 9, PromoCell GmbH, Heidelberg, Germany) and Luc2-IRES-tCD cell cultures (a gift from Dr. Pierre Busson group, Institut de Cancérologie Gustave Roussy, Villejuif, France) (Jiménez et al., 2011) were grown in advanced DMEM (Life Technologies, Merelbeke, Gent) supplemented with 2% fetal calf serum (Life Technologies) and 1% L-glutamine Penicillin-Streptomycin-Glutamin solution (Life Technologies) in an incubator set at 37°C and 5% CO_2.

6.3.3 Protein synthesis inhibition activity

Protein synthesis inhibition activity for non-reduced or reduced *S. nigra* RIPs (SNA-I, SNA-V or SNLRP) was determined using the TnT® T7 Quick Coupled Transcription/Translation System Kit (Promega, Mannheim, Germany) based on a cell-free system (Voss et al., 2006). According to manufacturer's instructions, the prepared mixture was incubated at 30°C for 10 min and chilled on ice. Afterwards, 2 μl PBS or PBS containing different concentrations of *S. nigra* RIPs or lectins were added to the reaction mixture and incubated for 30 min at 30°C. After addition of 35 μl nuclease-free water at room temperature the reaction samples were transferred to a luminometer plate (Greiner Labortechnik, Frickenhausen, Germany) containing 5 μl luciferase assay reagent at 25°C. The relative luciferase activities of the samples were determined at 562 nm for 10s using a microtiter top plate reader (Infinite 200, Tecan, Mannedorf, Switzerland) with an initial delay of 2s.

6.3.4 Cytotoxicity assay

To study the effect of different *S. nigra* RIPs and lectins on cell viability and proliferation, a total of 3,000 HeLa or NHDF cells were seeded in a 96-well plate (Greiner Labortechnik) and incubated at 37 °C and 5% CO_2 for 24 h. Subsequently, the medium was exchanged with medium supplemented with various concentrations of *S. nigra* RIPs or lectins (ranging from 0.1 to 2 μM), and incubated at 37°C and 5% CO_2 for 2 time points (24 h and 48 h), respectively. Phosphate buffered saline (Life Technologies) with/without 2 μM BSA was used in the control treatments (Oliveira et al., 2011). Four technical replicates were performed for each concentration, and each experiment was repeated three times.

Cell viability was determined by means of (resazurin-based) Presto Blue spectrophotometric assays (Life Technologies) according to manufacturer's instructions. In brief, the culture medium of each well was replaced with fresh culture medium containing 10% final concentration of Presto blue reagent. After incubation for 20 min in the dark at 37 °C and 5% CO_2 the fluorescence intensity of reduced resazurin was measured at 560/600 nm in a plate reader (Infinite 200, Tecan, Mannedorf, Switzerland).

Cell morphology was assessed using an inverted transmitted light microscope (Ti Eclipse, Nikon Instruments, Paris, France), with a 10x dry objective (Numerical aperture 0.5).

6.3.5   Labelling of *S. nigra* RIPs and lectins with fluorescein isothiocyanate

S. nigra RIPs and lectins were labeled with fluorescein isothiocyanate (FITC) (Sigma-Aldrich, St. Louis, USA). Lyophilized protein (10 mg/ml) was dissolved in 0.1 M carbonate/bicarbonate (1:9) buffer, pH 9. Afterwards, a 24-fold molar excess of FITC in dimethylformamide was added to the protein. After 2 h incubation in the dark at room temperature, the labeled protein was purified by gel filtration on a Sephadex G25 column (1 cm diameter/ 5 cm height) using PBS as running buffer. Subsequently, the labeled protein fraction was analyzed by SDS-PAGE and visualized by Fujifilm FLA 5100 (FUJIFILM Life Science, Japan). Protein concentrations and molar FITC/protein ratios were calculated to estimate the labeling efficiency according to manufacturer's instructions (Thermo scientific, Rockford, USA).

6.3.6   (Immuno-) fluorescence staining

HeLa cells were seeded on coverslips in a 12 well plate (3.8×10^4 cells/well) for at least 24 h, and cells were incubated with culture medium containing 50 nM FITC-labeled or non-labeled *S. nigra* proteins for fixed time periods. After washing with PBS, cells were fixed with 2% formaldehyde for 20 min, followed by three more PBS washes. Subsequently, cells were permeabilized in 0.5% Triton X-100 solution for 5 min, blocked with 50% fetal calf serum for 40 min at room temperature and incubated for 1 h at room temperature with one of the following primary antibodies: mouse anti-PDI (1:1000, Endoplasmic reticulum marker), anti-Golgin97 (1:2000, Golgi marker), rabbit anti-Rab5 (1:1000, Early endosome marker) or p62/SQSTM1 (1:100, autophagic flux marker, Santa Cruz Biotechnology Inc. Texas, USA). After three washes with PBS, cells were incubated for 1 h with goat anti-mouse IgG or goat anti-rabbit IgG Alexa Fluor-555 and after a final wash counterstained with DAPI (0.1 µg/ml) and mounted with Vectashield (Vector Laboratories Inc., Burlingame, CA, USA). Next to the immunostaining, lysosomes were visualized with LysoTracker (Life technologies, 50 nM) and lipid droplets were stained with BODIPY 493/503 (Life Technologies, 2 µg/ml).

6.3.7   *In cellula* luciferase assay

To study translation inhibition *in cellula*, a total of 3,000 HeLa cells (HG1-luc2-IRES-tCD cells (Voss et al., 2006)) were seeded per well in a 96-well plate (Greiner) and incubated at 37°C and 5% CO_2 for 24 h. After replacing the medium, the cells were

exposed to medium supplemented with 100 nM *S. nigra* RIPs and SNA-II, and incubated at 37°C and 5% CO_2 for another 24 h. Cycloheximide (10 µg/ml, Sigma-Aldrich) was used as the control treatment (Oliveira et al., 2011). Luciferase activity in cell extracts was assessed using the Promega Luciferase Assay System according to the manufacturer's instructions (Promega, Mannheim, Germany). After washing with PBS, cells were lysed with lysis buffer (Promega luciferase kit) for 2 min and half of the cell lysate was transferred to the luminometer plate (Greiner). After addition of the D-Luciferin substrate, luminescence was measured for a period of 10s. Recorded signals were normalized to the amount of viable cells as measured in a subsequent Presto blue assay. Four technical replicates were performed for each protein concentration, and each experiment was repeated three times.

6.3.8   Autophagic flux assay

The ptfLC3 expression vector from Dr. Tamotsu Yoshimori encoding an mRFP-EGFP-LC3 fusion construct (Kimura et al., 2007) was purchased from Addgene (Cambridge, MA USA, plasmid 21074). The expression vector was introduced into HeLa cells using Lipofectamine® 2000 (Life Technologies) according to the manufacturer's instructions. One day after transfection, the transfected cells were incubated with 100 nM SNA-I for 7 h. Subsequently the cells were analysed by confocal microscopy.

6.3.9   Microscopy and image analysis

Confocal images were acquired with a Nikon A1R confocal system, mounted on a Nikon Ti microscope body using a 40x (Numerical aperture 1.3) oil or 60x (Numerical aperture 1.4) oil objective and appropriate filters. The amount of internalized FITC-labeled *S. nigra* protein was quantified by measuring the total signal intensity per cell using a home-written script for FIJI image analysis freeware (http://fiji.sc/Fiji). More than 60 cells were analyzed for each treatment, and three repeats were performed for each experiment. The fluorescence signal data was normalized by the FITC labeling efficiency of the *S. nigra* proteins. Colocalization analysis was performed making use of the JaCoP plugin (Just Another Co-localization Plugin). Specifically, Manders' coefficients were retrieved for a fixed threshold setting per dye combination (Manders et al., 1993) and object-based colocalization was calculated using the centre-of-mass method (Bolte et al., 2006). An alternative object-based colocalization analysis was also performed using an in-house developed method that calculates the overlap of binarized channels per object (Verdoodt et al., 2012).

For quantification of p62 foci or BODIPY stained lipid-droplets, images were captured by widefield fluorescence microscopy (Nikon Ti) using a 40x oil objective (Numerical aperture 1.3). At least 25 randomly selected areas in each sample (3 repeats) were recorded using fixed acquisition settings. Per cell, metrics such as mean signal intensity, spot number, and mean spot intensity were measured using an in-house developed cytometric analysis pipeline for FIJI (InSCyDe, De Vos et al., 2010).

6.3.10 Mass spectrometry

The glycomic analyses were performed in collaboration with the group of Prof. Anne Dell (Faculty of Natural Sciences, Imperial College London, UK).

To acquire N- and O-glycans from glycoproteins, HeLa and NHDF samples were treated following an established protocol (Jang-Lee et al., 2006; North et al., 2010). Briefly, cells were suspended in lysis buffer (25 mM Tris, 150 mM NaCl, 5 mM EDTA and 1% CHAPS (v/v), pH 7.4) before homogenisation and sonication were performed. The homogenates were subsequently dialysed against a 50 mM ammonia bicarbonate buffer, pH 7.5, after which the samples were lyophilized. Extracted glycoproteins were reduced, carboxymethylated and tryptic digested prior to the release of protein linked N-glycans by PNGase F (Roche Applied Science) digest and O-linked glycans by reductive elimination. Released N- and O-glycans were permethylated prior to MS analysis. Sialidase cleavage was carried out using Sialidase S (Prozyme Glyko) and Sialidase A (Prozyme Glyko) in 50 mM sodium acetate, pH 5.5.

To acquire glycans from glycolipids another protocol was used as described previously (Jia et al., 2014). Briefly, the HeLa and NHDF samples were sonicated in ice-cold ultra-pure water. Glycolipids were extracted by chloroform/methanol/water, followed by the release of lipid-linked glycans via rEGCase II (Takara) digestion, and then the glycan purification using a Sep-pack C18 cartridge (Waters) and subsequently a Hypercarb column (Thermo Scientific). After this a deuteroreduction step was carried out. Sialic acids were cleaved using Sialidase S (Prozyme Glyko) and Sialidase A (Prozyme Glyko) in 50 mM sodium acetate, pH 5.5. The treated samples were lyophilized, permethylated and purified using Sep-Pak (C18; Waters).

MS data were obtained via a Voyager MALDI-TOF (Applied Biosystems) mass spectrometer. Purified permethylated glycans were dissolved in 10 µl methanol and

1 µl of the sample was mixed with 1 µl of matrix, 20 mg/ml 2,5-dihydroxybenzoic acid (DHB) in 70% (v/v) aqueous methanol and loaded on to a metal target plate. The instrument was run in the reflectron positive ion mode using an accelerating voltage of 20 kV.

MS/MS data were acquired using a 4800 MALDI-TOF/TOF mass spectrometer (AB SCIEX). In the MS/MS experiment the dissolved sample was dried and then re-dissolved in 10 µl methanol, 1 µl of the sample was mixed with 1 µl of matrix, 10 mg/ml diaminobenzophenone (DABP) in 70% (v/v) aqueous acetonitrile and loaded on to a metal target plate. The instrument was run in the reflectron positive ion mode. The collision energy was set to 1 kV with argon as the collision gas. The 4700 calibration standard (mass standards kit for the 4700 proteomics analyzer, Applied Biosystems) was used as the external calibrant for the MS and MS/MS modes.

The MS and MS/MS data were processed employing Data Explorer Software from Applied Biosystems. The processed spectra were annotated using a glycobioinformatics tool, GlycoWorkBench (Ceroni et al., 2008). Based on known biosynthetic pathways and susceptibility to PNGase F digestion, reductive elimination and rEGCase II digestion, all N-glycans are presumed to have a Manα1–6(Manα1–3)Manβ1–4GlcNAcβ1–4GlcNAc core structure; all O-glycans are assumed to have reducing end GalNAc; all glycolipid derived glycans are assumed to have a core of Galβ1-4Glc (North et al., 2010; Schachter 1991; Taylor and Drickamer 2011). The symbolic nomenclature used in the spectra annotation is the same as the one used by the Consortium for Functional Glycomics (CFG) (http://www.functionalglycomics.org/) and the Essentials for Glycobiology on-line textbook(http://www.ncbi.nlm.nih.gov/books/NBK1931/figure/ch1.f5/?report=objectonl).

6.3.11 Statistical analyses

Statistical analyses were performed using Prism version 5 (GraphPad, La Jolla, CA). One-way ANOVA (Dunnett's Multiple Comparison Test) was performed at the level of significance (*: $p < 0,05$; **: $p < 0,01$; ***: $p < 0,001$). The 50% lethal concentration (LC50) was determined using the non-linear regression analysis. Data were represented as means ± standard error (SE). Differences in cytotoxicity between different *S. nigra* proteins were statistically analyzed using SPSS (Tuckey's b) - IBM Statistical Package for the Social Sciences Statistics (IBM SPSS Statistics, IBM, New York, US).

6.4   Results

6.4.1   Elderberry RIPs inhibit protein synthesis *in vitro*

In an *in vitro* cell-free system, all non-reduced and reduced RIPs (SNA-I, SNA-V and SNLRP) from *S. nigra* clearly showed a concentration-dependent translation-inhibiting activity, albeit with strongly varying potency (Fig. 6.1A and 1B) (S1 Fig.). Compared to SNA-I (IC50= 5.48 nM), the IC50 values for *S. nigra* RIPs SNA-V and SNLRP were significantly lower (25 to 50 fold) (Fig. 6.1D), indicating that their activity was proportionally higher. The lectins SNA-II and SNA-IV, which are merely composed of the lectin chain, also started interfering with the translation process in the dose range of SNA-I (Fig. 6.1A). The protein synthesis inhibition activity was not enhanced by DTT-mediated reduction of the proteins since the IC50 values for the non-reduced and reduced SNA-I, SNA-V and SNLRP are very similar (Fig. 6.1).

6.4.2   *S. nigra* RIPs and lectins are more toxic towards HeLa than NHDF cells

To assess the antiproliferative activity of the *S. nigra* RIPs (SNA-I, SNA-V and SNLRP) and lectins (SNA-II and SNA-IV) on HeLa and NHDF cells, spectrophotometric viability assays were performed after incubation with different concentrations (0.1-2 µM) of the proteins (Fig. 6.2A and 2B). In HeLa cells, all proteins, except for SNA-IV, induced significant ($p < 0.05$) cytotoxicity after 48 h incubation at the lowest protein concentration tested (0.1 µM). Furthermore, SNA-IV also became cytotoxic at concentrations > 1.5 µM. There was a clear dose- and time-dependent effect on HeLa cell viability. The degree of cytotoxicity after 48 h was as follows: SNA-V > SNA-II > SNA-I > SNLRP > SNA-IV (Table 6.1). The cytotoxic effect on HeLa cells was accompanied by clear morphological changes such as cell rounding and blebbing (Fig. 6.2C). As evidenced by the increased LC50 values (Table 6.1), NHDF cells were much less susceptible to *S. nigra* proteins than HeLa cells. There was no statistically significant effect of SNA-IV and SNLRP on NHDF cell viability and proliferation after 24 h whereas all the other *S. nigra* proteins caused a significant cytotoxicity, though at much higher protein concentrations compared to HeLa cells. Only after 48 h, a significant effect on cell viability was witnessed for SNA-V ($p < 0.001$) at the lowest protein concentration (0.05 µM).
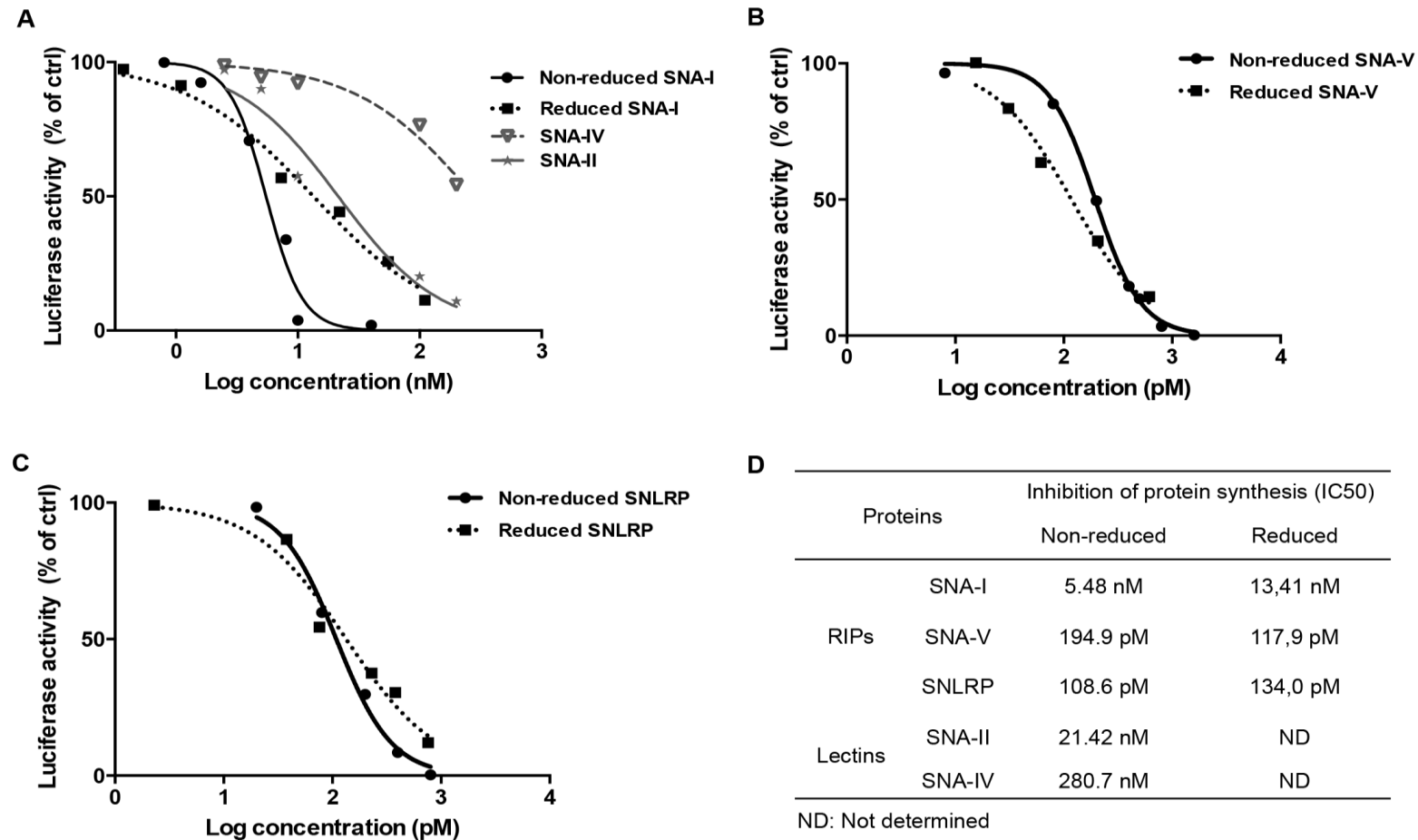
148

Figure 6.1. Effect of the *S. nigra* RIPs and lectins on protein synthesis in a cell-free translation assay. (A) Dose response curves of luciferase synthesis in treatments with SNA-I (non-reduced and reduced) and lectins (SNA-II, SNA-IV). (B and C) Dose response curves of luciferase synthesis in the treatments with non-reduced and reduced RIP for SNA-V and SNLRP, respectively. (D) IC50 values for the RIPs and lectins.

Table 6.1 Comparison of LC50 values for the *S. nigra* proteins in HeLa and NHDF cell lines.

	LC50 (μM)				
Time/Cell line	**SNA-I**	**SNA-II**	**SNA-IV**	**SNA-V**	**SNLRP**
24h HeLa	1.57 ± 0.32^{c}	0.72 ± 0.11^{a}	$>2.00^{b}$	0.74 ± 0.08^{a}	$>2.00^{b}$
48h HeLa	0.43 ± 0.04^{d}	0.27 ± 0.03^{d}	1.932 ± 0.20^{e}	0.11 ± 0.01^{d}	1.85 ± 0.44^{e}
24h NHDF	$>2.00^{f}$	$>2.00^{f}$	$>2.00^{f}$	$>2.00^{f}$	$>2.00^{f}$
48h NHDF	$1.70 \pm 0.35^{g,h}$	2.00 ± 0.77^{h}	$>2.00^{h}$	0.74 ± 0.12^{g}	$>2.00^{h}$

Data are shown as means ± SE based on 4 replications per treatment, and each experiment was repeated 3 times. Different letters (a-h) represent significant cytotoxicity differences (Duncan; $P < 0.05$) between different *S. nigra* proteins under each treatment.
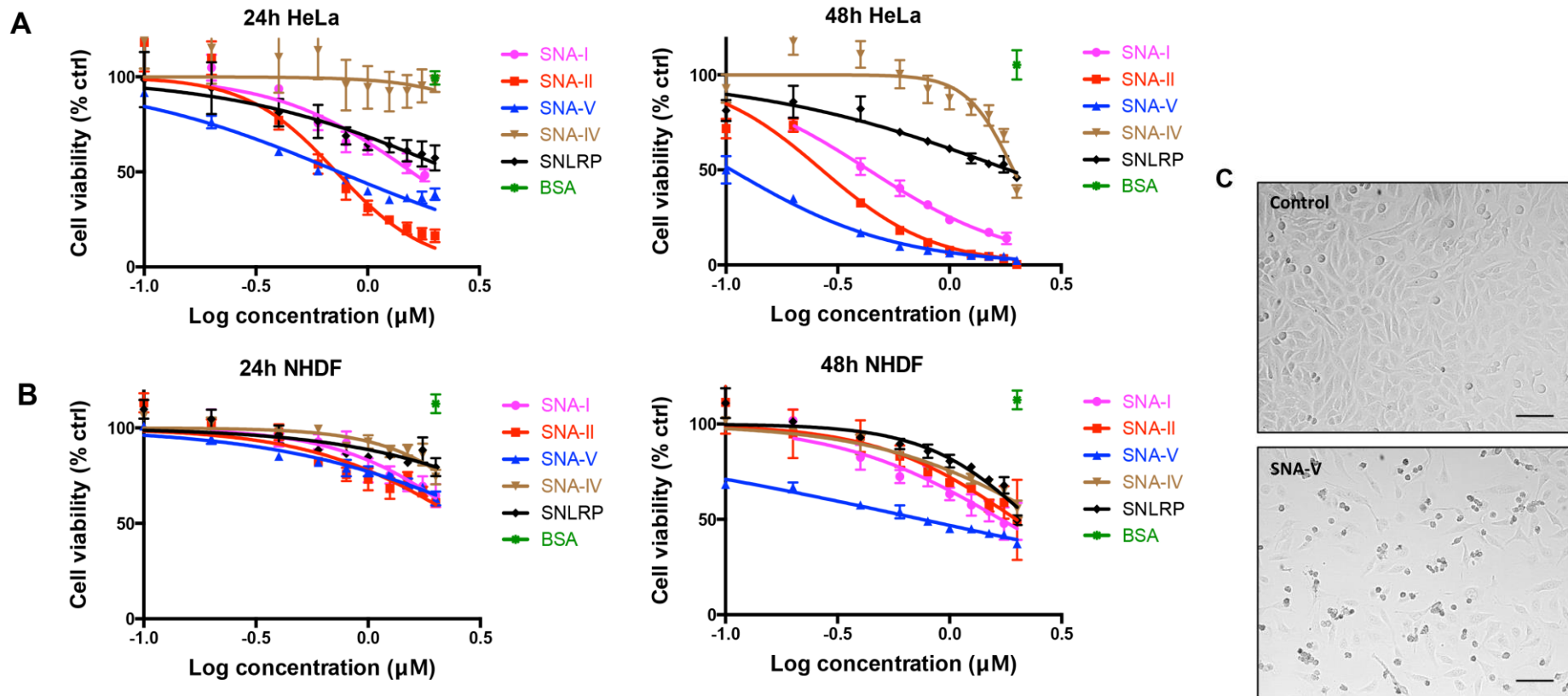
Figure 6.2 Dose response curve of the effect of *S. nigra* proteins on HeLa and NHDF cell viability after 24 and 48 h. (A) Dose-response curves for HeLa cells incubated for 24 and 48h with different concentrations of *S. nigra* RIPs/lectins. (B) Log concentration – cell viability curve of NHDF cells incubated for 24 and 48 h with different concentrations of *S. nigra* RIPs/lectins. % ctrl (treated/control X 100) = ratio of surviving treated cells/ surviving cells percent in control. All data are expressed as means ± SE of 3 biological replicates in 4 technical replicates (n=12). (C) Transmission light microscopy images of HeLa cells grown in the absence (control) and presence of 1.5 μM SNA-V for 24 h. Scale bars represent 100 μm.

6.4.3 *S. nigra* proteins are internalized by HeLa cells

To find out whether differences in cytotoxicity between *S. nigra* proteins were due to differences in cellular protein uptake, HeLa cells were incubated with FITC labeled RIPs and lectins, and monitored using live cell confocal imaging (Fig. 6.3A and supplementary Fig. S6.2). The binding and internalization kinetics of the proteins was quantified at different time points after incubation by measuring the intracellular fluorescence intensities (Fig. 6.3B). Within 0-5 min, we measured fluorescent signals that co-aligned with the plasma membrane, presumably reflecting lectin binding. At later time points, signals were also observed at intracellular locations. All proteins showed time-dependent internalization kinetics with a maximum fluorescent signal after 6 to 9 h of incubation. When fluorescently labelled SNA-I was added to the medium of HeLa cells, the protein attached to the cell surface within minutes. Within the first 40 min, fluorescent SNA-I became internalized and increasingly accumulated in spots close to the nucleus up till 9h (Fig. 6.3A). After 12h a decrease in fluorescent signal was observed, which probably reflects degradation and externalization of internalized lectin. A similar pattern was observed for SNA-V, albeit with a quicker turnover rate (max. at 6h) (supplementary Fig. S6.2B). The perinuclear accumulation was maintained even after mitosis. SNA-II (supplementary Fig. S6.2A) did not show a distinct tethering to the cell surface but also gradually accumulated inside the cell. Compared to SNA-V, intracellular accumulation of SNA-II was less pronounced. The same holds true for SNA-IV and SNLRP (supplementary Fig. S6.2C and D, captured with much higher laser power setting to be visible): the amount of bound protein to the HeLa cell surface was almost undetectable and the amount of internalized protein was low compared to SNA-I (supplementary Fig. S6.3B). After normalization for labeling efficiency, especially SNLRP internalization was negligible. During the time period of microscopic acquisition, HeLa cells incubated with the *S. nigra* proteins showed normal growth and cell division (supplementary Fig. S6.2B). Only a small subset of cells incubated with SNA-I, SNA-II or SNA-V showed morphological changes characteristic for apoptosis (supplementary Fig. S6.2A).
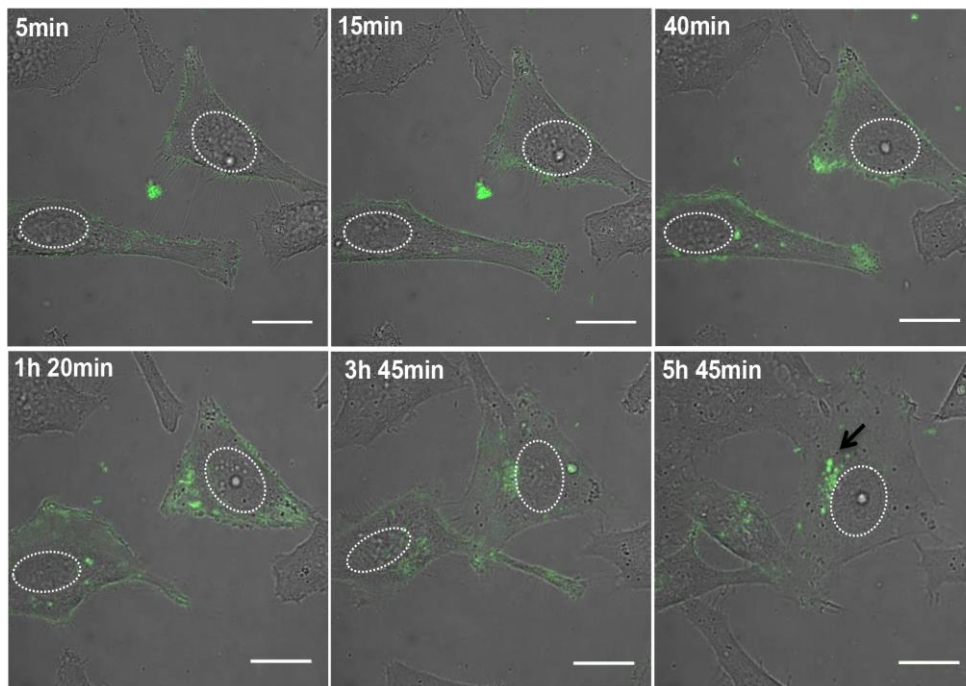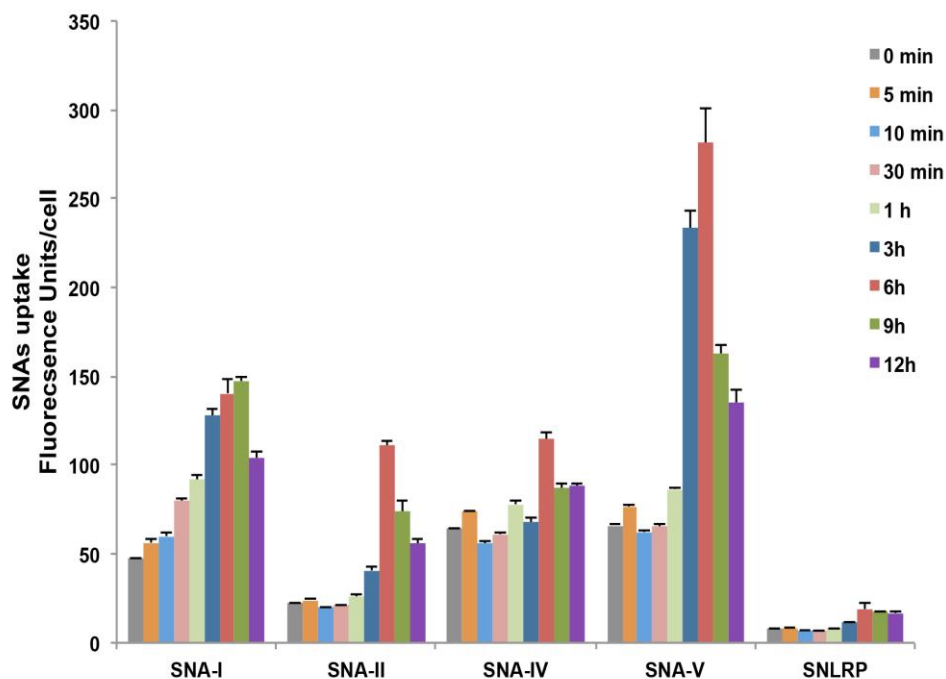
Figure 6.3 Internalization of FITC labeled *S. nigra* proteins in HeLa cells. (A) Confocal microscopic images of the uptake of SNA-I (25 nM) in HeLa cells after 6 hours incubation. The arrow indicates a spot where protein is accumulating. Nuclei have been delineated be in white. Scale bars represent 10 μm. (B) Uptake of 50 nM FITC labeled SNA-I, SNA-II, SNA-IV, SNA-V and SNLRP by HeLa cells after 0 min, 5 min, 30 min, 1 h, 3 h, 6 h, 9 h and 12 h incubation, based on fluorescence intensity, which was normalized by the FITC labeling efficiency. The pictures for quantification were acquired using identical confocal settings. Data are given as mean ± SE, based on at least 80 individual cell measurements per sample and each treatment was carried out with three independent replicates.

153

6.4.4 *S. nigra* proteins predominantly localize to lysosomes but are also found in other organelles.

To find out where the FITC-labeled *S. nigra* proteins are targeted to in the cell, a quantitative colocalization analysis was performed on confocal microscopy images after co-labeling various endovesicles (Fig. 6.4). Irrespective of the measurement method (Manders' coefficients or object-based colocalized coefficients), the analysis showed that a few discrete dots overlap with markers for ER or Golgi but the majority of the lectin/RIP-positive dots colocalized with the endosomes and lysosomes. In the case of SNA-I and SNA-IV higher Manders' coefficients were obtained for the ER, indicating relatively more colocalisation. It is also worth noting that the presence of SNA-IV and SNLRP in the Golgi compartment was clearly lower than for the other proteins.
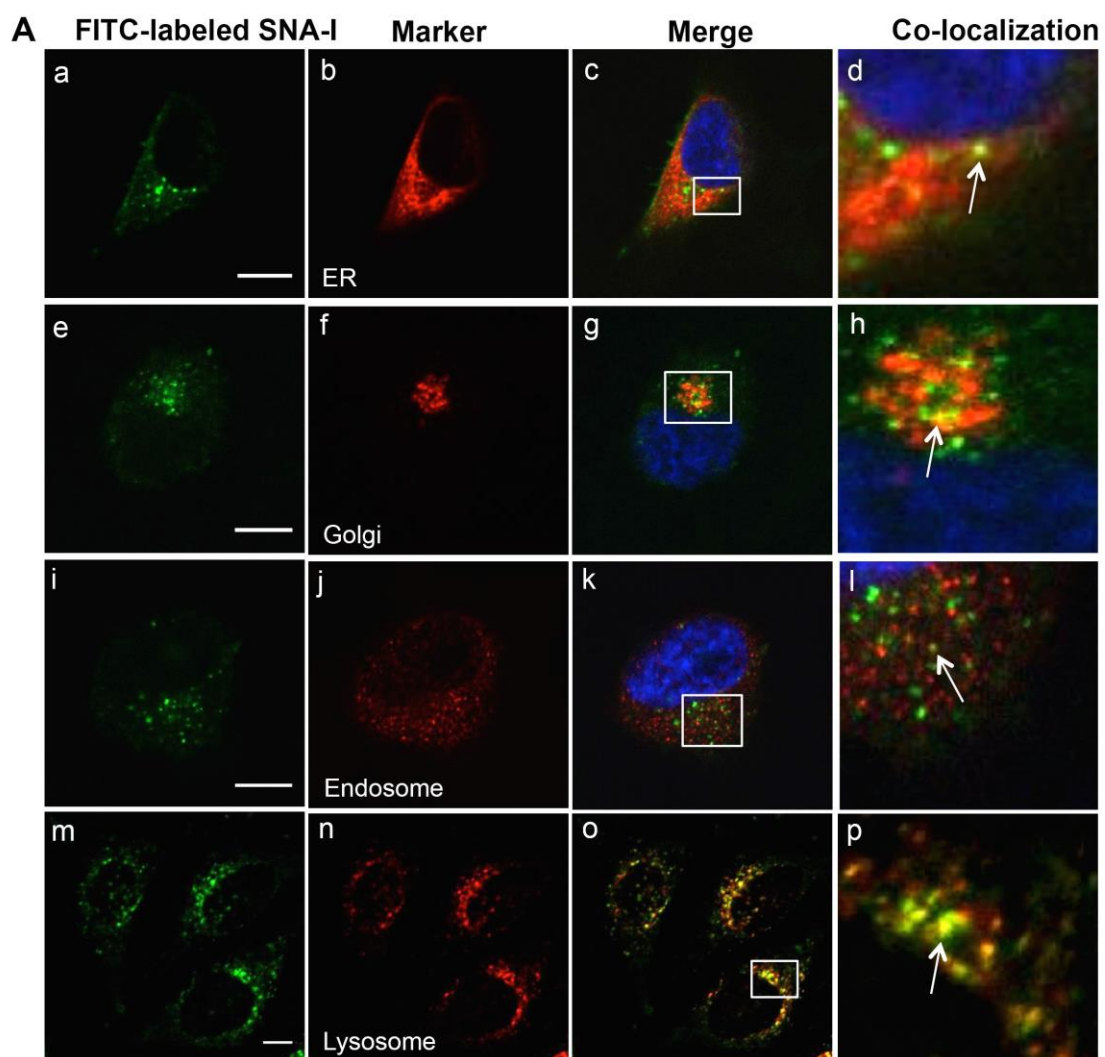
Figure 6.4A Legend on next page
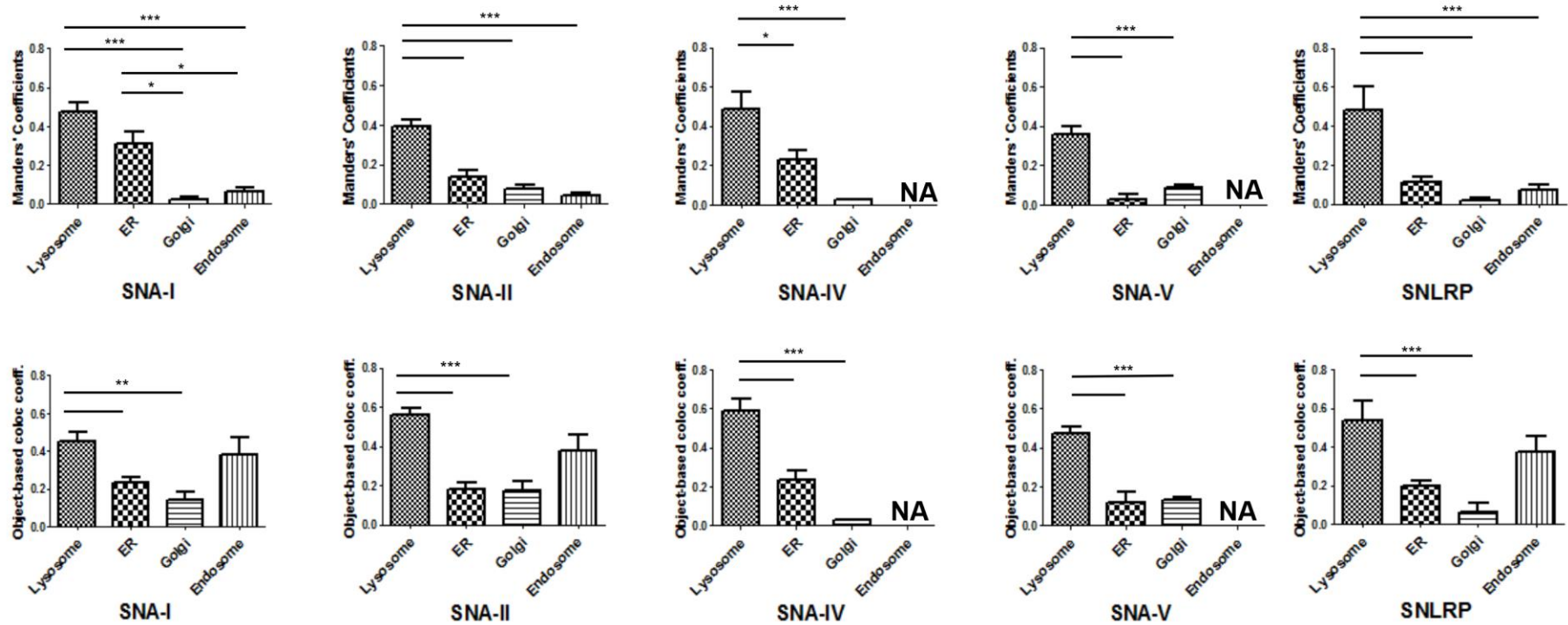
Figure 6.4 Confocal microscopic images and quantitative analysis of the colocalization. (A) Double immunofluorescence analysis of FITC-labeled SNA-I (a, e, i and m), and marker for ER (b, c and d), Golgi (f, g and h), endosomes (j, k and l) and lysosomes (n, o and p) in HeLa cells. The merged reconstructed images are shown in (d, h, l and p) with the green dots from FITC-labeled SNA-I and the red dots from the marker. The arrow indicates SNA-I dots overlapping with the marker. Scale bars represent 10 μm. (B) Manders' coefficients and object-based colocalization graphs of the colocalization image analysis study. Asterisks denote values significantly different from the lysosome (*: $p < 0,05$; **: $p < 0,01$; ***: $p < 0,001$).

6.4.5   Autophagy induced in HeLa cells

Given the fairly high load of proteins in the lysosomes, we reasoned that cellular uptake of some *S. nigra* proteins may trigger alternative degradation pathways such as autophagy. p62 is a direct substrate for autophagy that becomes included in autophagosomes, which is why we used it to monitor formation of autophagosomes (Bjørkøy et al., 2005). A quantitative analysis of the number of p62 puncta per cell revealed that the autophagosome formation increased significantly after administration of any of the different elderberry proteins (Fig. 6.5A and B). To determine whether the autophagic flux was altered, a tandem mRFP-GFP-tagged LC3 construct (Kimura et al., 2007; Mizushima et al., 2010) was used. This fusion construct relies on the properties of mRFP to withstand the acidic environment of the lysosomes and maintain its fluorescence, whereas GFP does not. A strong increase in red over yellow (green+red) foci suggested enrichment of LC3 positive autophagolysosomes and thus an increase in autophagic flux in HeLa cells incubated with SNAI (Fig. 6.5C and D).
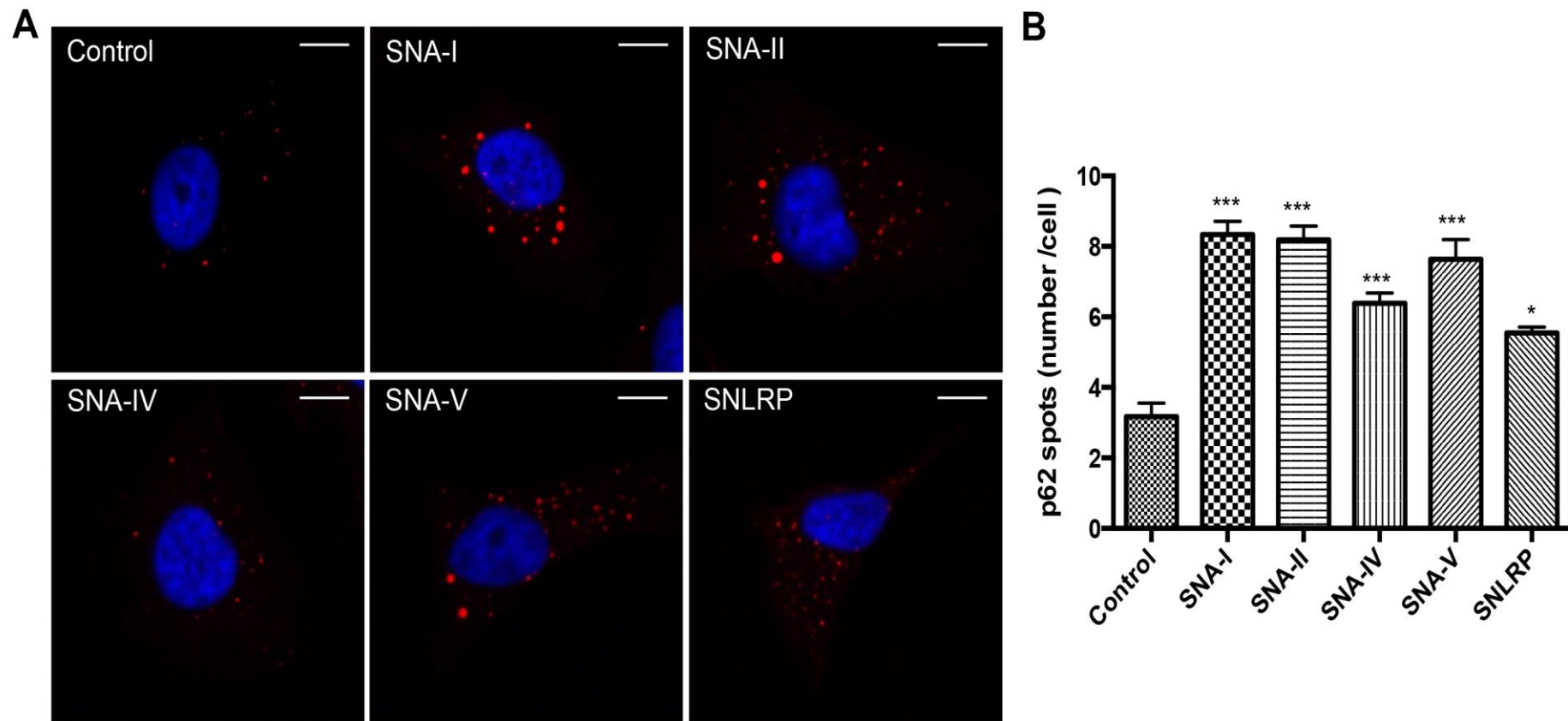
Figure 6.5 *S. nigra* proteins induce autophagy. (A) Confocal images of HeLa cells treated with *S. nigra* proteins, immuno-stained for p62 (red) and counterstained with DAPI (blue). (B) Quantification of p62 puncta numbers/cell (n>600 cells). Asterisks denote values significantly different from the cells incubated in the control (medium containing 1 x PBS) (*: $p < 0,05$; **: $p< 0,01$; ***: $p < 0,001$).
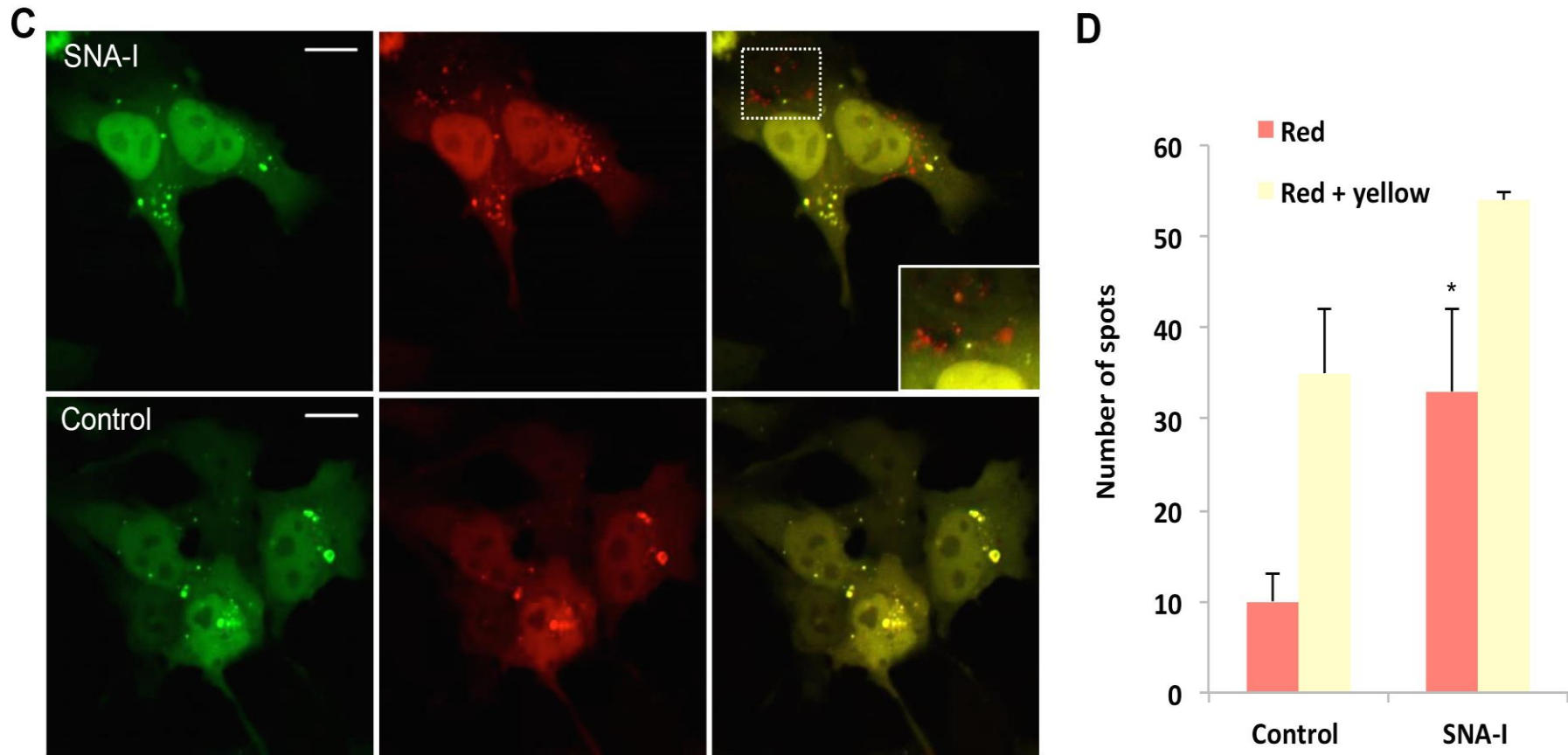
Figure 6.5 *S. nigra* proteins induce autophagy. (C) representative images of HeLa cells transfected with a tandem fluorescent mRFP-GFP-LC3 treated with 1x PBS (control) or SNA-I, (D) Quantification of yellow (autophagosomes) and red (autophagolysosomes) puncta reveals increased autophagy (total number of spots) as well as autophagic flux (red spots) in SNAI treated cells. The asterisk indicates a significant difference compared to the control with P-value < 0.05. Scale bars in panels A and C represent 10 µm and 15 µm, respectively.

6.4.6   Uptake of *S. nigra* proteins leads to translation inhibition *in cellula*

To ascertain protein translation inhibition activity within cells, we used the formation of lipid droplets (LDs) as a proxy (Suzuki 2012). Under ER stress, lipid droplets that increase in cultured cells are enriched with cholesterol esters (unpublished data, Suzuki et al., 2012). Detection of translational shutdown is one of the intermediate markers of ER stress (Bernales et al., 2006). HeLa cells have few small LDs when cultured in normal culture medium (Shibata et al., 2010), but show strong accumulation of LD's upon treatment with translation inhibitors such as cycloheximide (Suzuki 2012). When treated with 100 nM *S. nigra* RIPs SNA-I and SNA-V for 22 hours, there were significantly more LDs (Fig. 6.6A and B). This was not the case for SNLRP and the non-RIP lectins (SNA-II and SNA-IV), suggesting that the *S. nigra* RIPs do effectively exert their ribosome inactivating activity inside the cells. Experiments with a bioluminescent reporter cell line (HG1-luc2-IRES-tCD) supported this notion (Jiménez et al., 2011) (Fig. 6.6C). SNA-V significantly reduced the luminescent signal compared to the control. The other proteins showed no significant effect on the luminescent signal within the non-toxic range, possibly due to the weak sensitivity of the reporter cell line.
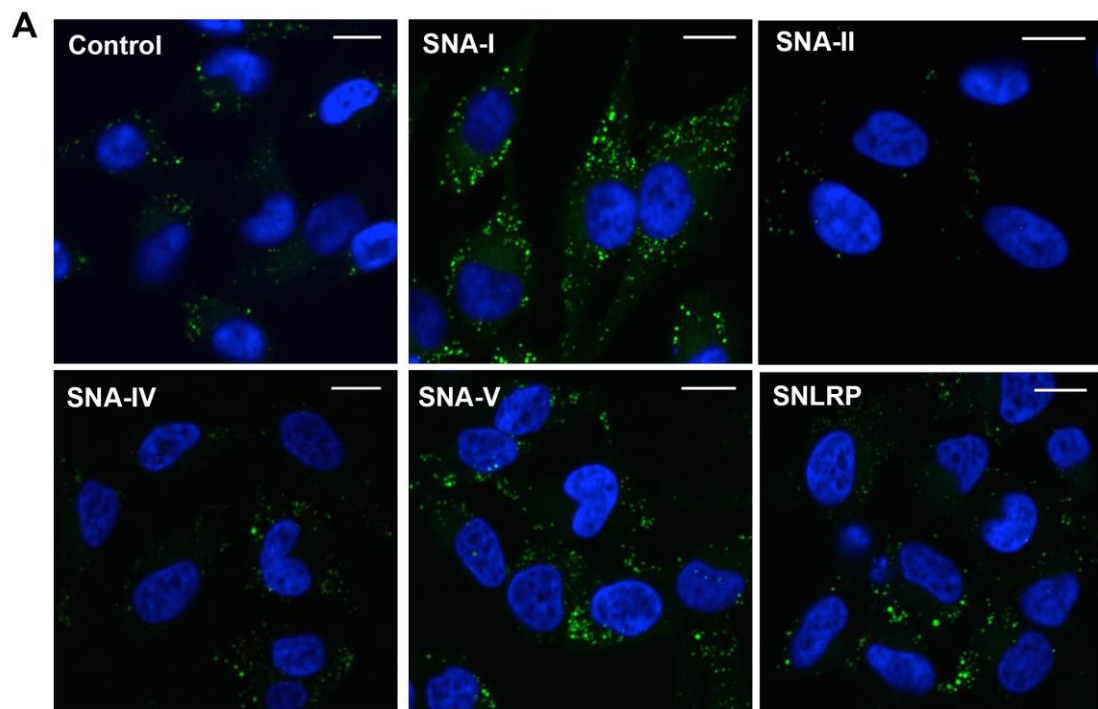

Figure 6.6 *In vivo* protein translation inhibition activity of *S. nigra* RIPs. (A) Merged confocal images of HeLa cells stained with DAPI (blue) and BODIPY (green). Scale bars represent 15 µm.
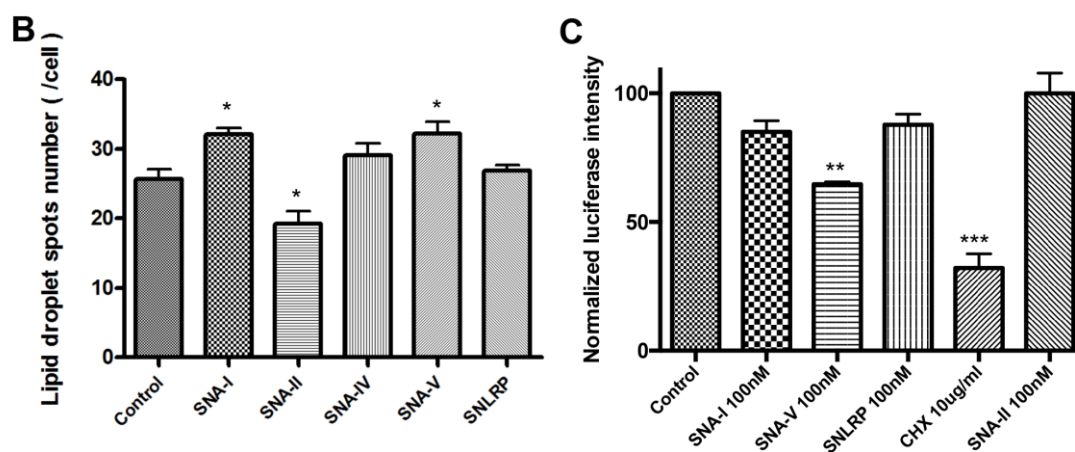
159

Figure 6.6 *In vivo* protein translation inhibition activity of *S. nigra* RIPs. (B) Average numbers of LDs/cell (n>400) (C) Luciferase activity measured in HG1-luc2-IRES-tCD cells incubated with *S. nigra* RIPs/lectins and controls. The treatment with 1 x PBS was selected as the negative control, and cycloheximide was used as a positive control. The luminescent signal was normalized by the fluorescence signal from the Presto blue assay to correct for variations in cell density. Asterisks denote values significantly different from the cells incubated with control (1 x PBS) (*: $p < 0,05$; **: $p < 0,01$; ***: $p < 0,001$).

6.4.7   Glycomic characterization of HeLa and NHDF cells

To assess whether differences in cytotoxicity between cell types and proteins were due to differences in carbohydrate binding to the cell surface, we analysed the glycome patterns on both glycoproteins and glycolipids of HeLa and NHDF cell samples using mass spectrometric methodologies (North et al., 2010). These experiments confirmed the presence of high mannose and complex glycans in both cell types. The major complex N-glycans in both HeLa and NHDF cells are sialylated with N-acetylneuraminic acid (NeuAc) or are terminated with uncapped galactose (Gal) (supplementary Fig. S6.3). To determine the sialic acid linkages, the glycans were digested with sialidase S, which specifically removes α2-3 linked sialic acid, or sialidase A, which cleaves all non-reducing terminal sialic acid residues. Quantification of terminal Gal and terminal NeuAc on glycans from each cell line was performed by comparing the relative abundance of LacNAc (Gal-GlcNAc) antenna and sialylated LacNAc antenna. The result (Fig. 6.7) showed that before Sialidase S digestion, the percentage of glycans terminated with Gal was approximately 54% in NHDF cells, which is significantly higher than in HeLa cells (approximately 30%). After Sialidase S digestion, the percentage of glycans terminated with α2-6 linked NeuAc in

HeLa cells is around 17%, which is considerably higher than the 3% observed in NHDF cells, Sialidase A digestion removed all NeuAc supporting the glycomic assignments.

MALDI-TOF spectra of O-glycans from HeLa and NHDF cells are shown in supplementary Fig. S6.4. The profile demonstrated the presence of both core 1 and core 2 structures in NHDF cells whilst in HeLa cells the majority of the glycan structures are of the core 1 type, although minor core 2 glycans were observed after sialidase digestion (Table 6.2). In both cell types the O-glycans are either sialylated with NeuAc or terminated with uncapped Gal. Comparison of the abundances of the O-glycans (Table 6.2) indicated that the glycans terminated with Gal are more prominent in NHDF cells than in HeLa cells, while the relative abundance of the glycans terminated with the α2-6 linked NeuAc (NeuAc(α2-6)GalNAc) is higher in HeLa cells.

MALDI-TOF data from glycans derived from the glycolipids of HeLa and NHDF cells are shown in supplementary Fig. S6.5. Table 6.3 summarises our structural conclusions which are derived from the glycomics experiments, taking into account biosynthetic considerations. The major glycans are sialylated, and glycans terminated with uncapped Gal represent only a minor fraction. In addition, a glycan (m/z 1101) terminated with HexNAc is present in HeLa cells. Sialidase digestion of HeLa samples confirmed the α2-3 linkage of the peripheral NeuAc of GM3, GM1b and GD1a (supplementary Table S6.1).
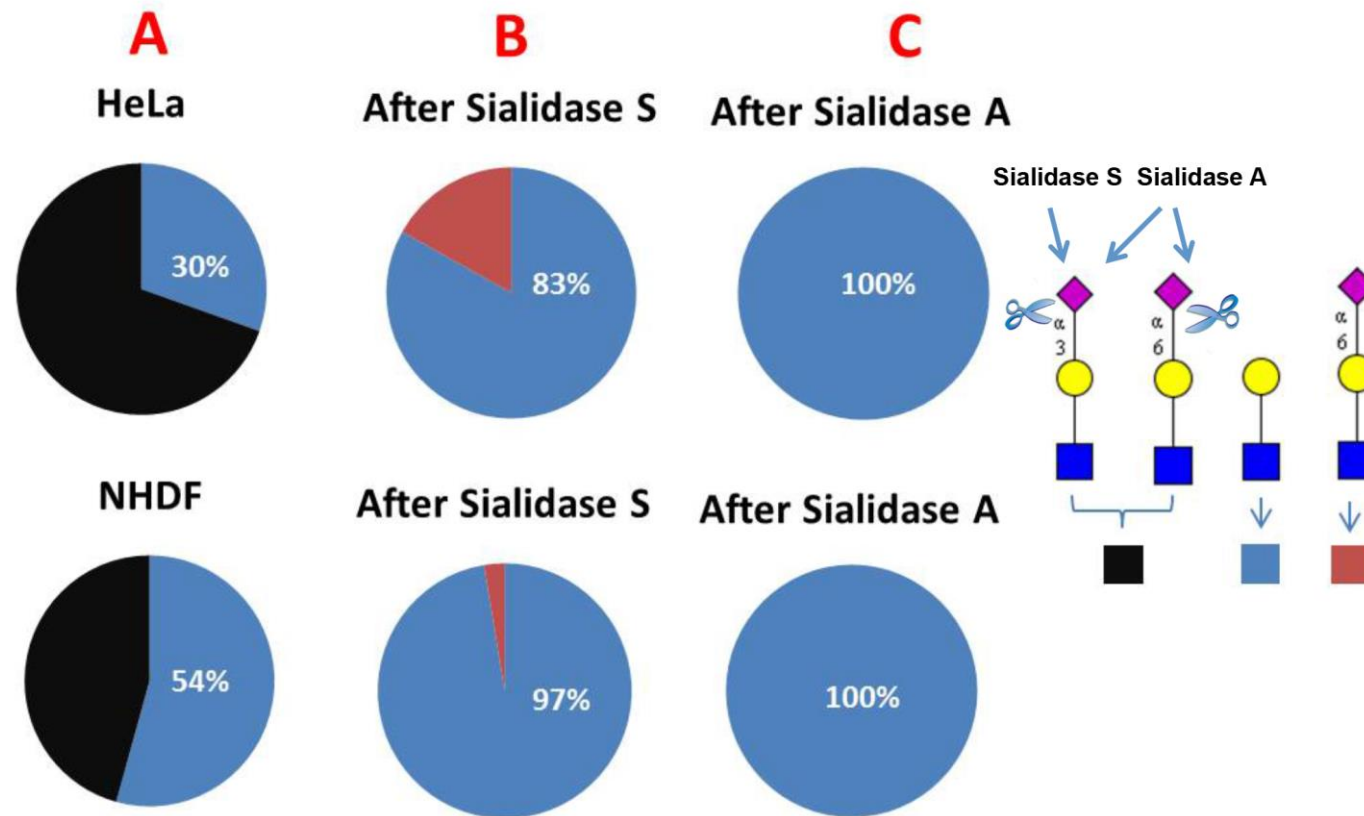
Figure 6.7 Comparative analysis of the relative intensities of LacNAc antenna and sialylated LacNAc antenna in all complex glycans in HeLa and NHDF cells (A), and in Sialidase S treated (B) and Sialidase A treated (C) samples. Black colour, relative intensity of α2-3 and α2-6 sialylated LacNAc antenna; blue colour, relative intensity of LacNAc antenna; red colour, relative intensity of α2-6 sialylated LacNAc antenna. ■ GlcNAc, ○ Gal, ◆ NeuAc.

Table 6.2 O-glycan structures observed in the MALDI-TOF MS spectra of Hela and NHDF glycoproteins. All glycans are permethylated and shown in the form of [M+Na]$^+$. Glycan structures and linkages are drawn based on the molecular weight, O-glycan biosynthetic pathway and MS/MS data. ND, not detected. *=minor (<20%), **=medium (20-50%), ***=major (>50%). □ GalNAc ■ GlcNAc, ○ Gal, ◆ NeuAc.
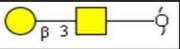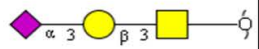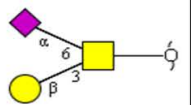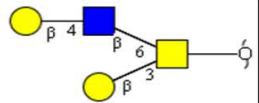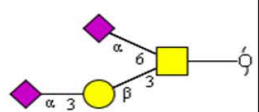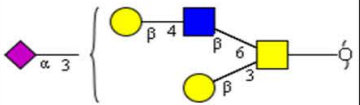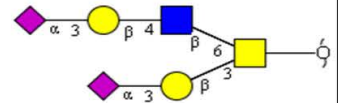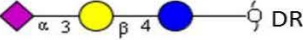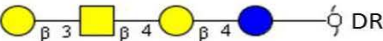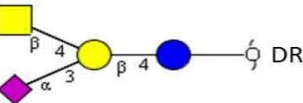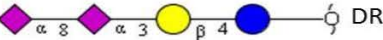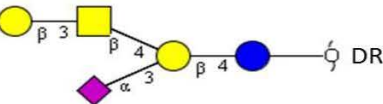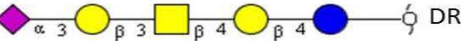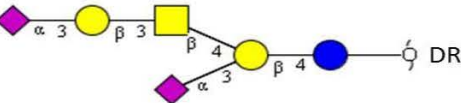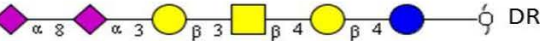
m/z	Structures	Relative abundance in					
		HeLa	NHDF	HeLa, Sialidase S treated	NHDF, Sialidase S treated	HeLa, Sialidase A treated	NHDF, Sialidase A treated
534		ND	**	**	**	***	***
895		**	**	ND	ND	ND	ND
895		ND	ND	***	*	ND	ND
984		ND	*	*	***	*	**
1257		***	**	ND	ND	ND	ND
1345		ND	*	ND	ND	ND	ND
1706		ND	*	ND	ND	ND	ND

Table 6.3 Structures of glycans derived from glycolipids observed in the MALDI-TOF MS spectra of Hela and NHDF cells. All glycans are deuteroreduced (DR), permethylated and shown in the form of [M+Na]$^+$. These glycan structures and linkages are drawn based on the molecular weight, glycolipid glycan biosynthetic pathway and MS/MS data. ND, not detected. *=minor (<20%), **=medium (20-50%), ***=major (>50%). ☐ GalNAc, ● Glc, ○ Gal, ◆ NeuAc.

m/z	Structures	Relative abundance in 35% acetonitrile fraction		Relative abundance in 50% acetonitrile fraction	
		HeLa	NHDF	HeLa	NHDF
855	GM3	*	***	ND	**
943	GA1	*	*	ND	ND
1101	GM2	***	ND	*	ND
1217	GD3	ND	**	ND	***
1305	GM1a / GM1b	**	*	*	*
1666	GD1a	*	ND	***	*
1666	GD1c	ND	ND	ND	*

164

6.5 Discussion

We have performed a comprehensive analysis of the cytotoxic activity of *S. nigra* proteins, including the type 2 RIPs (SNA-I, SNA-V and SNLRP) and lectins (SNA-II and SNA-IV), towards HeLa and NHDF cells. The results illustrate striking differences in terms of cytotoxicity and uptake between cell types and proteins. An important observation is that HeLa cell cultures are more sensitive to incubation with elderberry proteins than human fibroblasts. This can be explained by cell-type dependent differences at three levels, namely at the level of attachment, uptake and/or intracellular destination. Lectin binding to cell-type specific glycosylated proteins on the cell surface might lead to blocking of specific adhesion complexes or activate cell death factor receptors. For instance, galectin-1 induces apoptosis of activated T-cells and T leukaemia cell lines but does not affect resting T cells (Perillo et al., 1995). This difference in cytotoxicity depends on the expression of primary receptors (e.g. glycoproteins-CD43, CD45 and CD7) on the activated T-cell surface (Rabinovich et al., 2005). Specific (glycan-dependent) or aspecific (cell-type dependent) differences in endocytotic flux may in turn affect uptake efficiency and different cells may also sort or allocate the ingested proteins towards different organelles. Around 2000 genes are expressed at much higher levels in HeLa cells than in 16 normal human tissues (of which 805 are protein-coding). These genes typically relate to proliferation (cell cycle phase), transcription (RNA processing, rRNA transcription) and DNA repair (Landry et al., 2013). Therefore, the specific cytotoxicity towards HeLa cells, may also point to a specific, modulatory role in cell proliferation and/or cell cycle-dependent processes. This notion also implies potential anti-carcinogenic activity of these elderberry proteins, which would enable the exploration of natural lectins as anti-cancer compounds.

The protein translation inhibition activity of SNLRP and SNA-V was significantly higher than that of SNA-I in the *in vitro* cell-free system. The IC50 values for SNA-I and SNA-V correspond well with earlier estimations derived from studies using rabbit reticulocyte lysates (Jiménez et al., 2014). Barbieri et al. reported that the translation inhibition activity in a cell-free system was considerably higher for the reduced protein compared to the non-reduced type 2 RIPs (e.g. riproximin, ricin and volkensin) (Barbieri et al., 2004). Similarly Voss et al. (Voss et al., 2006) reported a 2-fold higher activity for the purified A chain of the type 2 RIP from *Ximenia americana,* suggesting that the translation inhibition activity of the A-chain from this type 2 RIP is inhibited due to steric hindrance by the B-chain (Voss et al., 2006).

However, as also shown by Barbieri et al. (Barbieri et al., 2004) this result cannot readily be generalized since the reduction of type 2 RIPs such as SNA-I and SNLRP does not affect their activity on protein synthesis in a rabbit reticulocyte lysate. Our analyses revealed no significant influence of reduction on the activity of SNA-I, SNA-V and SNLRP, suggesting that there is no adverse impact of the lectin domain on the activity of these RIPs. Surprisingly, SNA-II also showed some modest RIP activity when tested at high concentration (>10 nM). This may be due to SNA-II binding to ribosomal proteins leading to inactivation of the ribosomes, but at present the exact modus operandi remains speculative.

Another surprising finding is that the order of the *in vitro* protein synthesis inhibition activity of *S. nigra* proteins (SNLRP > SNA-V > SNA-I > SNA-II > SNA-IV) did not mirror their cytotoxicity towards HeLa cells (SNA-V > SNA-II > SNA-I > SNLRP > SNA-IV). In line with this, it was shown that SNLRP exhibits at least 250-fold lower RIP activity *in cellula* than *in vitro* (Battelli et al., 1997b), while for ricin, RIP activity is in a comparable range *in cellula* and *in vitro* (Jiménez et al., 2014). The lectin SNA-II proved to be even more cytotoxic than some of the RIPs, despite the absence of a RIP domain. This suggests that alternative or even complementary activities take place at the level of the cell. Several non-exclusive mechanisms that rely on lectin-carbohydrate interactions may explain this conundrum. One possibility is the differential uptake efficiency of the proteins in the cell; another is the inefficient targeting of the ribosomes (RIPs) or aspecific binding to and blocking of the ribosomes (lectins).

When assessing internalization kinetics, we observed that SNA-V is internalized most efficiently, whilst SNLRP was taken up least efficiently in HeLa cells. This could explain why these two proteins are at opposite ends of the cytotoxicity spectrum, despite their comparable *in vitro* protein translation inhibition activity. Indeed, lower binding to and uptake in the cells has been related to lower toxicity of type 2 RIPs, (e.g. ebulin 1) (Citores et al., 1996; Pascal et al., 2001). During cellular uptake, SNA-I, SNA-IV and SNA-V first bind to the cell surface and then accumulate around the nucleus. But, SNA-II and SNLRP enter the cells with much less attachment to the cell membrane. It is known that internalization of proteins in cells is not a must to provoke toxicity: some lectins can block cell surface receptors and thereby cause cytotoxicity (Lichtenstein et al., 2013). In this respect, we note that SNA-V and SNA-II are Gal binding proteins whereas SNA-I and SNA-IV are sialic acid binding proteins. In

contrast to the other proteins, SNLRP specifically recognizes GlcNAc oligomers. Thus, the differential cytotoxicity of the elderberry proteins could (in part) be caused by differences in the efficiency of binding to the cell membrane and the different number of binding sites present on the cell surface. To get a better view on the available glycan moieties, we performed a glycomic analyses. This revealed similar sialylation of the glycoproteins in the two cell types, a higher level of sialylation of the HeLa O-glycome compared with NHDF, and a variety of differences in the N-glycomes. In particular, N-glycomic analysis revealed that there were substantially more α2-6 linked sialic residues in glycoproteins from HeLa cells compared to NHDF cells. At least for SNA-I this could explain the increased cytotoxicity towards HeLa cells. Similarly, the higher overall level of sialylation of N- and O-glycans in HeLa cells compared with NHDF cells, could explain the higher cytotoxicity of SNA-IV for HeLa cells. SNA-II and SNA-V showed more cytotoxicity to the HeLa than to NHDF cell line, possibly evidenced by their specific binding to Core 1 glycans on glycolipids. Furthermore, SNA-V is the only protein that demonstrated significant cytotoxicity towards NHDF cells. This could be due to the high abundance of terminal Gal residues in these cells. SNLRP recognizes the core chitobiose moiety of N-glycan structures (Shang and Van Damme, 2014), so in theory, it could interact with all N-glycans. However, the LC50 values for SNLRP are very high, suggesting low binding to the cell surface glycoconjugates. Furthermore the amount of SNLRP internalized in HeLa cells was extremely low, suggesting that SNLRP binding to the chitobiose core is prevented e.g. by steric hindrance.

Although the MS data provided new insights on potential carbohydrate binding sites that correlate with cell binding/uptake for *S. nigra* proteins, it is clear that this interaction is complex and not sufficient to explain the cytotoxic activity of the proteins under study. For example, it remains unclear why the SNA-V and SNA-II are more toxic than SNA-I, despite the amount of terminal Gal on HeLa and NHDF cells being considerably lower than the amount of sialic acid.
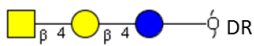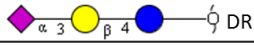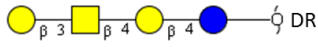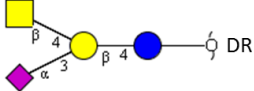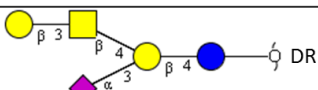
When looking at the cellular destination via colocalization analysis, it became clear that most of the *S. nigra* proteins end up in the lysosomes. However, a small fraction, which varied per protein, also reached the Golgi apparatus or the ER. For ricin, the Golgi complex has typically been considered to be the crucial intermediate subcellular compartment for delivery into the cytosol (Van Deurs et al., 1987), defining the cytotoxic potential of ricin (Sandvig et al., 1991; Yoshida et al., 1991;

Citores et al., 2002). Our results show low accumulation of the *S. nigra* proteins in the Golgi complex, but still significant toxicity. We reasoned that the protein fraction accumulating in the lysosomes may overload these organelles, causing saturation and subsequent activation of alternative degradation pathways such as autophagy. By scoring p62 positive foci, as well as LC3 foci, we confirmed an upregulation of the autophagic flux in the presence of all *S. nigra* proteins, suggesting that indeed such a pathway becomes activated, which in turn may provoke cell death (Klionsky et al., 2012). Autophagic cell death pathways have also recently been described for Concanavalin A and *Polygonatum cyrtonema* lectin (Fu et al., 2011; Liu et al., 2010; Lei et al., 2009) and may present a valuable venue for novel cancer therapeutic strategies.

In summary, the cellular uptake of *S. nigra* RIPs and lectins follows differential routing depending on their molecular structures, carbohydrate-binding properties and interaction with glycans present on the cell surface, which together determine the cytotoxic activity. Until now, it was believed that the lectin domain only facilitated internalization of the proteins, but we now show that the lectin domain can also exert a cytotoxic activity as such. This inherent cytotoxic potential may be due to one or a combination of the following mechanisms: blocking cell membrane receptors, a synergistic role in protein translation inhibition activity and/or lysosome saturation triggering autophagy. Our data helps filling in pieces of the puzzle of RIP induced cell death. Furthermore, a better understanding of the interaction of RIPs with a variety of carbohydrate-binding properties with different cell types may contribute to the development of more specific immunotoxins for future medical applications.

6.6 Supplemental data

Table S6.1 Structures of glycans derived from glycolipids observed in the MALDI-TOF MS spectra of HeLa cells. All glycans are deuteroreduced (DR), permethylated and $[M+Na]^+$. Glycan structures are drawn based on molecular weight, glycolipid glycan biosynthetic pathway and MS/MS data. ND, not detected. *=minor (<20%), **=medium (20-50%), ***=major (>50%). ☐ GalNAc, ● Glc, ○ Gal, ◆ NeuAc.

m/z	Structures		Relative abundance in	
		HeLa	Sialidase S treated	Sialidase A treated
739	GA2 — GalNAc(β4)–Gal(β4)–Glc–DR	ND	ND	*
855	GM3 — NeuAc(α3)–Gal(β4)–Glc–DR	ND	ND	ND
943	GA1 — Gal(β3)–GalNAc(β4)–Gal(β4)–Glc–DR	ND	***	***
1101	GM2 — GalNAc(β4)–[NeuAc(α3)]Gal(β4)–Glc–DR	**	*	ND
1305	GM1a — Gal(β3)–GalNAc(β4)–[NeuAc(α3)]Gal(β4)–Glc–DR	**	**	ND
1305	GM1b — NeuAc(α3)–Gal(β3)–GalNAc(β4)–Gal(β4)–Glc–DR		ND	ND
1666	GD1a — NeuAc(α3)–Gal(β3)–GalNAc(β4)–[NeuAc(α3)]Gal(β4)–Glc–DR	*	ND	ND

169
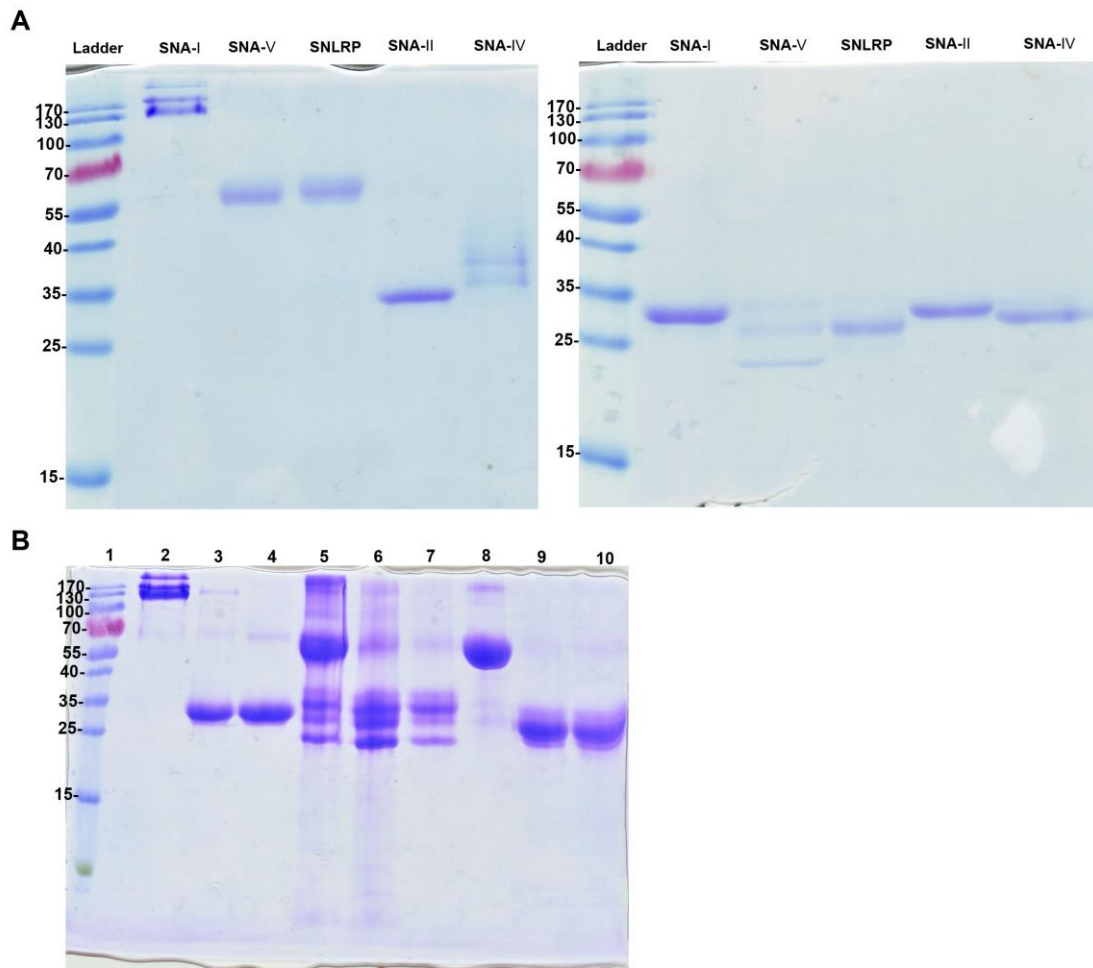
Figure S6.1 SDS-Polyacrylamide gel electrophoresis of *S. nigra* proteins. (A) Purified *S. nigra* proteins were analyzed under non-reducing (left) and reducing conditions (with 2 % β-mercaptoethanol) (right). Samples (3 µg) were loaded as follows: lane 1- Page Ruler Prestained Protein Ladder (Fermentas); lane 2- SNA-I; lane 3- SNA-V; lane 4- SNLRP; lane 5-SNA-II; lane 6- SNA-IV. (B) Non-reduced (without treatment) and reduced (incubation with 0,025 M DTT at 37 °C for 1 h or 2 h) *S. nigra* proteins for *in vitro* protein synthesis inhibition assay. Samples (7.5 µg) were loaded as follows: Lane 1- Page Ruler Prestained Protein Ladder; lane 2, 5 and 8- non-reduced SNA-I, SNA-V and SNLRP, respectively; lane 3, 6 and 9-reduced SNA-I, SNA-V and SNLRP treated with DTT for 1 h 37 °C, respectively; lane 4, 7 and 10- reduced SNA-I, SNA-V and SNLRP treated with DTT for 2 h at 37 °C, respectively.
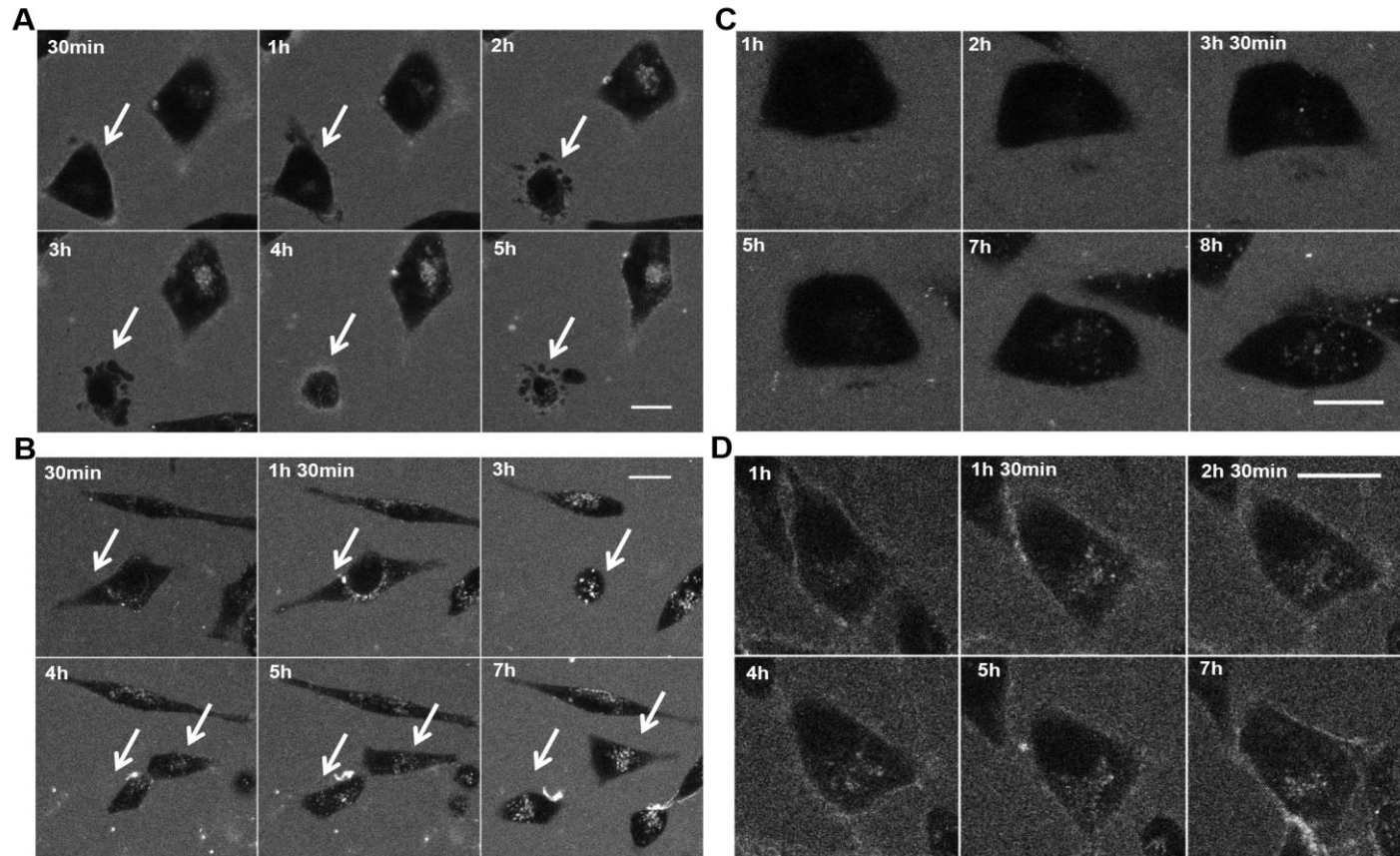
Figure S6.2 Internalization of FITC labelled *S. nigra* proteins in HeLa cells at different time points during a long incubation period. Confocal microscopic images of the uptake of SNA-II (A), SNA-V (B), SNLRP (C) and SNA-IV (D) in HeLa cells during incubation for a maximum of 8 hours. A small subset of HeLa cells incubated with SNA-II and SNA-V showed morphological changes characteristic for mitosis and apoptosis, which were showed by arrows. To visualize the cellular uptake clearly, the live cell images were captured with different settings (much higher laser power settings for SNA-IV and SNLRP and gain visibility). Scale bars represent 20µm.
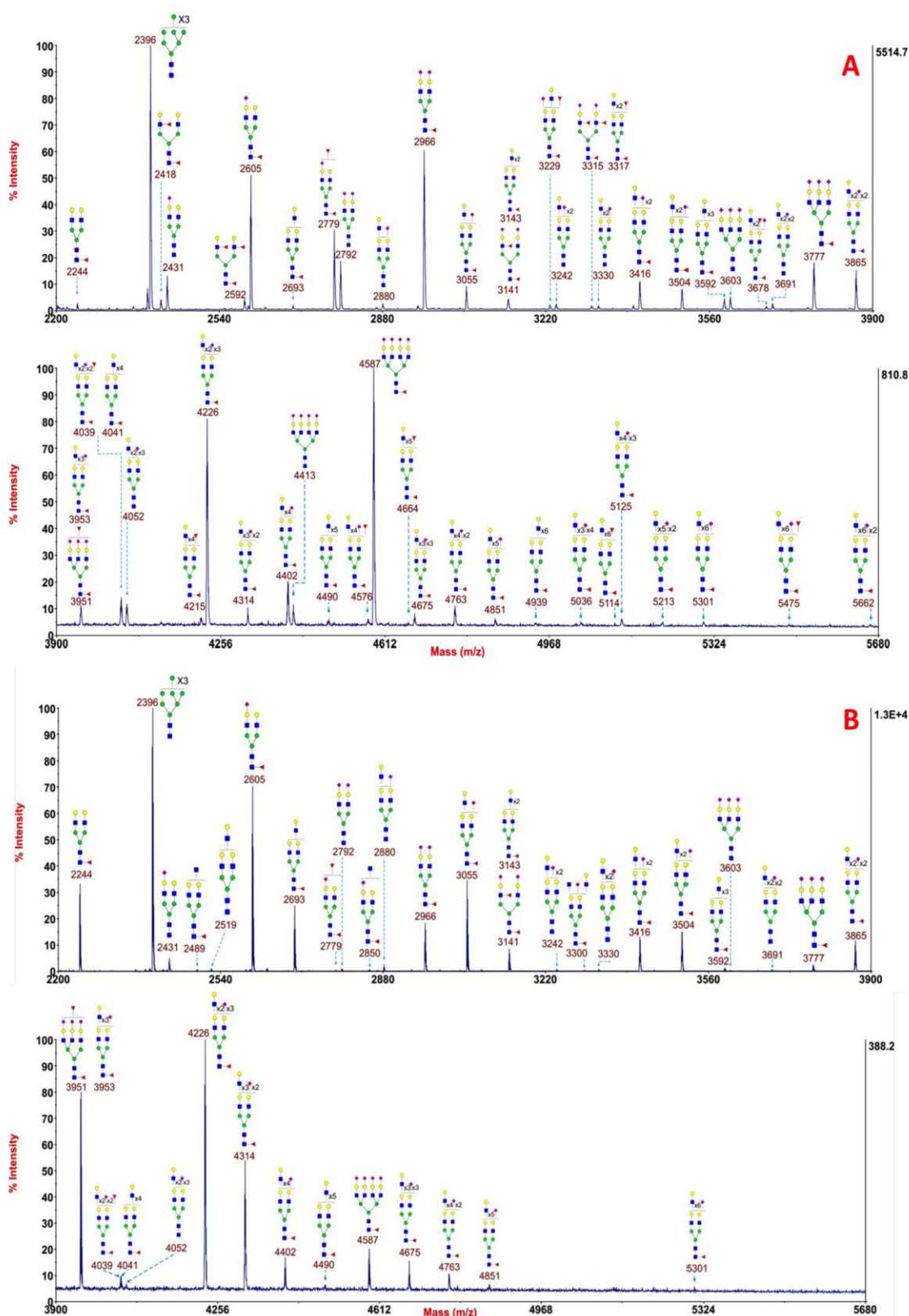
Figure S6.3 Annotated MALDI-TOF MS spectra of permethylated N-glycans in Hela (A) and NHDF (B) cells. Profiles were obtained from the 50% acetonitrile fraction from a C18 Sep-Pak column. All ions are [M+Na]$^+$. Putative structures are based on the molecular weight, N-glycan biosynthetic pathway and MS/MS data. ■ GlcNAc, ● Man, ○ Gal, ▲ Fuc, ◆ NeuAc.
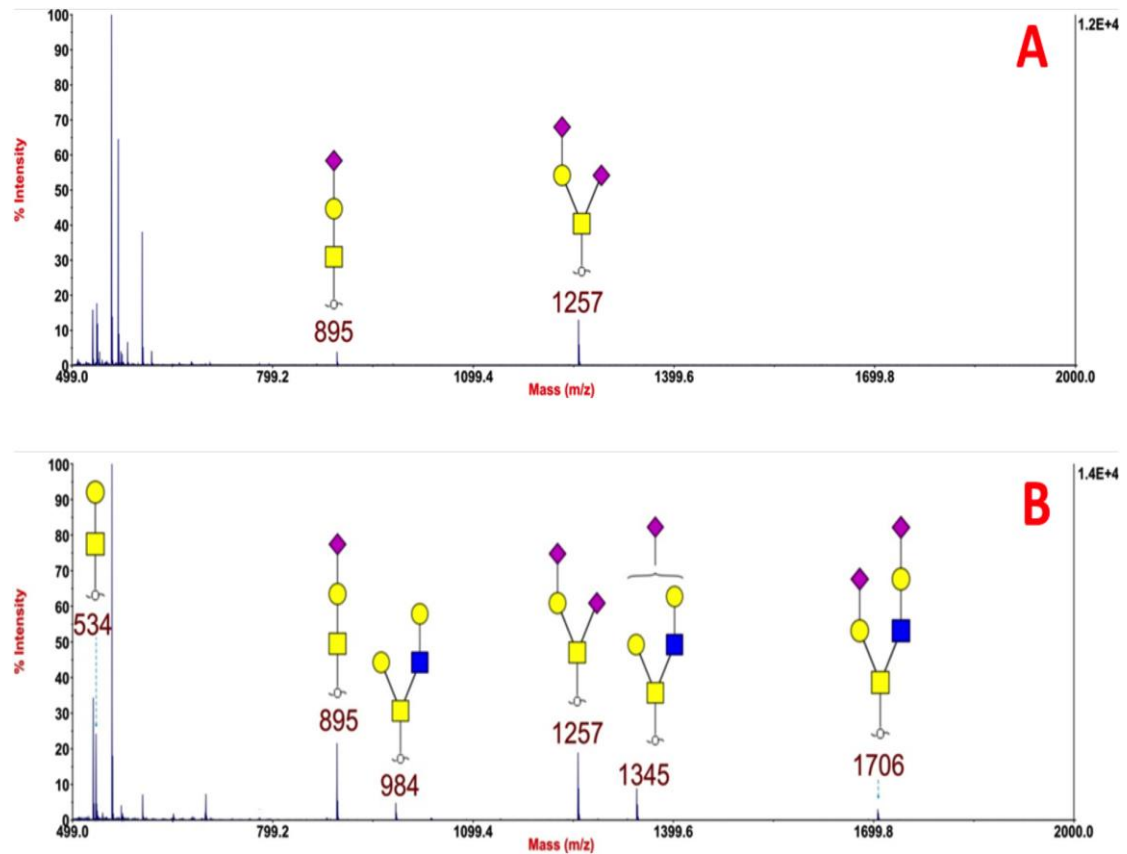
Figure S6.4 Annotated MALDI-TOF MS spectra of permethylated O-glycans in Hela (A) and NHDF (B) cells. Profiles were obtained from the 35% acetonitrile fraction from a C18 Sep-Pak column. All ions are [M+Na]$^+$. Putative structures are based on the molecular weight, O-glycan biosynthetic pathway and MS/MS data. □ GalNAc ■ GlcNAc, ○ Gal, ◆ NeuAc.
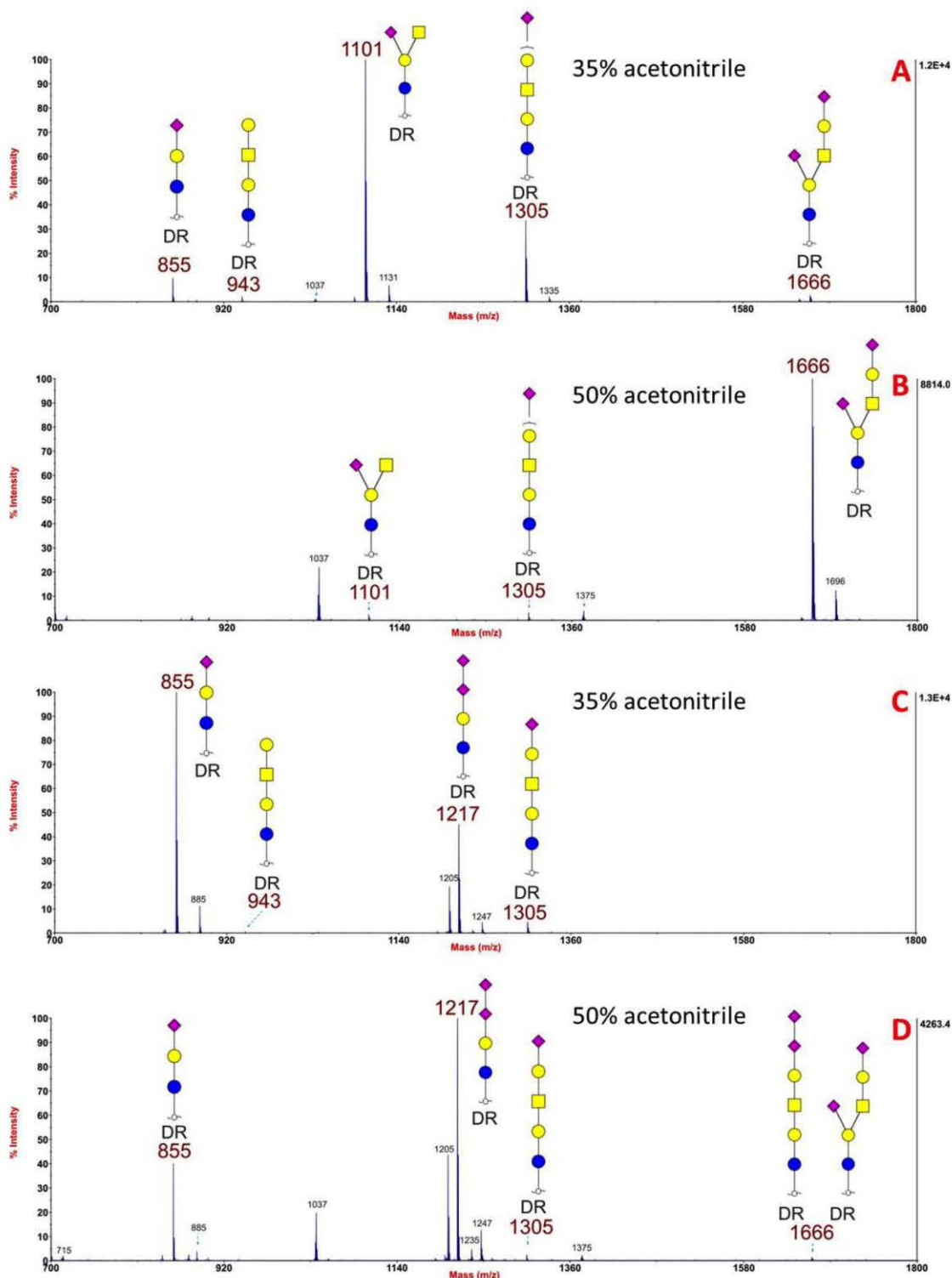
Figure S6.5 Annotated MALDI-TOF MS spectra of deuteroreduced, permethylated glycolipid derived glycans from Hela (A, B) and NHDF (C, D) cells. These profiles were obtained from the 35% and 50% acetonitrile fractions from a C18 Sep-Pak column. All ions are [M+Na]$^+$. Putative structures are based on the molecular weight, glycolipid glycan biosynthetic pathway and MS/MS data. ☐ GalNAc, ● Glc, ○ Gal, ◆ NeuAc.

Chapter 7

General discussion and perspectives for future research

Throughout their development plants are continuously threatened by attacks from micro-organisms, insects, herbivores and mammals. To survive in such a highly competitive environment, each plant must elaborate a complex set of different defense mechanisms, involving both physical adaptations (spines or leathery leaves) and synthesis of biochemical compounds with defense properties (alkaloids, toxins, lectins, ribosome-inactivating proteins, chitinases, …) (Muthamilarasan and Prasad, 2013; Wirthmueller et al., 2013; Lev-Yadun and Halpern, 2008; Vargas and Carlini, 2014). During the last decades, plant toxins, in particular RIPs, have attracted a lot of attention from researchers in different scientific disciplines. Several studies confirmed that RIPs play an important role in plant defense (Peumans et al., 2001; Van Damme, 2001; Krivdova et al., 2014). However, taking into account the toxic properties of these proteins RIPs have also been investigated for their biomedical applications, e.g. as tools in the battle against tumor cells.

New RIPs and RIP sequences are still being discovered regularly. Both genome and transcriptome sequences have resulted in new insights concerning the occurrence and physiological importance of RIPs. The recent discovery of RIP sequences in genome and transcriptome databases from daily consumed fruits, such as e.g. apple also raises questions with respect to food safety. However, the direct purification of apple RIPs from mature fruit failed, suggesting that levels of the level of RIP in apple are low. Nevertheless these proteins could play an important role in the plant. For instance, RIPs expressed in edible fruit could be useful due to their antiviral, antifungal or insecticidal activity, without any toxic effect to humans. Taking into account the widedistribution of RIPs (especially type 1 RIPs) in edible plants and their low toxicity to mammals both *in vitro* and *in vivo*, genes encoding RIPs might be candidate transgenes to enhance the resistance of plants against insects, fungi and viruses.

In this PhD thesis, the biological activities and physiological role(s) of RIPs have been investigated in detail. The apple RIPs have been studied for their molecular structure and biological activities, their developmental expression, their localization in the cell, and their involvement in plant defense. In addition, the effects of elderberry RIPs and lectins on mammalian cells were investigated with respect to their interaction with the cell surface, uptake and internalization by the cells and their cytotoxicity.

7.1 Characterization and biological properties of RIPs from apple

The first aim of this PhD research was to characterize the type 1 and type 2 RIPs from apple. The molecular structure, N-glycosidase activity, carbohydrate binding specificity and cytotoxicity of apple RIPs were investigated in detail in **chapter 2**. Due to the low expression of RIPs in the apple tissues (**chapter 3**), it was impossible to purify the native apple RIPs directly from apple tissues. Thus, heterologous expression systems were selected to express recombinant apple RIPs. Afterwards, the protein synthesis inhibition activity of recombinant RIPs was studied in a cell free system and their toxicity towards cells and plant predators as well as pathogens was investigated.

7.1.1 Molecular evolution

In some families (e.g. Euphorbiaceae and Poaceae) RIP genes are found in all sequenced genomes whereas in others (e.g. Rosaceae) RIP genes occur in some genomes (*Malus domestica* and *Prunus persica*) but are absent from others (*Fragaria vesca*) (described in chapter 1). It was found that apple (*Malus* sp.) and pear (*Pyrus* sp.) express both type 1 and type 2 RIPs whereas *Prunus* sp. (e.g. apricot and peach) expresses a complex set of type 1 RIPs. On the basis of a phylogenetic analysis, it was suggested that most type 1 RIPs found in dicots are evolutionary related to type 2 RIPs (Peumans and Van Damme, 2010). Sequence alignment of the coding sequences of the type 1 RIP and the type 2 RIP gene from *Malus domestica* demonstrated that after deletion of the C-terminus of the A domain and the entire B-domain minus the last amino acids at the C-terminus, both sequences can readily be aligned at the nucleotide level. However, due to the introduction of two frame shifts the type 1 RIP sequence lacks the signal peptide as well as the C-terminus of the type 2 RIP (Fig. 7.1). Therefore, type 1 RIPs from Rosaceae can be considered as "deletion" products of type 2 RIPs.

Besides domain deletion events type 1 RIP genes can also be generated by 'truncation" of type 2 RIP B chimers through "more simple" genetic events such as the introduction of a stop codon or a frame shift or the insertion of a transposable element. All these events shaped the complex RIP gene family.
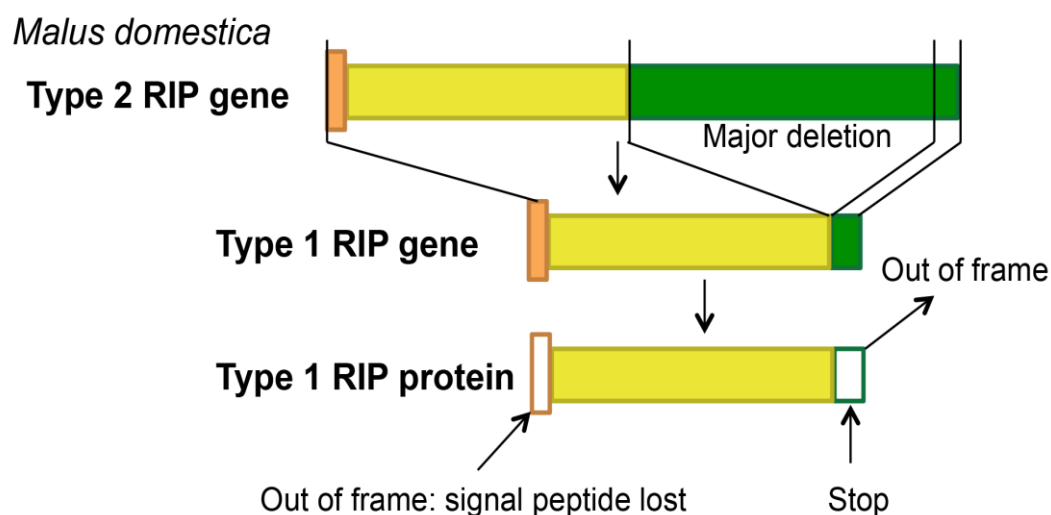
Figure 7.1 Documented domain deletion events that illustrate the conversion of apple type 2 RIP into type 1 RIP gene.

7.1.2   Molecular structure

The recombinant apple type 2 RIP is a multimeric protein as also suggested by the different forms observed on the SDS-PAGE analysis (**chapter 2**). This oligomerization is similar as shown for SNA-I and ebulin f. SNA-I, a type 2 RIP from *S. nigra*, is a tetrameric ($[(A-S-S-B)_2]_2$) protein in which the two B chains of two heterodimers are linked by a disulfide bond. Ebulin f, a type 2 RIP from *S. ebulus* L., is polymerized with other ebulin f or SELd (lectin B-B) molecules to form multimeric proteins (Citores, et al., 1998). Similar to ebulin f, the recombinant apple type 2 RIP occurs as a polymerized protein, whereby dimeric and monomeric type 2 RIPs probably coexist (**chapter 2**).

Normally, type 2 RIPs are chimeric proteins, consisting of an N-terminal enzymatic domain (the A chain) and a C-terminal lectin domain (the B chain) linked by a disulfide bridge. Unlike all other type 2 RIPs, the processing step consisting of the excision of the linker between the A and B chain from the precursor polypeptide does not seem to occur in native apple type 2 RIP (**chapter 2**). In addition, the native type 2 RIP from 10-day old fruits from pear was not reduced by betamercaptoethanol (data not shown). In contrast, the recombinant type 2 RIPs, either purified from whole transgenic tobacco leaves (**chapter 4**) or from the extracellular space between tobacco cells (data not shown), do show a clear A and B chain after reduction with betamercaptoethanol. To our knowledge this is the first report of a type 2 RIP where the A and B chains are not separated during processing of the precursor polypeptide into the mature RIP. It is not completely clear why this

178

processing step does not take place. Western blot analysis suggests that A and B chain remain linked in the native type 2 RIP, at least in 10-day old fruits from apple (**chapter 2**).

Similarly, the question remains why the linker sequence is not processed during the recombinant expression of apple type 2 RIP in BY-2 cells. Interestingly, the expression of the apple RIP sequence in the tobacco plants showed cleavage of the precursor into the A and B chain. Possibly, the sequence of apple type 2 RIP is insensitive to the proteolytic cleavage of the linker sequence. Moreover, it is possible that some particular protease necessary to process the linker sequence between A chain and B chain is present in the tobacco plant system but is absent in BY-2 cells.

7.1.3   Binding of apple type 2 RIP to sialic acid

The carbohydrate binding properties of the recombinant type 2 RIP from apple were defined by agglutination inhibition assays as well as glycan array analyses, and indicated that the apple type 2 RIP specifically recognizes sialic acid residues. The carbohydrate binding properties of the apple RIP are similar to those of SNA-I, a well-known type 2 RIP from elderberry (*Sambucus nigra*) (Van Damme et al., 1996a; Kaku et al., 2007; Shang and Van Damme, 2014). However, this carbohydrate binding specificity is very different from the majority of type 2 RIPs that specifically react with galactose or galactose derivatives. It is commonly accepted that sialic acid is absent in plants, although researchers did many efforts to confirm the occurrence of sialylated glycoconjugates in plant cells (Zeleny et al., 2006, Takashima et al., 2009). However, sialic acid is widely spread from bacteria to animal tissues, and plays an important role in cell communication, adhesion and protein targeting (Varki and Schauer, 2009). Similar to SNA-I, the sialic acid binding specificity of the apple type 2 RIP may also protect plants from plant diseases e.g. fungi, insects or viruses.

7.1.4   Cytotoxicity of apple type 2 RIP on mammalian cells

The type 2 RIP from apple showed toxicity to both HeLa and NHDF cell lines. Mass spectrometry allowed to analyse the glycome patterns on both glycoproteins and glycolipids of HeLa and NHDF cell samples and revealed that sialylated glycans with NeuAc are abundant on both cell lines (**chapter 6**). Furthermore this analysis provided evidence for the toxicity of sialic acid binding apple type 2 RIP on mammalian cells. Due to the lectin domain, it is much easier for the type 2 RIP to recognize the specific glycans on the cell surface and enter the cells by endocytosis

(Spooner and Lord 2014). Unlike type 2 RIPs, the pathway of type 1 RIPs (lacking the lectin domain) to enter cells is binding to cell surface receptors or via pinocytosis. This was shown for trichosanthin and saporin (de Vergilio et al., 2010), and these type 1 RIPs showed toxicity to mammalian cells after successful internalization. In our analysis, both HeLa and NHDF cells were not susceptible to the apple type 1 RIP. The question remains whether enough molecules of the RIP succeeded in getting into the cells?

Further research is needed to validate whether the type 1 RIP is able to bind to receptors on the cell surface. FITC labeling of the RIPs under study would be useful to follow the internalization of the proteins by microscopic analysis. Furthermore it might be interesting to check if the type 1 and type 2 RIPs can act synergistically. In addition, in view of possible future applications, the toxicity of the apple RIPs for human cells should be assessed in more detail.

7.2 Expression of RIPs in different apple tissues and during fruit development

In **chapter 3**, the tissue-specific expression of RIPs was quantitatively analyzed by studying the transcripts encoding apple type 1 and type 2 RIPs in different apple tissues, throughout plant and fruit development. The relative expression levels for the RIPs were normalized to the expression of two reference genes (18S rRNA and GAPDH) (Schaffer et al., 2007; Foster et al., 2006). In this study, all the apple tissues were sampled under natural growth conditions at the faculty campus during spring-autumn of 2013.

The apple genome contains three sequences encoding type 1 RIP sequences in particular type 1 RIP gene A (accession number: >MDP0000918923), gene B (>MDP0000134012) and gene C (>MDP0000223290). We have to mention that only one type 1 RIP gene, in particular gene A was analyzed in our study, instead of all three type 1 RIP genes from the apple genome. Type 1 RIP expression for gene A was not detected, most probably due to its very low expression. Based on the analysis from one gene encoding type 1 RIP, we can not conclude that in general the type 1 RIP has no or low expression in apple tissues. Possibly, genes B and C show a different expression pattern than gene A. At present, there is no information from transcriptome analysis about which tissue expresses type 1 RIP genes A and C. The transcriptome analysis showed that the type 1 RIP gene B is possibly expressed in young leaves. It was reported before that some type 1 RIPs are present only in some particular tissues, e.g. seeds (*Basella rubra* and *Cinnamonum camphora*), leaves

(*Phytolacca americana*, *Sambucus ebulus* L., *Beta vulgaris* and *Bougainvillea spectabilis*), roots (*Mirabilis jalapa*) and bulbs (Iris and *Charybdis maritima*) (Ng and Wong et al., 2014). For instance, the distribution of saporin (type 1 RIP from *Saponaria officinalis* L.) was detected throughout different plant tissues but was most abundant in seeds (Tartarini et al., 2010). Another example is beetin (a type 1 RIP from *Beta vulgaris*), it accumulates in adult plants but not in germs or young plants (Iglesias, et al., 2008). Luffin, a type 1 RIP from *Luffa cylindrica*, accumulates in seeds, leaves and stems (Di Cola et al., 1999). Possibly, some type 1 RIPs are also expressed in some particular tissues (e.g. roots) or are expressed only during a very specific time during development.

The apple genome contains only one sequence (>MDP0000711911) for a type 2 RIP gene. qRT-PCR analyses indicated that the apple type 2 RIP preferably accumulates in the early growth stages (young leaves, flower buds and 10 day-old fruits) and the expression level gradually decreases throughout plant/ tissue development. Compared to many other documented type 2 RIPs (e.g. ricin, SNA-I, abrin…) that can directly be purified from raw plant tissues, the transcript levels for the apple type 2 RIP are quite low. Interestingly, the type 2 RIP was found to accumulate in spring bark from apple trees collected in 2013. Similarly, SNA-I, possessing a similar carbohydrate binding specificity as the apple type 2 RIP, was reported as an abundant protein in the protein bodies of *S. nigra* bark as well (Van Damme et al., 1996a, Greenwood et al., 1986). In addition, the transcript level of apple type 2 RIP in mature seeds was quite low compared to the other tissues. Likely, ricin particularly accumulates in the last stage of seed development and early stage of the seed germination (Barnes, et al., 2009, Loss-Morais et al., 2013). These data suggest that ricin protects the seeds from invading pests and pathogens (Nielsen and Boston, 2001). The accumulation of apple type 2 RIP in particular tissues may suggest that the RIP is involved in plant defense.

It has been noticed that changes in mRNA levels are not congruent to the changes in protein levels, depending on the transcriptional and translational rates (Feussner and Polle, 2015). Our data provided some first evidence for the expression of RIPs at mRNA level in different apple and pear tissues. A quantitative measurement at the protein level would give a more solid statement about the presence of these enzymes in fruit or tree samples (e.g. western blot).

7.3 Apple type 1 RIP in cytoplasm and nucleus

All type 1 RIP sequences from apple are synthesized without a signal peptide. Using different experimental setups to study the localization (**chapter 3**) of the type 1 RIP-sequence A, we could show that the protein locates to the cytoplasm and the nucleus. These data are in agreement with the fact that due to the absence of a signal peptide, the protein is synthesized on free ribosomes in the cytoplasm of cells and partly targeted into the nucleus.

Type 1 RIP sequence A contains a clear nuclear targeting sequence at the C terminus of the sequence: ^{298}KKKK^{301}. Similar to the type 1 RIP gene A, type 1 RIP genes B and C from apple also contain a classical nuclear targeting sequence (^{307}KKPR^{310} and ^{300}KKPH^{303} for genes B and C, respectively). Therefore, it is hypothesized that all the type 1 RIPs from apple localize in the cytoplasm and the nucleus. In contrast to many other RIPs that are sequestered from the host ribosomes in e.g. vacuoles, the apple type 1 RIP is present in the cytosolic compartment which is similar to the localization pattern observed for the classical cereal type 1 RIPs (Nielsen and Boston, 2001). They are synthesized without a signal peptide and therefore will reside in the same cell compartment as the ribosomes (Nielsen et al., 2001). This raises some questions about their physiological importance and interaction with the own plant ribosomes. Some of these cereal RIPs have been shown to have little activity against plant ribosomes, while other cereal RIPs exert their function by interacting with the ribosomes of the host plant. For example the working mechanism of JIP60 nicely illustrates the endogenous function of some cereal RIPs during senescence (Rustgi et al., 2014). Similarly tritin is a cytosolic type 1 RIP from wheat, which is produced in senescing coleoptiles and plays an important role in the senescing of these coleoptiles (Sawasaki et al., 2008). However, it was also reported that some plant ribosomes are insensitive to RIPs compared to fungal and mammalian ones (Girbés et al., 2004). For instance, the ribosomes from sugar beets are resistant to beetins (type 1 RIP from sugar beet) (Iglesias et al., 2008). At present no extensive studies have been performed to unravel the physiological role of these proteins in the plant, but beetins have been reported as virus-inducible type 1 RIPs in adult leaves of *Beta vulgaris* L. Western blot analysis revealed the presence of beetin forms in adult plants but not in germ or young plants, indicating that the expression of these proteins is developmentally regulated. Furthermore, treatment of *B. vulgaris* leaves with mediators of plant-acquired resistance such as salicylic acid and hydrogen peroxide promoted the expression of beetin by induction of its transcript, but only in adult plants. Taking into consideration that the low-expressed RIPs are more

widespread in the plant kingdom than their abundant counterparts there is a reasonable chance that these RIPs play a very specific role in the plant. To unravel whether the apple type 1 RIP recognizes and interacts with plant ribosomes and/or exhibits N-glycosidase activity, *in vivo* analyses can be set up in order to test the effect of the RIPs on plant cell cultures/protoplasts or plant ribosomes (Dunaeva et al., 1999; Krawetz and Boston, 2000; Rustgi et al., 2014).

7.4 Secretion of apple type 2 RIP

Microscopic analyses revealed that the type 2 RIP sequence from apple contains a signal peptide, and the protein is secreted to the extracellular space (**chapter 3**). The apple type 2 RIP is synthesized on ribosomes on the rough ER and secreted into intercellular apoplastic space (Drakakaki and Dandekar, 2013). These data are in good agreement with the secretion of the RIP in the cell culture as evidenced by the successful purification of the recombinant type 2 RIP from stably transformed BY-2 medium (**Chapter 2**). According to their final subcellular localization RIPs synthesized on the ER can be divided in three main groups (Di Cola et al., 1999): (i) RIPs accumulating in the intercellular space, e.g. PAP (type 1 RIP from *Phytolacca americana*) and luffin; (ii) RIPs in the vacuolar compartment, e.g. ricin (Tully and Beevers, 1976); (ii) RIPs in both the extracellular space and the vacuole, e.g. saporin, gypsophilin (type 1 RIP, *Gypsophila elegans*). Being present in the extracellular space, apple type 2 RIPs can form a natural barrier against pathogen attack.

Besides using GFP fusion proteins, immunostaining would be another good choice to study the localization of apple RIPs. The use of antibodies would have been a preferred method as targeting of tagged proteins may not reveal the behavior of the endogenous protein. Since a specific antibody directed against apple RIPs is available, the experiments can be performed to study the localization of RIPs directly on different apple tissues by immunostaining.

7.5 Antifungal, antiviral and insecticidal properties of RIPs from apple

Most plant pathogens (fungi, bacteria and viruses) infect the plant tissue through intercellular spaces, which allows fast spreading of the pathogen. Plants produce various defense proteins in the intercellular space. Except for the basic PR proteins predominantly located in the vacuole, most acidic PR proteins are located in the intercellular space (Ng, 2004, Ebrahim et al., 2011). Many RIPs have also been reported as plant defense proteins accumulating in the intercellular space, such as PAP, ricin and saporin. Apple type 2 RIP is secreted into the extracellular apoplastic

space (**chapter 3**), which is in good agreement with its involvement in plant defense. Nevertheless, further research is needed to elucidate the physiological roles of apple RIPs (fruit RIPs) in the plant response to stress treatments and to investigate their application for plant improvement.

7.5.1 Antifungal activity of apple RIPs

Type 1 and Type 2 RIPs from apple showed antifungal activity when detached transgenic tobacco leaves were tested with the necrotrophic pathogenic *B. cinerea* (**chapter 4**). A hypothesis to define the function of apple RIPs was hypothesized as described in Fig. 7.2. The antifungal activity of RIPs is less potent compared to other antifungal proteins as described in chapter 1 (Ng, 2004, Nielsen and Boston, 2001). Nevertheless, the antifungal activity of apple RIPs can still be useful in plant defense and crop protection. The plant immune responses can be triggered by the infection of plant pathogens, both by biotrophs and necrotrophs. All the responses (biochemical, cellular and molecular events…) have one main goal, namely to limit the proliferation of the pathogens (Wen, 2013). The hypothesized mechanisms to explain the mode of action of RIPs on fungi are either to directly inactivate ribosomes from fungi (Krivdova et al., 2014) or to up-regulate endogenous host plant defenses (e.g. secondary metabolites, hormones and antimicrobial peptides). Many RIPs show the ability to depurinate fungal ribosomes, e.g. curcin 2 (a type 1 RIP from *Jatropha curcas*). To determine whether the RIP concentration is a factor determining the higher antifungal activity of the type 2 RIP, it would be nice to calculate the correlation between the antifungal activity and RIP expression in the future. Furthermore, the germination and development of Botrytis spores was clearly inhibited after incubation with 100 ng recombinant apple type 1 or type 2 RIPs in an *in vitro* antifungal assay (Fig. 4.5). A quantitative bioassay is necessary to gain better knowledge of the activity of the RIPs against fungi. For instance, experiments whereby the same concentration of recombinant type 1 or type 2 RIP is incubated with the fungus will allow to determine which protein has the highest antifungal activity. Investigation of the depurination activity of apple RIPs on fungal ribosomes can be considered in future studies. Furthermore, the contribution of other plant defense related compounds should be analyzed. Moreover, it would also be interesting to check whether the expression of apple RIPs can induce the expression of pathogenesis-related genes, which can be determined by analysis of the transcript levels of PR protein genes in transgenic plants attacked by pathogens or insects.
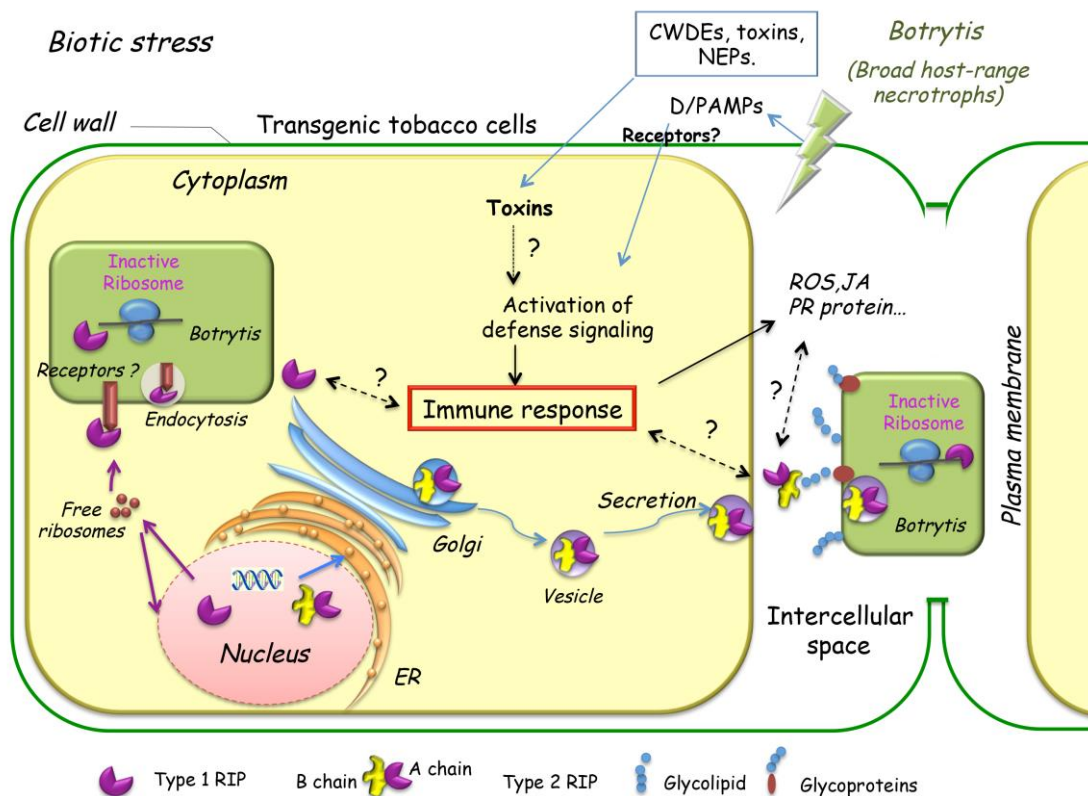
Figure 7.2 Schematic overview of the infection process of *Botrytis cinerea* on transgenic tobacco plants expressing RIPs from apple. *B. cinerea* (broad host-range necrotroph) produces diverse D/PAMPs that activate plant immune responses as well as virulence factors that suppress immune response (Mengiste, 2012). This scheme illustrates how the type 2 RIP from apple could be involved in plant defense. D/PAMPs, damage/pathogen-associated molecular patterns. NEPs, necrosis and ethylene-inducing proteins. CWDEs, cell wall-degrading enzymes. The cells and organelles are not drawn to scale. Only organelles relevant to the results of this study are shown.

The interaction of pathogens with the plant cell surface is an important step for the pathogens to get access to the intercellular space. It can be envisaged that type 2 RIPs might also enter the pathogens after binding of the lectin chain to the glycoconjugates on the surface. Although there is no information about the glycan structures on Botrytis, research confirmed there many carbohydrates are present on the surface of pathogens. For instance, lactose and galactose were detected on *Aspergillus nidulans* (Fekete et al., 2008). The surface glycans of *Candida albicans* consist of glucan (D-glucose polymer with glycosidic bonds), mannan (mannose polymers), chitin and sialic acids (Masuoka, 2004, Soares, 2000). Furthermore, sialic acids have been found in the cell wall of some plant pathogens, such as *Ascocalyx abietina* (Benhamou and Ouellette, 1986) and *Aspergillus fumigatus* (Warwas et al., 2007), and therefore these pathogens possess potential target carbohydrates for the sialic acid binding apple RIP (**chapter 2**). Immediate adhesion of *Botrytis cinerea* was

not significantly influenced by lectins (concanavalin A, soybean agglutinin, *Lotus tetragonolobus* lectin, and *Ulex europaeus* lectin) (Doss et al., 1993).

Apple RIPs also showed antifungal activity *in vitro* by reducing the growth of hyphae (**chapter 4**). In contrast to the apple type 2 RIP, incubation of fungal spores with different concentrations of the recombinant B chain alone did not affect fungal spore germination and growth. This experiment suggests that the antifungal activity of the RIP was due to its enzymatic activity, and that the lectin chains probably only helped the RIP to enter the fungal cells. Since the glycan structure for *B. cinerea* are not known, it would be interesting to analyse the glycans present on the fungal surface and the glycosylation of the effector proteins. These analyses may provide new insights to elucidate the mechanism of RIPs in plant defense against fungi, or in interaction with fungi evading the host plant innate immunity.

7.5.2 Antiviral activity of apple RIPs

Transgenic tobacco plants overexpressing a type 1 RIP or a type 2 RIP from apple showed clear antiviral activity against TMV infection (**chapter 4**). It was reported that SNA-I, SNA-V and SNLRP were inactive on plant ribosomes, but, displayed *in vitro* depurination activity on TMV RNA (Vandenbussche et al., 2004b; Tejezo et al., 2015). These elderberry type 2 RIPs as well as SNAI' also showed good antiviral activity *in planta* (chen et al., 2002a). As described in chapter 1 (Fig. 1.4), three mechanisms are hypothesized to explain the antiviral activities of RIPs. To determine which mechanism is applicable to apple RIPs, the depurination activity of RIPs on tobacco ribosomes and TMV RNA should be tested. Furthermore, a study of the expression of PR proteins (e.g. PR1, PR2), regulation of SA and activities of some antioxidant enzymes (e.g. superoxide dismutase and catalase…) in these plants after viral infection can provide better insights for the antiviral activity of apple RIPs.

7.5.3 Insecticidal activity of apple RIPs

The artificial diet assay revealed the insecticidal activity of recombinant RIPs from apple on nymphs of *Acyrtosiphon pisum.* The type 2 RIP from apple was clearly more toxic to aphids compared to the type 1 RIP most probably due to its carbohydrate binding activity. It will also be interesting to study the effect apple RIPs on other important pest insects, such as piercing-sucking aphids (e.g. peach-potato aphid (*M. persicae*)) or biting-chewing lepidopteran caterpillars (e.g. beet armyworm (*S. exigua*)). The effects of apple RIPs on proliferation and adult survival should be

investigated by long-term experiments with transgenic tobacco plants. To complete the experiments, it will be interesting to investigate the effects of apple RIPs on pests in *planta*. For example, *Spodoptera exigua* can be fed on the transgenic tobacco plants expressing apple RIPs and the development from larvae to pupa can be investigated. The larval weight and larval growth can be measured to determine the effect of apple RIPs on insect development. Furthermore, larvae can be fed with fluorescently labeled proteins (e.g. FITC-RIPs) to determine the internalization of apple RIPs in insect cells.

7.6 Mode of action of elderberry RIPs on mammalian cells

Our results show that the cytotoxicity of elderberry RIPs is not solely determined by their inhibitory activity on protein translation. Interestingly, it was found that the accumulation of *S. nigra* proteins in the lysosomes might cause saturation and subsequent activation of alternative degradation pathways such as autophagy due to overloading of these organelles (Fig. 7.3) (**chapter 6**). In addition, an increase of autophagy was detected when cells were incubated in the presence of all *S. nigra* proteins, suggesting that these proteins provoke additional cell stress and cell death (Klionsky et al., 2012). The apoptosis induced by RIPs was documented well (**chapter 1**), only few RIPs were reported to show an autophagic cell death phenotype (e.g. curcin, Mohamed et al., 2014). It would be interesting to know more about the cell death pathway caused by the *S. nigra* RIPs. Some further experiments can be performed to study e.g. the DNA fragmentation in cells treated with RIPs, cell cycle distribution of cells (by flow cytometric analysis), generation of ROS (DCFH-DA dye and fluorescence detection), mitochondrial stress (mitochondrial membrane transition pore assay) and caspase activation (extrinsic-caspase-8/-10 or intrinsic-caspase-3/-9)...
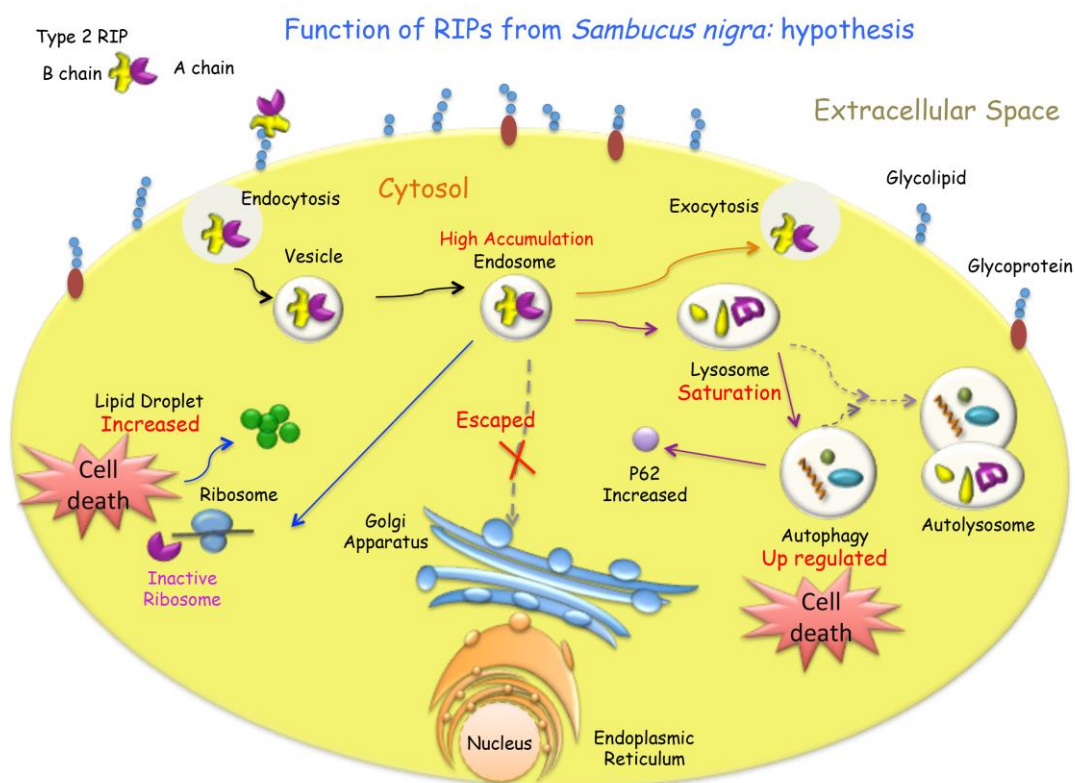
Figure 7.3 Hypothesis of cell death mechanism of RIPs from *S. nigra* in HeLa cells. The cells and organelles are not drawn to scale. Only organelles relevant to the results of this study are shown.

7.7 Final remarks

To conclude, research was performed to achieve some predefined objectives. This PhD research attempted to elucidate the physiological role and biological activities of ribosome-inactivating proteins from apple and elderberry. The recombinant type 1 and type 2 RIPs from apple were successfully characterized as functional RIPs possessing protein translation inhibition activity. The apple type 2 RIP is a chimeric protein with specificity for sialic acid and shows cytotoxicity towards mammalian cells (**Objective 1**). Our results have shown that the type 1 RIP is located in the cytoplasm and nucleus of the plant cell whereas the type 2 RIP is a secreted protein which is targeted to the apoplastic space. Furthermore, the type 2 RIP is especially abundant in the young tissues from the apple tree (**Objective 2**). Based on our results, it can be concluded that apple RIPs play an important role in plant defense against fungi, viruses and insects (**Objective 3**). The carbohydrate binding properties of the *S. nigra* lectins and type 2 RIPs have been investigated in detail by glycan array screening. Finally, the effects of *S. nigra* lectins and type 2 RIPs on mammalian cells indicated that HeLa cells are more susceptible to these proteins than NHDF cells. We showed that the enzymatic domain of the RIPs is not the only factor that determines

the cytotoxicity of the protein (**Objective 4**). Taken all these results together, we believe that this study contributed significantly to the understanding of the importance and biological activity of RIPs from apple and elderberry.

Summary

Ribosome-inactivating proteins are a family of proteins that damage ribosomes, which can be classically subdivided into two major groups: type 1 RIPs with enzymatic activity and type 2 RIPs consisting of a domain with enzymatic activity linked to a carbohydrate binding domain. Although RIP genes occur in bacteria, some fungi and invertebrates, most research was focused on RIPs from flowering plants. In the past, RIPs under study were abundant proteins that accumulated in storage tissues (barks, seeds and roots…) and hence could directly be purified from the plant materials. Furthermore, a lot of attention was given to the biological activities and possible applications of these RIPs in medicine (antiviral and anticancer therapy) and agriculture (plant defense against fungi, bacteria, viruses and insects).

The occurrence of protein homologs of some extremely toxic RIPs (such as e.g. ricin and abrin) in several food plants might be of concern with respect to food safety. In this PhD thesis, type 1 and type 2 RIPs originating from *Malus domestica* (apple) and type 2 RIPs as well as lectins from *Sambucus nigra* (elderberry) were chosen as study objects to investigate the biological activities of RIPs. It is interesting to check the cytotoxicity of especially the type 2 RIPs expressed in fruits. Furthermore, a detailed analysis of protein expression can give a lot of information on the specific role of these RIPs in the plant.

The type 1 and type 2 RIPs from apple were characterized and their cytotoxicity towards mammalian cells was investigated. Because of the low expression of RIPs in the apple tissues, the proteins were expressed recombinantly. Molecular cloning of the type 1 RIP and type 2 RIP sequences enabled the heterologous expression in *Pichia pastoris* and tobacco BY-2 cells. The recombinant type 1 RIP was purified using a combination of ion exchange chromatography and metal affinity chromatography. Similarly, the recombinant type 2 RIP was purified by a combination of hydrophobic interactions chromatography and affinity chromatography. Subsequently, a eukaryotic cell free translation system was used to show the effect(s) of the proteins on protein translation inhibition. Moreover, the analysis of a glycan array containing human glycans demonstrated that recombinant type 2 RIP from apple specifically recognizes carbohydrate structures containing sialic acid. The recombinant type 2 RIP showed cytotoxicity on both HeLa and NHDF cell lines, whereas the type 1 RIP demonstrated low cytotoxicity to mammalian cells.

To gain more insight on the expression of the proteins under study at cell and plant level, subcellular localization studies of apple RIPs were done using microscopy and analysis of RIP gene expression at transcript level was performed using qPCR

analysis. It was shown that the type 1 RIP fusion construct with EGFP yielded fluorescence in nucleus and the cytoplasm. These data were confirmed in different plant systems, such as the transient expression in *N. benthamiana* leaves, *Arabidopsis* suspension cells and *Arabidopsis* protoplasts, as well as the stable expression in *Arabidopsis* plants. Unlike the type 1 RIP, expression of the Type 2 RIP coupled with EGFP was detected in the ER and in vesicles, both in *Arabidopsis* suspension cells and in *Arabidopsis* protoplasts. Moreover, the type 2 RIP was also observed in the intercellular space from stably transformed *Arabidopsis* plants. Our data allowed to conclude that the type 2 RIP sequence which –unlike the type 1 RIP- contains with a signal peptide is synthesized following the secretory pathway. Furthermore, a quantitative analysis of the transcript levels of apple RIPs was performed in different tissues of an apple tree and throughout fruit development. Apple type 2 RIP transcripts accumulated at higher levels in young tissues (leaf buds, young leaves, unopened flower buds) and barks, and expression levels were low in the flower and the fruit. qPCR analysis did not allow to detect transcripts for the type 1 RIP from apple in any of the tissues tested.

In an attempt to determine the biological activities of RIPs from apple and their involvement in disease resistance, both apple RIPs were overexpressed in tobacco and the performance of the transgenic tobacco plants was investigated after infection with different plant pathogens. In addition, the recombinant RIPs purified in chapter 2 were tested in an artificial diet to study the insecticidal activity of the apple RIPs. The transgenic tobacco lines overexpressing type 1 and type 2 RIPs from apple were constructed and transformation of the lines was confirmed on RNA, DNA and protein level. A selection of the transgenic plants was used to investigate the effects of overexpression of the RIP genes on plant development and on their disease resistance to tobacco mosaic virus (TMV) and fungal (*Botrytis cinerea*) infection. Our results revealed that tobacco plants overexpressing apple RIPs showed clear antifungal activity after inoculation of *B. cinerea* conidial spores to detached leaves. Microscopic analysis indicated that the transgenic tobacco leaves inhibited the growth of the fungal hyphae at an early stage of development. The tobacco plants overexpressing the apple RIPs obviously also limited the disease spreading of TMV compared to wild type plants. Furthermore addition of the recombinant RIPs to an artificial diet revealed that the recombinant apple RIPs showed lethal effects on nymphal survival of *Acyrtosiphum pisum*.

The biological activities of the RIPs (SNA-I, SNA-V and SNLRP) and the lectins (SNA-II and SNA-IV) from *S. nigra* were investigated in detail. First the carbohydrate specificity of all *S. nigra* proteins was analyzed and compared in detail. Furthermore, the biological activity of several *S. nigra* proteins on different human cell lines was tested to study the cytotoxicity of the proteins. It was clearly shown that *S. nigra* proteins were more toxic to HeLa cells than to NHDF cells. Furthermore the data also suggest a much lower toxicity of the elderberry proteins than observed for the classical type 2 RIPs. The *in vitro* and *in vivo* protein synthesis inhibition activities of several *S. nigra* proteins indicated that type 2 RIPs from elderberry inhibit protein translation. The internalization and intracellular localization of the proteins showed clear differences among the elderberry proteins under study. These results probably relate to the differential binding and interaction of the elderberry proteins to glycans present on the cell surface due to the differences in carbohydrate binding specificity. Furthermore, glycan analysis (N- and O-glycans) of cell surface glycoproteins and glycolipids revealed a clear correlation with the results from cytotoxicity and internalization studies, indicating the importance of protein-carbohydrate interactions for the entry process of the proteins in the cell.

Throughout the PhD research, our knowledge of the biological activity of ribosome-inactivating proteins from apple and elderberry increased considerably. Obviously, apple RIPs are probably involved in plant defenses against several pathogens and insect predators. Nevertheless, more research is needed to confirm the physiological importance of RIPs from edible fruits. Ultimately this research might lead to applications in crop protection.

Samenvatting

Ribosoom-inactiverende proteïnen (kortweg RIP's) zijn een groep van eiwitten die, zoals hun naam doet vermoeden, ribosomen kunnen beschadigen. Deze enzymen worden ingedeeld in twee grote groepen. De eerste groep bevat de zogenaamde type 1 RIP's, welke zijn opgebouwd uit één enkel domein verantwoordelijk voor de enzymatische activiteit. De type 2 RIP's daarentegen beschikken naast dit enzymatisch domein over een tweede, koolhydraat bindend domein of lectine domein. Hoewel RIP genen voorkomen in bacteriën, sommige schimmels en invertebraten, zijn het vooral de RIP's uit zaadplanten waarnaar het meeste onderzoek gebeurt. Dit onderzoek focuste in het verleden vooral op RIP's die typisch in grote hoeveelheden voorkomen in opslagorganen (schors, zaden, wortels,...) en die bijgevolg zonder problemen uit de plantenweefsels konden opgezuiverd worden. Er werd veel aandacht besteed aan de biologische activiteit van deze eiwitten en hun mogelijke toepassingen in de geneeskunde (antivirale werking en gebruik in kankertherapie) en de landbouw (gewasbescherming tegen schimmels, bacteriële en virale pathogenen, insecten).

De aanwezigheid van homologen van enkele zeer toxische RIP's (zoals ricine en abrine) in voedingsgewassen is uiteraard van groot belang met betrekking tot voedselveiligheid. Type 1 en type 2 RIP's afkomstig uit appel (*Malus domestica*) en type 2 RIP's en enkele lectinen uit de vlier (*Sambucus nigra*) vormen het studieonderwerp van dit doctoraat. Het is interessant om de mogelijke cytotoxische eigenschappen van vooral de type 2 RIP's die voorkomen in fruit na te gaan. Daarnaast kan een gedetailleerde analyse van de eiwitexpressie ons meer leren over de functie die deze RIP's vervullen in de plant.

De type 1 en type 2 RIP uit appel werden gekarakteriseerd en hun cytotoxiciteit tegenover dierlijke cellen werd bepaald. Ten gevolge van het lage expressieniveau van deze eiwitten in verschillende weefsels van de appel/appelboom, dienden deze recombinant aangemaakt te worden. Met behulp van moleculaire klonering werd de heterologe expressie van de RIP's in *Pichia pastoris* en tabakscellen (BY-2) mogelijk gemaakt. Het recombinante type 1 RIP werd opgezuiverd door middel van een combinatie van ionuitwisselingschromatografie en metaal affiniteitschromatografie. Het type 2 RIP werd op een gelijkaardige manier opgezuiverd door gebruik te maken van een combinatie van hydrofobe interactie chromatografie en affiniteitschromatografie. Vervolgens werd het effect van deze recombinante RIP's op de eiwitsynthese bevestigd aan de hand van een celvrij *in vitro* translatiesysteem. Verder toonde een glycaan array analyse aan dat het type 2 RIP uit appel specifiek

siaalzuur-bevattende suikerstructuren herkent. Het recombinante type 2 RIP vertoonde cytotoxiciteit tegenover zowel HeLa cellen als NHDF cellen, terwijl het type 1 RIP slechts een lage cytotoxiciteit vertoonde tegenover dierlijke cellen.

Om een beter inzicht te verwerven in de expressie van de bestudeerde eiwitten, zowel op celniveau als op plantniveau, werden subcellulaire lokalisatiestudies uitgevoerd door middel van microscopie en aangevuld met qPCR analyses uitgevoerd om de RIP genexpressie in kaart te brengen. Er werd aangetoond dat een fusieconstruct waarbij het type 1 RIP gekoppeld werd aan eGFP aanleiding gaf tot een fluorescent signaal in de kern en het cytoplasma. Dit werd bevestigd in verschillende plantsystemen zoals transiënte expressie in *N. benthamiana* bladeren, *Arabidopsis* suspensieculturen en *Arabidopsis* protoplasten, alsook in stabiel getransformeerde *Arabidopsis* planten. In tegenstelling tot het type 1 RIP, werd expressie van het fusieconstruct van het type 2 RIP met eGFP gedetecteerd in het ER en in vesikels van zowel *Arabidopsis* suspensiecellen als *Arabidopsis* protoplasten. Daarnaast werd het type 2 RIP ook waargenomen in de intercellulaire ruimte van stabiel getransformeerde *Arabidopsis* planten. Gebaseerd op deze data werd geconcludeerd dat het type 2 RIP, dat in tegenstelling tot het type 1 RIP beschikt over een signaalpeptide, de secretorische pathway volgt. Verder werd ook een kwantitatieve analyse uitgevoerd van de transcriptniveaus van de appel RIP's in verschillende weefsels van een appelboom en doorheen de vruchtontwikkeling. Transcripts van het type 2 appel RIP bleken vooral abundant te zijn in jonge weefseltypes (bladknoppen, jonge bladeren, ongeopende bloemknoppen) en in schors, terwijl de expressie laag was in de bloem en de vrucht. Met behulp van qPCR was het niet mogelijk om expressie van het type 1 appel RIP te detecteren.

Om de biologische functie van de appel RIP's te achterhalen en hun mogelijke betrokkenheid in de plantafweer te onderzoeken, werden beide RIP's tot overexpressie gebracht in transgene tabaksplanten en de gevoeligheid van de overexpressielijnen tegen verschillende pathogenen werd onderzocht. Daarnaast werd ook de insecticidale werking van de RIP's getest door de opgezuiverde recombinante RIP's uit hoofdstuk 2 toe te voegen aan een artificieel dieet voor bladluizen. De transformatie van tabak voor de overexpressie van de type 1 en type 2 RIP's werd bevestigd op DNA, RNA en eiwitniveau. Een selectie van de transgene planten werd gebruikt om het effect van de overexpressie op de ontwikkeling van de plant en op de resistentie tegen het tabak mozaiekvirus (TMV) en tegen schimmelinfectie (*Botrytis cinerea*) te onderzoeken. Onze resultaten tonen aan dat

tabaksplanten die de appel RIP's tot overexpressie brengen duidelijke antifungale activiteit vertonen na de inoculatie van *B. cinerea* sporen op losse transgene tabaksbladeren. Uit microscopische analyse bleek dat de transgene tabaksbladeren de groei van de fungale hyfen in een vroeg stadium van ontwikkeling inhibeerden. Bij de tabaksplanten die de RIP's tot overexpressie brachten was de verspreiding van TMV duidelijk minder dan bij wild type planten. Het toevoegen van de recombinante RIP's aan een artificieel dieet onthulde dat de RIP's een letaal effect hadden op nymfen van *Acyrtosiphum pisum*.

De biologische activiteiten van de RIP's (SNA-I, SNA-V en SNLRP) en de lectinen (SNA-II en SNAIV) uit *S. nigra* werden in detail onderzocht. Allereerst werd de suikerspecificiteit van alle *S. nigra* proteïnen geanalyseerd en onderling vergeleken. Vervolgens werd de cytotoxiciteit van verschillende *S. nigra* eiwitten op verschillende humane cellijnen getest. Er werd duidelijk aangetoond dat de *S. nigra* eiwitten toxischer waren voor HeLa cellen dan voor NHDF cellen. Verder doen de data ook vermoeden dat de eiwitten van de vlier veel minder toxisch zijn dan waargenomen voor klassieke type 2 RIP's. Type 2 RIPs van de vlier waren in staat om de proteïnesynthese zowel *in vitro* als *in vivo* te inhiberen. Onder de bestudeerde proteïnen uit *S. nigra* waren er grote verschillen wat betreft hun internalisatie en intracellulaire lokalisatie in de HeLa cellen. Dit is hoogstwaarschijnlijk te verklaren door de verschillende suikerspecificiteit van de eiwitten waardoor deze met verschillende suikerstructuren aanwezig op het celoppervlak gaan interageren. Glycaan analysen (N- en O-glycanen) van glycoproteïnen op het celoppervlak onthulde dan ook een sterke correlatie tussen de resultaten van de cytotoxiciteitstesten en de internalisatiestudies, wat wijst op het belang van eiwit-koolhydraat interacties bij het binnentreden van de eiwitten in de cel.

Hoofdstuk 7 geeft een algemene discussie van de belangrijkste resultaten van dit doctoraat, alsook worden enkele perspectieven en ideeën voor toekomstige studies besproken. Doorheen deze doctoraatsstudie is onze kennis van de biologische activiteit van ribosoom-inactiverende proteïnen uit appel en vlier aanzienlijk toegenomen. De appel RIP's zijn hoogstwaarschijnlijk betrokken in de verdediging van de plant tegen verschillende pathogenen en insecten. Niettegenstaande is verder onderzoek nodig om de fysiologisch rol van RIP's in eetbare vruchten te bevestigen. Uiteindelijk kan dit onderzoek leiden tot toepassingen in gewasbescherming.

Reference list

Achuo, E. A., Audenaert, K., Meziane, H. and Höfte, M. (2004) The salicylic acid-dependent defense pathway is effective against different pathogens in tomato and tobacco. Plant Pathol. **53**, 65–72

Al Atalah, B., Fouquaert, E., Vanderschaeghe, D., Proost, P., Balzarini, J., Smith, D. F., Rougé, P., Lasanajak, Y., Callewaert, N. and Van Damme, E. J. M. (2011) Expression analysis of the nucleocytoplasmic lectin '*Orysata*' from rice in *Pichia pastoris*. FEBS J. **278**, 2064-79

Al Atalah, B., Vanderschaeghe, D., Bloch, Y., Proost, P., Plas, K., Callewaert, N., Savvides, S. N. and Van Damme, E. J. M (2014a) Characterization of a type D1A EUL-related lectin from rice expressed in *Pichia pastoris*. Biol. Chem. **395**, 413-424

Al Atalah, B., Smagghe, G. and Van Damme, E. J. M. (2014b) Orysata, a jacalin-related lectin from rice, could protect plants against biting-chewing and piercing-sucking insects. Plant Sci. **221–222**, 21–28

Alexander, J., Andersson, H. C., Bernhoft, A., Brimer, L., Cottrill, B., Fink-Gremmels, J., Galli, C. L., Grandjean, P., Gzyl, J., Heinemeyer, G., Johansson, N., Mutti, A., Schlatter, M., van Leeuwen, R., Van Peteghem, C. and Verger, P. (2008) Ricin (from *Ricinus communis*) as undesirable substances in animal feed: scientific opinion of the panel on contaminants in the food chain. The EFSA J. **726**, 1-38

Aoki, K., Perlman, M., Lim, J. M., Cantu, R., Wells, L. and Tiemeyer, M. (2007) Dynamic developmental elaboration of N-linked glycan complexity in the *Drosophila* melanogaster embryo. J. Biol. Chem. **282**, 9127-9142

Asselbergh, B., Curvers, K., Franca, S. C., Audenaert, K., Vuylsteke, M., Van Breusegem, F. and Höfte, M. (2007) Resistance to *Botrytis cinerea* in sitiens, an abscisic acid-deficient tomato mutant, involves timely production of hydrogen peroxide and cell wall modifications in the epidermis. Plant Physiol. **144**, 1863–1877

Audenaert, K., De Meyer, G. B. and Höfte M. (2002) Abscisic acid determines basal susceptibility of tomato to *Botrytis cinerea* and suppresses salicylic acid- dependent signaling mechanisms. Plant Physiol. **128**, 491–501

Bagga, S., Hosur, M. V. and Batra, J. K. (2003) Cytotoxicity of ribosome-inactivating protein saporin is not mediated through alpha2-macroglobulin receptor. FEBS Lett. **541**, 16–20

Barbieri, L., Aron, G. M., Irvin, J. D. and Stirpe, F. (1982) Purification and partial characterization of another form of the antiviral protein from the seeds of Phytolacca americana L. (pokeweed). Biochem. J. **203**, 55–59

Barbieri, L., Bolognesi, A., Cenini, P., Falasca, A. I., Minghetti, A., Garofano, L., Guicciardi, A., Lappi, D., Miller, S. P. and Stirpe, F. (1989) Ribosome-inactivating proteins from plant cells in culture. Biochem. J. **257**, 801–807

Barbieri, L., Battelli, M. G. and Stirpe, F. (1993) Ribosome- inactivating proteins from plants. Biochim. Biophys. Acta **1154**, 237-282

Barbieri, L., Valbonesi, P., Bonora, E., Gorini, P., Bolognesi, A. and Stirpe, F., (1997) Polynucleotide: adenosine glycosidase activity of ribosome-inactivating proteins: effect on DNA, RNA and poly (A). Nucleic Acids Res. **25**, 518-522

Barbieri, L., Valbonesi, P., Govoni, M., Pession, A., and Stirpe, F., (2000a) Polynucleotide: adenosine glycosidase activity of saporin-L1: effect on various forms of mammalian DNA. Biochim. Biophys. Acta **1480**, 258-266

Barbieri, L., Valbonesi, P., Righi, F., Zucceri, G., Monti, F., Gorini, P., Samori, B. and Stirpe, F. (2000b) Polynucleotide: Adenosine glycosidase is the sole activity of ribosome-inactivating proteins DNA. J. Biochem. **128**, 883–889

Barbieri, L., Ciani, M., Girbés, T., Liu, W., Van Damme, E. J. M., Peumans, W. J. and Stirpe, F. (2004) Enzymatic activity of toxic and non-toxic type 2 ribosome-inactivating proteins. FEBS Lett. **563**, 219-222

Barbieri, L., Polito, L., Bolognesi, A., Ciani, M., Pelosi, E., Farini, V., Jha, A. K., Sharma, N., Vivanco, J. M., Chambery, A., Parente, A. and Stirpe F. (2006) Ribosome-inactivating proteins in edible plants and purification and characterization of a new ribosome-inactivating protein from *Cucurbita moschata*. Biochim Biophys Acta **1760**, 783-792

Barnes, D. J., Baldwin, B. S. and Braasch, D. A. (2009) Ricin accumulation and degradation during castor seed development and late germination. Industrial Crops Products **30**, 254-258

Bass, H. W., Krawetz, J. E., Zinselmeier, C., Habben, J. E. and Boston, R. S. (2004) Maize ribosome-inactivating proteins (RIPs) with distinct expression patterns have similar requirements for proenzyme activation. J. Exp. Bot. **55**, 2219–2233

Battelli, M. G., Citores, L., Buonamici, L., Ferreras, J. M., de Benito, F. M., Stirpe, F. and Girbés, T. (1997a) Toxicity and cytotoxicity of nigrin b, a two-chain ribosome-inactivating protein from *Sambucus nigra*: Comparison with ricin. Arch. Toxicol. **71**, 360–364

Battelli, M. G., Barbieri, L., Bolognesi, A., Buonamici, L., Valbonesi, P., Polito, L., Van Damme, E. J. M., Peumans, W. J. and Stirpe. F. (1997b) Ribosome-inactivating lectins with polynucleotide: adenosine glycosidase activity. FEBS L. **408**, 355-359

Battelli, M. G., Musiani, S., Buonamici, L., Santi, S., Riccio, M., Maraldi, N. M., Girbés, T. and Stirpe, F. (2004) Interaction of volkensin with HeLa cells: Binding, uptake, intracellular localization, degradation and exocytosis. Cell Mol. Life Sci. **61**, 1975–1984

Bayer, H., Ey, N., Wattenberg, A., Voss, C. and Berger, M. R. (2012) Purification and characterization of riproximin from *Ximenia americana* fruit kernels. Protein Expr. Purif. **82**, 97-105

Becker, N. and Benhar, I. (2012) Antibody-based immunotoxins for the treatment of cancer. Antibodies **1**, 39-69

Bendtsen, J. D., Jensen, L. J., Blom, N., von Heijne, G. and Brunak, S. (2004) Feature-based prediction of non-classical and leaderless protein secretion. Protein Eng. Des. Sel. **17**, 349–356

Benhamou, N. and Ouellette, G. B. (1986) Ultrastructural localization of glycoconjugates in the fungus *Ascocalyx abietina*, the Scleroderris canker agent of conifers, using lectin-gold complexes. J. Histochem. Cytochem. **34**, 855-67

Berbee, M. L. and Taylor, J. W. (2010) Dating the molecular clock in fungi – how close are we? Fungal Biol. Rev. **24**, 1-16

Berger, S., Sinha, A. K. and Roitsch, T. (2007) Plant physiology meets phytopathology: plant primary metabolism and plant–pathogen interactions. J. Exp. Bot. **58**, 4019-4016

Bertholdo-Vargas, L. R., Martins, J. N., Bordin, D., Salvador, M., Schafer, A. E., Barros, N. M., Barbieri, L., Stirpe, F. and Carlini, C. R. (2009) Type 1 ribosome inactivating proteins entomotoxic, oxidative and genotoxic action on *Anticarsia gemmatalis* (Hubner) and *Spodoptera frugiperda* (J. E. Smith) (Lepidoptera, Noctuidae) J. Insect Physiol. **55**, 51–58

Bieri, S., Potrykus, I. and Fütterer, J. (2003) Effects of combined expression of antifungal barley seed proteins in transgenic wheat on powdery mildew infection. Mol. Breeding. **11**, 37-48

Bieri, S., Potrykus, I. and Fütterer, J. (2000) Expression of active barley seed ribosome-inactivating protein in transgenic wheat. Theor. Appl. Genet. **100**, 755-763

Bjørkøy, G., Lamark,T., Brech, A., Outzen, H., Perander, M., Øvervatn, A., Stenmark, H. and Johansen, T. (2005) p62/SQSTM1 forms protein aggregates degraded by autophagy and has a protective effect on huntingtin-induced cell death. J. Cell Biol. **171**, 605- 614

Blixt, O., Head, S., Mondala, T., Scanlan, C., Huflejt, M.E., Alvarez, R., Bryan, M. C., Fazio, F., Calarese, D., Stevens, J., Razi, N., Stevens, D. J., Skehel, J. J., Van Die, I., Burton, D. R., Wilson, I.A., Cummings, R., Bovin, N., Wong, C.H. and Paulson, J. C. (2004) Printed covalent glycan array for ligand profiling of diverse glycan binding proteins. Proc. Natl. Acad. Sci. U. S. A. **101**, 17033-17038

Bolognesi, A., Barbieri, L., Abbondanza, A., Falasca, A. I., Carnicelli, D., Battelli, M. G. and Stirpe, F. (1990) Purification and properties of new ribosome-inactivating proteins with RNA N-glycosidase activity. Biochim. Biophys. Acta **1087**, 293–302

Bolognesi, A., Polito, L., Olivieri, F., Valbonesi, P., Barbieri, L., Battelli, M. G., Carusi, M. V., Benvenuto, E., Del Vecchio Blanco, F., Di Maro, A., Parente, A., Di Loreto, M. and Stirpe, F. (1997) New ribosome-inactivating proteins with polynucleotide: adenosine glycosidase and antiviral activities from *Basella rubra* L. and *Bougainvillea spectabilis* Willd. Planta **203**, 422-429

Bolognesi, A., Polito, L., Lubelli, C., Barbieri, L., Battelli. M. G., Parente, A. and Stirpe, F. (2002) Ribosome-inactivating and adenine polynucleotide glycosylase activities in *Mirabilis jalapa* L. tissues. J. Biol. Chem. **277**, 13709-13716

Bolognesi, A., Polito, L., Scicchitano, V., Orrico, C., Pasquinelli, G., Musiani, S., Santi, S., Riccio, M., Bortolotti, M. and Battelli, M. G. (2012) Endocytosis and intracellular localisation of type 1 ribosome-inactivating protein saporin-s6. J. Biol. Regul. Homeost. Agents **26**, 97–109

Bolte, S. and Cordelières, F. P. (2006) A guided tour into subcellular colocalization analysis in light microscopy. J. Microsc. **224**, 213-232

Bora, N., Gadadhar, S. and Karande, A. A. (2010) Signaling different pathways of cell death: abrin induced programmed necrosis in U266B1 cells. Int. J. Biochem. Cell Biol. **42**, 1993-2003

Boscher, C., Dennis, J. W. and Nabi, I. R. (2011) Glycosylation, galectins and cellular signaling. Curr. Opin. Cell. Biol. **23**, 383-392

Bradford, M. M. (1976) A rapid and sensitive method for the quantitation of microgram quantities of protein utilizing the principle of protein–dye binding. Anal. Biochem. **72**, 248–254

Brandhorst, T., Dowd, P. F. and Kenealy, W. R. (1996) The ribosome-inactivating protein restriction deters insect feeding on *Aspergillus restrictus*. Microbiol-Sgm. **142**, 1551-1556

Brandizzi, F., Irons, S. L., Johansen, J., Kotzer, A. and Neumann, U. (2004) GFP is the way to glow: bioimaging of the plant endomembrane system. J. Microsc. **214**, 138–158

Broekaert, W. F., Nsimba-lubaki, M., Peeters, B. and Peumans, W. J. (1984) A lectin from elder (*Sambucus nigra* L.) bark. Biochem. J. **221**, 163-169

Broekaert, W. F., Terras, F. R. G., Cammue, B. P. A. and Vanderleyden, J. (1990) An automated quantitative assay for fungal growth inhibition. FEMS Microbiol. Lett. **69**, 55–60

Buntru, M., Vogel, S., Spiegel, H. and Schillberg, S. (2014) Tobacco BY-2 cell-free lysate: an alternative and highly-productive plant-based in vitro translation system. BMC Biotechnology **14**, 37-48

Butterworth, A.G. and Lord, J. M. (1983) Ricin and *Ricinus communis* agglutinin subunits are all derived from a single-size polypeptide precursor. Eur. J. Biochem. **137**, 57–65

Carlini, C. R. and Grossi-de-Sá, M. F. (2002) Plant toxic proteins with insecticidal properties. A review on their potentialities as bioinsecticides. Toxicon, **40**, 1515-1539

Carzaniga, R., Sinclair, L., Fordham-Skelton, A. P. Harris, N. and Croy, R. R. D. (1994) Cellular and subcellular distribution of saporins, type 1 ribosome-inactivating proteins in soapwort (*Saponaria officinalis* L.). Planta. **194**, 461-470

Ceriotti, A. and Roberts, L. M. (2006) Endoplasmic reticulum-associated protein degradation in plant cells. Robinson, D. G. (eds.) In *Plant Cell Monographs*: The Plant *Endoplasmic Reticulum* pp. 75–98. Springer-Verlag, Berlin/Heidelberg, Germany

Reference list

Ceroni, A., Maass, K., Geyer, H., Geyer, R., Dell, A. and Haslam, S. M. (2008) GlycoWorkbench: A tool for the computer-assisted annotation of mass spectra of glycans. J. Proteome Res. **7**, 1650-1659

Chan, W. Y., Wong, J. H. and Ng, T. Z. (2014) Embryotoxic and abortifacient activities of ribosome-inactivating proteins. Stirpe, F. and Lappi, D. A. (eds.) Ribosome-inactivating proteins: ricin and related proteins, pp. 270-280. Wiley Blackwell Press, NJ, USA

Chaudhry, B., Müller-Uri, F., Cameron-Mills, V., Gough, S., Simpson, D., Skriver, K. and Mundy, J. (1994) The barley 60 kDa jasmonate-induced protein (JIP60) is a novel ribosome-inactivating protein. Plant J. **6**, 815-824

Chen, H., Wang, Y., Yan, M. G., Yu, M. K. and Yao, Q. Z. (1996) The phosphatase activity of five ribosome-inactivating proteins. Chin. Biochem. J. **12**, 125-129

Chen, Y., Peumans, W. J. and Van Damme, E. J. M. (2002a) The *Sambucus nigra* type-2 ribosome-inactivating protein SNA-I' exhibits in planta antiviral activity in transgenic tobacco. FEBS Lett. **516**, 27-30

Chen, Y., Peumans, W. J., Hause, B., Bras, J., Kumar, M., Proost, P., Barre, A., Rougé, P. and Van Damme, E. J. M. (2002b) Jasmonic acid methyl ester induces the synthesis of a cytoplasmic/nuclear chito-oligosaccharide-binding lectin in tobacco leaves. FASEB J. **16**, 905–907

Chen, Y., Rougé, P., Peumans, W. J. and Van Damme, E. J. M. (2002c) Mutational analysis of carbohydrate-binding activity of the NeuAc(α-2,6)Gal/GalNAc-specific type 2 ribosome-inactivating protein from elderberry (*Sambucus nigra*) fruits. Biochem. J. **364**, 587-592

Chhikara, S., Chaudhury, D., Dhankher, O. P. and Jaiwal, P. K. (2012) Combined expression of a barley class II chitinase and type I ribosome inactivating protein in transgenic *Brassica juncea* provides protection against *Alternaria brassicae*. Plant Cell Tiss. Org. **108**, 83-89

Choquer, M., Fournier, E., Kunz, C., Levis, C., Pradier, J. M., Simon, A. and Viaud, M. (2007) *Botrytis cinerea* virulence factors: new insights into a necrotrophic and polyphageous pathogen *FEMS Microbiol. Lett.* **277**, 1–10

Chuang, W. P., Herde, M., Ray, S., Castano-Duque, L., Howe, G. A. and Luthe, D. S. (2014) Caterpillar attack triggers accumulation of the toxic maize protein RIP2. New Phytol. **201**, 928-939

Citores, L., Munoz, R., De Benito, F. M., Iglesias, R., Ferreras, J. M. and Girbes, T. (1996) Differential sensitivity of HELA cells to the type 2 ribosome-inactivating proteins ebulin l, nigrin b and nigrin f as compared with ricin. Cell. Mol. Biol. (Noisy-le-Grand, France) **42**, 473-476

Citores, L., de Benito, F. M., Iglesias, R., Ferreras, J. M., Argüeso, P., Jiménez, P., Méndez, E. and Girbés, T. (1998) Presence of polymerized and free forms of the non-toxic type 2 ribosome-inactivating protein ebulin and a structurally related new homodimeric lectin in fruits of *Sambucus ebulus* L.. Planta **204**, 310-317

Citores, L., Ferreras, J. M., Muñoz, R., Benítez, J., Jiménez, P. and Girbés, T. (2002) Targeting cancer cells with transferrin conjugates containing the non-toxic type 2 ribosome-inactivating proteins nigrin b or ebulin 1. Cancer Lett. **184**, 29-35

Citores, L., Munoz, R., Rojo, M. A., Jiménez, P., Ferreras, J. M. and Girbés, T. (2003) Evidence for distinct cellular internalization pathways of ricin and nigrin b. Cell. Mol. Biol. **49**, OL461–OL465

Clough, S. J. and Bent, A. F. (1998) Floral dip: a simplified method for Agrobacterium-mediated transformation of *Arabidopsis thaliana*. Plant J. **16**, 735–743

Corrado, G., Bovi, P. D., Ciliento, R., Gaudio, L., Di Maro, A., Aceto, S., Lorito, M. and Rao R. (2005) Inductible expression of a *Phytolacca heterotepala* ribosome-inactivating protein leads to enhanced resistance against major fungal pathogens in tobacco. Phytopathol. **95**, 206-215

Corrado, G., Scarpetta, M., Alioto, D., di Maro, A., Polito, L., Parente, A. and Rao, R. (2008) Inducible antiviral activity and rapid production of the Ribosome-Inactivating Protein I from *Phytolacca heterotepala* in tobacco. Plant Sci. **174**, 467–474

Coleman, W. H. and Roberts, W. K. (1981) Factor requirements for the tritin inactivation of animal cell ribosomes. Biochim. Biophys. Acta **654**, 57-66

Cummings, R. D. and Etzler, M. E. (2009) "R-type lectins,". Varki, E., Cummings, R. D., Esko, J. D., Freeze, H. H., Stanley, P. Bertozzi, C. R., Hart, G. W. and Etzler, M. E. (eds) Essentials of Glycobiology, 2nd Edn, Chapt 28, Cold Spring Harbor, Cold Spring Harbor Laboratory Press, NY, USA

Dang, L. and Van Damme, E.J.M. (2015) Toxic proteins in plants. Phytochemistry **117**, 51-64.

Dangl, J. L., Horvath, D. M. and Staskawicz, B. J. (2013). Pivoting the plant immune system from dissection to deployment. Science **341**, 746-751

Das, M. K., Sharma, R. S. and Mishra, V. (2012) Induction of apoptosis by ribosome inactivating proteins. Important of N-glycosidase activity. Appl. Biochem. Biotechnol. **166**, 1552-1561

Day, P. J., Lord, J. M. and Roberts, L. M. (1998) The deoxyribonuclease activity attributed to ribosome inactivating proteins is due to contamination. Eur. J. Biochem. **258**, 540–545

de Benito, F. M. Citores, L., Iglesias, R. Ferreras, M. Camafeita, E., Méndez, E. and Girbés, T. (1997) Isolation and partial characterization of a novel and uncommon two-chain 64-kDa ribosome-inactivating protein from the bark of elder (*Sambucus nigra* L.). FEBS Lett. **413**, 85-91

de Benito, F. M., Iglesias, R., Ferreras, J. M., Citores, L., Camafeita, E., Méndez, E. and Girbés, T. (1998) Constitutive and inducible type 1 ribosome-inactivating proteins (RIPs) in elderberry (*Sambucus nigra* L.). FEBS Lett. **428**, 75–79

Deeks, E. D., Cook, J. P., Day, P. J., Smith, D. C., Roberts, L. M. and Lord, J. M. (2002) The low lysine content of ricin A chain reduces the risk of proteolytic degradation after translocation from the endoplasmic reticulum to the cytosol. Biochem. **41**, 3405-3413

Delporte, A., De Vos, W. H. and Van Damme, E. J. M. (2014) *In vivo* interaction between the tobacco lectin and the core histone proteins. J. Plant Physiol. **171**, 1149-1156

De Marcos Lousa, C., Gerschlick D. C. and Denecke, J. (2012) Mechanisms and concepts paving the way towards a complete transport cycle of plant vacuolar sorting receptors. Plant Cell **24,** 1714-1732

Denecke, J., Aniento, F., Frigerio, L., Hawes, C., Hwang, I., Mathur, J., Neuhaus, J. M. and Robinson, D. G. (2012) Secretory pathway research: the more experimental systems the better. Plant Cell **24**, 1316-1326

Desmyter, S., Vandenbussche, F., Hao, Q., Proost, P., Peumans, W. J. and Van Damme, E. J. M. (2003) Type-1 ribosome-inactivating protein from *iris* bulbs: a useful agronomic tool to engineer virus resistance? Plant Mol. Biol. **51**, 567-576

de Virgilio, M., Lombardi, A., Caliandro, R. and Fabbrini, M. (2010) Ribosome-inactivating proteins: From plant defense to tumor attack. Toxins **2**, 2699-2737

De Vos, W. H., Van Neste, L., Dieriks, B., Joss, G. H. and Van Oostveldt, P. (2010) High content image cytometry in the context of subnuclear organization. Cytometry Part A **77A**, 64-75

Di Cola, A., Marcozzi, G. Balestrini, R. and Spanò, L. (1999) Localization of the type 1 ribosome-inactivating protein, luffin, in adult and embryonic tissues of *Luffa cylindrical* L. Roem. J. Exp. Bot. **50**, 573-579

Di Cola, A., Frigerio, L., Lord, J.M., Ceriotti, A. and Roberts, L.M. (2001) Ricin A chain without its partner B chain is degraded after retrotranslocation from the endoplasmic reticulum to the cytosol in plant cells. Proc. Natl Acad. Sci. USA **98**, 14726–14731

Di Cola, A., Frigerio, L., Lord, J. M., Roberts, L. M. and Ceriotti, A. (2005) Endoplasmic reticulum-associated degradation of ricin A chain has unique and plant-specific features. Plant Physiol. **137**, 287–296

Di Maro, A., Citores, L., Russo, R., Iglesias, R. and Ferreras, J. M. (2014) Sequence comparison and phylogenetic analysis by the maximum likelihood method of ribosome-inactivating proteins from angiosperms. Plant Mol. Biol. **85**, 575-588

Dodds, N. P. and Rathjen, J. P. (2010) Plant immunity: towards an integrated view of plant-pathogen interactions. Nature Rev. **11**, 539-548

Domashevskiy, A. V., Miyoshi, H. and Goss, D. J. (2012) Inhibition of pokeweed antiviral protein (PAP) by turnip mosaic virus genome-linked protein (VPg). J. Biol. Chem. **287**, 29729–29738

Domashevskiy, A. V. and Goss, D. J. (2015) Pokeweed antiviral protein, a ribosome inactivating protein: activity, inhibition and prospects. Toxins. **7**, 274-298

Dowd, P. F., Mehta, A. D. and Boston, R. S. (1998) Relative toxicity of the maize endosperm ribosome-inactivating protein to insects. J. Agricultural Food Chem. **46**, 3775-3779

Dowd, P. F., Zuo, W. N., Gillikin, J. W., Johnson, E. T. and Boston, R. S. (2003) Enhanced resistance to *Helicoverpa zea* in tobacco expressing an activated form of maize ribosome-inactivating protein. J. Agric. Food Chem. **51**, 3568–3574

Dowd, P. F., Johnson, E. T. and Price, N. P. (2012) Enhanced pest resistance of maize leaves expressing monocot crop plant-derived ribosome-inactivating protein and agglutinin. J. Agric. Food Chem. **60**, 10768-10775

Doss, R. P., Potter, S. W., Chastagner, G. A. and Christian, J. K. (1993) Adhesion of nongerminated *Botrytis cinerea* conidia to several substrata. Appl. Environ. Microbial. Applied. **59**, 1786-1791

Drakakaki, G. and Dandekar, A. (2013) Protein secretion: how many secretory routes does a plant cell have? Plant Sci. **203**, 74-8

Duggar, B. M. and Armstrong, J. K. (1925) The effect of treating the virus of tobacco mosaic with the juice of various plants. Annals of the Missouri Botanical Garden **12**, 359-366

Dunaeva, M., Goevel, C., Wasternack, C., Parthier, B. and Goerschen, E. (1999) The jasmonate-induced 60 kDa protein of barley exhibits N-glycosidase activity *in vitro*. FEBS Lett. **452**, 263-266

Duvet, S., Foulquier, F., Mir, A. M., Chirat, F. and Cacan, R. (2004) Discrimination between lumenal and cytosolic sites of deglycosylation in endoplasmic reticulum-associated degradation of glycoproteins by using benzyl mannose in CHO cell lines. Glycobiology **14**, 841-849.

Ebrahim, S. Usha, K. and Singh, B. (2011) Pathogenesis Related (PR) proteins in plant defense mechanism. pp 1043-1054. Méndez-Vilas, A. (eds) Science against microbial pathogens: communicating current research and technological advances. Formatex Research Center, Badajoz, Spain

Elmore, S. (2007) Apoptosis: a review of programmed cell death. Toxicol. Pathol. **35**, 495-516

Emanuelsson, O., Nielsen, H., Brunak S. and von Heijne. G. (2000) Predicting subcellular localization of proteins based on their N-terminal amino acid sequence. J. Mol. Biol. **300**, 1005-1016

Emmanuel, F., Turpin, E., Alfsen, A. and Frénoy, J. P. (1988) Separation of ricin A- and B-chains after dithiothreitol reduction. Anal. Biochem. **173**, 134-141

Endo, Y. (2014) Enzymology of the Ribosome-inactivating proteins. Stirpe, F. and Lappi, D. A. (eds.) Ribosome-inactivating proteins: ricin and related proteins, pp. 151-160. Wiley Blackwell Press, NJ, USA

Fang, E. F., Ng, T. B., Shaw, P. C. and Wong, R. N. (2011) Recent progress in medicinal investigations on trichosanthin and other ribosome-inactivating proteins. Curr. Med. Chem. **18**, 4410-4417

Febvay, G., Delobel, B. and Rahbé, Y. (1988) Influence of the amino acid balance on the improvement of an artificial diet for a biotype of *Acyrthosiphon pisum* (Homoptera:Aphididae). Can. J. Zool. **66**, 2449–2453

Fekete, E., Padra, J., Szentirmai, A. and Karaffa, L. (2008) Lactose and D-galactose catabolism in the filamentous fungus *Aspergillus nidulans*. Acta Microbiol. Immunol. Hung. **55**, 119-24.

Ferreras, J. M., Citores, L., Iglesias, R., Jiménez, P. and Girbés, T. (2010) *Sambucus* ribosome-inactivating proteins and lectins. (Lord, J.M., Hartley, M,R., Eds.), pp.122-123, Chapter 6. Toxic Plant Proteins, Plant Cell Monographs **18**, Springer-Verlag Berlin Heidelberg

Ferreras, J. M., Citores, L., Iglesias, R., Jiménez, P. and Girbés, T. (2011) Use of ribosome-inactivating proteins from *sambucus* for the construction of immunotoxins and conjugates for cancer therapy. Toxins **3**, 420-441

Feussner, I., Hause, B., Vörös, K., Parthier, B. and Wasternack, C. (1995) Jasmonate-induced lipoxygenase forms are localized in chloroplasts of barley leaves (*Hordeum vulgare* cv. Salome). Plant J. **7**, 949-957

Foster, T., Kirk, C., Jones, W. T., Allan, A. C., Espley, R., Karunairetnam, S. and Rakonjac, J. (2006) Characterisation of the DELLA subfamily in apple (*Malus x domestica* Borkh.). Tree Genetics & Genomes **3**, 187-197

Fouquaert, E., Hanton, S. L., Brandizzi, F., Peumans, W. J. and Van Damme. E. J. M. (2007) Localization and topogenesis studies of cytoplasmic and vacuolar homologs of the *Galanthus nivalis* agglutinin. Plant Cell Physiol. **48**, 1010–1021

Fracasso, G., Stirpe, F. and Colombatti, M. (2010) Ribosome-inactivating protein-containing conjugates for therapeutic use, in Lord, J. M. and Hartley, M. R. (Eds.), Toxic Plant Proteins. pp. 225-263.Springer Berlin Heidelberg, Germany.

Freeman, B. C. and Beattie, G. A. (2008) An overview of plant defenses against pathogens and herbivores. The Plant Health Instructor. DOI: 10.1094/PHI-I-2008-0226-01

Frigerio, L. and Roberts, L. M. (1998) The enemy within: Ricin and plant cells. J. Exp. Bot. **49**, 1473-1480

Frigerio, L., Jolliffe, N. A., Cola, A. D., Felipe, D. H., Paris, N., Neuhaus, J. M., Lord, J. M., Ceriotti, A. and Roberts, L. M. (2001) The internal propeptide of the ricin precursor carries a sequence-specific determinant for vacuolar sorting. Plant Physiol. **126**, 167–175

Fu, L. L., Zhou, C. C., Yao, S., Yu, J. Y., Liu, B. and Bao, J. K. (2011) Plant lectins: targeting programmed cell death pathways as antitumor agents. Int. J. Biochem. Cell Biol. **43**, 1442-1449

Gadadhar, S. and Karande, A. A. (2013) Abrin immunotoxin: targeted cytotoxicity and intracellular trafficking pathway. PLoS One **8**, e58304-e58319

Galvez, L. C., Banerjee, J., Pinar, H. and Mitra, A. (2014) Engineered plant virus resistance. Plant Sci. **228**, 11-25

Gareth, D. G. (2014) Ribosome-inactivating proteins: Pathology from cells to organs. Stirpe, F. and Lappi, D. A. (eds.) Ribosome-inactivating proteins: ricin and related proteins, pp. 179-198. Wiley Blackwell Press, NJ, USA

Gatehouse, A. M. R., Barbieri, L., Stirpe, F. and Croy, R. R. D. (1990) Effects of ribosome inactivating proteins on insect development differences between lepidoptera and coleoptera. Entomol. Exper. Appl. **54**, 43-51

Gilabert-Oriol, R., Weng, A., von Mallinckrodt, B., Melzig, M. F., Fuchs, H. and Thakur, M., (2014) Immunotoxins constructed with ribosome-inactivating proteins and their enhancers: a lethal cocktail with tumor specific efficacy. Curr. Pharm. Des. **20**, 6584-6643

Girbés, T., Ferreras, J. M., Arias, F. J., Muñoz R., Iglesias, R., Jimenez, P., Rojo, M. A., Arias, Y., Perez, Y., Benitez, J., Sanchez, D. and Gayoso, M. J. (2003) Non-toxic type 2 ribosome-inactivating proteins (RIPs) from Sambucus: occurrence, cellular and molecular activities and potential uses. Cell. Mol. Biol. **49**, 537-545

Girbés, T., Ferreras, J. M. Arias, F. J and Stirpe, F. (2004) Description, distribution, activity and phylogenetic relationship of ribosome-inactivating proteins in plants, fungi and bacteria. Mini Rev. Med. Chem. **4**, 461-476

Glazebrook, J. (2005) Contrasting mechanisms of defense against biotrophic and necrotrophic pathogens. Annu. Rev. Phytophatol. **43**, 205-227

Greenwood, J. S., Stinissen, H. M., Peumans, W. J. and Chrispeels, M. J. (1986) *Sambucus nigra* agglutinin is located in protein bodies in the phloem parenchyma of the bark. Planta **167**, 275-278

Griffiths, G. D. (2014) The potential for misuse of ribosome-inactivating proteins. Stirpe, F. and Lappi, D. A. (eds.) Ribosome-inactivating proteins: ricin and related proteins, pp. 281-286. Wiley Blackwell Press, NJ, USA

Hao, Q., Van Damme, E. J. M., Hause, B., Barre, A., Chen, Y., Rougé, P. and Peumans, W. J. (2001) *Iris* bulbs express type 1 and type 2 ribosome-inactivating proteins with unusual properties. Plant Physiol. **125**, 866-76

Harrison, S. J., Mott, E. K., Parsley, K., Aspinall, S., Gray, J. C. and Cottage A. (2006) A rapid and robust method of identifying transformed *Arabidopsis thaliana* seedlings following floral dip transformation. Plant Methods **2**, 19-26

Hazes, B. (1996) The $(QxW)_3$ domain: A flexible lectin scaffold. Protein Sci. **5**, 1490-1501

He, X., Gao, L. and Ma, N. (2013) One-step instant synthesis of protein-conjugated quantum dots at room temperature. Sci. Rep. **3**, 2825-2836

Hellemans, J., Mortier, G., De Paepe, A., Speleman, F. and Vandesompele, J. (2007) qBase relative quantification framework and software for management and automated analysis of real-time quantitative PCR data. Genome Biol. **8**, R19-33

Helmy, M., Lombard, S. and Pieroni, G. (1999) Ricin RCA60: evidence of its phospholipase activity. Biochem. Biophys. Res. Commun. **258**, 252-255

Hiraiwa, N., Kondo, M., Nishimura, M. and Hara-Nishimura, I. (1997) An aspartic endopeptidase is involved in the breakdown of propeptides from storage proteins in protein storage vacuoles of plants. Eur. J. Biochem. **246**, 133–141

Hoekema, A., Hirsch, P. and Hooykass, P. P. (1983) A binary plant vector strategy based on separation of the vir and TDNA regions of the *Agrobacterium tumefaciens* Ti plasmid. Nature **303**, 179–180

Hong, Y., Saunder, K., Hartley, M. R. and Stanley, J. (1996) Resistance to geminivirus infection by virus-indeced expression of dianthin in transgenic plants. Virology **220**, 119-127

Honjo, E., Dong, D., Motoshima, H. and Watanabe, K. (2002) Genomic clones encoding two isoforms of pokeweed antiviral protein in seeds (PAP-S1 and S2) and the N-glycosidase activities of their recombinant proteins on ribosomes and DNA in comparison with other isoforms. J. Biochem. **131**, 225–231

Horsch, R. B., Fry, J. E., Hoffmann, N. L., Eichholtz, D., Rogers, S. G. and Fraley, R. T. (1985) A simple and general method for transferring genes into plants. Science **227**, 1229–1231

Howe, G. A. and Jander, G. (2008) Plant immunity to insect herbivores. Annu. Rev. Plant Biol. **59**, 41–66

Hu, D., Tateno, H., Kuno, A., Yabe, R. and Hirabayashi, J. (2012) Directed evolution of lectins with sugar-binding specificity for 6-sulfogalactose. J. Biol. Chem. **287**, 20313–20320

Huang, H., Hou, H., Wei, Q., Xu Y. and Chen F. (2008) A ribosome-inactivating protein (curin 2) induced from *Jatropha curcas* can reduce viral and fungal infection in transgenic tobacco. Plant Growth. Reg. **54**, 115-123

Hudak, K. A., Wang, P. and Tumer, N. E. (2000a) A novel mechanism for inhibition of translation by pokeweed antiviral protein: Depurination of the capped RNA template. RNA **6**, 369–380

Hudak, K. A., Wang, P. and Tumer, N. E. (2000b) Pokeweed antiviral protein inhibits translation of capped RNAs independently of ribosome depuration by acting directly on the RNA template. Nucleic Acids Res. **34**, 1174–1181

Hudak, K. A., Bauman, J. D. and Tumer, N. E. (2002) Pokeweek antiviral protein binds to the cap structure of eukaryotic mRNA and depurinates the mRNA downstream of the cap. RNA. **8**, 1148-1159

Hur, Y., Hwang, D. J., Zoubenko, O., Coetzer, C., Uckun, F. H. and Tumer, N. E. (1995). Isolation and characterization of pokeweed antiviral protein mutations in *Saccharomyces cerevisiae*: identification of residues important for toxicity. Proc. Natl. Acad. Sci. USA **92**, 8448–8452

Iglesias, R., Pérez, Y., de Torre, C., Ferreras, J. M., Antolín, P., Jiménez, P., Rojo, M. Á., Méndez, E. and Girbés, T. (2005) Molecular characterization and systemic induction of single-chain ribosome-inactivating proteins (RIPs) in sugar beet (Beta vulgaris) leaves. J. Exp. Bot. **56**, 1675-1684

Iglesias, R., Pérez, Y., Citores, L., Ferreras, J. M., Méndez, E. and Girbés, T. (2008) Elicitor-dependent expression of the ribosome-inactivating protein beetin is developmentally regulated. J. Exp. Bot. **59**, 1215-1223

Ikawatti, Z., Widyaningshi Elly, S., Puspitasari, D. and Sismindari (2003) Induction of apoptosis by protein fraction isolated from the leaves of *Mirabilis jalapa* L. on HeLa and Raji cell line. Oriental Pham. Exp. Med. **3**, 151-156

Ippoliti, R. and Fabbrin, S. (2014) A long journey to the cytosol: what do we know about entry of type 1 RIPs inside a mammalian cells? Stirpe, F. and Lappi, D. A. (eds.) Ribosome-inactivating proteins: ricin and related proteins, pp. 161-177. Wiley Blackwell Press, NJ, USA

Irvin, J. D. and Uckun, F. M. (1992) Pokeweed antiviral protein: Ribosome inactivation and therapeutic applications. Pharmacol. Ther. **55,** 279–302

Ishizaki, T., Megumi, C., Komai, F., Masuda, K. and Oosawa, K. (2002) Accumulation of a 31-kDa glycoprotein in association with the expression of embryogenic potential by spinach *callus* in culture. Physiol. Plant. **114**, 109–115

Jang-Lee, J., North, S. J., Sutton-Smith, M., Goldberg, D., Panico, M., Morris, H., Haslam, S. M. and Dell, A. (2006) Glycomic profiling of cells and tissues by mass spectrometry: fingerprinting and sequencing methodologies. Meth. Enzymol. **415**, 59-86.

Jia, N., Barclay, W. S., Roberts, K., Yen, H. L., Chan, R. W., Lam, A. K., Air, G., Peiris, J. M., Dell, A., Nicholls, J. M. and Haslam, S. M. (2014) Glycomic characterisation of respiratory tract tissues of ferrets: implications for its use in influenza virus infection studies. J. Biol. Chem. **289**, 28489-28504

Jiang, S. Y., Ramamoorthy, R., Bhalla, R., Luan, H. F., Venkatesh, P. N., Cai, M. and Ramachandran, S. (2008) Genome-wide survey of the RIP domain family in Oryza sativa and their expression profiles under various abiotic and biotic stresses. Plant Mol. Biol. **67**, 603-614

Jiang, S. Y., Bhalla, R., Ramamoorthy, R., Luan, H. F., Venkatesh, P. N., Cai, M. and Ramachandran, S. (2012) Over- expression of OSRIP18 increases drought and salt tolerance in transgenic rice plants. Transgenic Res. **21**, 785-795

Jiménez, A. Z., Gressette, M., Barjon, C., Wei, M., Gourzones, C. and Busson, P. (2011) Rapid obtention of stable, bioluminescent tumor cell lines using a tCD2-luciferase chimeric construct. BMC Biol. **11**, 26-35

Jiménez, P., Gayoso, M. J. and Girbés, T. (2014) Non-toxic type 2 ribosome-inactivating proteins. Stirpe, F. and Lappi, D. A. (eds.) Ribosome-inactivating proteins: ricin and related proteins, pp. 67-82. Wiley Blackwell Press, NJ, USA

Jolliffe, N. A., Ceriotti, A., Frigerio, L. and Roberts, L. M. (2003) The position of the proricin vacuolar targeting signal is functionally important. Plant Mol. Biol. **51**, 631-641

Kadirvelraj, R., Grant, O. C., Goldstein, I. J., Winter, H. C., Tateno, H., Fadda, E. and Woods, R. J. (2011) Structure and binding analysis of *Polyporus squamosus* lectin in complex with the Neu5Acα2-6 Galβ1-4GlcNAc human-type influenza receptor. Glycobiology **21**, 973-984

Kageyama, A., Kusano, I., Tamura, T., Oda, T. and Muramatsu, T. (2002) Comparison of the apoptosis- inducing abilities of various protein synthesis inhibitors in U937 cells. Biosci. Biotechnol. Biochem. **66**, 835-839

Käll, L., Krogh, A. and Sonnhammer, E. L. L. (2007) A combined transmembrane topology and signal peptide prediction method. J. Mol. Biol. **338**, 1027-1036

Kanzaki, H., Nirasawa, S., Saitoh, H., Nishihara, M. I. M., Terauchi, R. and Nakamura, I. (2002) Overexpression of the wasabi defensin gene confers enhanced resistance to blast fungus (*Magnaporthe grisea*) in transgenic rice. Theor. Appl. Genet. **105**, 809–814

Kaku, H., Peumans, W. J. and Goldstein, I. J. (1990) Isolation and characterization of a second lectin (SNA-II) present in elderberry (*Sambucus nigra* L.) bark. Arch. Biochem. Biophys. **277**, 255-262

Kaku, H., Kaneko, H., Minamihara, N., Iwata, K., Jordan, E. T., Rojo, M. A., Minami-Ishii, N., Minami, E., Hisajima, S. and Shibuya, N. (2007) Elderberry bark lectins evolved to recognize Neu5Acα2,6Gal/GalNAc sequence from a Gal/GalNAc binding lectin through the substitution of amino-acid residues critical for the binding to sialic acid. Biochem. J. **142**, 393-401

Karimi, M., Inzé, D. and Depicker, A. (2002) GATEWAY^{TM} vectors for *Agrobacterium*-mediated plant transformation. Trends Plant Sci. **7**, 193–195

Kazan, K. and Manners, J. M. (2012) JAZ repressors and the orchestration of phytohormone crosstalk. Trends Plant Sic. **17**, 22-31

Kim, I., Xu, W. and Reed, J. C. (2008) Cell death and endoplasmic reticulum stress: disease relevance and therapeutic opportunities. Nat. Rev. Drug Discov. **7**, 1013–1030

Kim, Y. and Robertus, J. D. (1992) Analysis of several key active site residues of ricin A chain by mutagenesis and X-ray crystallography. Protein Eng. **5**, 775-779

Kimura, S., Noda, T. and Yoshimori, T. (2007) Dissection of the autophagosome maturation processby a novel reporter protein, tandem fluorescent-tagged LC3. Autophagy **3**, 452-460

Klionsky, D. J. (2007) Autophagy: from phenomenology to molecular understanding in less than a decade. Nat. Rev. Mol. Cell Biol. **8**, 931-937

Klionsky, D. J. et al. (2012) Guidelines for the use and interpretation of assays for monitoring autophagy. Autophagy **8**, 445–544

Krawetz, J. E. and Boston, R. S., (2000) Substrate specificity of a maize ribosome-inactivating protein differs across diverse taxa. Eur. J. Biochem. **267**, 1966-1974

Kreb, H. and Warburg, O. (1981) Cell physiologist, biochemist and eccentric. Oxford: Clarendon Press, **47**.

Kreitman, R. J. (2006) Immunotoxins for targeted cancer therapy. AAPS J. **8**, e532-E551

Krivdova, G., Neller, K. C. M., Parikh, B. A. and Hudak, K. (2014) Antiviral and antifungal properties of RIPs. **Stirpe, F. and Lappi, D. A.** (eds.) Ribosome-inactivating proteins: ricin and related proteins, pp. 198-211. Wiley Blackwell Press, NJ, USA

Krivdova, G., Neller, K. C. M., Parikh, B. A. and Hudak, K. (2014) Antiviral and antifungal properties of RIPs. Stirpe, F. and Lappi, D. A. (eds.) Ribosome-inactivating proteins: ricin and related proteins, pp. 198-211. Wiley Blackwell Press, NJ, USA

Kumar, M. A., Timm, D. E., Neet, K. E., Owen, W. G., Peumans, W. J. and Rao, A. G. (1993) Characterization of the lectin from the bulbs of *Eranthis hyemalis* (winter aconite) as an inhibitor of protein synthesis. J. Biol. Chem. **268**, 25176-25183

Kurinov, I.V. and Uckun, F.M. (2003) High resolution X-ray structure of potent anti-HIV pokeweed antiviral protein-III. Biochem. Pharmacol. **65,** 1709–1717

Lacadena, J., Alvarez-García, E., Carreras-Sangrà, N., Herrero-Galán, E., Alegre-Cebollada, J., García-Ortega, L., Oñaderra, M., Gavilanes, J. G. and Martínez del Pozo, A. (2007) Fungal ribotoxins: molecular dissection of a family of natural killers. FEMS Microbiol. Rev. **31**, 212-37

Lam, Y. H., Wong, B., Wang, R. N. S., Yeung, H. W. and Shaw, P. C. (1996) Use of trichosanthin to reduce infection by turnip mosaic virus. Plant Sci. **114**, 111-117

Lam, S. K. and Ng, T. B. (2001a) Hypsin, a novel thermostable ribosome-inactivating protein with antifungal and antiproliferative activities from fruiting bodies of the edible mushroom *Hypsizigus marmoreus*. Biochem. Biophys. Res. Commun. **285**, 1071-1075

Lam, S. K. and Ng, T. B. (2001b) First simultaneous isolation of a ribosome inactivating protein and an antifungal protein from a mushroom (*Lyophyllum shimeji*) together with evidence for synergism of their antifungal effects. Arch. Biochem. Biophys. **393**, 271-280

Landry, J. J., Pyl, P. T., Rausch, T., Zichner, T., Tekkedil, M. M., Stütz, A, M, Jauch, A., Aiyar, R. S., Pau, G., Delhomme, N., Gagneur, J., Korbel, J. O., Huber, W. and Steinmetz, L. M. (2013) The genomic and transcriptomic landscape of a HeLa cell line. G3(Bethesda). **3**, 1213-1224

Lannoo, N., Vervecken, W., Proost, P., Rougé, P. and Van Damme, E. J. M. (2007) Expression of the nucleocytoplasmic tobacco lectin in the yeast *Pichia pastoris*. Protein Expr. Purif. **53**, 275–282

Lannoo, N. and Van Damme, E. J. M. (2014) Lectin domains at the frontiers of plants defense. Front. Plant Sci. **5**, 397

Lanzanova, C. Torri, A., Motto, M. and Balconi, C. (2011) Characterization of the maize b-32 ribosome inactivating protein and its interaction with fungal pathogen development. Maydica. **14**, 164-172

Lanzanova, C., Giuffrida, M. G., Motto, M., Baro, C., Donn, G., Hartings, H., Lupotto, E., Careri, M., Elviri, L. and Balconi, C. (2009) The *Zea mays* b-32 ribosome-inactivating protein efficiently inhibits growth of *Fusarium verticillioides* on leaf pieces *in vitro*. Eur. J. Plant Pathol. **124**, 471-482

Lapadula, W. J., Puerta, M. V. S. and Ayub, M. J. (2013) Revising the taxonomic distribution, origin and evolution of ribosome inactivating protein genes. PLoS One **8**, e72825

Leah, R., Tommerup, H., Svendsen, I. and Mundy, J. (1991) Biochemical and molecular characterization of 3 barley seed proteins with antifungal properties. J. Biol. Chem. **266**, 1564-1573

Lei, H. Y. and Chang, C. P. (2009). Lectin of Concanavalin A as an anti-hepatoma therapeutic agent. J. Biomed. Sci. **16**, 10-1186

Lev-Yadun, S. and Halpern, M. (2008) External and internal spines in plants insert pathogenic microorganisms into herbivore's tissues for defence. Van Dijk, T. (eds) Microbial ecology research trends, pp. 155-168. Nova Science Publishers, NY, USA

Li, J., Gu, L., Aach, J., and Church, G. M. (2014) Improved cell-free RNA and protein synthesis system. PLoS Once **9**, e106232-e106243

Li, X. D., Liu, W. Y. and Niu, C. L. (1996) Purification of a new ribosome-inactivating protein from the seeds of *Cinnamomum porrectum* and characterization of the RNA N-glycosidase activity of the toxic protein. Biol. Chem. **377**, 825-831

Liao, P., Liu, W., Li, H., Gao, H., Wang, H., Li, N., Xu, N., Li, J., Wan, J., Liu, L. and Sun, Y. (2012) Morphological changes of ricin toxin-induced apoptosis in human cervical caner cells. Toxicol. Ind. Health. **28**, 439-448

Lichtenstein, R. G. and Rabinovich, G. A. (2013) Glycobiology of cell death: when glycans and lectins govern cell fate. Cell Death Differ. **20**, 976–986

Liu, B., Bian, H. J. and Bao, J. K. (2010) Plant lectins: potential antineoplastic drugs from bench to clinic. Cancer Lett. **287**, 1-12

Lorberboum-Galski, H. (2011) Human toxin-based recombinant immunotoxins/chimeric proteins as a drug delivery system for targeted treatment of human diseases. Expert Opin. Drug Delivery. **8**, 605-621

Lord, J. M. and Roberts, L. N. M. (1998) Toxin entry: retrograde transport through the secretory pathway. J. Cell Biol. **140**, 733–736

Lord, J. M., Roberts, L. M. and Lencer, W. I. (2005) Entry of protein toxins into mammalian cells by crossing the endoplasmic reticulum membrane: Co-opting basic mechanisms of endoplasmic reticulum-associated degradation. Curr. Top. Microbiol. Immunol. **300**, 149–168

Lord, J. M. and Hartley, M. R. (Eds.) (2010) Toxic Plant Proteins. Springer Berlin Heidelberg, Germany.

Lodge, J. K., Kaniewski, W. K. and Tumer, N. E. (1993) Broad-specrum virus resistance in transgenic plants expressing pokeweed antiviral protein. Pro. Natl. Acad. Sci. USA **90**, 7089-7093

Lombardi, A., Bursomanno, S., Lopardo, T., Traini, R., Colombatti, M., Ippoliti, R., Flavell, D. J., Flavell, S. U., Cerotti, A. and Fabbrini, M. S. (2010) *Pichia pastoris* as a host for secretion of toxic saporin chimeras. FASEB J. **24**, 253–265

Longemann, J., Jach, G., Tommerup, H., Mundy, J. and Schell, J. (1992) Expression of a barley ribosome-inactivating protein leads to increased fungal protein in transgenic tobacco plants. Nat. Biotechnol. **262**, 615-623

Losey, J. E. and Eubanks, M. D. (2000) Implications of pea aphid host-plant specialization for the potential colonization of vegetables following post-harvest emigration from forage crops. Environ. Entomol. **29**, 1283-1288

Loss-Morais, G., Turchetto-Zolet, A. C., Etges, M., Cagliari, A., Körbes, A. P., Maraschin Fdos, S., Margis-Pinheiro, M. and Margis, R. (2013) Analysis of castor bean ribosome-inactivating proteins and their gene expression during seed development. Genet. Mol. Biol. **36**, 72-86

Mach, L., Waltraud, S., Ammann, M., Poetsch, J., Bertsch, W., Marz, L. and Glossl, J. (1991) Purification and partial characterization of a novel lectin from elder (*Sambucus nigra* L.) fruit. Biochem. J. **278**, 667-671

Mach, L., Kerschbaumer, R., Schwihla, H. and Glossl, J. (1996) Elder (*Sambucus nigra* L.) fruit lectin (SNA-IV) occurs in monomeric, dimeric and oligomeric isoforms. Biochem. J. **315**, 1061

Magy, B., Tollet, J., Laterre, R., Boutry, M. and Navarre, G. (2014) Accumulation of secreted antibodies in plant cell cultures varies according to the isotype, host species and culture conditions. Plant Biotech. J. **12**, 457–467

Malhotra, J. D. and Kaufman, R. J. (2007) The endoplasmic reticulum and the unfolded protein response. Semin. Cell Dev. Biol. **18**, 716–731

Mandal, M. K., Fischer, R., Schillberg, S. and Schiermeyer, A. (2014) Inhibition of protease activity by antisense RNA improves recombinant protein production in *Nicotiana tabacum* cv. Bright Yellow 2 (BY-2) suspension cells. Biotech. J. **9**, 1065–1073

Manders, E. M. M, Verbeek, F. J. and Aten, J. A. (1993) Measurement of co-localization of objects in dual-colour confocal image. J. Microsc. **169**, 375-382

Mansouri, S., Nourollahzadeh, E. and Hudak, K. A. (2006) Pokeweed antiviral protein depurinates the sarcin/ricin loop of the rRNA prior to binding of aminoacyl-tRNA to the ribosomal A-site. RNA **12**, 1683-1692

Marshall, R. S., D'Avila, F., Di Cola, A., Traini, R., Spanò, L., Fabbrini, M. S. and Ceriotti, A. (2011) Signal peptide-regulated toxicity of a plant ribosome-inactivating protein during cell stress. Plant J. **65**, 218-229

Martin, S. J., Lennon, S. V., Bonham, A. M. and Cotter, T. G. (1990) Induction of apoptosis (programmed cell death) in human leukemic HL-60 cells by inhibition of RNA or protein synthesis. J. Immunol. **145**, 1859-1867

Masuoka, J. (2004) Surface Glycans of Candida albicans and Other Pathogenic Fungi: Physiological Roles, Clinical Uses, and Experimental Challenges. Clin. Microbiol. Rev. **17**,281–310

Matsuoka, K. and Nakamura, K. (1991) Propeptide of a precursor to a plant vacuolar protein required for vacuolar targeting. Proc. Natl. Acad. Sci. USA **88**, 834–838

Maveyraud, L., Niwa, H., Guillet, V., Svergun, D. I., Konarev, P. V., Palmer, R. A., Peumans, W. J., Rouge, P., Van Damme, E. J. M., Reynolds, C. D. and Mourey, L. (2009) Structural basis for sugar recognition, including the Tn carcinoma antigen, by the lectin SNA-II from *Sambucus nigra*. Proteins **75**, 89-103

Reference list

Mayerhofer, P. U., Cook, J. P., Wahlman, J., Pinheiro, T. T., Moore, K. A., Lord, J. M., Johnson, A. E. and Roberts, L. M. (2009) Ricin A chain insertion into endoplasmic reticulum membranes is triggered by a temperature increase to 37 °C. J. Biol. Chem. **284**, 10232–10242

Meng, Y., Lin, S., Liu, S., Fan, X., Li, G. and Meng, Y. (2014) A Novel Method for Simultaneous Production of Two Ribosome-Inactivating Proteins, α-MMC and MAP30, from *Momordica charantia L.* PLoS One **9**, e101998-e10205

Mengiste, T. (2012) Plant immunity to necrotrophs. Annu. Rev. Phytophathol. **50**, 267-94

Mizushima, N., Yoshimorim, T. and Levine, B. (2010) Methods in mammalian autophagy research. Cell **140**, 313-326

Mo, H., Winter, H. C. and Goldstein, I. J. (2000) Purification and characterization of a Neu5Ac α2-6Galβ1-4Glc/GlcNAc-specific lectin from the fruiting body of the polypore mushroom *Polyporus squamosus.* J. Biol. Chem. **275**, 10623-10629

Mohamed, M. S., Veeranarayanan, S., Minegishi, H., Sakamoto, Y., Shimane, Y., Nagaoka, Y., Aki, A., Poulose, A. C., Echigo, A., Yoshida, Y., Toru Maekawa, T. and Kumar, D. S. (2014) Cytological and subcellular response of cells exposed to the type-1 RIP curcin and its hemocompatibility analysis. Sci. Rep. **4**, 5747

Montfort, W., Villafranca, J. E., Monzingo, A. F., Ernst, S. R., Katzin, B., Rutenber, E., Xuong, N. H., Hamlin, R. and Robertus, J. D. (1987) The three-dimensional structure of ricin at 2.8 Å. J. Biol. Chem. **262**, 5398-5403

Mondal, H. A., Chakraborti, D., Majumder, P., Roy, P., Roy, A., Bhattacharya, G. S. and Das, S. (2011) Allergenicity assessment of *Allium sativum* leaf agglutinin, a potential candidate protein for developing sap sucking insect resistant food crop. PLoS One **6**, 27716-27724

Montanaro, L., Sperti, S., Mattioli, A., Testoni, G. and Stirpe, F. (1975) Inhibition by ricin of protein synthesis *in vitro*. Inhibition of the biding of elongation factor 2 and of adenosine diphosphate-ribosylated elongation factor 2 to ribosomes. Biochem. J. **146**, 127-131

Moon, Y. H., Song, S. K., Choi, K. W. and Lee, J. S. (1997) Expression of a cDNA encoding *Phyolacca insularis* antiviral protein confers virus resistance on transgenic potato plants. Mol. Cells **7**, 807-815

Müller, M., Dues, G., Balconi, C., Salamini, F. and Thompson, R. D. (1997) Nitrogen and hormonal responsiveness of the 22 kDa α-zein and b-32 genes in maize endosperm is displayed in the absence of the transcriptional regulator Opaque-2. Plant J. **12**, 281–291

Muñoz, R., Arias, Y., Ferreras, J. M., Jiménez, P., Rojo, M. A. and Girbés, T. (2001) Sensitivity of cancer cell lines to the novel non-toxic type 2 ribosome-inactivating protein nigrin b. Cancer Lett. **167**, 163-169

Murashige, T. and Skoog, F. (1962) A revised medium for rapid growth and bioassays with tobacco tissue cultures. Physiol. Plant. **15**, 473–497

Muthamilarasan, M. and Prasad, M. (2013) Plant innate immunity: An updated insight into defense mechanism. J. Biosci. **38**, 433-449

Narayana, S., Surolia, A. and Karande, A. A. (2004) Ribosome-inactivating protein and apoptosis: abrin causes cell death via mitochondrial pathway in Jurkatt cells. Biochem. J. **377**, 233-240

Narayanan, S., Surendranath, K., Bora, N., Surolia, A. and Anjali, A. K. (2005) Ribosome inactivating proteins and apoptosis. FEBS Lett. **579**, 1324–1331

Nielsen, K. and Boston, R. S. (2001) Ribosome-inactivating proteins: a plant perspective. Plant Mol. Biol. **52**, 785-816

Nielsen, K., Payne, G. A. and Boston, R. S. (2001) Maize ribosome-inactivating protein inhibits normal development of *Aspergillus nidulans* and *Aspergillus flavus*. Mol. Plant-Microbe Interactions **14**, 164-172

Ng, T. B. and Wang, H. X. (2001) Panaxagin, a new protein from Chinese ginseng possesses anti-fungal, anti-viral, translation-inhibiting and ribonuclease activities. Life Sci. **68**, 739-749

Ng, T. B. and Parkash, A. (2002) Hispin, a novel ribosome-inactivating protein with antifungal activity from hairy melon seeds. Protein Exres. Purif. **26**, 211-217

Ng, T. B. (2004) Antifungal proteins and peptides of leguminous and non-leguminous origins. Peptides **25**, 1215-1222

Ng, T. B. and Wong, J. H. (2014) Ribosome-inactivating proteins in Caryophyllaceae, Cucurbitaceae and Euphorbiaceae. Stirpe, F. and Lappi, D. A. (eds.) Ribosome-inactivating proteins: ricin and related proteins, pp. 212-222. Wiley Blackwell Press, NJ, USA

North, S. J., Jang-Lee, J., Harrison, R., Canis, K., Ismail, M. N., Trollope, A., Antonopoulos, A., Pang, P. C., Grassi, P., Al-Chalabi, S., Etienne, A. T., Dell, A. and Haslam, S. M. (2010) Mass spectrometric analysis of mutant mice. Methods Enzymol. **478**, 27-77

Obrig, T. G. (1997) Shiga toxin mode of action in *E. coli* O157:H7 disease. Front Biosci. **15**, d635-642

Oliveira, C., Felix, W., Moreira, R. A., Teixeira, J. A. and Domingues, L. (2008) Expression of frutalin, an α-D-galactose-binding jacalin-related lectin, in the yeast *Pichia pastoris*. Protein Expr. Purif. **60**, 188-193

Oliveira, C., Nicolau, A. , Teixeira, J. A. and Domingues, L. (2011) Cytotoxic effects of native and recombinant frutalin, a plant galactose-binding lectin, on HeLa cervical cancer cells. *J. Biomed. Biotechnol.* **2011**, 568932-568941

Olmo, N., Turnay, J., González, de Buitrago, G., López de Silanes, I., Gavilanes, J. G. and Lizarbe, M. A. (2001) Cytotoxic mechanism of the ribotoxin a-sarcin: induction of cell death via apoptosis. Eur. J. Biochem. **268**, 2113-2123

Padler-Karavani, V., Song, X., Yu, H., Hurtado-Ziola, H., Huang, S., Muthana, S., Chokhawala, H. A., Cheng, J., Verhagen, A., Langereis, M. A., Kleene, R., Schachner, M., De Groot, R. J., Lasanajak, Y., Matsuda, H., Schwab,

R., Chen, X., Smith, D. F., Cummings, R. D. and Varki, A. (2012) Cross-comparison of protein recognition of sialic acid diversity on two novel sialoglycan microarrays. J. Biol. Chem. **287**, 22593-22608

Papadopoulos, J. S. and Agarwala, R. (2007) COBALT: constraint-based alignment tool for multiple protein sequences. Bioinformatics **23**, 1073-1079

Parente, A., Chambery, A., Di Maro, A., Russo, R. and Severino, V. (2014) Ribosome-inactivating proteins from Phytolaccaceae. Stirpe, F. and Lappi, D. A. (eds.) Ribosome-inactivating proteins: ricin and related proteins, pp. 28-43. Wiley Blackwell Press, NJ, USA

Park, S. W. Stevens, N. M. and Vivanco, J. M. (2002a) Enzymatic specificity of three ribosome-inactivating proteins against fungal ribosomes, and correlation with antifungal activity. Planta. **216**, 227-234

Park, S. W., Lawrence, C. B., Linden, J. C. and Vivanco, J. M. (2002b) Isolation and characterization of a novel ribosome-inactivating protein from root cultures of pokeweed and its mechanism of secretion from roots. Plant Physiol. **130**, 164-178

Park, S. W., Vepachedu, R., Owens, R. A. and Vivanco, J. M. (2004a) The N-glycosidase activity of ribosome-inactivating protein ME1 targets single-stranded regions of nucleic acids independent of sequence or structural motifs. J. Biol. Chem. **279**, 34165–34174

Park, S. W., Vepachedu, R., Sharam, N. and Vivanco, J. M. (2004b) Ribosome-inactivating proteins in plant biology. Planta **219**, 1093–1096

Parkash, A., Ng, T. B. and Tso, W. W. (2002) Isolation and characterization of luffacylin, a ribosome inactivating peptide with anti-fungal activity from sponge gourd (Luffa cylindrica) seeds. Peptides. **23**, 1019-1024

Pascal, J. M., Day, P. J., Monzingo, A. F., Ernst, S. R., Robertus, J. D., Iglesias, R., Pérez, Y., Férreras, J. M., Citores, L. and Girbés, T. (2001) 2.8-Å Crystal structure of a nontoxic type-II ribosome-inactivating protein, ebulin l. Proteins: Structure, Function, and Genetics **43**, 319-326

Pereira-Lorenzo, S., Ramos-Cabrer, A. M. and Fischer, M. (2009) Breeding apple (*Malus x domestica* Borkh). Breeding Plantation Tree Crops: Temperate Species. pp. 33-81 Springer, NY.

Perillo, N. L., Pace, K. E., Seilhamer, J. J. and Baum, L. G. (1995) Apoptosis of T cells mediated by galectin-1. Nature **378**, 736-739

Petersen, L. K. and Stowers, R. S. (2011) A gateway multisite recombination cloning tool kit. PLoS One **6**, e24531-24548

Peumans, W. J., Kellens, J. T. C., Allen, A. K and Van Damme, E. J. M. (1991) Isolation and characterization of a seed lectin from elderberry (*Sambucus nigra*) and its relationship to the bark lectins. Carbohydr. Res. **213**, 7-17

Peumans, W. J., Roy, S., Barre, A., Rougé, P., Van Leuven, F. and Van Damme, E. J. M. (1998) Elderberry (*Sambucus nigra*) contains truncated Neu5Ac(α-2,6)Gal/GalNAc-binding type 2 ribosome-inactivating proteins. FEBS Lett. **425**, 35-39

Peumans, W. J., Hao, Q. and Van Damme, E. J. M. (2001) Ribosome-inactivating proteins from plants: more than RNA N-glycosidases? FEBS J. **15**, 1494-1506

Peumans, W. J. and Van Damme, E. J. M. (2010) Evolution of plant ribosome-inactivating proteins. Lord, J.M. and Hartley, M. R. (eds) pp. 1-26. Plant Cell Monographs, Springer, NY, USA

Peumans, W. J., Shang, C. and Van Damme, E. J. M. (2014) Updated model of the molecular evolution of RIP genes. Stirpe, F. and Lappi, D. A. (eds.) Ribosome-inactivating proteins: ricin and related proteins, pp. 134-150. Wiley Blackwell Press, NJ, USA

Pieterse, C. M., Van der Does, D., Zamioudis, C. Leon-Reyes, A. and Van Wees, S. C. (2012) Hormonal modulation of plant immunity. Annu. Rev. Cell Dev. Biol. **28**, 489-521

Polito, L., Bortolotti, M., Mercatelli, D., Battelli, M. G. and Bolognesi, A. (2013a) Saporin-S6: A Useful Tool in Cancer Therapy. Toxins **5**, 1698-1722

Polito, L., Bortolotti, M., Mercatelli, D., Mancuso, R., Baruzzi, G., Faedi, W. and Bolognesi, A. (2013b) Protein synthesis inhibition activity by strawberry tissue protein extracts during plant life cycle and under biotic and abiotic stresses. Int. J. Mol. Sci. **14**, 15532-15545

Prestle, J., Schönfelder, M., Adam, G. and Mundry, K. W. (1992) Type 1 ribosome- inactivating protein depurinate plant 25S rRNA without species specificity. Nucleic Acids Res. **20**, 3179–3182.

Puri, M., Kaur, I., Perugini, M. A. and Gupta, R. C. (2012) Ribosome-inactivating proteins: current status and biomedical applications. Drug Discov. Today **17**, 774-83

Qian, Q., Huang, L., Yi, R., Wang, S. and Ding, Y. (2014) Enhanced resistance to blast fungus in rice (*Oryza sativa* L.) by expressing the ribosome-inactivating protein alpha-momorcharin. Plant Sci. **217-218**, 1-7

Qin, W., Huang, M. X., Xu, Y., Zhang, X. S. and Chen, F. (2005) Expression of a ribosome inactivating protein (curcin 2) in *Jatropha curcas* is induced by stress. J. Biosci. **30**, 351-357

Rabinovich, G. A. (2005) Galectin-1 as a potential cancer target. Br. J. Cancer **92**, 1188-1192

Rao, P. V. Jayaraj, R., Bhaskar, A. S., Kumar, O., Bhattacharya, R., Saxena, P., Dash, P. K. and Vijayaraghavan, R. (2005) Mechanism of ricin-induced apoptosis in human cervical cancer cells. Biochem. Pharmacol. **69**, 855-865

Ready, M., Wilson, K., Piatak, M. and Robertus, J. D. (1984) Ricin-like plant toxins are evolutionarily related to single-chain ribosome-inhibiting proteins from *Phytolacca*. J. Biol. Chem. **259**, 15252–15256

Ready, M. P., Brown, D. T. and Robertus, J. D. (1986) Extracelular localization of pokeweed antiviral protein. Proc. Natl. Acad. Sci. USA **83**, 5053-6

Reinbothe, S., Mollenhauer, B. and Reinbothe, C. (1994a) JIPs and RIPs: The regulation of plant gene expression by jasmonates in response to environmental cues and pathogens. Plant Cell **6**, 1197–1209

Reinbothe, S., Reinbothe, C., Lehmann, J., Becker, W., Apel, K. and Parthier, B. (1994b) JIP60, a methyl jasmonate-induced ribosome-inactivating protein involved in plant stress reactions. Proc. Natl. Acad. Sci. USA **91**, 7012–7016

Reisbig, R., Olsnes, S. and Eiklid, K. (1981) The cytotoxic activity of Shigella toxin. Evidence for catalytic inactivation of 60S ribosomal subunit. J. Biol. Chem. **256**, 8739-8744

Remi Shih, N. R., McDonald, K. A., Jackman, A. P., Girbes, T. and Iglesias, R. (1997) Bifunctional plant defense enzymes with chitinase and ribosome-inactivating activities from *Trichosanthes kirilowii* cell cultures. Plant Sci. **130**, 145-150

Rendic, D., Wilson, I. B. H. and Paschinger, K. (2008) The glycosylation capacity of insect cells. Croatica Chemica. Acta **81**, 7-21

Reyes, A. G., Geukens, N., Gutschoven, P., De Graeve, S., De Mot, R., Mejía, A. and Anné, J. (2010) The *Streptomyces coelicolor* genome encodes a type I ribosome-inactivating protein. Microbiology **156**, 3021-3030

Reyes, A. G., Anné, J. and Mejía, A. (2012) Ribosome-inactivating proteins with an emphasis on bacterial RIPs and their potential medical applications. Future Microbiol. **7**, 705-17

Rhodes, J. M., Campbell, B. J. and Yu, L. G. (2008) Lectin-epithelial interactions in the human colon. *Biochem. Soc. Trans.* **36**, 1482-1486

Rippmann, J. F., Michalowski, C. B., Nelson, D. E. and Bohnert, H. J. (1997) Induction of a ribosome-inactivating protein upon environmental stress. Plant Mol Biol. **35**, 701–709

Rojo, E. and Denecke, J. (2008). What is moving in the secretory pathway of plants? Plant Physiol. **147**, 1493–1503

Robertus, J. D., Ready, M. P. (1984) Ricin B-chain and discoidin I share a common primitive protein fold. J. Biol. Chem. **259**, 13953-13956

Roth, J. Kemph, A. Reuter, G. Schauer, R. and Gehring, W. J. (1992) Occurrence of sialic acids in *Drosophila melanogaster*. Science **256**, 673-675

Rustgi, S., Pollmann, S., Buhr, F., Springer, A., Reinbothe, C., von Wettstein, D. and Reinbothe, S. (2014) JIP60-mediated, jasmonate- and senescence-induced molecular switch in translation toward stress and defense protein synthesis. Proc. Natl. Acad. Sci. USA **111**, 14181-14186

Rutenber, E., Ready, M. and Robertus, J. (1987) Structure and evolution of ricin B-chain. Nature **326,** 624-626

Rutenber, E. and Roberus, J. D. (1991) Structure of ricin B-chain at 2.5 Å resolution. Proteins **10**, 240-250

Sadeghi, A., Van Damme, E. J. M., Michiels, K., Kabera, A. and Smagghe, G. (2009a) Acute and chronic insecticidal activity of a new mannose-binding lectin from *Allium porrum* against *Acyrthosiphon pisum* via an artificial diet. Can. Entomol. **141**, 1–7

Sadeghi, A., Van Damme, E. J. M. and Smagghe, G. (2009b) Evaluation of the susceptibility of the pea aphid, *Acyrthosiphon pisum*, to a selection of biorational insecticides using an artificial diet. J. Insect Sci. **9**, 1–8

Sandvig, K., Olsnes, S. and Pihl, A. (1978) Binding, uptake and degradation of the toxic proteins abrin and ricin by toxin-resistant cell variants. Eur. J. Biochem. **82**, 13–23

Sandvig, K., Prydz, K., Hansen, S. H. and Van Deurs, B. (1991) Ricin transport in brefeldin A-treated cells: correlation between Golgi structure and toxic effect. J. Cell Biol. **115,** 971–981

Sandvig, K. and van Deurs, B. (2000) Entry of ricin and Shiga toxin into cells: molecular mechanisms and medical perspectives. EMBO J. **19**, 5943–5950

Sandvig, K. and van Deurs, B. (2005) Delivery into cells: lessons learned from plant and bacterial toxins. Gene Ther. **12**, 865-872

Sawasaki, T., Nishihara, M. and Endo, Y. (2008) RIP and RALyase cleave the sarcin/ricin domain, a critical domain for ribosome function, during senescence of wheat coleoptiles. Biochem. Biophys. Res. Commun. **370**, 561-565

Schaart, J. G., Tinnenbroek-Capel, I. E. M. and Krens, F. A. (2010) Isolation and characterization of strong gene regulatory sequences from apple, *Malus × domestica*. Tree Genet. Genomes **7**, 135-142

Schachter, H. (1991) The 'yellow brick road' to branched complex N-glycans. Glycobiology **1**, 453-461.

Schaffer, R. J., Friel, E. N., Souleyre, E. J., Bolitho, K.,Thodey, K., Ledger, S., Bowen, J. H., Ma, J. H., Nain, B., Cohen, D., Gleave, A. P., Crowhurst, R. N., Janssen, B. J., Yao, J. L. and Newcomb, R. D. (2007) A genomics approach reveals that aroma production in apple is controlled by ethylene predominantly at the final step in each biosynthetic pathway. Plant Physiol. **144**, 1899-1912

Seifi, H. S., Curvers, K., De Vleesschauwer, D., Delaere, I., Aziz, A. and Höfte M. (2013) Concurrent overactivation of the cytosolic glutamine synthetase and the GABA shunt in the ABA-deficient sitiens mutant of tomato leads to resistance against *Botrytis cinerea*. New Phytol. **199**, 490-504

Selitrennikoff, C. P. (2001) Antifungal proteins. Appl. Environ. Microbiol. **67**, 2883-2284

Seo, S., Katou, S., Seto, H., Gomi, K. and Ohashi, Y. (2007) The mitogen-activated protein kinases WIPK and SIPK regulate the levels of jasmonic and salicylic acids in wounded tobacco plants. Plant J. **49**, 899-909

Sevrioukova, I. F. (2011) Apoptosis-inducing factor: structure, function, and redox regulation. Antioxid. Redox Singal. **14**, 2545-2579

Shah, J. and Veluthambi, K. (2010) Dianthin, a negative selection marker in tobacco, is non-toxic in transgenic rice and confers sheath blight resistance. Biol. Plantarum. **54**, 443-450

Shahidi-Noghabi, S., Van Damme, E. J. M. and Smagghe, G. (2006) Bioassays for insecticidal activity of iris ribosome-inactivating proteins expressed in tobacco plants. Commun. Agric. Appl. Biol. Sci. **71**, 285-289

Shahidi-Noghabi, S., Van Damme, E. J. M. and Smagghe, G. (2008) Carbohydrate-binding activity of the type-2 ribosomes-inactivating protein SNA-I from elderberry (*Sambucus nigra*) is a determining factor for its insecticidal activity. Phytochem. **69**, 2972-2978

Shahidi-Noghabi, S., Van Damme, E. J. M. and Smagghe, G. (2009) Expression of *Sambucus nigra* agglutinin (SNA-I') from elderberry bark in transgenic tobacco plants results in enhanced resistance to different insect species. Transgenic Research **18**, 249-259

Shahidi-Noghabi, S,, Van Damme, E. J. M., Mahdian, K. and Smagghe, G. (2010a) Entomotoxic action of *Sambucus nigra* agglutinin i in *Acyrthosiphon pisum* aphids and *Spodoptera exigua* caterpillars through caspase 3 like dependent apoptosis. Arch. Insect Biochem. Physiol. **75**, 207–220

Shahidi-Noghabi, S., Van Damme, E. J. M., Iga, M. and Smagghe, G. (2010b) Exposure of insect midgut cells to *Sambucus nigra* L. agglutinins I and II causes cell death via caspase-dependent apoptosis. J. Insect Physiol. **56**, 1101-7

Shahidi-Noghabi, S., Van Damme, E. J. M., De Vos, W. H. and Smagghe, G. (2011) Internalization of *Sambucus nigra* agglutinins I and II in insect midgut CF-203 cells. Arch. Insect Biochem. Physiol. **76**, 211-22

Shang, C., Madej, M., De Vos, W. and Van Damme, E. J. M. (2013) The ribosome-inactivating proteins (RIPs) from elderberry (*Sambucus nigra*) in the battle against cancer?? Glycoconj. J. **30**, 355

Shang, C., Peumans, W. J. and Van Damme, E. J. M. (2014) Occurrence and taxonomical distribution of ribosome-inactivating proteins belonging to the ricin/shiga toxin superfamily. Stirpe, F. and Lappi, D. A. (eds.) Ribosome-inactivating proteins: ricin and related proteins, pp. 11-27. Wiley Blackwell Press, NJ, USA

Shang, C. and Van Damme, E. J. M. (2014) Comparative analysis of carbohydrate binding properties of *Sambucus nigra* lectins and ribosome-inactivating proteins. Glycoconj. J. **31**, 345-354

Shibata, M., Yoshimura, K.,Tamura, H., Ueno, T., Nishimura, T., Inoue, T., Sasaki, M., Koike, M., Arai, H., Kominami, E. and Uchiyama, Y. (2010) LC3, a microtubule-associated protein1A/B light chain3, is involved in cytoplasmic lipid droplet formation. *Biochem*. *Biophys*. *Res*. Commun. **393**, 274-279

Shibuya, N., Goldstein, I. J., Broekaert, W. F., Nsimba-Lubaki, M., Peeters, B. and Peumans, W. J. (1987) The elderberry (*Sambucus nigra* L.) bark lectin recognizes the NeuAc(α2,6)-Gal/GalNAc sequence. J. Biol. Chem. **262**, 1596-1601

Shibuya, N., Tazaki, K., Song, Z. W., Tarr, G. E., Goldstein, I. J. and Peumans, W. J. (1989) A comparative study of bark lectins from three elderberry (*Sambucus*) species. J. Biochem. **106**, 1098-1103

Shih, S. F., Wu, Y. H., Hung, C. H., Yang, H. Y. and Lin, H. Y. (2001) Abrin triggers cell death by inactivating a thiol-specific antioxidant protein. Journal of Biological Chemistry, **276**, 21870–21877

Sikriwal, D., Ghosh, P. and Batra, J. K. (2008) Ribosome inactivating protein saporin induces apoptosis through mitochondrial cascade, independent of translation inhibition. Int. J. Biochem. Cell Biol. **40**, 2880–2888

Sikriwal, D., and Batra, J. K. (2010) Ribosome inactivating proteins and apoptosis. Lord, J. M. and Hartley, M. R. (Eds.) Plant cell monographs. Toxic plant proteins. pp. 107–132. Springer-Verlag, Berlin, Germany

Smallshaw, J. E., Ghetie, V., Rizo, J., Fulmer, J. R., Trahan, L. L., Ghetie, M. A. and Vitetta, E. S. (2003) Genetic engineering of an immunotoxin to eliminate pulmonary vascular leak in mice. Nat. Biotechnol. **21**, 387-391

Smirnov, S., Shulaev, V. and Tumer, N. E. (1997) Expression of pokeweed antiviral protein in transgenic plants induces virus resistance in grafted wild-type plants independently of salicylic acid accumulation and pathogenesis-related protein synthesis. Plant Physiol. **114**, 1113-1121

Smith, D. F., Song, X. and Cummings, R. D. (2010) Use of glycan microarrays to explore specificity of glycan-binding proteins. Methods Enzymol. **480**, 417-444

Smolik, M. and Krzysztoszek, O. (2010) Evaluation of genetic variability in choosen apple (*Malus×domestica* Borkh.) cultivars by ISSR-PCR analysis. Russ. J. Genet. **46**, 819-827

Soares, R. M., de A Soares, R. M., Alviano, D. S., Angluster, J., Alviano, C. S. and Travassos, L. R. (2000) Identification of sialic acids on the cell surface of *Candida albicans*. Biochim. Biophys. Acta. **1474**, 262-8

Song, S. K., Choi, Y., Moon, Y. H., Kim, S. G., Choi, Y. D. and Lee, J. S. (2000) Systemic induction of a *Phytolacca insularis* antiviral protein gene by mechanical wounding, jasmonic acid, and abscisic acid. Plant Mol. Biol. **43**, 439–450

Song, X., Yu, H., Chen, X., Lasanajak, Y., Tappert, M. M., Air, G.M., Tiwari, V. K., Cao, H., Chokhawala, H. A., Zheng, H., Cummings, R. D. and Smith, D. F. (2011) A sialylated glycan microarray reveals novel interactions of modified sialic acids with proteins and viruses. J. Biol. Chem. **286**, 31610-31622

Spooner, R. A., Hart, P. J., Cook, J. P., Pietroni, P., Rogon, C., Hohfeld, J., Roberts, L. M. and Lord, J. M. (2008) Cytosolic chaperones influence the fate of a toxin dislocated from the endoplasmic reticulum. Proc. Natl. Acad. Sci. USA **105**, 17408–17413

Spooner, R. A. and Lord, J. M. (2012) How ricin and shiga toxin reach the cytosol of target cells: retrotranslocation from the endoplasmic reticulum. Current Top Microbiol. Immunol. **357**, 19-40

Spooner, R. A. and Lord, J. M. (2014) The intracellular journey of type 2 ribosome-inactivating proteins. Stirpe, F. and Lappi, D. A. (eds.) Ribosome-inactivating proteins: ricin and related proteins, pp. 83-96. Wiley Blackwell Press, NJ, USA

Stanley, P. and Cummings, R. D. (2009) Structures common to different glycans. Varki, A., Cummings, R. D., Esko, J. D., Freeze, P., Stanley, P., Bertozzi, C. R., Hart, G. W. and Etzler, M. E. (eds.) Essentials of Glycobiology, 2nd, pp. 175-198. Cold Spring Harbor Laboratory Press, NY

Reference list

Stevens, W. A., Spurdon, C., Onyon, L. J. and Stirpe, F. (1981) Effect of inhibitors of protein synthesis from plants on tobacco mosaic virus infection. Experientia **37,** 257-259

Stillmark, P. H. (1888) Über Ricin, ein giftiges Ferment aus den Samen von *Ricinus communis* L. und einigen anderen Euphorbiaceen [doctoral thesis]. Vol. Ph.D. Dorpat: University of Dorpat.

Stirpe, F., Olsnes, S. and Phil, A. (1980) Gelonin, a new inhibitor of protein-synthesis, nontoxic to intact-cells-isolation, characterization, and preparation of cytotoxic complexes with concanavalin-A. J. Biol. Chem. **255**, 6947-6953

Stirpe, F., Williams, D. G., Onyon, L. J., Legg, R. F. and Stevens, W. A. (1981) Dianthins, ribosome-inactivating proteins with anti-viral properties from *Dianthus caryophyllus* L. (carnation). Biochem. J. **195**, 399-405

Stirpe, F. (1982) On the action of ribosome-inactivating proteins: are plant ribosomes species-specific? Biochem. J. **202**, 279-280

Stirpe, F., Gasperi-Campani., Barbieri, L., Falasca, A., Abbondanza, A. and Stevens, W. A. (1983) Ribosome-inactivating proteins from the seeds of *Saponaria officinalis* L. (soapwort), of *Agrostemma githago* L. (corn cockle) and of *Asparagus officinalis* L. (asparagus), and from the latex of *Hura crepitans* L. (sandbox tree).Biochem, J. **216**, 617-625

Stirpe, F., Barbieri, L., Battelli, M. G., Falasca, A. I., Abbondanza, A., Lorenzoni, E. and Stevens, W. A. (1986) Bryodin, a ribosome-inactivating protein from the roots of *Bryonia dioica* L. (white bryony). Biochem. J. **240**, 659-665

Stirpe, F., Barbieri, L., Gorini, P., Valbonesi, P., Bolognesi, A. and Polito, L. (1996) Activities associated with the presence of ribosome-inactivating proteins increase in senescent and stressed leaves. FEBS Lett. **382**, 309-312

Stirpe F. (2004) Ribosome-inactivating proteins. Toxicon. **44**, 371–383

Stirpe, F. and Battelli, M. G. (2006) Ribosome-inactivating proteins: progress and problem. Cell. Mol. Life Sci. **63**, 1850-1866

Stirpe, F. (2014) Introduction and History. Stirpe, F. and Lappi, D. A. (eds.) Ribosome-inactivating proteins: ricin and related proteins, pp. 1-10. Wiley Blackwell Press, NJ, USA

Stirpe, F. and Lappi, D. A. (eds.) (2015) Ribosome-inactivating proteins: ricin and related proteins. Wiley Blackwell Press, NJ, USA

Suzuki, H. (2012) Translation inhibitors induce formation of cholesterol ester-rich lipid droplets. PLoS One **7**, 42379-42387

Svinth, M., Steighardt, J., Hernandez, R., Suh, J. K., Kelly, C., Day, P., Lord, M. G., Girbés, T. and Robertus, J. D. (1998) Differences in cytotoxicity of native and engineered RIPs can be used to assess their ability to reach the cytoplasm. Biochem. Biophys. Res. Commun. **249**, 637 – 642

Szalai K, Schöll I, Förster-Waldlw E, Politoz L, Bolognesiz A, Untersmayr E, Riemer AB, Boltz-Nitulescu G, Stirpez F. and Jensen-Jarolim E. (2005) Occupational sensitization to ribosome-inactivating proteins in researchers. Clin. Exp. Allergy **35**, 1354-1360

Takashima, S., Seino, J., Nakano, T. Fujiyama, K. Tsujimoto, M., Ishida, N. and Hashimoto, Y. (2009) Anlysis of CMP-sialic acid transporter-like proteins in plants. Phytochem. **70**, 1973-1981

Tan, Q. Q., Dong, D. X..Yin, X. W., Sun, J., Ren, H. J. and Li, R. X. (2009) Comparative analysis of depurination catalyzed by ricin A-chain on synthetic 32mer and 25mer oligoribonucleotides mimicking the sarcin/ricin domain of the rat 28S rRNA and *E. coli* 23S rRNA. J. Biotechnol. **139**, 156-162

Tartarini, A., Pittaluga, E., Marcozzi, G., Testone, G., Rodrigues-Pousada, R. A., Giannino, D. and Spanò, L. (2010) Differential expression of saporin genes upon wounding, ABA treatment and leaf development. Physiol. Plant. **140**, 141-152

Taylor, S., Massiah, A., Lomonossoff, G., Roberts, M., Lord, J. M. and Hartley, M. (1994) Correlation between the activities of five ribosome-inactivating proteins in depurination of tobacco ribosomes and inhibition of tobacco mosaic virus infection. Plant J. **5**, 827-835

Taylor, M. E. and Drickamer, K. (2011) Introduction to glycobiology, 3rd edition, Oxford University Press, Oxford, UK.

Tejero, J., Jiménez, P., Quinto, E. J., Cordoba-Diaz, D., Garrosa, M., Cordoba-Diaz, M., Gayoso, M. J. and Girbés, T. (2015) Elderberries: A source of ribosome-inactivating proteins with lectin activity. Molecules, **20**, 2364-2387

Tesh, V. L. (2012) The induction of apoptosis by Shiga toxins and ricin. Curr. Topics Microbiol. Immunol. **357**, 137-178

Thompson, J. D., Higgins, D. G. and Gilson, T. J. (1994) CLUSTAL W: improving the sensitivity of progressive multiple sequence alignment through sequence weighting, position-specific gap penalties and weight matrix choice. Nucleic Acids Res. **22**, 4673-4680

Tumer, N. E., Hwang, D. J. and Bonness, M. (1997) C-terminal deletion mutant of pokeweed antiviral protein inhibits viral infection but does not depurinate host ribosomes. Proc. Natl. Acad. Sci. USA **94**, 3866-3871

Tumer, N. E. and Li, X. P. (2012) Interaction of ricin and shiga toxins with ribosomes. Curr. Top Microbiol. Immunol. **357**, 1-18

Vago, R., Marsden, C. J., Lord, J. M., Ippoliti, R., Flavell, D. J., Flavell, S. U., Ceriotti, A. and Fabbrini, M. S. (2005) Saporin and ricin A chain follow different intracellular routes to enter the cytosol of intoxicated cells. FEBS J. **272**, 4983-4995

Vallejo, A. N., Pogulis, R. J. And Rease, L. R. (1994) In vitro synthesis of novel genes: mutagenesis and recombination by PCR. Genome Res. **4**, S123-S130

Van Damme, E. J. M., Barre, A., Rougé, P., Van Leuven, F. and Peumans, W. J. (1996) The NeuAc(α-2,6)Gal/GalNAc binding lectin from elderberry (*Sambucus nigra*) bark, a type-2 ribosome-inactivating protein with an unusual specificity and structure. Eur. J. Biochem. **235**, 128–137

Van Damme, E. J. M., Barre, A., Rougé, P., Leuven, F. V. and Peumans ,W. J. (1996a) The NeuAc(a-2,6) Gal/ Gal-NAc-binding lectin from elderberry (*Sumbucus nigra*) bark, a type-2 ribosome-inactivating protein with an unusual specificity and structure. Eur. J. Biochem. **235**, 128-137

Van Damme, E. J. M., Barre, A., Rougé, P., Leuven, F. V. and Peumans, W. J. (1996b) Characterization and molecular cloning of *Sambucus nigra* agglutinin V (nigrin b), a GalNAc-specific type-2 ribosome-inactivating protein from the bark of elderberry (*Sambucus nigra*). Eur. J. Biochem. **237**, 505-513

Van Damme, E. J. M., Roy, S., Rarre, A., Rougé, P., Leuven, F. V. and Peumans, W. J. (1997a) The major elderberry fruit protein is a lectin derived from a truncated type 2 ribosome-inactivating protein. Plant J. **12**, 1251-1260

Van Damme, E. J. M., Barre, A., Rougé, P., Van Leuven, F. and Peumans, W. J. (1997b) Isolation and molecular cloning of a novel type 2 ribosome-inactivating protein with an inactive B-chain from elderberry (*Sambucus nigra*) bark. J. Biol. Chem. **272**, 8353-8360

Van Damme, E. J. M., Roy, S., Barre, A., Citores, L., Mostafapous, K., Rougé, P., Van Leuven, F., Girbés, T., Goldstein, I. J. and Peumans, W. J. (1997c) Elderberry (*Sambucus nigra*) bark contains two structurally different Neu5Ac(α-2,6)Gal/GalNAc-binding type 2 ribosome-inactivating proteins. Eur. J. Biochem. **245**, 648-655

Van Damme, E. J. M., Peumans, W. J., Barre, A. and Rougé, P. (1998) Plant lectins: a composite of several distinct families of structurally and evolutionary related proteins with diverse biological roles. Crit. Rev. Plt. Sci. **17**, 575-692

Van Damme, E. J. M., Hao, Q., Chen, Y., Barre, A., Vandenbussche, F., Desmyter, S., Rougé, P. and Peumans, W. J. (2001) Ribosome-inactivating proteins: a family of plant proteins that do more than inactivate ribosomes. Crit. Rev. Plant Sci. **20**, 395-465

Van Damme, E. J. M., Smith, D. F., Cummings, R. and Peumans, W. J. (2011) Glycan arrays to decipher the specificity of plant lectins. Adv. Exp. Med. Biol. **705,** 757-768

Vandenbussche, F., Peumans, W. J., Desmyter, S., Proost, P., Ciani, M. and Van Damme, E. J. M. (2004a) The type-1 and type-2 ribosome-inactivating proteins from *Iris* confer transgenic tobacco plants local but not systemic protection against virus. Planta **220**, 211-221

Vandenbussche, F., Desmyter, S., Ciani, M., Proost, P., Peumans, W. J. and Van Damme, E. J. M. (2004b) Analysis of the *in planta* antiviral activity of elderberry ribosome-inactivating proteins. Eur. J. Biochem. **271**, 1508-1515

Van Deurs, B., Petersen, O. W., Olsnes, S. and Sandvig, K. (1987) Delivery of internalized ricin from endosomes to cisternal Golgi elements is a discontinuous, temperature-sensitive process. Exp. Cell Res. **171**, 137–152

Van Hove, J., Fouquaert, E., Smith, D. F., Proost, P. and Van Damme, E. J. M. (2011) Lectin activity of the nucleocytoplasmic EUL protein from *Arabidopsis thaliana*. Biochem. Biophys. Res. Commun. **14**, 101-105

Van Leene, J., Stals, H., Eeckhout, D., Persiau, G., Van De Slijke, E., Van Isterdael, G., De Clercq, A., Bonnet, E., Laukens, K., Remmerie, N., Henderickx, K., De Vijlder, T., Abdelkrim, A., Pharazyn, A., Van Onckelen, H., Inzé, D., Witters, E. and De Jaeger, G. (2007) A tandem affinity purification-based technology platform to study the cell cycle interactome in *Arabidopsis thaliana*. Mol. Cell. Proteomics **6**, 1226–1238

Vargas, L. R. B. and Carlini. C. R. (2014) Insecticidal and antifungal activities of ribosome-inactivating proteins. Stirpe, F. and Lappi, D. A. (eds.) Ribosome-inactivating proteins: ricin and related proteins, pp. 212-222. Wiley Blackwell Press, NJ, USA

Varki, A. and Schauer, R. (2009). Sialic acids. Varki, A., Cummings, R. D. Esko, J. D. Freeze, H. H. Stanley, P., Bertozzi, C. R. Hart, G. W. and Etzler, M. E. (eds.) Essentials of Glycobiology (2nd edition), Ch. 14. Cold Spring Harbor Press, NY, USA

Velasco, R., Zharkikh, A., Affourtit, J., Dhingra, A., Cestaro, A., Kalyanaraman, A., Fontana, P., Bhatnagar, S. K., Troggio, M., Pruss, D., Salvi, S., Pindo, M., Baldi, P., Castelletti, S., Cavaiuolo, M., Coppola, G., Costa, F., Cova, V., Dal Ri, A., Goremykin, V., Komjanc, M., Longhi, S., Magnago, P., Malacarne, G., Malnoy, M., Micheletti, D., Moretto, M., Perazzolli, M., Si-Ammour, A., Vezzulli, S., Zini, E., Eldredge, G., Fitzgerald, L. M., Gutin, N., Lanchbury, J., Macalma, T., Mitchell, J. T., Reid, J., Wardell, B., Kodira, C., Chen, Z., Desany, B., Niazi, F., Palmer, M., Koepke, T., Jiwan, D., Schaeffer, S., Krishnan, V., Wu, C., Chu, V. T., King, S. T., Vick, J., Tao, Q., Mraz, A., Stormo, A., Stormo, K., Bogden, R., Ederle, D., Stella, A., Vecchietti, A., Kater, M. M., Masiero, S., Lasserre, P., Lespinasse, Y., Allan, A. C., Bus, V., Chagné, D., Crowhurst, R. N., Gleave, A. P., Lavezzo, E., Fawcett, J. A., Proost, S., Rouzé, P., Sterck, L., Toppo, S., Lazzari, B., Hellens, R.P., Durel, C.E., Gutin, A., Bumgarner, R. E., Gardiner, S. E., Skolnick, M., Egholm, M., Van de Peer, Y., Salamini, F. and Viola, R. (2010) The genome of the domesticated apple (*Malus x domestica Borkh*). Nat. Genet. **42**, 833-839

Verdoodt, F., Willems, M., Dhondt, I., Houthoofd, W., Bert. W. and De Vos, W. H. (2012) Measurement of S-phase duration of adult stem cells in the flatworm *Macrostomum lignano* by double replication labelling and quantitative colocalization analysis. Cell Biol. Int. **36**, 1251-1259

Verfaillie, T., Salazar, M., Velasco, G and Agostinis, P. (2010) Linking ER stress to autophagy: potential implications for cancer therapy. Int. J. Cell Biol. **2010**, 930509

Vitale, A. and Raikhel, N. V. (1999) What do proteins need to reach different vacuoles? Trends Plant Sci. **4**, 149-156

Reference list

Voorhees, R. M., Schmeing, T. M., Kelley, A. C. and Ramakrishnan, V. (2010) The mechanism for activation of GTP hydrolysis on the ribosome. Science **330**, 835–838

Voss, C., Eyol, E. , Frank, M., Von Der Lieth, C. W. and Berger, M. R. (2006) Identification and characterization of riproximin, a new type II ribosome-inactivating protein with antineoplastic activity from *Ximenia americana*. FASEB J. **20**, 1194-1196

Vlot, A. C., Dempseym, D. A. and Klessig, D. F. (2009) Salicylic acid, a multifaceted hormone to combat disease. Annu. Rev. Phytopathol. **47**, 177-206

Walsh, T. A., Morgan, A. E. and Hey, T. D. (1991) Characterization and molecular cloning of a proenzyme form of a ribosome-inactivating protein from maize. Novel mechanism of proenzyme activation by proteolytic removal of a 2.8-kilodalton internal peptide segment. J. Biol. Chem. **266**, 23422-23427

Wang, P., Zoubenko, O. and Tumer, N. E. (1998) Reduced toxicity and broad spectrum resistance to viral and fungal infection in transgenic plants expression pokeweed antiviral protein II. Plant Mol. Biol. **38**, 957-964

Wang, P. and Tumer, N. E. (1999) Pokeweed antiviral protein cleaves double-stranded supercoiled DNA using the same active site required to depurinate rRNA. Nucleic Acids Res. **27**, 1900–1905

Wang, Y., Yu, G., Han, Z., Yang, B., Hu, Y., Zhao, X., Wu, J., Lv, Y. and Chai, W. (2011) Specificities of *Ricinus communis* agglutinin 120 interaction with sulfated galactose. FEBS Lett. **585**, 3927–3934

Walski, T., Van Damme, E. J. M. and Smagghe, G. (2014) Penetration through the peritrophic matrix is a key to lectin toxicity against *Tribolium castaneum*. J. Insect Physiol. **70**, 94-101

Warwas, M. L., Waston, J. N.m Bennet, A. J. and Margo, M. M. (2007) Structure and role of sialic acids on the surface of *Aspergillus fumigatus* conidiospes. Glycobiology 17, 401-410

Watanabe, K., Kawasaki, T., Sako, N., Funatsu, G. (1997) Actions of pokeweed antiviral protein on virus-infected protoplasts. Biosci. Biotechnol. Biochem. **61**, 994-997

Wei, G. Q., Liu, R. S., Wang, Q. Q. and Liu, W. Y. (2004) Toxicity of two type II ribosome-inactivating proteins (cinnamomin and ricin) to domestic silkworm larvae. Arch. Insect Biochem. Physiol. **57**, 160-165

Wen, L. (2013) Cell death in plant immune response to necrotrophs. Plant Biochem. Physiol. **1**, e103-105

Wirthmueller, L., Maqbool, A. and Banfield, M. J. (2013) On the front line: structural insights into plant-pathogen interactions. Nat. Rev. Microbiol. **11**, 761-776

Wong, Y. T., Ng, Y. M., Mark, N. S., Sze, K. H., Wong, K. B. and Shaw, P. C. (2012) Maize ribosome-inactivating protein uses lys158– lys161 to interact with ribosomal protein P2 and the strength of interaction Is correlated to the biological activities. PLoS. One **7**, e49608-18

Wu, D., Chu, J., Hao, Y. Y., Zhuang, Y. P. and Zhang, S. L. (2012) Incomplete proteins disulphide bond conformation and decreased protein expression result from high cell growth during heterologous protein expression in *Pichia pastoris*. J. Biotechnol. **157**, 107-112

Xiang, L., Le Roy, K., Bolouri-Moghaddam, M. R., Vanhaecke, M., Lammens, W., Rolland, F. and Van den Ende, W. (2011) Exploring the neutral invertase-oxidative stress defence connection in *Arabidopsis thaliana*. J. Exp. Bot. **62**, 3849-3862

Xiang, L. (2012). Localization and fuction of plant invertases and fructan metabolizing enzymes. PhD thesis.

Xiang, L., Etxeberria, E. and Van den Ende, W. (2013) Vacuolar protein sorting mechanisms in plants. FEBS J. **4**, 979-993

Xu, J., Wang, H. and Fan, J. (2007) Expression of a ribosome-inactivating protein gene in bitter melon is induced by *Sphaerotheca fuliginea* and abiotic stimuli. Biotechnol Lett. **29**, 1605–1610

Yabe, R., Suzuki, R., Kuno, A., Fujimoto, Z., Jigami, Y. and Hirabayashi, J. (2007) Tailoring a novel sialic acid-binding lectin from a ricin-B chain-like galactose-binding protein by natural evolution-mimicry. J. Biochem. **141**, 389–399

Yang, Y., Li, R. and Qi, M. (2000) In vivo analysis of plant promoters and transcription factors by agroinfiltration of tobacco leaves. Plant J. **22**, 543–551

Yang, Z., Bennett, E. P., Jørgensen, B., Drew, D. P., Arigi, E., Mandel, U., Ulvskov, P., Levery, S. B., Clausen, H. and Petersen, B. L. (2012) Toward stable genetic engineering of human O-glycosylation in plants. Plant Physiol. **160**, 450–463

Yoo, S. D., Cho, Y. H. and Sheen, J. (2007) *Arabidopsis* mesophyll protoplasts: a versatile cell system for transient gene expression analysis. Nat. Protoc. **2**, 1565–1572

Yoshida, T., Chen, C. C., Zhang, M. S. and Wu, H. C. (1991) Disruption of the Golgi apparatus by brefeldin A inhibits the cytotoxicity of ricin, modeccin, and *Pseudomonas* toxin. Exp. Cell Res. **192**, 389–395

Yuan, H., Ming, X., Wang, L., Hu, P., An, C. and Chen, Z. (2002) Expression of a gene encoding trichosanthin in transgenic rice plants enhances resistance to fungus blast disease. Plant Cell Rep. **20**, 992-998

Zeleny, R., Kolarich, D., Strasser, R. and Altmann, F. (2006) Sialic acid concentrations in plants are in the range of inadvertent contamination. Planta **224**, 222-227

Zhang, W., Yang, X., Qiu, D., Guo, L., Zeng, H., Mao, J. and Gao, Q. (2011) PeaT1-induced systemic acquired resistance in tobacco follows salicylic acid-dependent pathway. Mol. Biol. Rep. **38**, 2549–2556

Zhou, X., Li, X. D., Yuan, J. Z., Tang, Z. H. and Liu, W. Y. (2000) Toxicity of cinnamomin-A new type II ribosome-inactivating protein to bollworm and mosquito. Insect Biochem. Mol. Biol. **30**, 259–264

Zhu, F., Zhang, P., Meng, Y. F., Zhang, D. W., Cheng, J., Lin, H. H. and Xi. D. H. (2013) Alpha-momorcharin, a RIP produced by bitter melon, enhances defense response in tobacco plants against diverse plant viruses and shows antifungal activity *in vitro*. Planta **237**, 77-88

Zong, W. X. and Thompson, C. B. (2006) Necrotic death as a cell fate. Genes Dev. **20**, 1-15

Zoubenko, O., Uckun, F., Hur, Y., Chet, I. and Tumer, N. E. (1997) Plant resistance to fungal infection induced by nontoxic pokeweed antiviral protein mutants. Nat. Biotechnol. **15,** 992–996

Acknowledgements

Past years have been a truly exciting and unforgettable experience in my life. Here, I would like to take this opportunity to thank all the people that have helped me throughout this wonderful journey.

First and foremost, I was most fortunate to work in the Glyco team under the supervision of my promoter Prof. Els Van Damme. It would not have been possible to complete this dissertation without her insightful and encouraging suggestions and guidance. She taught me the various aspects of conducting research. Besides her professional expertise and technical guidance, she has always been very kind and helpful. I would like to express my special thanks to Dr. Willy Peumans for his invaluable discussions and advices.

I am extremely thankful to the reading committee: Prof. Winnok H. De Vos, Prof. Monica Höfte, Prof. Guy Smagghe, Prof. Danny Geelen, Prof. John Van Camp, Prof. Kris Audenaert, Prof. Nico Boon, Prof. Wim Van den Ende, for their precious time in reading this thesis and providing me critical suggestions to improve it. I would like to thank the China Scholarship Council (CSC) and the Special Research Fund (BOF co-funding) for the financial support.

I would like to express my sincerest gratitude to Prof. Winnok H. De Vos for his valuable input, advice and implementing ideas during our collaborative study on the effects of *S. nigra* proteins on mammalian cells. CSI boys, Tom and Tobias, have provided their support in every aspect of technical help for which I am forever thankful. I really appreciate Prof. Monica Höfte for her instructive advice and useful suggestions during the collaboration on the biotic stress experiments. I would also like to thank Prof. Guy Smagghe for his useful discussions and advice. I am very thankful to Prof. Anne Dell and Dr. Stuart M. Haslam and Qiushi Chen (Imperial College London) for the glycomics data analyses.

How can I forget my dear Glyco's? We spent the beautiful PhD life together by sharing the joy of discovery and investigation. I owe a great debt of gratitude for your patience, optimism and inspirational attitude. Thank you very much for your help and support in the past years and providing me such a great working environment. Nausicaä has been always a great info desk for everybody. Jonas, besides the science, you also bring me a lot of knowledge about European songs and culture. Lore, all different interesting stories construct the memories of you in my mind. Sofie, you are so sweet and always very patient with me. You are the one who transmits a lot of happiness to all glyco's. Liuyi and Ying, thank you for speaking Chinese with me ☺, and I wish you a lot of success to finalize your PhD. Let's meet in China! Jeroen, massive thanks to you for your kindness and for translating the summary into Dutch. I will remember Kristof as a thoughtful and friendly person answering my various questions. I would like to thank Tomasz for kindly providing me FITC labeled proteins, which was very handy. Na, thank you a lot for the setting up the aphid experiments. You are always

so helpful with everything. It was a good experience to work with Hamshou, and I wish you all the best with your insects. Mariya, you are just starting the PhD life and I believe you will overcome all the problems. Subramanyam, I hope you will enjoy the life in Glyco group and I wish you good luck with your project.

I will never forget the people who have already left: Bassam, Annelies, Elke, Megumi, Kirsten, Romina, Dieter, Gianni, Isabel and Karolina. My previous dear office mates, Annelies "ciwiz" and Bassam, you were always willing to help me and work out my problems, especially during the early stage of my PhD. I really miss the days we spent together. Pauline, Ona, Mariusz and Katlijn, thank you for being such nice students, and I wish you a lot of success in your future career. I would also like to extend my gratitude to Geert, Fien and Sofie. You helped me a lot and made my life easy. I would thank all the people from the department of Molecular Biotechnology.

I am so lucky to have made so many great friends who were always there for me no matter for the ups and downs: Mei, Lili, Lizi, Sabine, Bilal, Julia, Chuan, Yueqi, Yanrong, Linxin, Jianyun, Guokun, Renfei, Jinzhi, Wenkun, Huajun, Xianyu, Haidong, Wangxiang, Zongwang, Wanzhao, Huaihan, Lidan, Baoyu, Jisheng, Zhengliang, Guangzhi, Liubing, Lifan, Guoliang, Yuming, Caojun, Wuyan, Lixiao, Wuting, Tiantian, Ouyang Lin, Dongfei, Mery, Dora, Hennok, Annelien, Cintia, Marina, Clauvis and Ruben.

I would also like to thank Prof. Lizhe An, Prof. Huang Zhang and Dr. Xiule Yue (Lanzhou University, China) who brought me into the world of biotechnology during the third year of my bachelor, and their passion for science made me decide to further pursue the PhD.

Although impossible to express in words as it deserves, I would like to mention my deepest gratitude to my beloved parents for their never ending support, love and compassion. They have been my greatest mentors and source of aspiration throughout my life to overcome all the difficulties. Last but not least I specially thank my husband Yang for his love, tolerance and understanding towards me regardless of all the work.

Chenjing
June 2015

Curriculum vitae

Curriculum vitae

1. Personal information

First name: Chenjing

Family name: Shang

Birth date: 22nd Dec. 1985

Nationality: China

Civil status: Married

E-mail: shangchenjing@gmail.com

2. Education

2010 - 2015   PhD in Applied Biological Sciences, Faculty of Bioscience Engineering, Ghent University, Belgium.

   PhD thesis, " Biological activity of ribosome-inactivating proteins from *Malus sp.* (apple) and *Sambucus nigra* (elderberry)"

2009 – 2010   Master study of Botany, Faculty of Life Sciences, Lanzhou University, China

2005 – 2009   Bachelor of Biotechnology, Faculty of Life Sciences, Lanzhou University, China

   Bachelor thesis, "Cloning and sequence analysis of gene F200 from *Chorispora bangeana* using suppression subtractive hybridization"

3. Career

Other experiences

2007-2008   **Project,** "The primary study the anti-freeze gene from *Chorispora bangeana* by using suppression subtractive hybridization", Lanzhou University

2008-2009   **Project,** "The effect of silencing gene STAT-3 upon breast cancer cell MCF-7", Lanzhou University

Supervision of undergraduate and master students

Pauline Depuydt (2012.08 - 2013.06) "The ribosome-inactivating proteins in apple (*Malus* sp.)"

Mariusz Madej (2012. 09 - 2013. 04) "The effect(s) of ribosome-inactivating proteins and lectins from elderberry (*Sambucus nigra*) on mammalian cell lines"

Ona Corominas (2013. 09 - 2014. 01) "Analysis of transgenic tobacco lines expressing ribosome-inactivating proteins from apple"

Katlijn Haerick (2014. 02-2014. 06) "Kunnen ribosoominactiverende proteïnen uit appel helpen in de verdediging van tabak tegen pathogenen?"

4. Languages

Chinese   Mother tongue

English   Fluent

5. Publications with peer-reviewed journals

Shang, C., Van Damme, E. J. M. (2014) Comparative analysis of carbohydrate binding properties of *Sambucus nigra* lectins and ribosome-inactivating proteins. Glycoconj. J. **31**, 345-354

Ji, H., Gheysen, G., Ullah, C., Verbeek, R., **Shang, C.**, De Vleesschauwer, D., Höfte, M. and Kyndt, T. (2015) The role of thionins in rice defence against root pathogens. Mol. Plant Pathol. *In press*

Shang, C., Chen, Q., Dell, A., Haslam, S. M., De Vos, W. H. and Van Damme, E. J. M. (2015) The cytotoxicity of elderberry lectins is not solely determined by their N-glycosidase activity. PLoS One, in press

6. Patent

An, L., **Shang, C.**, Zhang, H. and Fan, X.: A method of transformation of embryogenic suspension cultures in *Chorispora bungeana*. Patent No. ZL 2010 1 0241353.2 (Authorized: 13th Mar. 2013)

7. Book chapters

Shang, C., Peumans, W. J. and Van Damme, E. J. M. (2014) Occurrence and taxonomical distribution of ribosome-inactivating proteins belonging to the ricin/shiga toxin superfamily. In: Ribosome-inactivating proteins: ricin and related proteins. Stirpe, F. and Lappi, D. A. (eds.) pp. 11-27. Wiley Blackwell Press, NJ, USA

Peumans, W. J., **Shang, C.** and Van Damme, E. J. M. (2014) Updated model of the molecular evolution of RIP genes. In: Ribosome-inactivating proteins: ricin and related proteins. Stirpe, F. and Lappi, D. A. (eds.) pp. 134-150. Wiley Blackwell Press, NJ, USA

Shang, C., Dang, L. and Van Damme, E. J. M. (2015) Plant AB toxins with lectin domains. In: Toxinology: Plant Toxins. Gopalakrishnakone, P., Carlini, C. R. and Ligabue-Braun, R. (Eds.) Springer, Berlin, Germany. In press

8. Conferences

With oral Presentation

Shang, C., Madej, M., De Vos, W. H. and Van Damme, E. J. M. (23-28th June, 2013) The ribosome-inactivating proteins (RIPs) from elderberry (*Sambucus nigra*) in the battle against cancer??" The 22nd International Glycoconjugate Symposium, Dalian, China.

Shang, C. and Van Damme, E. J. M. (05th Feb., 2014) Localization study of ribosome-inactivating proteins from apple (*Malus* sp.) The 6th Plant Research FBW meeting, Ghent, Belgium.

Shang, C., Seifi, S. H., Delaere, I., Höfte, M. and Van Damme, E. J. M. (19th May, 2014) Effect(s) of overexpression of ribosome-inactivating proteins from apple on disease resistance. The 66th International Symposium on Crop Protection, Ghent, Belgium

With poster presentation

Shang, C., Peumans, W. J. and Van Damme, E. J. M. (24-26th Nov., 2013) Ribosome-inactivating proteins in apple (*Malus* sp.). The 24th Joint Glycobiology Meeting, Wittenberg, Germany

Shang, C., Peumans, W. J. and Van Damme, E. J. M. (23-28th June, 2013) Ribosome-inactivating proteins in apple (*Malus* sp.). The 22nd International Symposium on Glycocojugates , Dalian, China

Shang, C., De Vos, W. H. and Van Damme, E. J. M. (14-16th Sept., 2014) Interaction of ribosome-inactivating proteins (RIPs) from elderberry (*Sambucus nigra*) with surface glycans of mammalian cells. The 25th Joint Glycobiology Meeting, Ghent, Belgium

9.   Academic Honors

Best Poster Presentation, *25th Joint Glycobiology Meeting*, Belgium, 2014

Best Poster Presentation, *24th Joint Glycobiology Meeting*, Germany, 2013

Excellent paper and travel grant, *The 22nd International Symposium on Glycoconjugates*, China, 2013

Academic Scholarship (CSC), *China Scholarship Council*, 2010-2014

BOF Co-funding, Ghent University, 2011-2014